18.4

DOE/SF/11438-T1(Vol.1)
(DE82001663)

CONCEPTUAL DESIGN OF A SOLAR COGENERATION FACILITY INDUSTRIAL PROCESS HEAT

Executive Summary and Final Report for the Period September 30, 1980–August 14, 1981

By
Patrick Joy
Martin Brzeczek
Harold Seielstad
Carl Silverman
George Yenetchi

July 1981

Work Performed Under Contract No. AC03-80SF11438

Exxon Research and Engineering Company
Linden, New Jersey

and

Badger Energy, Inc.
Cambridge, Massachusetts

Martin Marietta
Denver, Colorado

and

Pacific Gas & Electric
San Raymon, California

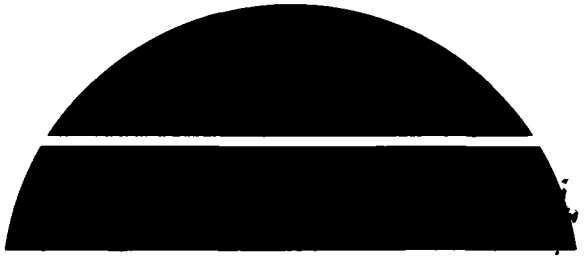

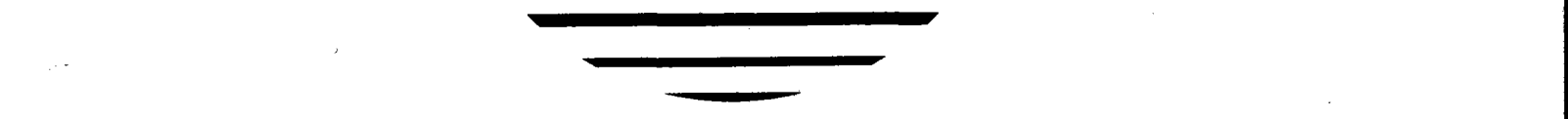

U.S. Department of Energy

Solar Energy

DISCLAIMER

DOE/SF/11438-T1(Vol.1)
(DE82001663)
Distribution Category UC-62c

VOLUME I - EXECUTIVE SUMMARY AND FINAL REPORT

CONCEPTUAL DESIGN OF A SOLAR COGENERATION FACILITY INDUSTRIAL PROCESS HEAT

Final Report for the Period September 30, 1980 - August 14, 1981

by
Patrick Joy
Martin Brzeczek
Harold Seielstad
Carl Silverman
George Yenetchi

CONTRACTORS

Advanced Energy Systems Lab
Exxon Research and Engineering Company
P.O. Box 45
Linden, New Jersey 07036

Badger Energy, Inc.
Cambridge, Mass 02142

Martin Marietta
Denver Division
Denver, Colorado, 80201

Pacific Gas & Electric
3400 Crow Canyon Road
P.O. Box 31
San Raymon, CA 94583

PREPARED FOR THE U.S. DEPARTMENT OF ENERGY
UNDER CONTRACT DE-AC0380SF-11438

VOLUME I - TABLE OF CONTENTS

TABLE OF CONTENTS (Continued)

VOLUME II - TABLE OF CONTENTS

LIST OF TABLES

LIST OF TABLES

LIST OF FIGURES

LIST OF FIGURES (Continued)

LIST OF FIGURES (Continued)

LIST OF FIGURES

1.0 EXECUTIVE SUMMARY

Exxon Research and Engineering Company, in association with Martin Marietta Denver Aerospace, Badger Energy, Incorporated and Pacific Gas and Electric Company, submits this final report to the United States Department of Energy (DOE) in fulfillment of contract DE-AC0380SF-11438 entitled "Designs for Solar Cogeneration, Category A Industrial Process Heat." Purpose of the DOE procurement is to design economic, technically feasible, site specific systems which use solar central receiver technology to cogenerate both thermal energy and electricity. In accordance with this procurement, we have devloped conceptual designs for a solar central receiver Cogeneration Facility with molten salt storage to generate process steam for Exxon Company USA's enhanced oil recovery operations at the Edison field near Bakersfield, California, and electricity to power the solar system and to sell to PG&E Company. This system is designed to displace the consumption of a total of 22,237 m^3 [139,547 barrels (bbl.)] of oil per year including 10,000 m^3 (62,114 bbl.) displaced for the enhanced oil recovery process and 12,237 m^3 (77,433 bbl.) displaced for electric power generation.

1.1 PROJECT SUMMARY

The Solar Cogeneration Facility summarized in this report can simultaneously provide process steam for Exxon Company USA's enhanced oil recovery operations and electricity to the Pacific Gas and Electric Company without the consumption of and emissions from fossil fuels. A number of technical, economic and programmatic conclusions have evolved from this conceptual design study. These conclusions are presented herein.

1.1.1 Technical Conclusions

1) Solar Central Receiver technology can provide steam temperatures and pressures required by the thermal enhanced oil recovery (TEOR) process at the Edison field.

2) The high pressure requirements for TEOR steam and high turbine water purity requirements preclude the use of a turbine topping-process bottoming cogeneration cycle, and dictate a design which is essentially separate and parallel process steam and electric power producing subsystems.

3) Second generation heliostats and a two cavity receiver, now in the prototype development stages, appear to offer significant technical advantages over earlier heliostat designs and over external receivers.

4) The use of energy storage is essential to allow efficient turbine operation and is preferable to allow uniform steam flow to the TEOR process.

5) Molten salt is preferred over sodium and water for the receiver heat transfer fluid for reasons of cost, controllability, safety and compatibility with energy storage.

6) Molten salt was also selected as the energy storage medium due to its cost, performance and safety advantages over oil/rock and pressurized water.

1.1.2 Non-Technical Conclusions

1) Of the various system sizes considered in this study,, the larger cogeneration system size, which is limited by available land at Edison, is more cost effective than smaller alternatives due to economics of scale and the value of the additional electricity produced by the facility and sold to PG&E.

2) Using reasonable economic assumptions and cost estimates consistent with this conceptual design study, the levelized energy cost ($\overline{LEC}$) of steam from the Solar Cogeneration Facility is \$51/MWh_t. This is significantly higher than the $\overline{LEC}$ of an oil fired steam boiler facility of comparable capacity which is \$35/MWh_t.

3) The $\overline{LEC}$ of the Solar Cogeneration Facility is very sensitive to capital, O&M, tax credits and depreciation schedules. For the range of economic sensitivities considered in this study, the solar facility $\overline{LEC}$ ranges from a low of \$16/MWh_t to a high of \$112/MWh_t. The conventional oil fired facility $\overline{LEC}$ ranges from \$22/MWh_t to \$63/MWh_t.

4) Uncertainties in the economic parameters listed in 3) above combined with uncertainties in the regulation of, and revenues from, small electric power producers in California cause great difficulty in predicting the future economic worth of this Solar Cogeneration Facility.

5) The impact of taxes on crude oil paid by the producer is to provide an economic incentive to burn a portion of the crude oil produced at Edison rather than buying such crude at prevailing market prices including all taxes. This imposes a lower $\overline{LEC}$ target for solar in this application than would be encountered for solar in a non-oil producing application.

6) In an earlier Exxon study of solar enhanced oil recovery (contract DE-AC03-79C530307), it was determined that a TEOR potential of 8,400 MW_t exists in Kern County, and of this, approximately 3,200 MW_t could potentially be satisfied (assuming reasonable land costs) with solar thermal energy by the year 2000.

1.2 INTRODUCTION

Several energy and legislative issues form a background for this conceptual design study of a Solar Cogeneration Facility at Exxon's Edison field.

First is the dual potential for conserving domestic crude oil normally burned in the thermal enhanced oil recovery process and reducing combustion related emissions by using solar thermal energy to produce steam for enhanced oil recovery. Second, is Federal and state legislation aimed at discouraging the use of oil and gas in industries and encouraging cogeneration and small electric power producers by requiring utilities to buy and sell electricity to cogenerators and small power producers at just and reasonable rates. Third is a combination of high direct normal insolation, constant demand for process steam, accessable land and process steam requirements compatible with solar central receiver technology. These factors combine to create a logical setting for a conceptual design study of solar energy to produce steam for Exxon Company USA's enhanced oil recovery process and electricity for powering the solar facility and for sale to Pacific Gas and Electric Company.

The objectives of the sponsoring DOE procurement include the development of site specific designs which use solar central receiver technology to produce both process steam and electricity from a single cogeneration facility. Such designs are to have the following characteristics: potential for construction and reliable operation by 1986; potential for cost effective operation; high potential for commercial success and potential for significant savings of critical oil and gas fuels.

The technical approach to this conceptual design study was to first identify all technical, economic, regulatory, site and process parameters which bear on this study and then to develop several site specific designs which satisfy the program parameters and select the most cost effective of the candidate designs. The use of solar central receiver technology in which a field of computer driven, tracking mirrors or heliostats reflects and concentrates sunlight into a central, stationary receiver mounted on top of a tower, was dictated by the DOE procurement. In addition, the solar system size was influenced by the program requirements to generate steam for the users' industrial process plus at least an additional 10% to be used to generate electricity for sale to the local utility. The upper limit on system size for this study was fixed by the available land at Edison which is contained within public highways; the lower limit on size was set by the aforementioned 10% requirement for electricity production.

This conceptual design study was executed for the DOE by an industrial/utility team led by the prime contractor, Exxon Research and Engineering Company in association with Badger Energy Incorporated, Martin Marietta Denver Aerospace and Pacific Gas and Electric Company.

Exxon was responsible for program management, system integration, system performance, cost estimating and electric power generating system design. Badger provided design, performance and cost data for the thermal storage and thermal transport subsystems. Martin provided design, performance and cost data for the solar subsystems including collectors, receiver and tower and the overall master controller. PG&E provided information on rate structures, interface requirements, interfacing equipment and cogeneration regulations.

The solar cogeneration facility conceptual design is shown in the artist concept of Figure 1.2-1. The north field of 3295 second generation Martin Marietta heliostats is shown to be carefully integrated within the existing oil wells and other site facilities allowing ample space for access to current and planned wells. The 137 m (450 ft) concrete tower is shown at center right and supports two independent cavity receivers each cooled by molten salt. The hot and cold salt thermal storage tanks are shown at the tower base left. Other equipment shown in the artists rendition includes the twin oil fired steamers now in service at Edison, the heat exchange and water treatment facilities and master control room and turbine room. The wet cooling tower for the condensing turbine is shown above the control room. At the lower right is the existing PG&E substation which will interface with the Solar Cogeneration Facility.

1.3 FACILITY DESCRIPTION

The site selected for this design study is the Edison oil field in Kern County, California. The Edison field is located approximately 11 km (7 mi) southeast of Bakersfield at the south end of the San Joaquin Valley. The latitude is about 35° north. Figure 1.3-1 shows the location relative to Bakersfield. The terrain is very flat (Figure 1.3-2), is at an average elevation of 180 m (600 ft.) above mean sea level and has very slight slope of 1.5% from the northeast to the southwest.

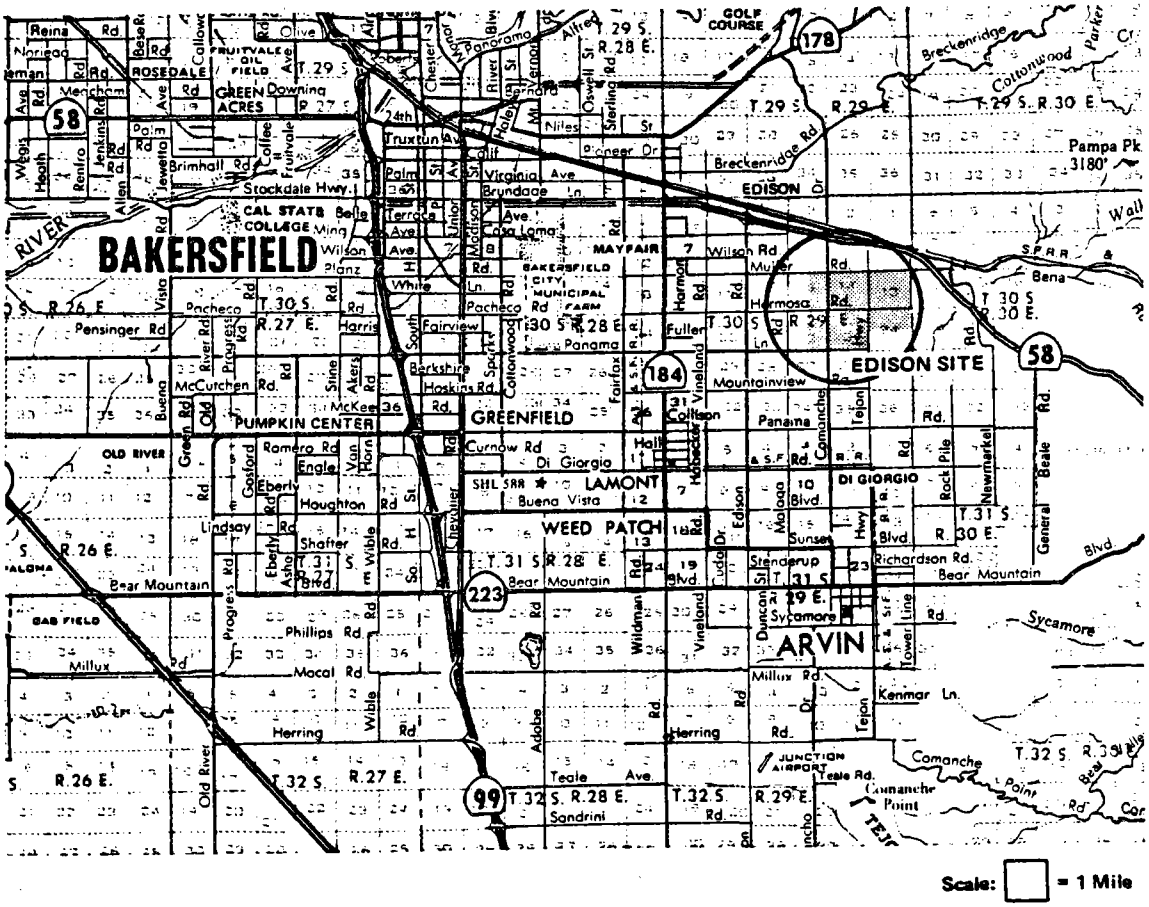

Figure 1.3-1 Bakersfield Area Map

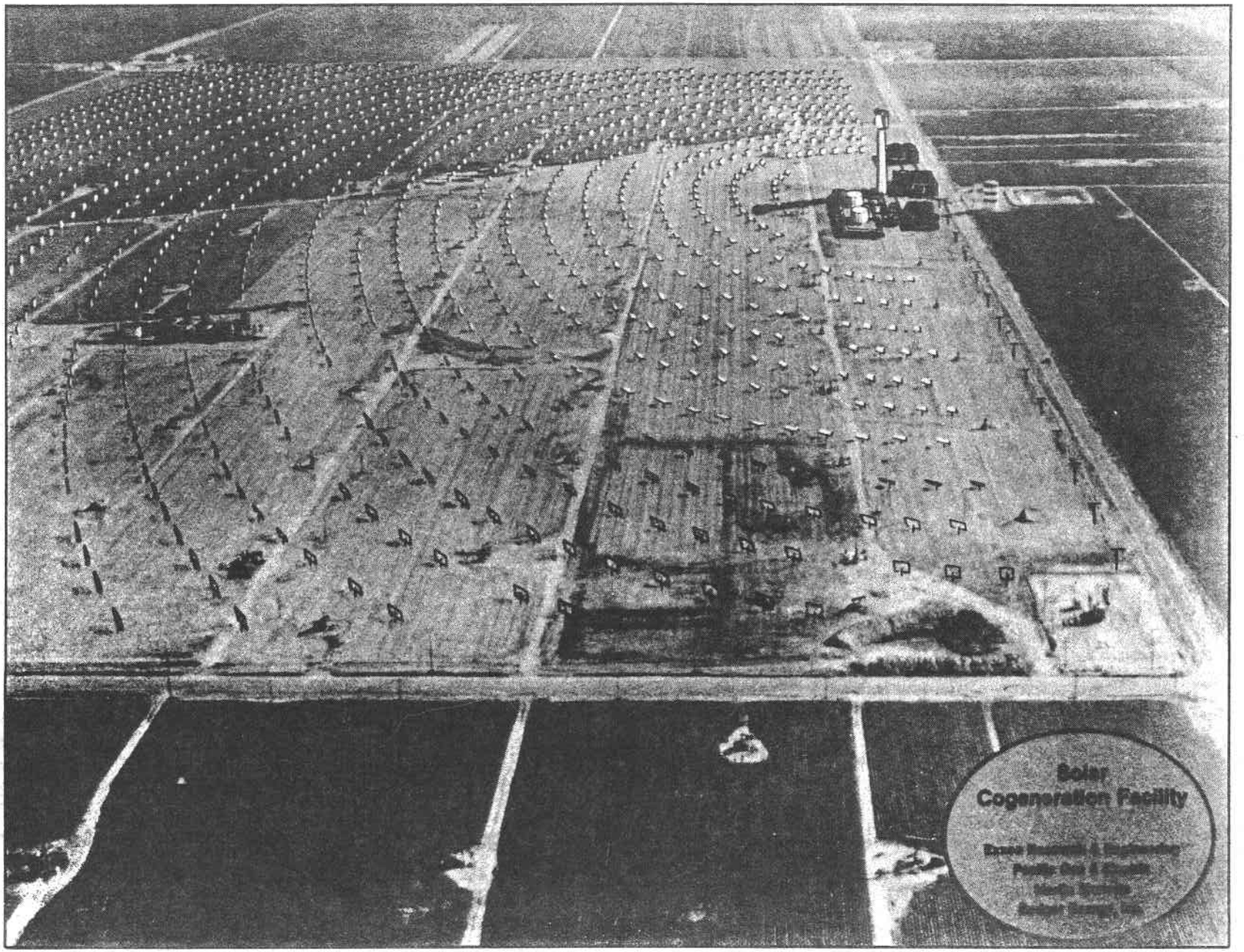

Figure 1.2-1 Conceptual Design

A map of the zone to be served by the cogeneration system is shown in Figure 1.3-3. There are 74 producing wells on this site and another 70 are planned to be drilled. When the drilling program is complete the average oil well density will be one well per 5060 m^2 (1.25 acres). The entire cogeneration facility will be located on leases 808794, 808795, 808796 and 808797, which measures 1610 m (5280 ft.) by 805 m (2640 ft.).

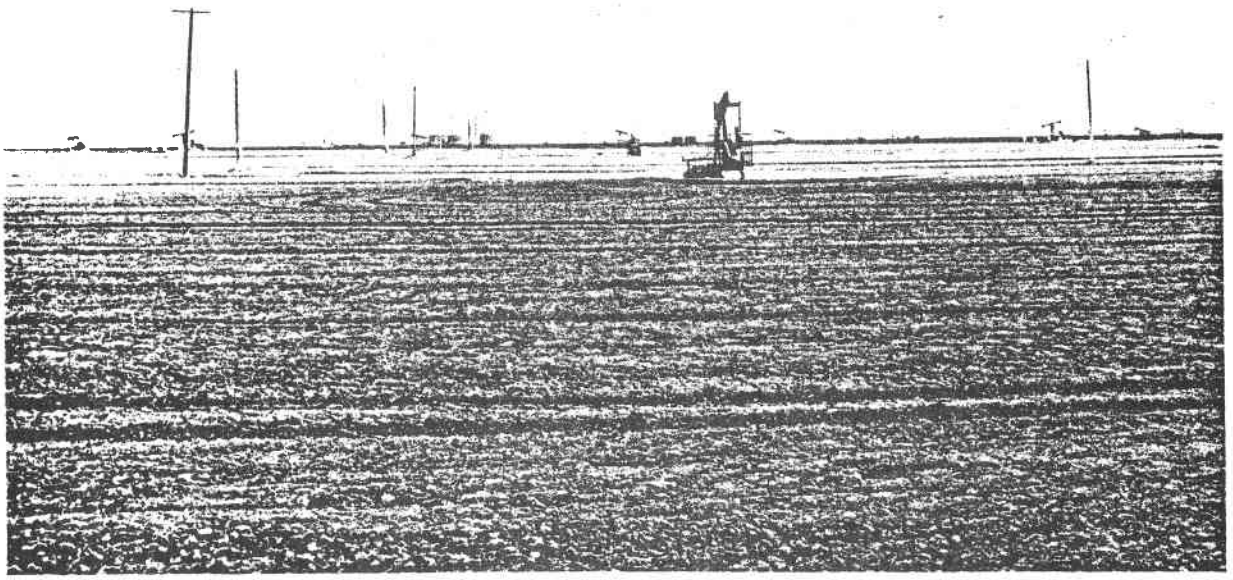

Figure 1.3-2 Exxon's Edison Field Looking South from Tank Battery Location

The annual average direct normal insolation in this general area of California ranges from 6 to 7 kW/m^2 per day. The closest location to the site for which detailed measured insolation data are available is Fresno, 174 km (108 miles) to the northwest, which averages 6.21 kW/m^2 per day. Exxon has taken direct normal and total horizontal insolation measurements for the entire year 1980 at the Edison field and has found these measurements to agree within 5% of Fresno data. The climate is warm and semiarid. Average daily temperatures range from 9°C (48°F) in the winter to 29°C (84°F) in the summer. Cumulative precipitation averages 15 cm (5.8 in.) annually, nearly all of which is in the form of rain.

Exxon presently uses two crude oil-fired boilers, each rated at 7.3 MW_t (25 MBtu/hr output power) in their steaming operations. The boilers, fuel and feedwater storage tanks and feedwater treatment module are all portable units that can be moved about the field. The Edison field is presently operated in the steam stimulation mode. Steam is injected into a single well at a time continuously for about 7 days, then the well is capped and allowed to soak for about 4 days. After pumping is resumed, the initial production rate is several times greater than before the injection process (Figure 1.3-4). The production

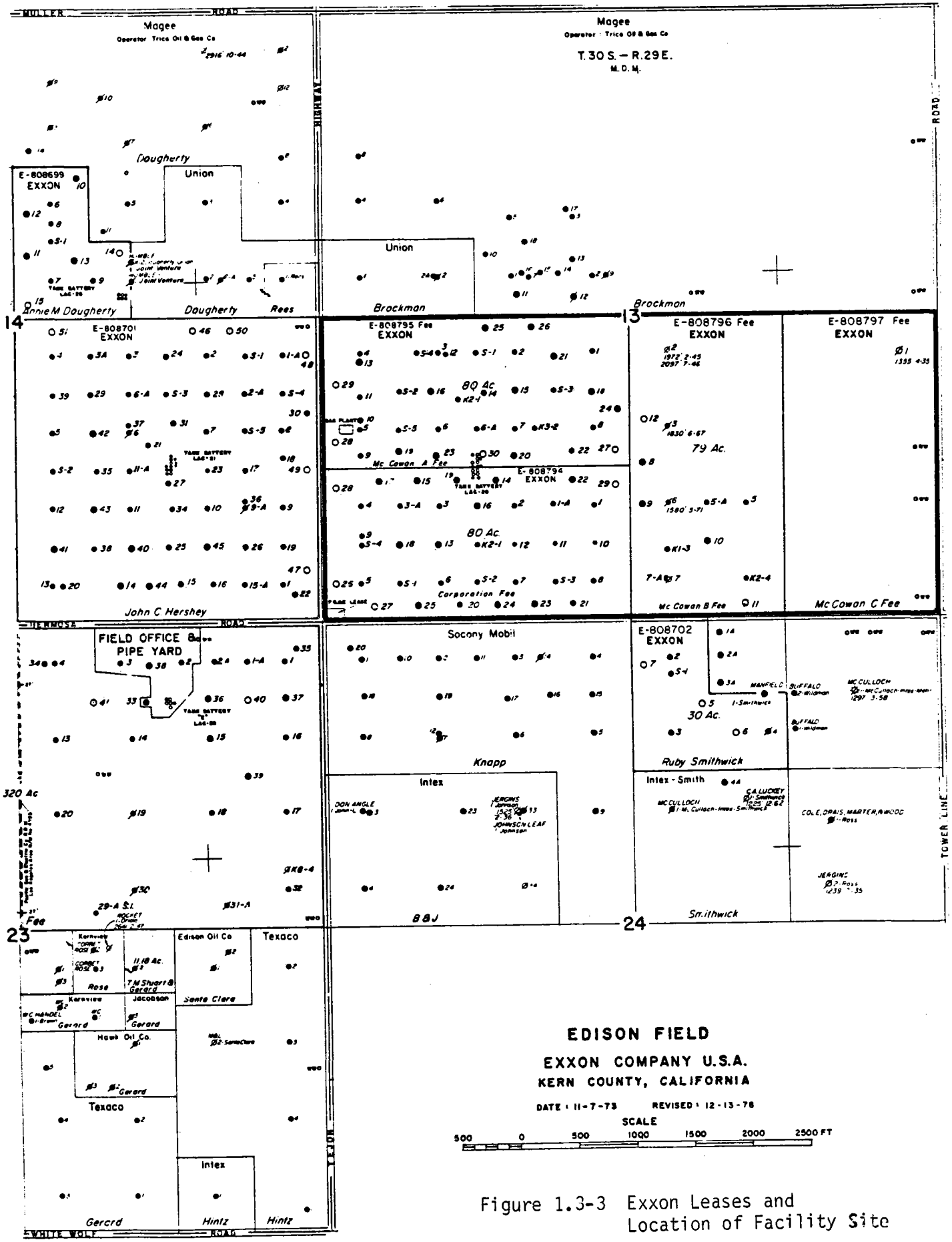

EDISON FIELD

EXXON COMPANY U.S.A.

KERN COUNTY, CALIFORNIA

DATE : 11-7-73 REVISED : 12-13-78

SCALE

500 0 500 1000 1500 2000 2500 FT

Figure 1.3-3 Exxon Leases and Location of Facility Site

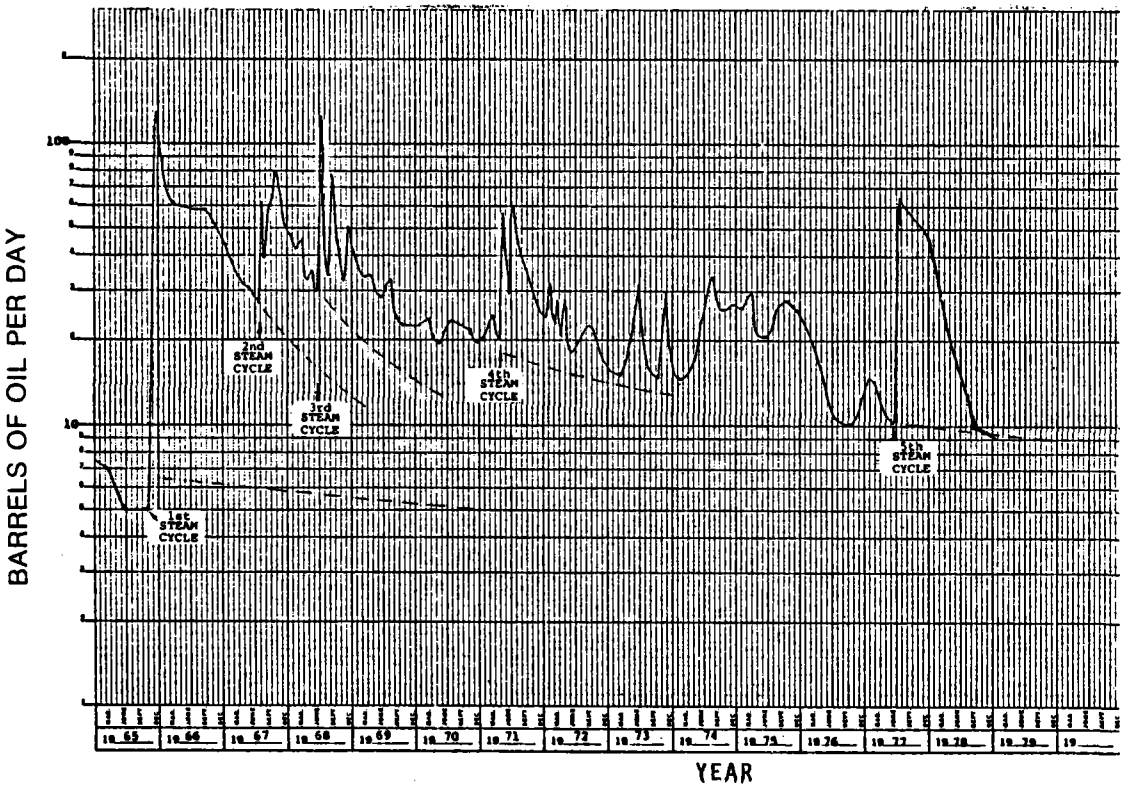

Figure 1.3-4 Typical Production History-Steam Stimulation

rate declines with time until the next steaming cycle is performed. The interval between stimulations for any given well varies from one to several years.

1.4 CONCEPTUAL DESIGN DESCRIPTION

The conceptual design of the Solar Cogeneration Facility at Exxon's Edison field employs central receiver solar thermal technology and molten salt heat transfer fluid and energy storage medium to supply thermal energy to two salt/steam boilers. These, in turn, provide steam for both the enhanced oil recovery process and the rankine cycle turbine generator which supplies electricity to the Solar Cogeneration Facility and to the PG&E grid. The major elements of the facility are shown schematically in Figure 1.4-1. Molten salt is pumped from the cold storage tank at 288°C (550°F) to the receiver where concentrated solar energy is converted to thermal energy, which is absorbed in the molten salt, raising its temperature to 566°C (1050°F). The molten salt returns to the hot salt storage tank. From this tank separate molten salt transfer loops convey the salt to separate salt/steam boilers. The process steam boiler uses well water from onsite wells which is treated and sent to the process steam boiler which generates steam at 290°C (560°F), 80% quality. This steam is then fed into the steam distribution network along with steam from existing fossil boilers for injection into the wells. The turbine steam boiler also uses treated well water to provide make up water for the turbine. Steam is generated in the turbine steam boiler at 538°C and fed into the single reheat steam turbine. Salt returns from both boilers at 288°C(550°F) to the cold salt storage tank. The steam turbine drives a 20.4 MW_e (gross) generator which interfaces with the on site PG&E substation to provide electricity to the grid. Some turbine extraction steam is used to preheat water for the process steam.

The Solar Cogeneration Facility is sized to provide, on an annual basis, 106,000 MWh_t of thermal energy for the enhanced oil recovery process and 43,000 MWh_e of net electrical energy to the PG&E grid.

The collector subsystem consists of 3295 Martin Marietta second generation heliostats arranged in a north field configuration (see figure 1.4-2). The heliostats are arranged in a radially staggered semicircular pattern with open areas to provide access to current and planned oil wells. As a result of well clearances the heliostat field is skewed, with 1858 heliostats in the east (lower portion of figure 1.4-2) and 1437 heliostats in the west half. Reflecting area per heliostat is 57.4 m^2 for a total reflecting field area of 189,000 m^2 (12.0 million ft^2). The heliostat field is contained within a land area of 1.3 million square meters (0.5 square miles).

On an annual basis, the collector subsystem directs 287,000 MWh_t of solar energy into the two cavity receiver for an annual collector efficiency of 67%.

The receiver design is a two cavity arrangement mounted on a 137 m (450 ft) concrete tower. Each cavity has a door (to reduce non-operating thermal losses) which is covered with ablative material for protection of the receiver in the event of a power loss. Each cavity aperture measures 11 m x 11 m (36 ft x 36 ft) and each cavity can operate independent of the other. Separate molten salt surge tanks at the receiver inlet and outlet are used to decouple receiver salt flow transients from supply and return piping transients and to provide an emergency storage capability to maintain salt flow through the receiver in the event of a salt pump failure. On an annual basis, the receiver delivers 243,600 MWh_t of thermal energy to the tower base and has a thermal conversion efficiency of 85%. (Martin Marietta has tested a similar molten salt receiver at the central receiver test facility in Albuquerque.) The energy storage subsystem consists of separate hot and cold molten salt storage tanks, each 15 m (49 ft) diameter by 11 m (36 ft) high. A third tank provides backup to either hot or cold tank. The total energy storage capacity is 380 MWh_t using molten salt at 566°C in the hot tank and 288°C in the cold tank. The energy storage capacity is sized to provide steam to the enhanced oil recovery process 24 hours/day and steam to drive the turbine generator 14 hours/day during the summer, when electric rates are higher. The 14 hour turbine operating time coincides with daily on peak and partial peak pricing periods defined by PG&E.

The process steam subsystem generates 5.56 kg/s (44,000 lb/hr) of 293°C (560°F) 80% quality steam for use in the enhanced oil recovery process. Four units of shell and tube design make up the heat exchanger train. The process steam subsystem also contains water treatment facilities to soften the onsite well water, which enters the heat exchanger at 21°C (70°F) is preheated in three stages to 293°C and then flashed to 7.81 MPa (1133 psig) steam for use in the process.

The turbine steam subsystem generates 20.9 kg/s (165,760 lb/hr) of superheated steam at 538 °C (1000°F) for use in the steam turbine and reheats 18.4 kg/s (145,830 lb/hr) of steam from 398°C to 538°C for use in the low pressure section

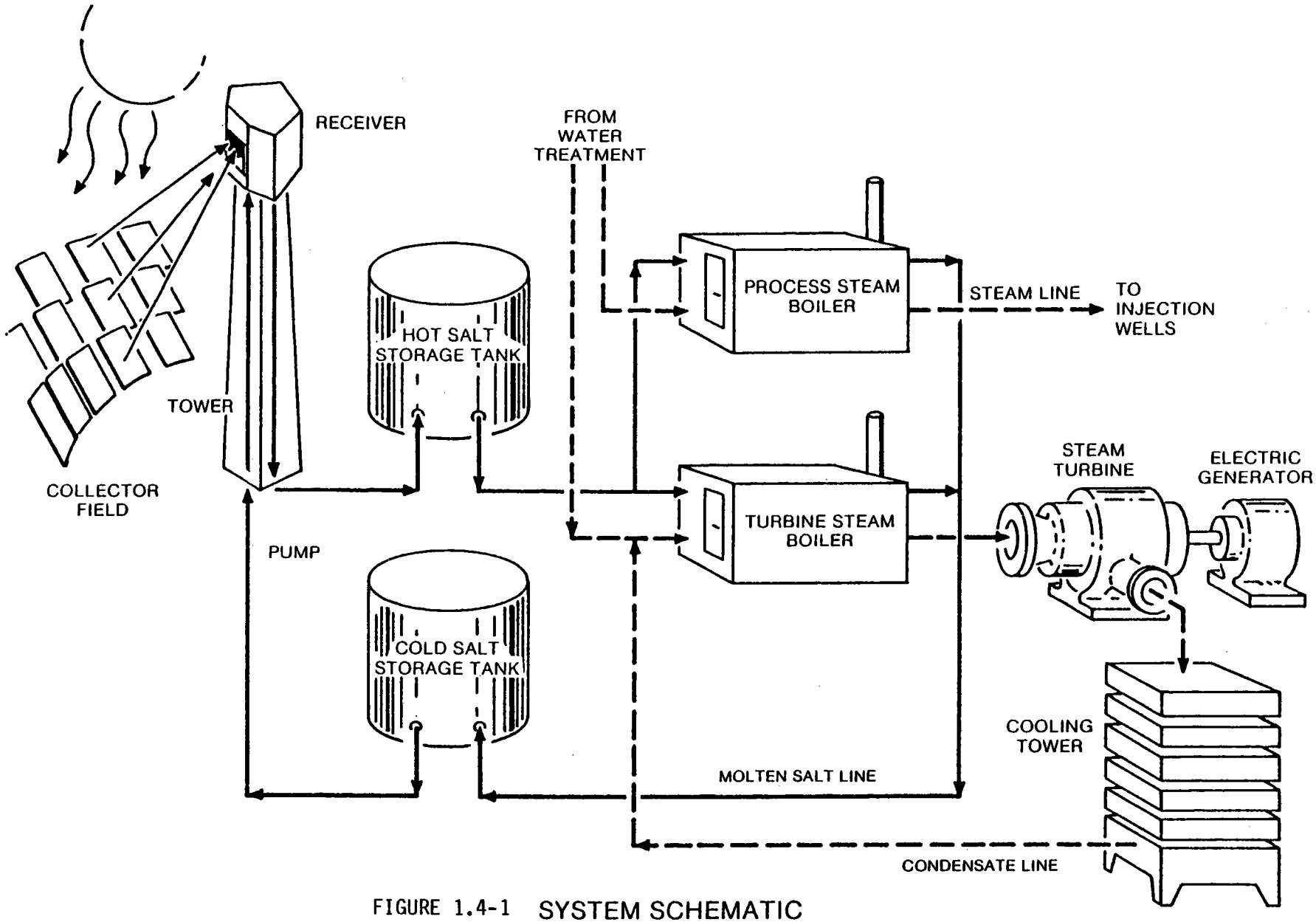

FIGURE 1.4-1 SYSTEM SCHEMATIC

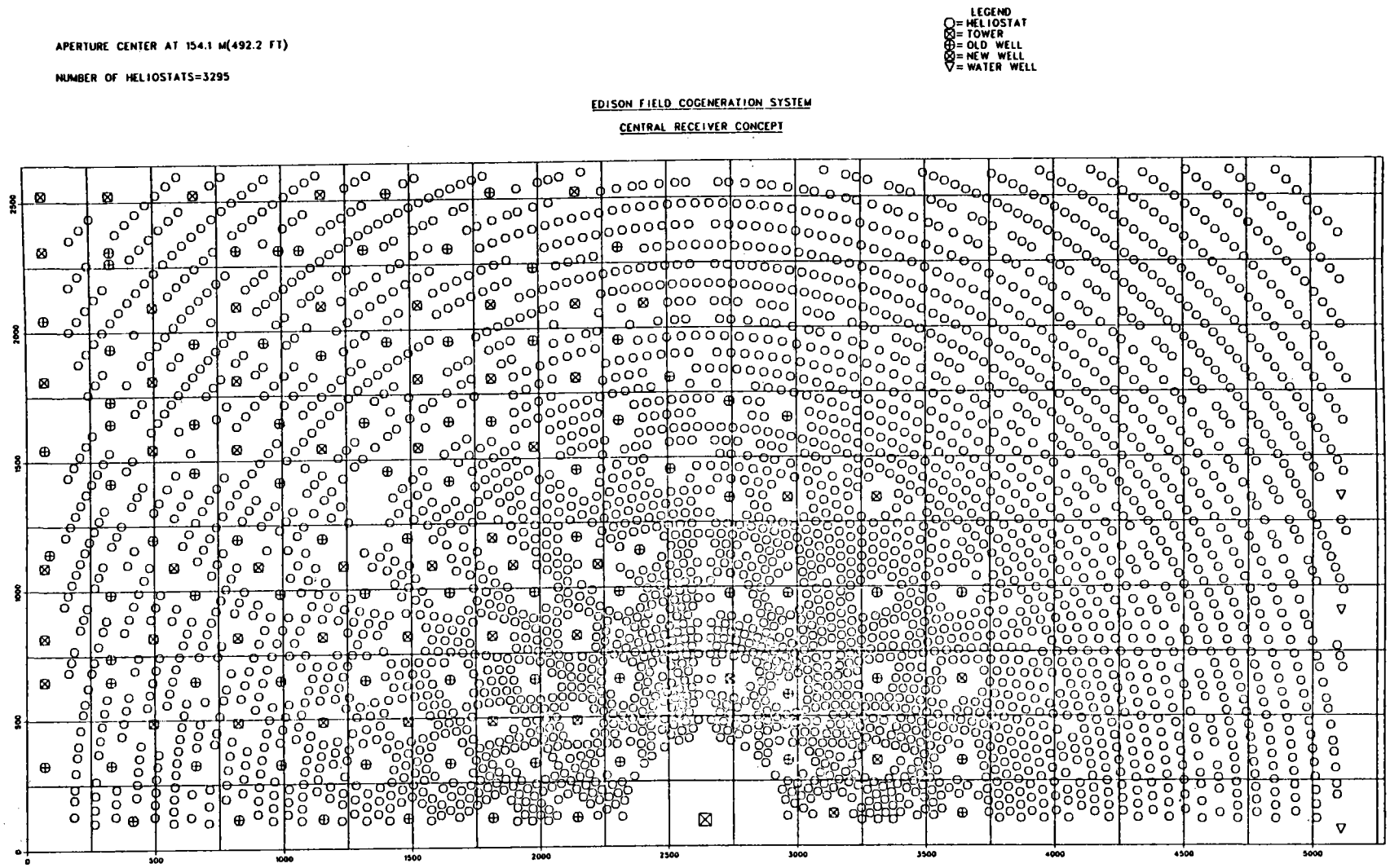

Figure 1.4-2 Collector Field Layout

of the turbine. This subsystem contains four shell and tube heat exchangers, one steam drum and water treatment facilities to provide high purity water for use in the turbine. The turbine steam subsystem is designed to operate independently of the process steam subsystem.

The electric power generating subsystem (EPGS) consists of a 20.4 MW_e (gross) turbine-generator set with feedwater heaters, condenser, a wet cooling tower and utility interconnection hardware. The rankine cycle turbine is a single reheat, multiple extraction, condensing type with inlet steam at 538°C (1000°F), 8.3 MPa (1200 psia), reheat steam at 538°C (1000°F), 2.6 MPa (380 psia) and exhaust pressure of 6.9 KPa (2 in Hg). Heat rejection is a mechanical draft wet cooling tower. The turbine generator set is sized to provide 20.4 MW_e of gross electrical power with 56 MW_t of steam inlet. Overall rankine cycle efficiency is 36%. The direct driven synchronous generator runs at 3600 RPM and outputs 20.4 MW_e at 12 KV.

On an annual basis the EPGS provides 43,000 MWh_e to the PG&E grid, 88% of this during peak and partial peak pricing periods. In addition, the turbine provides 11,400 MWh_t of extraction steam for preheating process boiler feedwater.

The entire Solar Cogeneration Facility is monitored and controlled by the master control subsystem which includes six functional subsystems, a data acquisition subsystem and an emergency control subsystem. The control subsystems include: collector, receiver, storage, process steam, turbine steam and power generation. The master control subsystem uses the supervisory control concept in which the six distributed digital control subsystems are responsible for first level control function, while the supervisory computer prescribes the proper operating instructions (set points) to meet operating objectives. Normal plant control is designed to be automatic although full time operators would be used.

The data acquisition system operates independent of the master controller and will provide instantaneous and long term performance information. The emergency control subsystem is programmed with out of tolerance conditions and can override the master controller if emergency conditions warrant.

A tabular summary of key design and performance features of the Solar Cogeneration Facility is given in table 1.4-1.

1.5 SYSTEM PERFORMANCE

The annual Solar Cogeneration Facility performance was calculated using the SOLMET TMY weather data for Fresno, CA, which has insolation levels similar to the Edison field. The mean daily annual direct normal insolation from the Fresno TMY tape is 6.21 Kwh/m^2-day, or an annual basis, 429,000 MWh of direct normal insolation is incident on the heliostat field.

Table 1.4-1

Conceptual Design Summary Table

1. Prime Contractor: Exxon Research and Engineering Company,
   Patrick Joy, Project Manager

2. Major Subcontractors: Martin Marietta Corporation, Martin Brzeczek
   Pacific Gas & Electric Company, Harold Seielstad
   Badger Energy Incorporated, Carl Silverman

3. Site Location: Exxon Edison field near Bakersfield, CA

4. Facility Characteristics:

   a. Turbine type: Single reheat, condensing turbine generator, 20.4 MW_e gross output
   b. Turbine inlet condition: 538°C (1,000°F), 8.27 MPa (1,200 psia)
   c. Turbine outlet conditions, each port:

	Temperature °C (°F)	Pressure kPa (psia)
	463 (865)	4,540 (659)
	399 (750)	2,760 (400)
	475 (887)	1,590 (231)
	373 (705)	750 (109)
	285 (545)	303 (44)
	60 (295)	60 (9.5)
Exhaust:	38 (101)	7 (2 in. Hg)

   d. Process fluid and purpose: 80% quality steam for enhanced oil recovery
   e. Process fluid conditions: 293°C (560°F), 7.6 MPa (1130 psia), 26.4 MW_t continuous

5. Design Point: Noon, Day 189 Fresno TMY Data, Insolation of .95 kw/m^2

6. Receiver:

   a. Receiver fluid: Molten salt 60% NaNO/40% KNO_3 by weight
   b. Configuration: Two cavity
   c. Type: Forced circulation, recirculating
   d. Elements: 12 absorber panels, in series, each of two cavity
   e. Temperature: 288°C (550°F) inlet, 566°C (1050°F) outlet
   f. Pressure: 2.5 MPa (363 psia)
   g. Tower: 137 m (450 ft)

7. Collector Field:

   a. No. of heliostats: 3295
   b. Mirror area per heliostat: 57.4 m^2 (618 ft^2)
   c. Cost - $/$m^2$ installed: 203 $/$m^2$ (direct cost)
   d. Type: Martin Marietta second generation
   e. Field configuration: 3.1 rad (180°) north field
   f. Total mirror area: 189,133 m^2 (2.03 x 10^6 ft^2)
   g. Total collector field area: 1,300,000 m^2 (320 acres)

8. Storage:

    a. 380 MWh_t capacity
    b. Molten Salt, 60% $NaNO_3$/40% KNO_3

9. Project Cost:

    a. Total Project Cost - including all capital, startup, and checkout cost but excluding O & M: $120 million

    b. Total Project Cost using installed heliostat cost of $260/$m^2$: $135 million

10. Construction Time: 3 years

11. Solar Facility Contribution at Design:

    a. Design Point; Noon, Day 189, 0.95 kW/m^2

        1. Receiver output: 122 MW_t, 460% of process thermal demand
        2. Electrical energy: 20.4 MW_e gross, 18.3 MW_e net after 2.1 MW_e plant demand (100%)
        3. Process energy: 13.2 MW_t + 2.55 MW_t preheat to fossil steamers, 60% of process thermal demand

    b. Design Day; Day 189 of Fresno, CA, TMY Data

        1. Receiver output: 1145 MWh_t, 181% of process thermal demand
        2. Electrical energy: 286 MWh_e gross, 256 MWh_e net after 29.4 MWh_e plant demand (100% during 14 hours of turbine operation)
        3. Process energy: 352 MWh_t, 56% of process thermal energy

12. Solar Facility Contribution, annual:

    a. Receiver output: 244,000 MWh_t, 116% of process thermal demand
    b. Electrical energy: 47,900 MWh_e gross, 43,000 net to grid after 100% of plant electric demand during turbine operation
    c. Process energy: 105,600 MWh_t, 50% of process thermal demand

13. Solar Fraction:

    a. Design point: 60%
    b. Design day: 56%
    b. Annual: 50%

14. Annual Fossil Energy Saved: 139,500 bbl crude oil equivalent (5.8×10^6 Btu/bbl)

15. Type of Fuel Displaced: Heavy Crude Oil

16. Ratio of $\frac{\text{Annual Energy Produced}}{\text{Total mirror area}}$: 1.25 MWh_t/m^2

17. Ratio of $\frac{\text{Capital Cost}}{\text{Annual Fuel Displaced}}$: \$506/MWh_t

18. Site insolation (direct normal):

a.	Design point:	950 W/m^2
b.	Daily average:	6.21 kWh/m^2
c.	Annual average:	2.27 MWh/m^2
d.	Source:	TMY SOLMET Tape - Fresno, CA
e.	Site measurements:	Direct normal, total horizontal insolation measured on site from January 1980 to January 1981, continuously

19. Cogeneration Utilization Efficiency:

$$\frac{\text{Facility Net Electrical and Thermal Energy Production}}{\text{Facility Total Energy Input}}$$

$$= \frac{110{,}000\ MWh_t\ (Fossil) + 105{,}600\ MWh_t\ (Solar) + 43{,}000\ MWh_e\ (Solar)}{145{,}000\ MWh_t\ (Fossil) + 287{,}200\ MWh_t\ (Solar)}$$

$$= 0.60$$

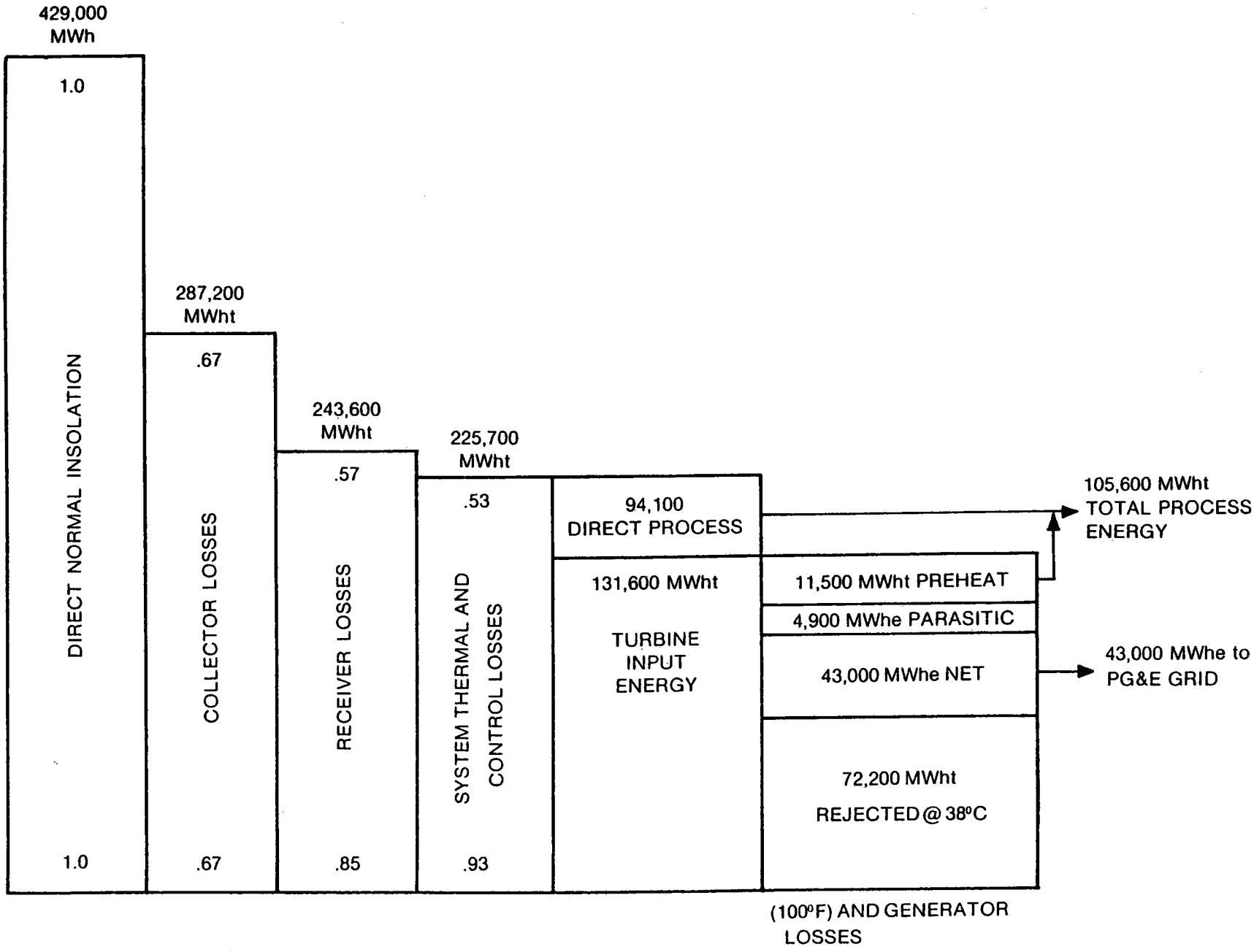

Figure 1.5-1

Solar Cogeneration Facility Annual Performance

Annual facility performance is depicted by the stairstep diagram in figure 1.5-1. Of the incident solar energy, 67% is reflected into the receiver aperture. Receiver losses account for another 10% of the incident energy, which results in annual solar thermal conversion efficiency of 57%. The nonsolar subsystems' account for another 4% loss due to thermal and control losses and turbine blanketing which leaves 53% (225,700 MWh_t) of the incident solar energy converted and delivered to the process and turbine as useful thermal energy. Of this 131,600 MWh_t is delivered to the turbine generator which converts this to 43,000 MWh_e of net electrical power delivered to the PG&E grid. Turbine extraction provides 11,400 MWh_t to the salt/process steam and fossil boilers for preheating and another 94,100 MWh_t is generated directly by the salt/process steam boiler for a total of 105,600 MWh_t delivered to the enhanced oil recovery process. The total net thermal energy, delivered to the turbine inlet and the TEOR process (including preheat energy from turbine extraction) is 237,100 MWh_t per year. This is equivalent to a saving of 139,500 bbl of oil per year or 3.63 million bbl over the projected 26 year lifetime of the Solar Cogeneration Facility.

1.6 ECONOMIC SUMMARY

The estimated capital cost to design, construct and startup the Solar Cogeneration Facility is $120 million. This estimate includes all direct capital costs, indirect costs such as contractors engineering and project management and a 25% construction contigency, which is appropriate for a project in the conceptual design stage. Figure 1.6-1 displays the consituents of the cost estimate according to major project subsystems, including all indirect costs and contingencies.

The economic analysis compared the levelized energy cost ($\overline{LEC}$) of the Solar Cogeneration Facility to the $\overline{LEC}$ of a conventional oil fired steam boiler facility delivering the same thermal energy to the enhanced oil recovery process. Results are shown in table 1.6-1 for the baseline economic assumptions of solar and conventional (refer to section 6 for details). The levelized cost of steam from the solar facility is calculated to be $51/$MWh_t$ compared to $35/$MWh_t$ for the conventional facility. The $\overline{LEC}$ of solar is quite sensitive to number of key parameters including capital, O&M and fixed charge rate. Conventional facility $\overline{LEC}$ is most sensitive to fuel escalation asumptions. These sensitivities are shown in figure 1.6-2 for the range of solar capital cost estimates and the range of fuel escalations studied. From Figure 1.6-2, equivalent solar-conventional $\overline{LEC}$ is shown to occur at a solar capital cost of $100 million, with 4% real fuel escalation assumed.

In addition to capital and O&M cost uncertainties which reflect the prototype stage of high temperature solar system development, there exist legislative uncertainties which can affect the tax credits, depreciation allowances, and electric revenues for solar cogeneration systems. These uncertainties combine to make solar system cost predictions much less accurate than conventional fossil fired systems.

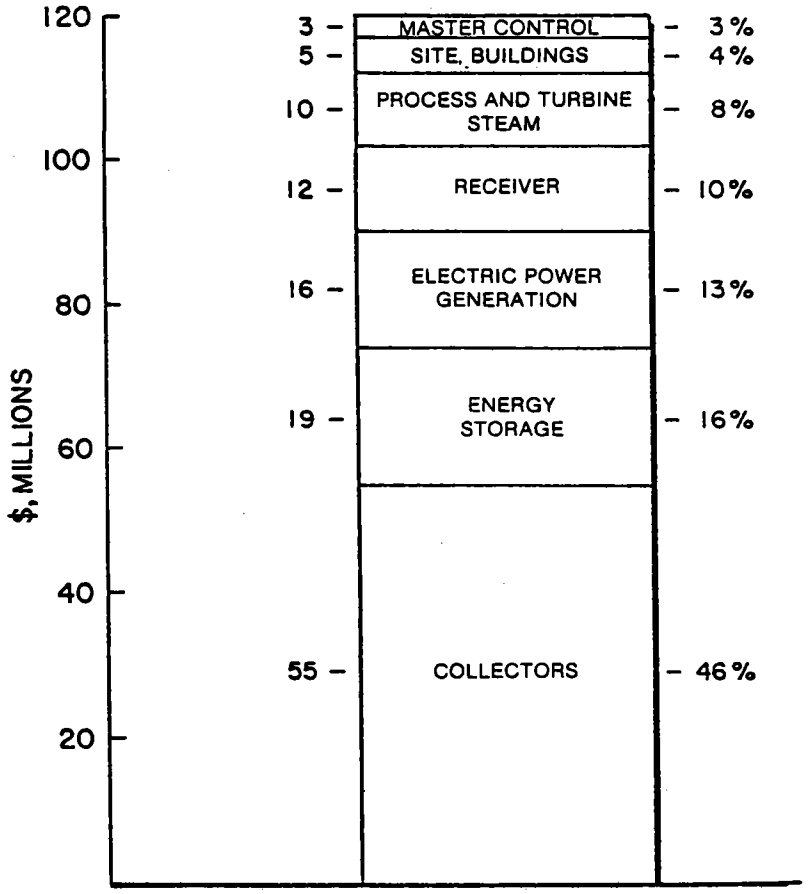

Figure 1.6-1 Cogeneration Facility Cost Estimate

Table 1.6-1

Baseline Economics, Solar vs. Conventional

Solar Cogeneration Facility	Conventional Oil Fired Steam Facility
$51/MWh$_t$ ($15/MBtu)	$35/MWh$_t$ ($10/MBtu)

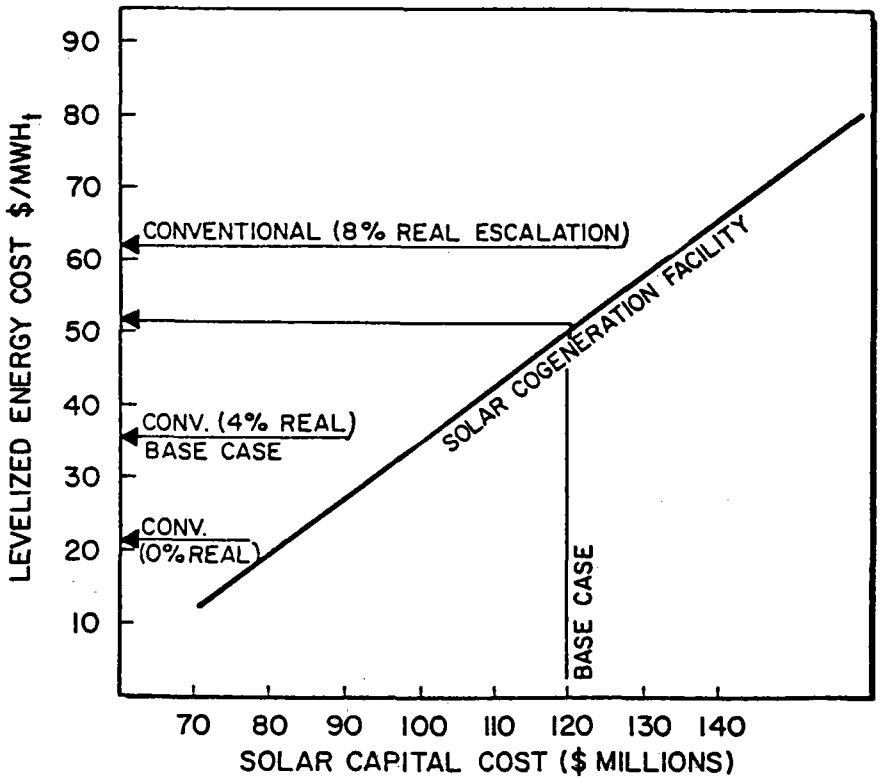

Figure 1.6-2

Solar Conventional $\overline{LEC}$

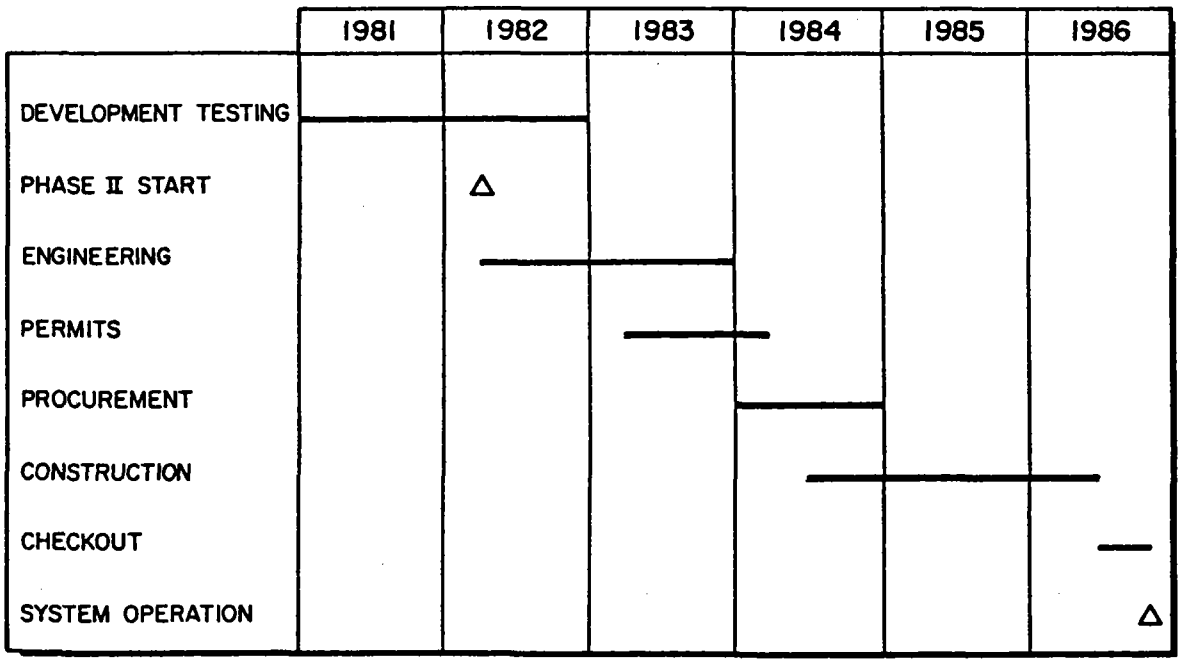

Figure 1.7-1

Cogeneration Development Schedule

1.7 DEVELOPMENT PLAN

The Solar Cogeneration Facility development plan is a logical sequence of project events beginning with development testing and concluding with facility startup in late 1986. The development plan is illustrated in figure 1.7-1. The development testing includes the steam drive pilot program, now underway at the Edison field, to determine the suitability of the field for the steam drive method of enhanced oil recovery. A second development test is the cold salt pump which has not yet been tested under cogeneration facility operating conditions.

DOE sponsored development testing of heliostats, receivers and complete central receiver systems such as the Barstow 10 MW_e Pilot Plant are either in progress or will start up by year end 1981. These related solar equipment tests will benefit the proposed cogeneration facility at Edison field. No other development testing is anticipated for this facility. The detailed engineering phase could commence in early 1982 followed by the securing of all required permits by late 1983. Procurement and contruction could begin in early 1984 and construction could be completed by mid 1986.

Following subsystem and system level checkout, the Solar Cogeneration Facility could be producing steam for enhanced oil recovery and electricity for the PG&E grid by December 1986.

As indicated below and in Section 7 of this report, Exxon does not intend to be involved in further development of this project beyond this contract.

1.8 SITE OWNER'S ASSESSMENT

Exxon will not pursue additional development of the Solar Cogeneration Facility at this time. The economic analysis conducted in this study shows the Solar Cogeneration Facility to be less attractive, for most cases studied, than the conventional oil-fired steam boiler. From an Exxon project viewpoint, the uncertainties surrounding the solar case are much larger than the uncertainty of the conventional case which is simply fuel cost escalation. Therefore, it is extremely risky to attempt to make a project decision in 1981 when the economic climate in 1986 may be considerably different and result in the solar project being even less economically attractive than it now appears. Major economic uncertainties affecting the Solar Cogeneration Facility at this time include the amount and certainty of revenues from the sale of electricity to PG&E (refer to Appendix D, Section A-18 for termination conditions), capital costs, solar tax credits and equipment depreciation allowances. Exxon does, however, endorse the results and conclusions of this conceptual design study of a Solar Cogeneration Facility at the Edison field. The design described in this report appears to be technically feasible, environmentally sound and provides an approach to meeting projected steam requirements at the Edison field without burning additional crude oil.

Although this design appears to be technically feasible, Exxon considers the demonstration of central receiver technology in an operational environment to be a necessary prelude to its widespread consideration and use in industrial process heat applications. Such demonstrations will provide important performance, economic and reliability data on central receiver systems and components. Systems demonstrations scheduled for near term operation in Barstow, Ca., and Almeria, Spain, coupled with DOE heliostat and receiver component development programs should provide valuable operational data.

Exxon has studied both the cogeneration approach and a simple solar process steam-only approach (Contract DE-AC03-79SF-10737) to provide steam for its enhanced oil recovery needs using solar central receiver technology. Within the accuracy of these conceptual design and cost studies, the solar steam-only approach appears to be more cost effective and less technically complex than the Solar Cogeneration Facility described in this report. This conclusion applies, of course, only to Exxon's enhanced oil recovery operations at the Edison field and the site specific solar designs which have been developed.

While Exxon has no other active TEOR sites in California, we have estimated as part of DOE Contract DE-AC03-79CS30307 that a solar potential of 3200 MW_t (10,900 MBtu/h) of installed steam capacity could exist in the Kern County area alone by the end of this century to help recover known heavy oil reserves. This potential presumes reasonable land costs. Further opportunities could exist in other heavy oil-producing areas including Texas and Venezuela. At the Edison field, the Solar Cogeneration Facility should satisfy the projected increased demand for steam, although such demand depends critically on geologic and economic factors which are under evaluation.

The conceptual design presents no severe or unusual safety or operational requirements and could be accommodated in the oil field production environment. The Solar Cogeneration Facility could result in a reduction of total ultimate atmospheric emissions, with the only negative impact being the loss of some 320 acres of irrigated cropland.

Two restrictions on energy use face Exxon at the Edison site -- restrictions imposed by the California Area Resources Board on emissions from fossil-fired steamers, and restrictions on use of oil imposed by the Fuel Use Act of 1978. Solar systems could assist in meeting both of these restrictions as an increased demand for heavy oil causes an increase in the use of TEOR in California.

2.0 INTRODUCTION

This report describes the conceptual design of a Solar Cogeneration Facility at Exxon's Edison oil field in California. This work was performed for the Department of Energy under contract DE-AC0380SF-11438, entitled "Designs for Solar Cogeneration." The contract was performed during the period 30 September, 1980 to 31, July, 1981 at a total cost of $419,856. Department of Energy project direction was provided by Sally Fisk, Larry Prince and Keith Rose. J.W. Smith of Sandia National Labs Livermore was the technical monitor. The Exxon Research and Engineering Company's prime contract was managed by George Yenetchi until 30 April, 1981, and by Patrick Joy to its conclusion. The Exxon mailing address is P.O. Box 592, Florham Park, N.J., 07932.

Other contributing organizations to this program were Martin Marietta Denver Aerospace under the management of Martin Brzeczek; Badger Energy, Inc. under the management of Carl Silverman, and Pacific Gas and Electric Company under the management of Harold Seielstad. Pacific Gas and Electric Company donated their services at no charge to the program.

2.1 STUDY OBJECTIVES AND BACKGROUND

2.1.1 Objectives

The objectives of the sponsoring DOE procurement for this project are to develop site specific conceptual designs which (1) make effective use of solar thermal energy from a solar central receiver system integrated into a cogeneration facility; (2) have the potential for construction and high reliability operation by 1986; (3) provide the best possible economics for the overall plant or facility application; (4) have the potential to achieve wide commercial success, and (5) offer the potential for significant savings in critical oil and gas fuels.

The specific objective of the DOE contract with Exxon is to develop a conceptual design for a solar powered cogeneration plant at Exxon's Edison oil field near Bakersfield, CA. Two categories of applications were defined in the DOE procurement: industrial process heat applications (Category A) and space conditioning, hot water applications (Category B). This contract is responsive to Category A.

2.1.2 Background

Two energy related factors have an important bearing on this study. The first is the potential for simultaneously conserving domestic crude oil and reducing combustion related pollutants in California by generating steam from solar energy for use in enhanced oil recovery.

The second factor is federal and state legislation aimed at discouraging the use of natural gas and oil in utilities and industries, and encouraging cogeneration and small power producers by requiring utilities to buy and sell electricity to cogenerators and small producers at just and reasonable rates. The combination of these factors with site specific factors such as climate and land suitability results in a background which compels the investigation of solar energy to produce both steam and electricity for use in enhanced oil recovery and electricity for sale to the local utility.

The United States in general and California in particular, contain large reserves of heavy crude oil that cannot be recovered by conventional primary recovery methods. The injection of steam to heat and pressurize oil bearing formations is a well established method of achieving economic production from existing reservoirs. The economic and performance potential of this method, known as thermal-enhanced oil recovery (TEOR) is limited in two ways. First, the steam generators used to recover the heavy crude oil consume a considerable amount of oil in the process. Typically, in TEOR, from .08 m^3 (.5bbl) to .16m^3 (1bbl) of oil is consumed in order to produce .48 m^3 (3bbl) of oil. Second, the California state air quality standards require costly methods of combustion gas cleanup which reduce the efficiency of the steam generating process. The use of solar energy to generate steam for thermal enhanced oil recovery (STEOR) would address both limitations by conserving the oil normally burned and preserving the quality of air in California.

Federal legislation, which forms a backdrop for this study, includes the bills comprising the National Energy Act of 1978 (PL93-617-through 621), the Fuel Use Act (FUA) (PL-95-020) and Public Utilities Regulatory Policy Act (PURPA) of 1978 (PL95-617).

The National energy Act of 1978 (PL 93-617 through 621) contains provisions designed to discourage the use of natural gas and petroleum in electric power plants and major fuel-burning installations, and encourage the substitution of coal and other alternate fuels as primary energy sources. Increased tax credits are provided for investment in equipment using renewable energy resources (such as solar energy).

The requirements of the Power Plant and Industrial Fuel Use Act P1-950-20 could impose a significant regulatory cost burden on organizations building installations in areas where environmental or other constraints would prevent the use of coal or other alternate fuels. The Solar Cogeneration Facility appears to provide advantages over other types of electric power plants or fuel burning installations since they are currently not classified as either electric power plants or major fuel burning installations and are therefore exempt from the requirements of the FUA according to the proposed rules for implementation published as of August 31, 1979.

The Public Utilities Regulatory Policy Act of 1978 PL 95-617, Section 210 requires that the Federal Energy Regulatory Commission (FERC) shall prescribe "such rules as it determines necessary to encourage cogeneration and small power production." These rules require electric utilities to offer to:

1) sell electric energy to qualifying cogeneration facilities and qualifying small power producing facilities and

2) purchase electric energy from such facilities.

These rules further require that the rates for sale and purchase be just and reasonable and not discriminate against the qualifying cogenerators and small power producers. The Act also specifies that for facilities which have capacities less than 30 megawatts, the FERC may prescribe rules under which these facilities are exempt from federal and state regulation, if such exemption is necessary to encourage cogeneration and small power production.

California state legislation has a bearing on the solar cogeneration study in two areas: first, the state income tax credits for solar and renewable energy equipment of 25% plus a three-year depreciation of the remaining 75% (AB-2036); and second, the state PUC regulations (formulated in response to PL 95-617), which mandate utilites to pay prices for cogenerated power and capacity based on the "avoided costs" or costs which the utility would actually incur if the utilty were to add additional generating capacity.

Exxon's utility partner in this cogeneration study is Pacific Gas and Electric Co. which serves a wide geographical area in northern California including the San Joaquin Valley.

PG&E has been actively involved in cogeneration for several decades. In the early 1940's, three oil-burning steam plants were built in the San Francisco Bay Area. The plants were designed to provide process steam to adjacent oil refineries and to provide 180 MW of electrical generation. These early cogeneration plants are still in operation today. PG&E has purchased surplus electricity from wood products industrial cogenerators since the 1950's. Today the PG&E system includes 433 MW_e of cogeneration capacity of which 264 MW_e is industry owned.

Table 2.1-1 is a representative listing of existing and planned PG&E industrial cogeneration projects. Figure 2.1-1 shows the location of existing and planned cogeneration facilities within the PG&E service area. Those in the northwest are typically wood product industries. Those in the Central Valley are biomass-fueled facilities. The greatest potential for cogeneration are the heavy oil fields in the southern portion of the service area.

Cogeneration is a preferred electrical generation technology. PG&E has in place the following program elements that are targeted to promote the maximum implementation of cogeneration by its industrial customers: An informational announcement has been mailed to over 12,000 industries in the service area. A consultant has completed a study to identify the service area cogeneration potential through 1990. PG&E has an internally organized cogeneration review committee and an oil field recovery cogeneration task force. Other program elements include: funding of several cogeneration feasibility studies, environmental and regulatory assistance to potential cogenerators, and an incentive gas rate for cogenerators (if approved by the California Public Utilities Commission).

Table 2.1-1

PG&E Cogeneration Projects

Project Name & Location	Project Description	Size MWe	Date of Operation
Georgia-Pacific Corporation Ft. Bragg. CA	Wood Waste-Fueled	10	Operating
Optimum Energy Development Kern River Oil Field	TEOR	66	1980-1984
Dow Chemical Pittsburg, CA	Gas Turbine	35	1965
Louisiana-Pacific Corporation Samoa, CA	Wood Waste-Fueled	7	Operating
California Power and Light Madera, CA	Biomass-Fueled	50	1982
PG&E Gerber, CA	Gas Turbine/Compressor	3.7	1981
Diamond/Sunsweet Incorporated Stockton, CA	Walnut Shell-Fueled	4.5	Dec. 1980
Imotek, Incorporated Sacramento, CA	Biomass-Fueled	7.5	1982
Texaco, Incorporated San Ardo, CA	Coal Gasification TEOR	210	DOE Funding for Studies Requested

In late 1979, the California PUC authorized PG&E to pay prices for cogenerated power and capacity that are based on the avoided costs of energy. Avoided costs are variable. They are dependent on demand and the generation mix required to meet that demand. For pricing purposes. the year is separated into two seasonal periods. A five month summer period (Period A) and a seven month winter period (Period B). Within each seasonal period are three periods reflecting electrical demand conditions; on-peak, partial-peak, and off-peak. Table 2.1-2 defines the pricing periods for Period A and Table 2.1-3 defines the pricing periods for Period B.

The following energy prices are in effect for the winter period February 1 to April 30 1981:

on-peak	65.80 mills/Kwh
partial peak	62.19 mills/Kwh
off-peak	55.53 mills/Kwh

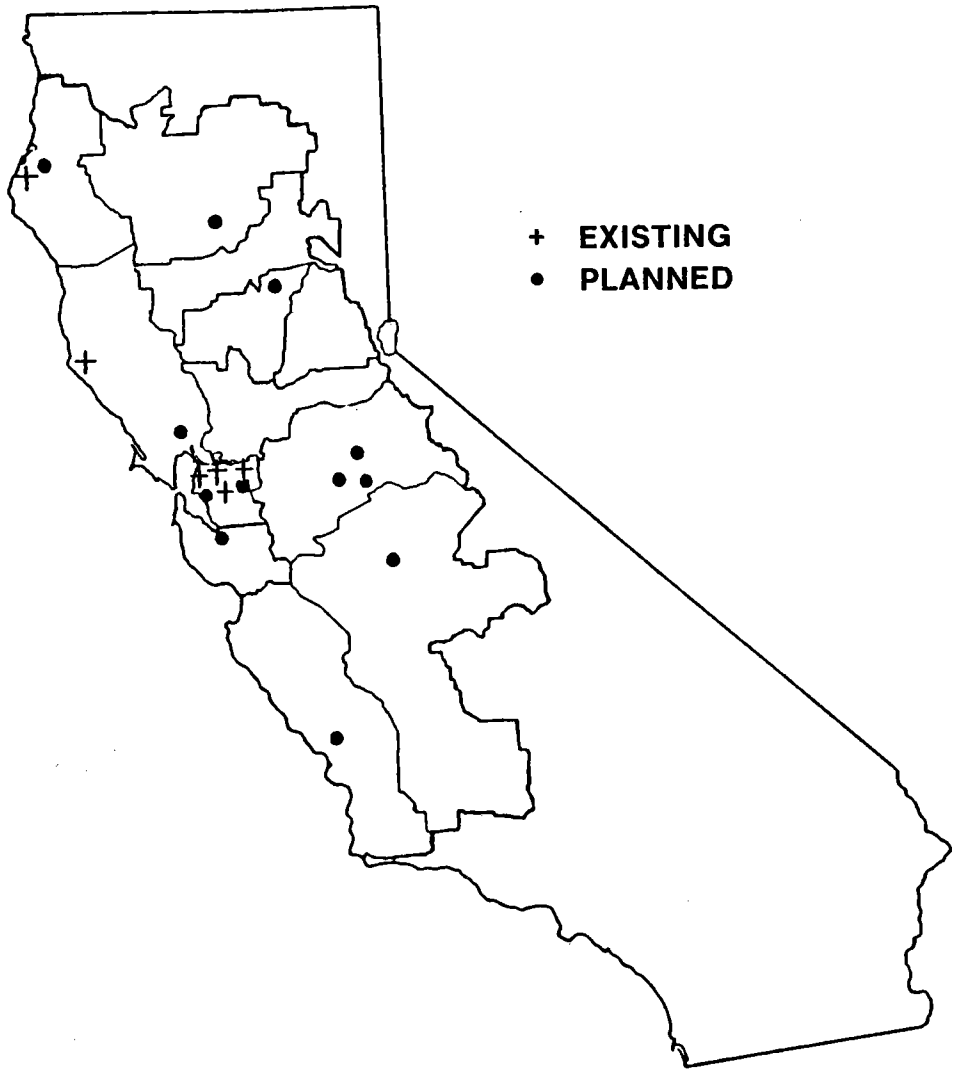

Figure 2.1-1

PG&E Cogeneration Project Locations

PG&E's energy prices are adjusted quarterly to reflect changes in the cost of incremental fuel oil.

The availability of new cogeneration capacity will permit PG&E to defer construction of new generation facilities. Accordingly there is a savings to PG&E. The savings can be calculated using PG&E's standard economic and financial assumptions for: new coventional unit costs, cost escalations, carrying charges, and cost of capital. This savings can be passed on to the cogenerators in the form of capacity payments if minimum requirements are met. These requirements and options for the manner in which capacity payments may be made are discussed in Appendix C.

The proposed solar cogeneration facility, if available in 1986 with an expected 26 year life, would be entitled to a non-escalating capacity payment of $100/kw-yr.

TABLE 2.1-2

COGENERATION PRICING TIME PERIODS — Period A: May 1 to September 30.

Cogeneration Pricing Time Periods	Monday through Friday*	Saturdays*	Sundays and Holidays
On-peak	12:30 P.M to 6:30 P.M.		
Partial-peak	8:30 A.M. to 12:30 P.M. 6:30 P.M. to 10:30 P.M.	8:30 A.M. to 10:30 P.M.	
Off-peak	10:30 P.M. to 8:30 A.M.	10:30 P.M. to 8:30 A.M.	12:00 A.M. to 12:00 A.M.

TABLE 2.1-3

COGENERATION PRICING TIME PERIODS — Period B October 1 to April 30

Cogeneration Pricing Time Periods	Monday through Friday*	Saturdays*	Sundays and Holidays
On-peak	4:30 P.M. to 8:30 P.M.		
Partial-peak	8:30 P.M. to 10:30 P.M. 8:30 A.M. to 4:30 P.M.	8:30 A.M. to 10:30 P.M.	
Off-peak	10:30 P.M. to 8:30 A.M.	10:30 P.M. to 8:30 A.M.	12:00 A.M. to 12:00 A.M.

*Except the following holidays: New Year's Day, Washington's Birthday, Memorial Day, Independence Day, Labor Day, Veteran's Day, Thanksgiving, and Christmas.

2.2 TECHNICAL APPROACH

A number of important criteria were accounted for in developing the conceptual design of the solar cogeneration faciity at the Edison field. First among these was the existing TEOR process and its particular steam conditions (pressure, temperature and flow rates). The existing TEOR process at Edison also imposes physical constraints (land area and well clearances); the characteristics of the existing fossil boilers and the current and future TEOR operations also were among the input criteria for the conceptual design.

The legal limit on electrical generating capacity for cogenerators or small power producers in California (30 MW_e) and the favorable rate structure for small power producers mandated by the California PUC are two important regulatory criteria which strongly impact the cogeneration design.

The DOE program requirements for this study specified the use of central receiver solar technology and on-site production of thermal energy for the industrial process (TEOR) and on-site production of electricity for both process needs and revenue generation. Central receiver technology is well suited to the TEOR requirements at Edison, as a previous Exxon conceptual design study has

shown (contract DE-AC03-79SF10737). Central receiver technology is capable of efficiently producing temperatures in the range of 600°C (1100°F) which results in high thermodynamic efficiency for the steam turbine which drives the electric generator. Another important technology criteria was the use of energy storage to decouple the intermittent supply of the solar energy from the constant demand for process steam and the daily peaking demand for electricity which somewhat lags the insolation resource.

The use of energy storage permits a uniform flow of steam to the TEOR process which matches the current practice and allows the turbine-generator to operate efficiently and on a schedule which maximizes electric power revenues.

A final technology criteria was the use of a master controller to coordinate, optimize, and synchronize the operation of the solar and storage subsystem with the process steam and electric power generation subsystems.

2.3 SITE LOCATION

Exxon's Edison field is located in parts of sections 13, 14, 15, 18, 19, 22, 23, and 24 of Kern County, California. The field is located on the east side of the San Joaquin Valley 11 km (7 mi) southeast of Bakersfield. Principal access is by California Highways 58 and 99 (Fig. 2.3-1).

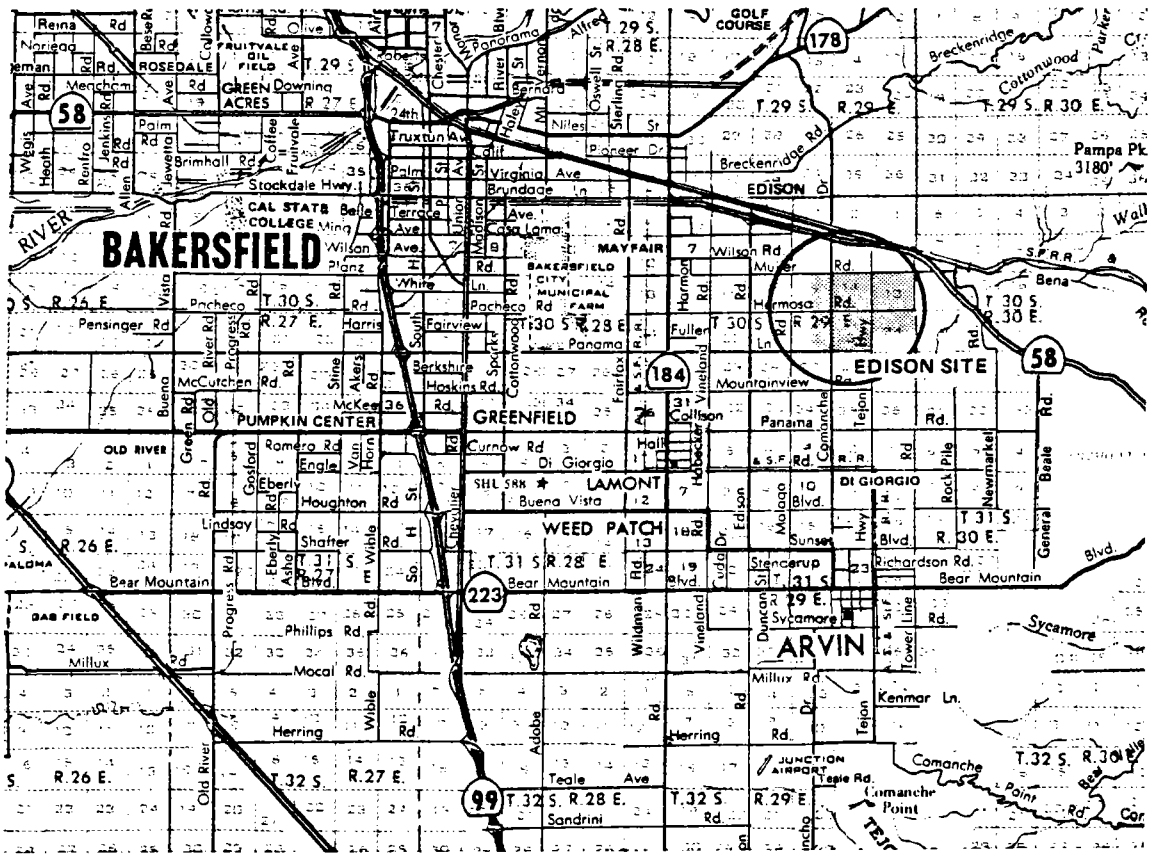

Figure 2.3-1 Bakersfield Area Map

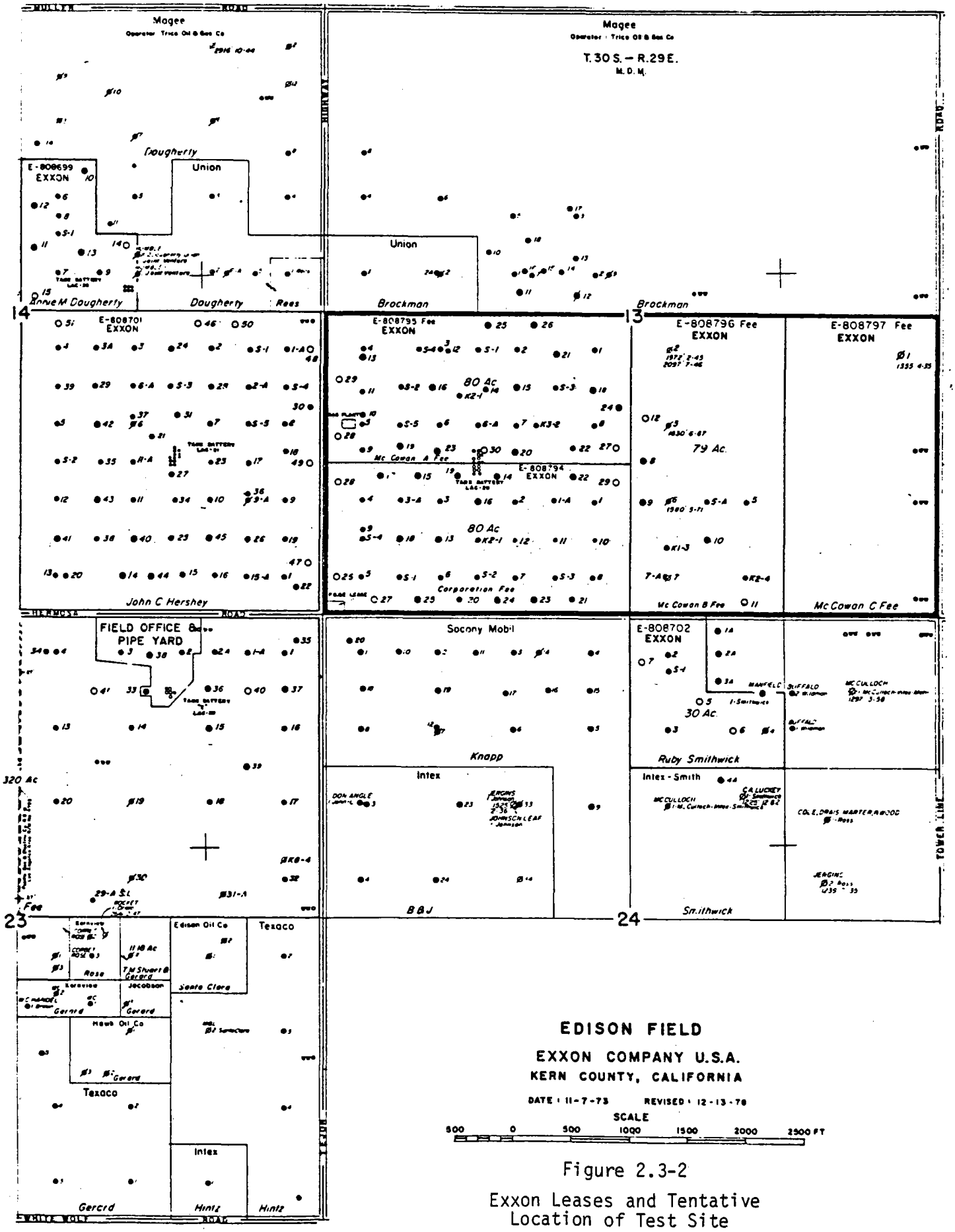

EDISON FIELD

EXXON COMPANY U.S.A.

KERN COUNTY, CALIFORNIA

DATE : 11-7-73 REVISED : 12-13-78

SCALE

500 0 500 1000 1500 2000 2500 FT

Figure 2.3-2

Exxon Leases and Tentative Location of Test Site

Figure 2.3-2 is a plot plan showing the Exxon leases at Edison and the location of the Solar Cogeneration Facility site. The site extends due east of Tejon Highway and north of Hermosa Road and includes Exxon leases, 808794, 808795, 808796 and 808797 it is approximately 0.3 km (1/2 mi) from the Exxon field office on Hermosa Road. The site area is approximately 1,311,000 m^2 (320 acres) and encompassses 74 operating wells. Access to the wells is from the west off Tejon Highway.

2.4 SITE GEOGRAPHY

At the proposed cogeneration site, both the surface and mineral rights are owned by Exxon. There are few zoning and no other use restrictions on this and surrounding land. It is 8 km (5 mi) to the outskirts of Bakersfield and no extensive residential or commercial activities are anticipated during the period while oil is being produced. Present-day residential and commercial activities in the Bakersfield area are expanding to the southwest of the city away from the intensive oil-producing activities in Kern County. Access to the site is by publicly owned roads adjacent to the site.

It is not anticipated that any structures sufficiently large enough to interfere with solar operations would ever be considered in the area. The closest lease to the south of the site is owned by Mobil and is in active oil production.

Figures 2.4-1 and 2.4-2 are photographs from a central point in the site showing the surface features as viewed to the southeast and southwest, respectively.

Kern County Airport is located approximately 32 km (20 mi) to the northwest of the site, which is outside the airport control zone.

Several structures already exist at the field. The principal building is the Exxon field office located on Hermosa Road. This building has available 65 m^2 (700 ft^2) of office space, 28 m^2 (300 ft^2) of locker and shower facilities and a small shop.

Shipments to the Edison field area can be made by truck, plane or railroad. The weight limitation on California Routes 58 and 99 and on local roads is 100 tons. Items measuring 3.7 by 30.5 m (12 by 100 ft) or larger can be shipped by truck but must be escorted. Heavy and bulky equipment is usally shiped by rail (Southern Pacific Railroad) to the freight depot at Edison, which is 8 km (5 mi) northwest of the field. There are no overpasses on the roads between the depot and the field.

The Edison site is a flat, alluvial plain ranging in elevation from about 0.21 km (700 ft) in the northeast to 0.15 km (500 ft) in the southwest. The area is free of standing water and is not subject to flooding. After heavy rains of one to two days' duration, it is sometimes necessary to wait one to five days before heavy equipment can be moved on the field.

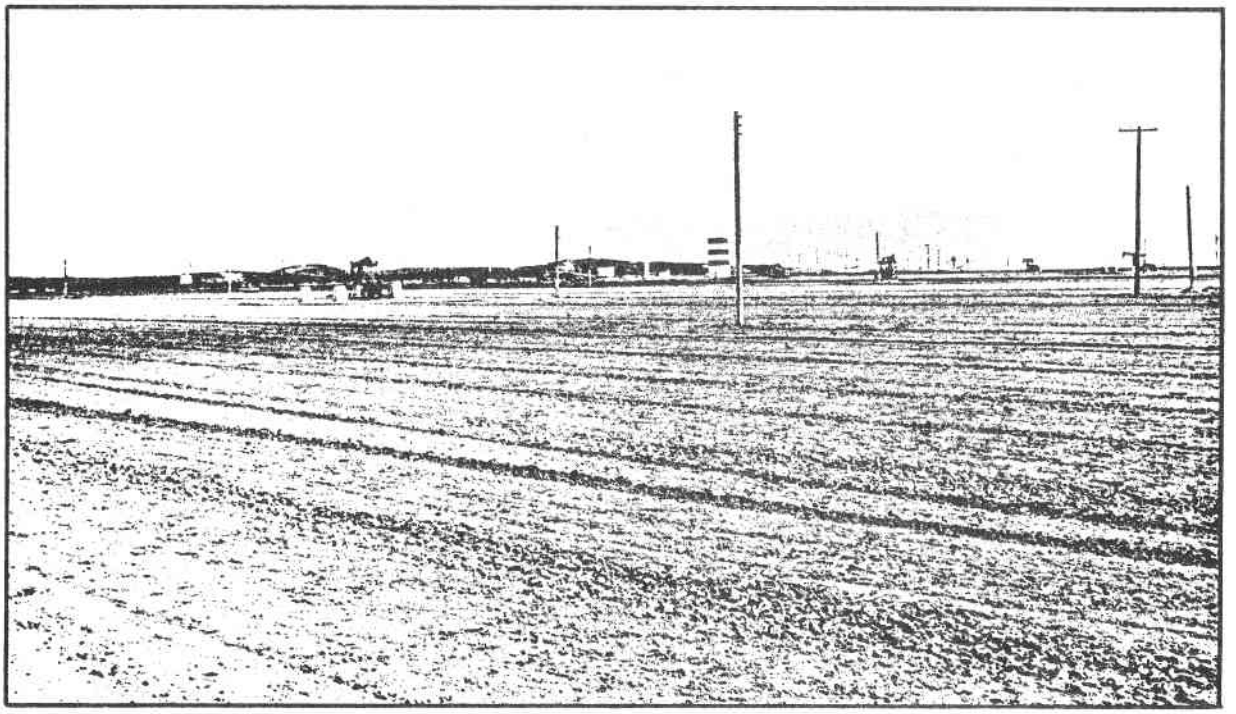

Figure 2.4-1

Cogeneration Site - Southeast View

Figure 2.4-2

Cogeneration Site - Southwest View

Bakersfield is considered a high earthquake risk area. It is classified Zone 4 in the Uniform Building Code and structures must be designed to appropriate specifications. The last major quake was in 1952 and measured 7.5 to 7.7 on the Richter scale. The Uniform Building Code puts the soil to the Edison field in Class 4 (SC), sand and clay.

The producing zones in the Edison field main area include the Kern River -- Chanac, Santa Margarita, Wicker, Nozu, Freeman-Jewett, Walker and Schist. The Kern River and Schist are the two most prolific. The Kern River is the shallowest producing zone and ranks first in productivity. Over the approximately 4.05 x 10^6 m^2 (1,000 acres) on Exxon property, depth averages about 0.34 km (1,000 ft.) below sea level. Net sand thickness varies from 9 to 61 m (30 to 200 ft.) in a gross interval. The nearly "dead" oil is produced by solution gas drive with limited water drive likely. Reservoir and oil characteristics for the Kern River formation are given in Table 2.4-1.

Table 2.4-1 Summary of Reservoir Data

	Kern River Sand Edison Field
Depth to formation top, m (ft.)	335 (1,100)
Oil gravity, °API	16-19
Current reservoir pressure, MPa (psig)	1.03 (150.0)
Average net sand thickness, m (ft.)	24 (80.0)
Reservoir temperature, °C (°F)	35 (95)
Oil viscosity at reservoir temperature, Pa-s (cp)	0.310 (310.0)
Average permeability to air, millidarcy	1,500
Average porosity, %	27
Average oil content, bbl/acre foot	1,150
Average oil saturation, % partial volume	55
Formation dip, rad (deg)	0.14-0.17 (3-10)
Pattern Size, m^2 (acres)	10,000-20,000 (2.5-5.0)

The Schist is the deepest producing zone and ranks second in productivity. Over the approximately 2.8 x 10^6 m^2 (700 acres) on Exxon property, depth varies from 9 m (30 ft.) to over 610 m (2,000 ft.) below sea level. The primary production mechanism is water influx, although solution gas drive and gravity drainage have been important in the past.

The water supply for steam generation is provided from an Exxon-owned and operated well. This well draws water from a depth of 300 m (1,000 ft.) at a rate of 9.5×10^{-3} m^3/s (150 gpm). Water is distributed to the stimulation side by portable lines. Water is treated in portable units containing ion exchange beds. Table 2.4-2 contains water quality information before and after treatment. No problems are anticipated with the quantity of incremental water required for the solar-derived steam.

Table 2.4-2 Water Quality Data - Impurities in ppm

Impurities	As produced from Well	After Treatment
Calcium	54.4	<0.5
Magnesium	12.6	<0.5
Sodium	50.6	210.0
Bicarbonates	298.9	0
Chlorides	36.1	326.0
Sulphates	2.2	0
Nitrates	0.44	0
Total Hardness as $CaCo_3$	187.66	0.5

Produced water is separated from oil in the separator tanks distributed throughout the field and indicated in Figure 2.3-2. This water, along with the waste water from the water treating plants, is reinjected into the Schist zone through wells on the Young Fee. The reinjected water currently averages 684 m^3/day (4,300 bbl/day).

Other wastes are handled as follows. Sanitary water is treated in the privately maintained septic system. Solid wastes, i.e., sludge from the gas scrubbing and oily waste, are trucked to a landfill operated by the town of Bakersfield.

Electric power produced by Pacific Gas and Electric services the field. An existing substation shown in Figure 2.3-2 at the southwest corner of Section 13 is rated for 1,900 kW. Currently, the maximum load is 500 kW. Electric power is brought to the site by an overhead cable on utility poles along Hermosa Road.

2.5 CLIMATE

The overall climate at Bakersfield is warm and semiarid. Average temperature is 18°C (65°F) and varies from 9°C (48°F) in winter to 29°C (84°F) in summer. Annual precipitation averages 15 cm (5.8 in.). Snow is rare and no accumulations of greater than 4 cm (1.5 in.) have been recorded. Southeasterly winds, originating in the Tehachapi Mountains can, at times, reach velocities of 26.82 mps (60 mph). The most recent severe wind storm occurred in December 1977, with gusts to 33.53 mps (75 mph). A complete summary of the local climatic conditions is given in Appendix B.

Annual average direct normal insolation based on Fresno long-term insolation data is 6.21 Kwh/m^2/day. Exxon measurements made at Edison during 1980 show similar insolation levels between Fresno and Edison field. Local factors which may impact insolation include the intensive agricultural operations in the San Joaquin Valley and winter fogs that can be trapped in the area bound by the coast ranges to the west, the Tehachapi Mountains to the south and the Sierra Nevadas to the northeast.

2.6 EXISTING PLANT DESCRIPTION

The existing process at Exxon's field is thermally enhanced oil recovery (TEOR) in which steam is injected into the oil bearing reservoir to increase the temperature and pressure of the reservoir to effect the flow and recovery of heavy crude oil. Steam is produced by portable steam generators which burn crude oil and some diesel fuel to produce steam for the TEOR process and electricity to power the boiler. TEOR operations began in 1965 and were expanded in 1979. The projected Solar Cogeneration Facility would supply steam to the TEOR process and electricity to power the planned solar facility, and electricity to sell to Pacific Gas and Electric.

2.7. EXISTING PLANT PERFORMANCE

Steam stimulation is the current method of TEOR at the Edison field. This method involves the following steps (Figure 2.7-1):

1) Saturated steam at 260 to 288°C (500 to 550°F) and 75 to 80% quality is injected into a well for 5 to 7 days. The steam flow rate is about 3.2 x 10^{-3} m^3/s (50 gpm) of water equivalent;

2) The well is closed and "steam-soaked" for about 4 days. The injected steam permeates and heats the oil/rock/sand formation and reduces the viscosity of the oil.

3) The well is opened and oil is pumped out for about the next 50 to 70 weeks, after which the steam soak process is repeated.

Currently two crude oil-fueled boilers (one put into operation in 1965, the other in 1979) are being used at Edison. Their characteristics are listed in Table 2.7-1. For each well stimulation, a boiler, portable Thermiotics water treating plant, and portable water, boiler fuel, and diesel fuel tanks (Figure 2.7-2) are moved to the well site.

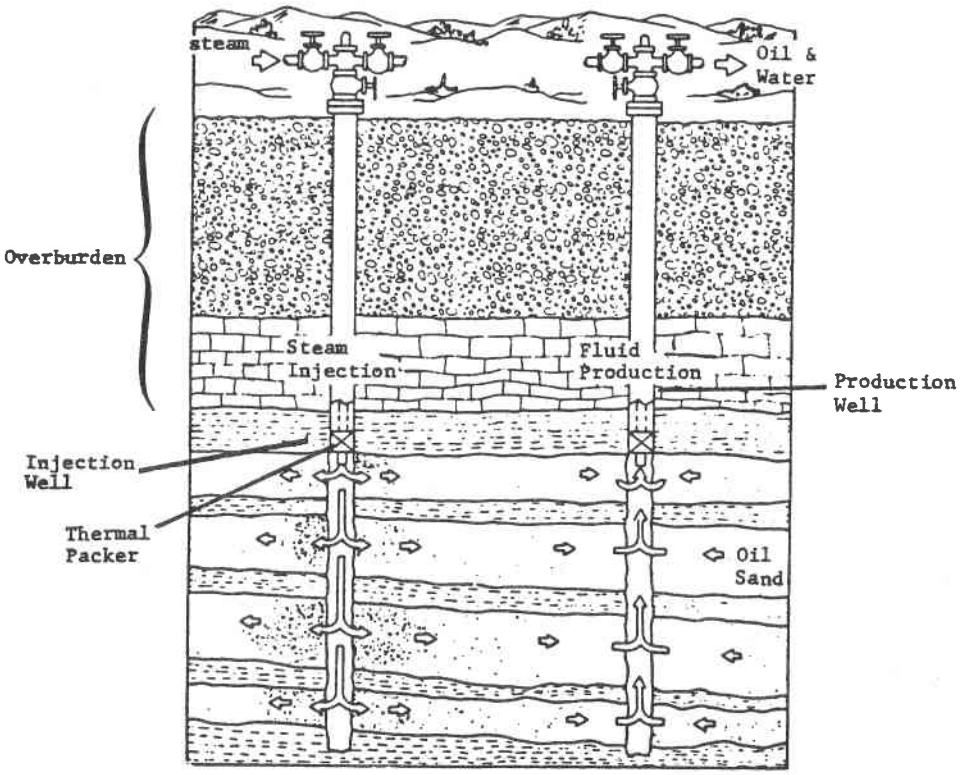

Figure 2.7-1
Steam Stimulation - TEOR

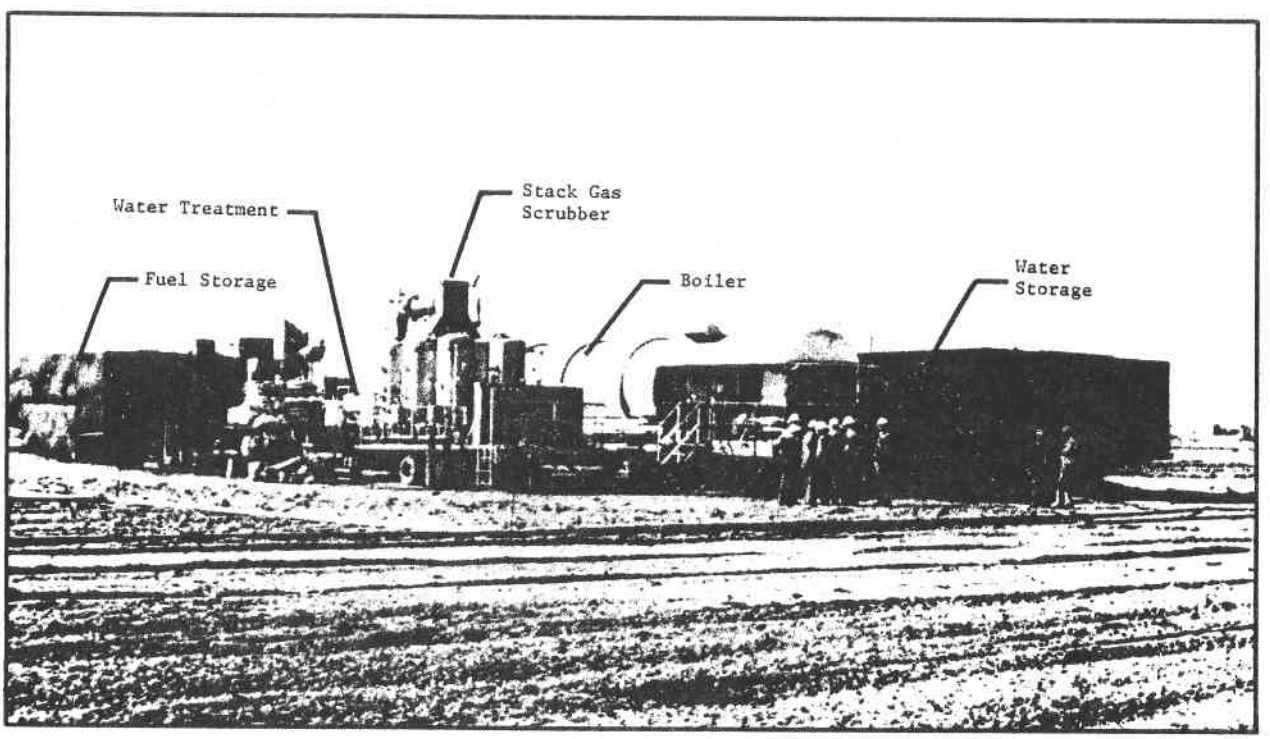

Figure 2.7-2
Existing Oil-Fired Steamer at Edison

In a typical operation, 1,590 m^3 (10,000 bbl) of water will be converted to steam and injected into the well (plus an additional 9 to 10% for the scrubber). To accomplish this, about 115 m^3 (724 bbl) of crude oil will be burned (about 106 m^3 of oil would be required if no scrubber were used).

The portable steamers currently in use at Edison are in service on an average 80% of the time. The remaining 20% is divided between 3% for maintenance and 15% for moving and reinstallation. Unscheduled downtime occurs rarely when an automatic overpressure or overtemperature sensor shuts down the steamer. In these cases the shutdown is discovered and the steamer restarted within a few hours.

Table 2.7-1 Steam Generator Design Data for Struthers Thermoflood® 25 Steamer

Design Steam Pressure	10.343 MPa (1,500 psig)
Design Steam Quality	80%
Design Steam Flow to Well	11,564.6 kg/h (25,500 lb./h)
Design Steam Flow to Oil Burner	72.56 kg/h (160 lb./h)
Condensate to Drain	18.14 kg/h (40 lb./h)
Design Steam Flow to Heater Outlet	11,655.3 kg/h (25,700 lb./h)
Heat to Well (Above 80°F Feed Temperature)	7.27 MW (24,797,808 Btu/h)
Heat to Produce Atomizing Steam	59.09 kW (201,600 Btu/h)
Heat to Preheat Fuel Oil (Recirculate)	37.44 kW (127,750 Btu/h)
Design Total Heat Output of Heater	7.91 MW (26,999,408 Btu/h)
Thermal Efficiency of Heater	89.99% (LHV Basis)
Thermal Efficiency of Process	89.12% (LHV Basis)
Burner Type	North American 5131-Fa
Burner Heat Release	8.14 MW (27,777,778 Btu/h)
Fuel	Crude Oil
Fuel Net Heating Value	10907 KWhr/m^3 (141,000 Btu/gal.)
Fuel Consumption	0.746 m^3/h (197 gal./h)
Pilot Fuel	Natural Gas or LPG
Combustion Air 11,900.2 kg/h (26,240 lb./h)	Flue Gas 12,598.6 kg/h (27,180 lb./h)
Flue Gas Temperature	190.6°C (375°F) at 20% Excess Air

2.8 PROJECT ORGANIZATION

This conceptual design study was executed by an industrial/utility team consisting of Exxon Research and Engineering Company, Martin Marietta Denver Aerospace, Badger Energy, Inc. and Pacific Gas and Electric Company. The organization and functional responsibilities are illustrated in Figure 2.8-1.

As prime contractor, Exxon provided overall program management and technical coordination and served as primary contact with DOE and its technical advisers. In addition, Exxon provided systems integration, system performance and economic analysis and electric power generation system design; and as owner/operator of the Edison field, provided process and site data for the enhanced oil recovery process at the Edison field on which this conceptual design study is based.

Martin Marietta Denver Aerospace was responsible for design, performance and cost data for the solar subsystem including collectors and receiver, and the master controller.

Badger Energy, Inc. provided design, performance and cost data for the energy storage and steam subsystems.

Pacific Gas and Electric Company provided data on the current rate structure for small power producers in their service area, and data on interfacing the cogeneration facility with the PG&E grid.

2.9 FINAL REPORT ORGANIZATION

This report is organized into two volumes. Volume I is the main technical report and Volume II contains all appendices. Volume I consists of an executive summary in Section 1 which presents a concise overview of the cogeneration design and important technical and economic conclusions. Section 2 is an introduction to the report and Sections 3, 4 and 5 describe the system selection process, the final conceptual design of the facility and technical details of each subsystem. The economic methods and conclusions are presented in Section 6 and the development plan is presented in Section 7.

Volume II, Appendices, contains the systems specification as Appendix A. Appendix B contains Bakersfield climatogical data and the Edison Field insolation data for 1980. PG&E's draft agreement and interconnect requirements are in Appendix C and collector operating and safety procedures are contained in Appendix D.

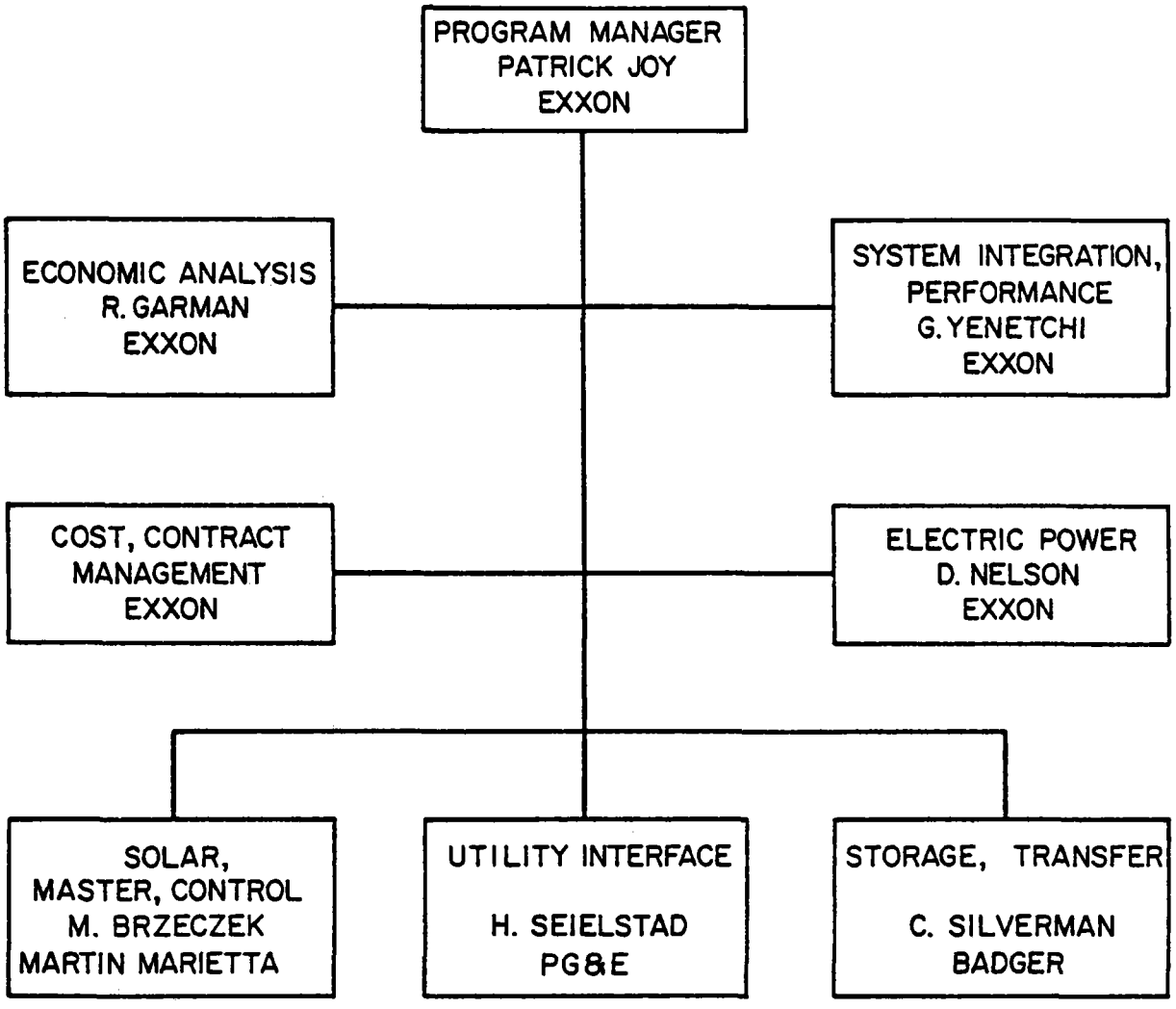

Figure 2.8-1

Cogeneration Program Organization

3.0 SELECTION OF PREFERRED SYSTEM

3.1 INTRODUCTION

In this chapter the process of selecting the final cogeneration system configuration is described and the various system level and subsystem level tradeoff studies are presented.

A number of technical and economic considerations entered into the system selection process. The selection process was essentially a three step process including: 1) identification of fixed system parameters; 2) determination of overall system energy flow configuration; 3) initial system sizing, subsystem selection and optimization and final system sizing.

The fixed system parameters are summarized in this section. Section 3.2 presents the system configuration study and 3.3 discusses the technology options. The system sizing study is explained in Section 3.4 and the subsystem trade studies are summarized in Sections 3.5, 3.6 and 3.7.

The first step in the system selection process is the identification of the system parameters which are considered to be fixed inputs to the design. These inputs are summarized in Table 3.1-1. The requirements of this DOE contract include the design of a facility to generate both thermal and electrical/mechanical energy for the users' process. In this case, Exxon's process is enhanced oil recovery which requires primarily steam with small amounts of electricity. The contract requires a facility design, in this case, which provides thermal energy to the EOR process and also produces electrical energy equal to greater than 10% of the thermal energy produced. This requirement sets the minimum electrical to thermal energy ratio and when coupled with the process thermal energy requirement, determines minimum electrical energy levels from the cogeneration facility. Other DOE contract program specified parameters include central receiver solar technology with a baseline heliostat design being the second generation heliostats currently under development, a facility startup date of 1986 and initial heliostat costs of $\$260/m^2$.

The governmental regulations which impact the facility design are the federal and state regulations governing renewable energy, equipment and cogeneration which are identified in Section 2 of this report.

A key input to the design process is the Pacific Gas and Electric Company's rate structure for cogenerators in their service area which was formulated in response to federal and state requirements. PG&E is required to purchase electricity from cogenerators and small power producers at prices wich reflect the "avoided energy costs" or those costs which the utility would incur if it were to construct new generating capacity or purchase additional power from conventional fuels, such as oil. (PG&E is also required to sell electricity to the same producers at fair rates.) Thus, PG&E will make purchases, from qualifying producers, of either energy alone or both energy and capacity.

Table 3.1-1

Cogeneration Fixed Design Parameters

Source	Parameters
DOE Specified Program Requirements	o Cogeneration - Thermal and Electrical/Mechanical - Electrical > 10% of Thermal o Central Receiver Solar Technology o 1986 Facility Start-Up o Initial Heliostat Direct Cost of $260/m^2$
Federal, State, Legislative	o FERC Regulations, re: Cogeneration, Small Power Producers o California PUC Rulings o PG&E Cogeneration Policies, Rate Structure
Exxon Site and Process	o EOR process steam demand - 293°C (560°F), 7.8 MPa (1130 psia), 26 MW_t continuous o Edison field land availability and access requirements o Edison field insolation, weather parameters

The projected revenues from the sale of electricity from the cogeneration facility were an important determinant in the system sizing study which is presented in Section 3.4.

Another fixed input to the design is the definition of cogenerator or small power producer. According to the FERC regulations mandated by PURPA (PL 95-617), all cogenerators and small power producers under 30 megawatts capacity are exempt from state and federal regulations pertaining to utilities. This 30 MW_e capacity places an upper limit on the size of the electric power subsystem.

The final fixed inputs to the system selection process are the site and process specific parameters. These include the process steam demand, the Edison field land area and access requirements and site specific environmental data such as direct normal insolation and windspeed. Future plans for the Edison field call for steaming the most productive section of the field at a rate of 954 m^3/day (6,000 bbl water per day) of steam into 12 to 14 injection wells at a time over a period of 26 years. This rate is equivalent to the output of four fossil fired boilers rated at 7.33 MW_t (25 MBtu/hr) capacity. Two steamers are currently in operation. Thus, the planned requirements for process steam for EOR at the Edison site called for the production of steam equivalent to two 7.33 MW_t fossil fuel boilers operating at full capacity.

Other site specific requirements include the available land on which Exxon owns both surface and mineral rights, the access requirements for the wells and the Edison field insolation and weather parameters.

3.2 SYSTEM CONFIGURATION

3.2.1 Series Vs. Parallel Energy Flow

Two basic system configurations which were examined in this study are series and parallel energy flows. The series flow configuration is possible because the solar receiver can deliver thermal energy at 566°C (1,050°F) and the EOR thermal process requires steam at 293°C (560°F). A steam turbine could operate between these two points making the series configuration a turbine topping-process bottoming cycle. However, the feedwater purity requirement for the turbine (about 50 ppb total dissolved solids) is much more stringent than the purity required for the process steam boiler. This necessitates the use of a heat exchanger to separate the turbine steam from the process steam. An energy flow diagram depicting this series flow configuration is shown in Figure 3.2-1. This system configuration can only produce a small amount of electricity (55 KW_e), which is less than the electrical demand of the solar cogeneration system and less than the 10% of the thermal process requirement which is a program requirement for this study.

The combination of process temperature requirement plus a separate turbine flow loop results in a very small enthalpy drop available to the turbine and thus, very low electric power generation. For this reason the series flow configuration was not pursued. A number of parallel energy flow configurations were examined in which the turbine and the process steam generator operate in parallel using separate heat transfer loops to produce steam from circulating molten salt. The analysis of alternative parallel configurations is presented in Section 3.4.

A key component in these flow configurations is the use of energy storage. Several important process and economic factors dictated the inclusion of energy storage in the design. These include:

1) The existing EOR process produces a uniform flow of steam to the injection wells. Although the reservoir can tolerate a certain range of steam flow rates, the use of energy storage allows the solar generated steam flow to be uniform, thus matching the existing process and introducing no potential reservoir problems such as sanding or channeling.

2) A turbine is required to generate electricity and it is essential that the steam flow to the turbine be extremely uniform, which permits high turbine efficiency.

3) All heat exchangers in the cogeneration plant would have to be sized for the peak instantaneous heat transfer rate in the absence of any energy storage. This peak rate would be about four times as high without storage, thus requiring all heat exchange equipment to be about four times larger in order to maintain the required heat transfer temperature differences. This would result in a severe economic penalty.

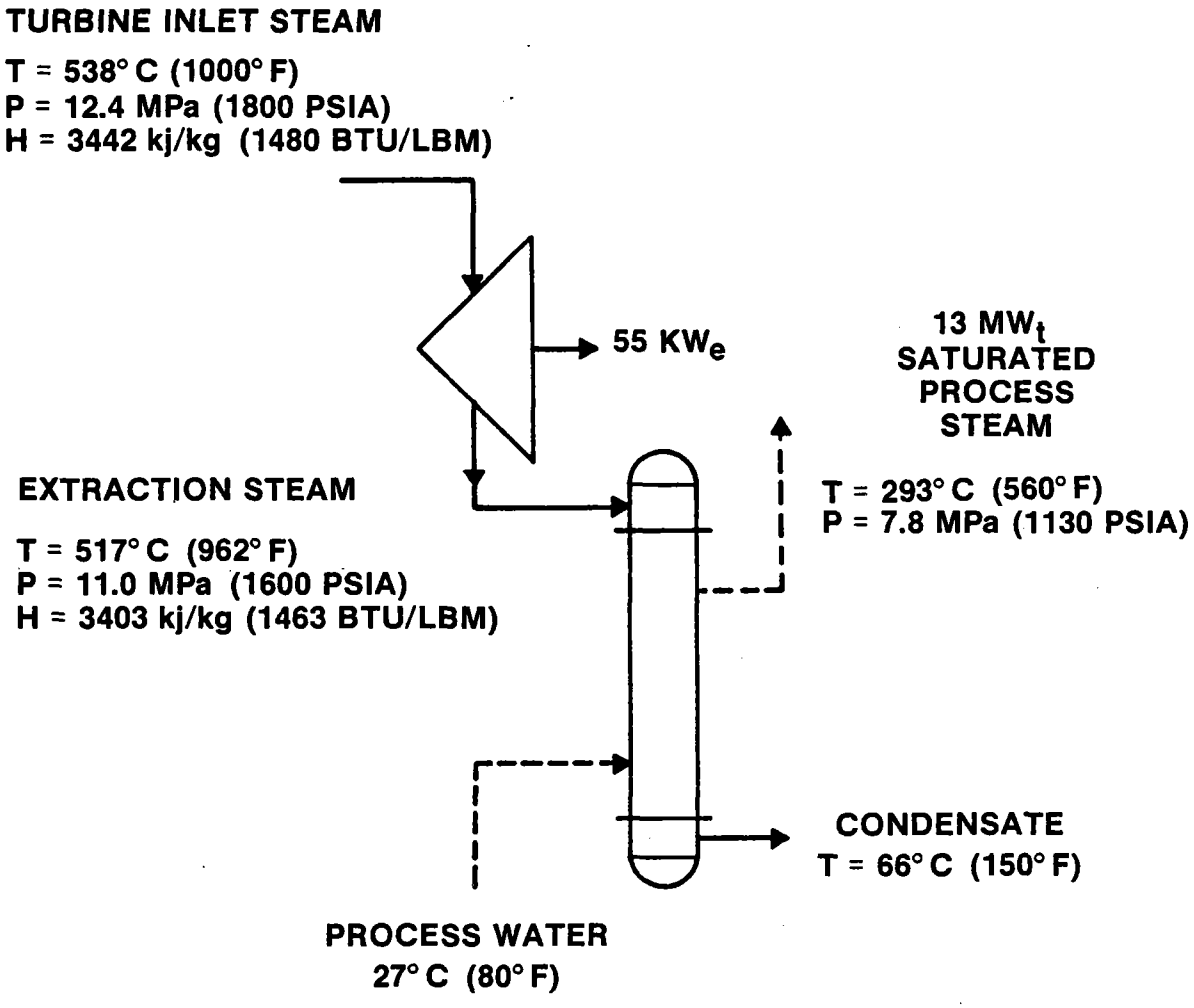

Figure 3.2-1 Series Flow Energy Diagram

4) The overall system control problem for a cogeneration facility without storage would be extremely difficult. Such a controller would have to control three independent flow loops (salt, turbine steam and process steam) to within narrow operating temperatures during wide variations of insolation.

Another key component in the facility is the Rankine cycle steam turbine. Its selection was based on technical maturity, availability and cost effectiveness. For these reasons, alternative thermal cycles such as Brayton and Stirling were not selected.

3.3 HEAT TRANSFER FLUID TECHNOLOGY

Each of the three alternative central reveiver heat transfer fluid technologies (water/steam, molten salt, molten sodium) were considered for use at the cogeneration facility. The molten salt technology was selected because of the advantages listed in Table 3.3-1. The sodium technology was considered but not selected because of concerns with the safety aspects and the lack of utility or industrial experience with liquid sodium. Sodium reacts violently with air and water and is toxic. Molten nitrate salt does not exhibit these characteristics and has been used safely for over forty years in the metals and chemical industries. Our evaluations show sodium and sodium hardware cost more than the salt equivalents and do not offer significant gains in efficiency to offset those disadvantages.

Table 3.3-1 Advantages of Molten Salt

Over Water/Steam - Decouples process heat input from solar energy collection - More cost-effective thermal storage High differential temperature Low cost of storage medium Simplification or elimination of components - Simpler receiver--single-phase fluid - Decoupled heat exchangers and receiver Cloud transients cannot affect turbine - Lower pressure operation Lower construction costs
Over Molten Sodium - Less costly - No violent reaction with air or water - Greater heat capacity and density Smaller piping and storage - Less costly components - No nuclear industry standards - Solar receiver test results not yet available

For all of the above reasons, the molten salt technology was selected by Exxon as best for a 1986 application. Previous Martin Marietta studies as referenced in the appendix have examined all aspects of the molten salt technology. These studies also concluded that large solar standalone plants based on molten salt technology can be cost-competitive in the late 1980s. The results of the Alternate Central Receiver Phase II program has proven the success of the solar receiver portion of the molten salt technology. This program designed, fabricated, and tested a cavity receiver at the Central Receiver Test Facility in Albuquerque, New Mexico. This test utilized the same 60% sodium nitrate, 40% potassium nitrate salt composition (similar receiver design points of 288°C (550°F) inlet and 566°C (1050°F) outlet with a nominal 5 MW_t solar input). The test receiver used Incoloy 800 material and was exposed to heat fluxes similar to those which the cogeneration facility receiver was conceptually designed to. Martin Marietta test work is continuing under a separate contract which will design, fabricate, and build a molten salt thermal storage subsystem. This program is funded by Sandia and is planned to be in testing by late 1981. In addition, Martin Marietta is teamed with Babcock & Wilcox and is under Sandia contract to conceptually design a molten salt steam generator.

3.4 SYSTEM SIZE

3.4.1 Constraints

Two constraints on system size are the available land area at the Edison field (upper limit) and the program requirement for the electrical energy produced to be equal to or greater than 10% of the thermal energy produced for the TEOR process (lower limit).

To examine the effect of system size and turbine operation, three parallel energy flow configurations were compared, each with varying levels of bottoming to preheat process feedwater.

3.4.2 Candidate Systems

The three candidate parallel flow systems are described below with advantages and disadvantages noted. The characteristics of each system are summarized in Table 3.4-1.

CASE 1 (selected as baseline system configuration)

The turbine-generator (TG) is sized to operate during peak periods only. This produces the highest electric revenues and capacity payment. The solar field is constrained by available land. Case 1 features include:

- o TG is always run (efficiently) at design conditions
- o Large TG is more efficient (better heat rate)
- o Large heliostat field shows favorable economies of scale
- o Preheats water only during turbine operation

Table 3.4-1

PRELIMINARY COGENERATION ALTERNATIVE DESIGNS

	CASE 1	CASE 2	CASE 3
Turbine - Generator Operation	Power Produced in Peak Periods	Power Produced 24 Hrs/Day	Power Produced 24 Hrs/Day
Turbine Size Criteria	Land Available for Solar Field	Land Available for Solar Field	All Exhaust Heat Recovered
Turbine - Generator Rating	16.2 MW_e	9.4 MW_e	1.7 MW_e
Turbine Inlet Conditions	1000°F, 1200 psig	1000°F, 1000 psig	1000°F, 400 psig
Heat Rate - Btu/Kwh	10530	11050	18850
Thermal Storage - MWH_t	340	460	260
Heliostats in Field	2900	2900	1680
Tower Height - m	125	125	75

CASE 2 (same number of heliostats as Case 1)

TG operates all day and uses about the same thermal energy as Case 1. It produces more off-peak electricity and a smaller capacity payment. Case 2 characteristics are:

- o Preheats process feedwater 24 hrs/day
- o Capital cost of TG and balance of EPGS is less than in Case 1
- o Requires larger energy storage than Case 1
- o TG Operates off design most of the time
- o Smaller TG is less efficient

CASE 3

The heliostat field is sized such that the TG operates 24 hrs/day and all exhaust heat is used to preheat process feedwater. This field size is the smallest of the three. It has the following characteristics:

- o Produces most electricity during the off-peak periods
- o Preheats process feedwater 24 hrs/day
- o Low capital cost for TG and balance of EPGS
- o TG Operates off design most of the time
- o Small TG has low efficiency
- o Heliostat field is smaller and has unfavorable economies of scale
- o Highest thermodynamic efficiency (no cooling tower required)

To compare the different configurations against each other, the electric and thermal energy produced was calculated for each Case. For all cases the turbine is a non reheat machine with an inlet temperature of 538°C (1000°F) and a condenser temperature of 66°C (150°F). The daily thermal energy collected is calculated using the daily direct normal insolation from the Fresno, CA, TMY data and preliminary collector field performance.

CASE 1

The hours of turbine operation are varied to use the available thermal energy at the design rate, therefore the amount of preheating by turbine extraction varies.

An energy balance leads to:

Turbine Thermal Energy	+	Process Energy (Turbine operating)	+	Process Energy (Turbine not operating)	=	Total Energy Collected

The process energy rate without preheating (no turbine operation) is 13.21 MW_t. The rate with preheating (turbine operating) is 10.89 MW_t. The heat input rate for the turbine is 50.3 MW_t to produce 16.2 MW_e. Let h_t be the hours of turbine operation for any one day. Then:

$$(h_t \times 50.3) + (h_t \times 10.89) + (24-h_t) \times (13.21) = \text{Total energy collected}$$

Solving for the hours of turbine operation yields

$$h_t = (\text{Total energy collected} - 317)/48$$

Once h_t is known, all other heat flows and electric energy production can be found:

Energy to turbine = (h_t x 50.3 MW_t)
Direct energy to process = Total collected - Energy to turbine
Preheat energy to process = (h_t x 2.32 MW_t)
Preheat energy to fossil boilers = (h_t x 2.55 MW_t)
Electric Energy = (h_t x 16.2 MW_e)

On days when the turbine operates less than 6 hrs. (summer) (4 hrs. (winter)) all electric energy produced is on peak. On days when the turbine operates longer, the additional electric energy is produced during the partial-peak period. When the energy collected is less than that required by the process, no electricity is generated and all available energy is used by the process.

The hours of turbine operation were calculated for each day of the year. The on, partial and off peak MWh_e of electricity (allowing for Saturdays, Sundays and holidays), process energy, and preheat energy were determined and the revenues calculated.

CASE 2

The heat input rate to the turbine is varied to match the available thermal energy and operate the turbine 24 hrs/day, provided there is at least enough energy to operate at 20% of design rating (otherwise all energy goes to the process). The process energy requirement with the turbine operating is 10.89 MW_t, so the thermal energy available to the turbine for a day is:

Turbine energy = Total energy collected - (24 x 10.89)

The electricity produced was determined from an estimate of the turbine efficiency as a function of percent of rated heat input.

CASE 3

The collector field and turbine were sized so that all exhaust heat can be used to preheat process feedwater. Because the process heat requirement is the same as Case 2, the total thermal energy available to the turbine was estimated on a seasonal basis and then converted to total electrical energy produced based on design rating turbine efficiency (this is conservative). The distribution of on, partial and off-peak hours is the same as Case 2, since the turbine operates 24 hrs/day. The electric and process energy revenues were then calculated.

3.4.3 Comparison

The thermal and electrical energy outputs for all three cases are summarized in Table 3.4.2. The estimated revenues for all three cases is shown in Table 3.4-3.

Due to the difference in field size between cases 1 & 2 and case 3, the cases are compared using a figure of merit, K defined as:

$$K = \frac{(\text{Net Present Value of Revenues})(1-\text{Tax Rate})(\text{Capital Recovery Factor})}{(\text{Present Value of Capital Cost})(\text{After Tax Fixed Charge Rate})}$$

Economic attractiveness is directly related to the magnitude of K

Table 3.4-4 shows a preliminary estimate of the capital costs and figure of merit for each case. Case 1 results in the highest value of K among the three candidate systems. This is due primarily to the higher electric revenues resulting from turbine operation during peak periods. This demonstrates that in this case the lower thermodynamic efficiency of the Case 1 configuration is balanced by the increase in the value of electricity produced.

There are additional advantages to Case 1 that go beyond these comparative economics and may be more important for an actual installation.

1) Steady Field Steam Injection Rates:

   In Case 1 the steam injection rate can be kept constant on any day that the total energy collected exceeds the process requirement. Excess energy is absorbed by the turbine-generator system which operates until the energy is exhausted. Case 2 also posseses some ability to do this. In Case 3 the turbine and process are linked so that daily swings in energy collected result in daily changes in injection rate, often to levels 2-3 times above normal.

2) Operation of Turbine at Rated Capacity

   In Case 1 the turbine always operates at rated capacity (point of highest performance). Daily energy variations are handled by varying the hours of turbine operation. In Case 2 and 3 the turbines operate 24 hours a day and on all but peak days would operate at less than rated capacity.

The facility configuration described by Case 1 was selected as the starting point for the conceptual design. The final facility design, performance and cost estimate are presented in Section 4 of this report.

Table 3.4-2

THERMAL AND ELECTRIC ENERGY PRODUCTION

	CASE 1			CASE 2			CASE 3		
	Winter	Summer	Annual	Winter	Summer	Annual	Winter	Summer	Annual
Total Thermal Energy - MWh_t	51918	49841	101759	57729	54576	112305	44900	60100	105000
Electric Energy - MWh_e									
Peak	5514	10219	15733	1425	4046	5471	396	832	1228
Partial Peak	4022	8453	12475	3912	6939	10851	1244	1363	2607
Off Peak	1520	3033	4553	5721	11053	16774	1713	2291	4004
TOTAL			32761			33096			7839

TABLE 3.4-3

ANNUAL REVENUE ESTIMATES

First Year in $ 1980
and
(Annualized Net Present Value After Tax)

REVENUE SOURCE	CASE 1	CASE 2	CASE 3
ELECTRIC			
Peak	$1,005,800 ($1,311,900)	$ 351,000 ($451,600)	$ 78,600 ($102,100)
Partial Peak	$ 763,800 ($922,600)	$ 622,900 ($804,400)	$ 159.200 ($196,100)
Off Peak	$ 242,700 ($275,500)	$ 894,100 ($1,015,500)	$ 213,000 ($244,000)
Capacity	$ 945,800 ($465,500)	$ 548,500 ($270,000)	$ 22,500 ($11,000)
PROCESS ENERGY	$1,736,300 ($2,729,700)	$1,916,200 ($3,012,600)	$1,791,600 ($2,816,700)
TOTAL ANNUALIZED NPV	($5,705,200)	($5,554,100)	($3,369,900)

Annualized NPV After Tax Revenue = Annual Revenue (NPV Factor)(Capital Recovery Factor)(1-Tax Rate)

TABLE 3.4-4

PRELIMINARY CANDIDATE SYSTEM

CAPITAL COST ESTIMATES
(In Millions of Dollars)

	CASE 1	CASE 2	CASE 3
Heliostats ($260/m^2)	43.3	43.3	25.1
Tower	2.80	2.80	1.29
Receiver	1.9	1.9	1.3
Piping	.21	.21	.13
Thermal Storage	2.0	2.5	1.7
Salt-Steam HX, Drum, Pump	1.0	.75	.65
Salt-Steam HX Piping	2.0	1.5	1.3
Master Control	.75	.75	.75
Turbine-Generator	1.9	1.5	.62
Balance of EPGS	5.0	5.0	4.0
Site Improvement	.1	.1	.1
Building	1.0	1.0	1.0
Direct Cost	61.96	61.31	37.95
Engineering, Indirects, Contingency	22.38	22.19	15.18
Present Value of Capital Investment	84.34	83.50	53.13
Figure of Merit, K (higher K is more economically attractive)	$1.124	$1.105	$1.054

Capital Recovery Factor, CRF = .1541.
After Tax Fixed Charge Rate, FCR = .06017
Tax Rate, t = .5086
Depreciation Factor DPF = .5825
Tax Credit = .385

3.5 COLLECTOR FIELD OPTIMIZATION

This section details the optimization of the collector field designed to transfer high quality solar energy to the receiver. The collector subsystem consists of:

1) Heliostats, including reflective surfaces,structural supports, drive units, control sensors, pedestals, foundations and cabling;

2) Controllers, including heliostat, heliostat array, and field controllers, interface electronics, and power supplies;

3) Support equipment for alignment, washing, operations and maintenance, and installation and removal.

The heliostat parameters used in the following studies are those of the Martin Marietta second generation heliostat, an advanced, mass producible heliostat design that provides both low life-cycle cost and improved performance. The design is based on a combination of new design concepts, high volume mass production capabilities, and Martin Marietta's experience gained in designing, fabricating, and testing several generations of heliostats.

The approach taken for conceptual design of the collector subsystem was to (1) determine the range of field sizes possible, considering our specific land area and other restraints, (2) select a collector subsystem size based on overall system requirements, (3) optimize the collector field to the most cost effective field configuration for the selected system size, and then (4) analyze the daily and annual peformance of the collector subsystem. The computer codes used to optimize the collector field design and analyze its performance, DELSOL, the RCELL package, MIRVAL and STEAEC, are explained in detail in Appendix A.

3.5.1 Preliminary System Sizing

As part of the system sizing studies described in section 3.4, the DELSOL computer code was used to optimize several collector/ receiver modules to a minimum figure of merit, using tower height as the independent variable. (Figure of merit is defined as the ratio of solar system direct capital cost to the annual energy produced by the plant.) As shown in Figure 3.5-1 a family of curves, one per tower height. A plot of these minima, presented in Figure 3.5-2, indicates that a solar system with an 80 meter tower producing 80 MW_t has the best figure of merit. However, this curve is not a basis for selecting that system because the important effects of indirect costs and economies of scale are ignored.

Results of the system sizing analysis by Exxon indicated that it is desirable to generate as much power as possible. As shown, higher towers resulted in more energy collection; thus, Exxon imposed a maximum tower height (neglecting the receiver) of 150 meters (500 ft).

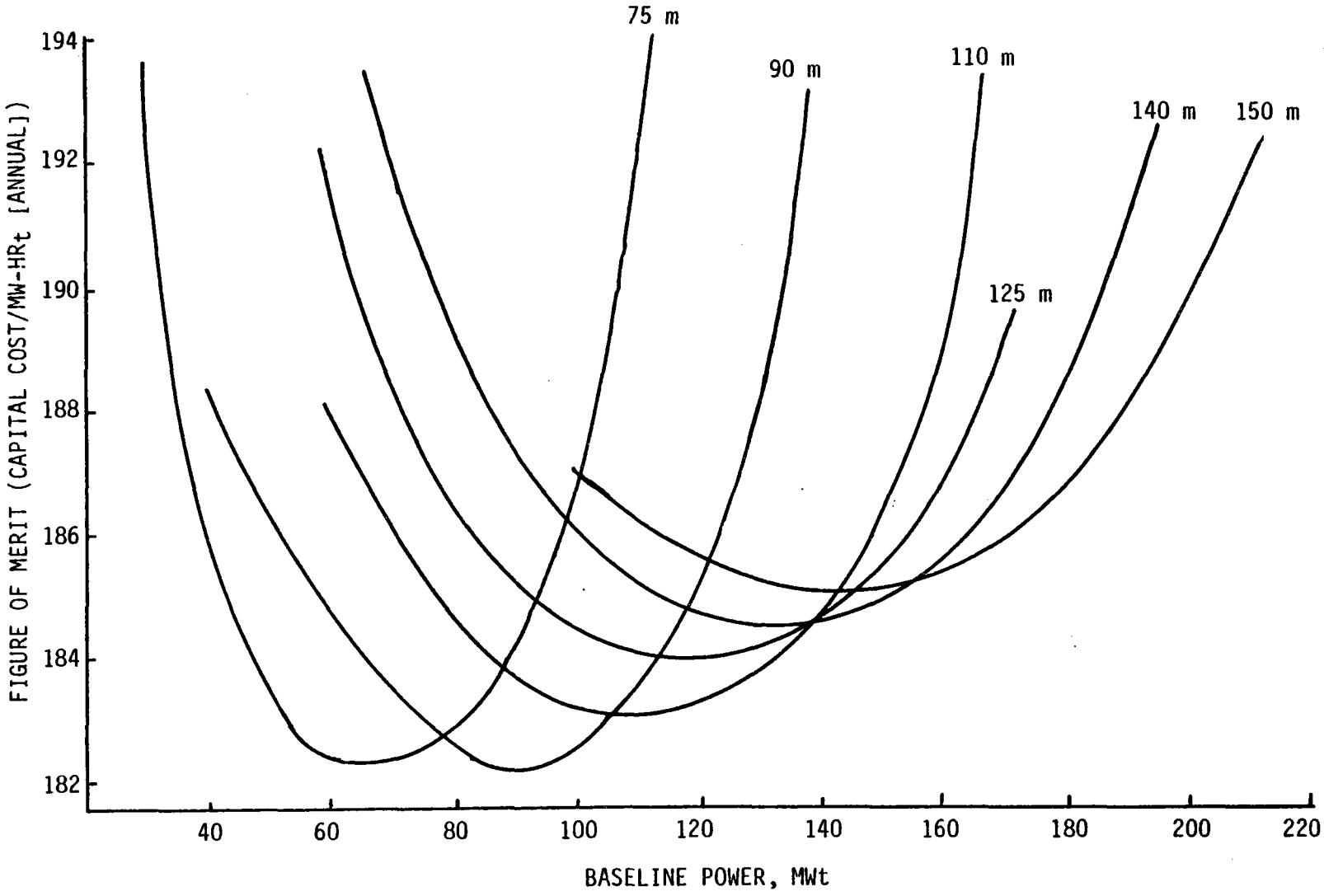

Figure 3.5-1 Power Level vs. Cost

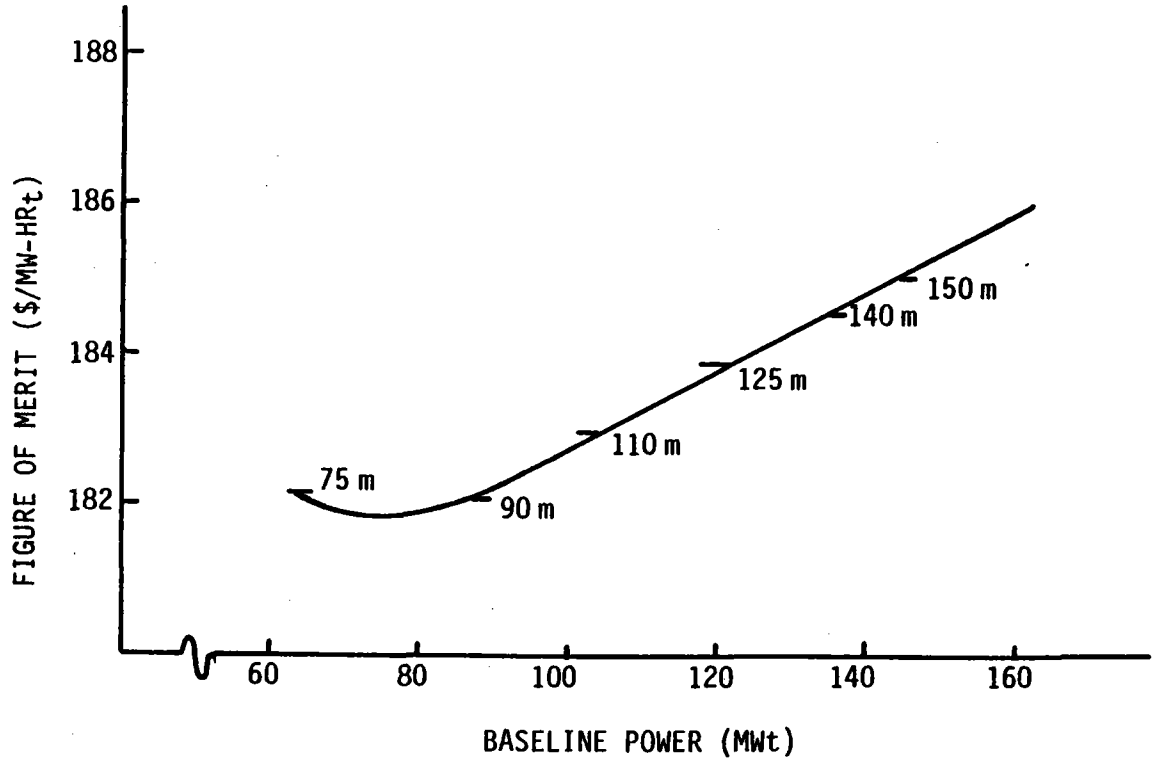

Figure 3.5-2 Optimum Power Level vs. Cost

3.5.2 Field Layout

After defining the tower height, the RCVR/RCELL program linkage was used to generate the radial and azimuthal coefficents defining the optimized collector field layout. For a given tower height, the RCVR/RCELL computer programs determine the optimum heliostat spacing based on minimum figure of merit, which is strongly affected by the heliostat capital cost. The more expensive the heliostats, the more important their performance versus land costs. RCVR/RCELL then minimizes shading and blocking by placing the heliostats further apart. Alternately, the less expensive the heliostats, the less crucial their performance. The program then acts to reduce land costs by increasing the heliostat density. Thus, for a given land area and tower height, annual energy production is strongly dependent on the direct cost of heliostats.

The optimized radial and azimuthal coefficients generated by RCVR/RCELL for the cogeneration facility were used by the LAYOUT program to provide the individual heliostat coordinates, all located within the site boundary. The resulting configuration is a rectangular north biased heliostat field, with the tower located just north of the center of the southern boundary. The coordinates of the heliostats as calculated by LAYOUT provide sufficient spacing for elimination of mirror physical interference, while at the same time allowing access by service vehicles, utility lines, and maintenance personnel. As shown in Figure 3.5-3, the minimum spacing between any two heliostat foundations in the field is 11.8 m (38.8 ft), satisfying the imposed requirement that all wells be accessible by roads of at least 9.1 m (30 ft) width. This spacing also allows a 1.2 m (4 ft) clearance between the reflective surfaces in any orientation. As shown in Figure 3.5-4, no heliostat is within 22.9 m (75 ft) of any existing or proposed well. A 9.1 m (30 ft) access area was allowed around the tank battery as well as the gas plant. A listing of the coordinates of each of the 3295 heliostats is provided in Appendix A.

3.6 RECEIVER SELECTION AND OPTIMIZATION

The receiver subsystem includes the receiver, supporting tower and foundation, horizontal and vertical piping, pumps,and valves. The basic function of this subsystem is to effectively intercept radiant solar flux directed from the collector subsystem and efficiently transfer that thermal energy to the molten salt working fluid.

The approach taken was to (1) select the receiver type, (2) optimize its design, and (3) analyze its performance. The computer codes used to optimize and analyze the receiver design--TRASYS, MITAS, and DRSP (Dynamic Receiver Simulation Program) are explained in Appendix A.

3.6.1 Cavity Vs Exposed

Numerous studies done previously by Martin Marietta have clearly demonstrated that, although external receivers enjoy an advantage in terms of lower receiver and tower costs, the higher thermal efficiency associated with cavity receivers

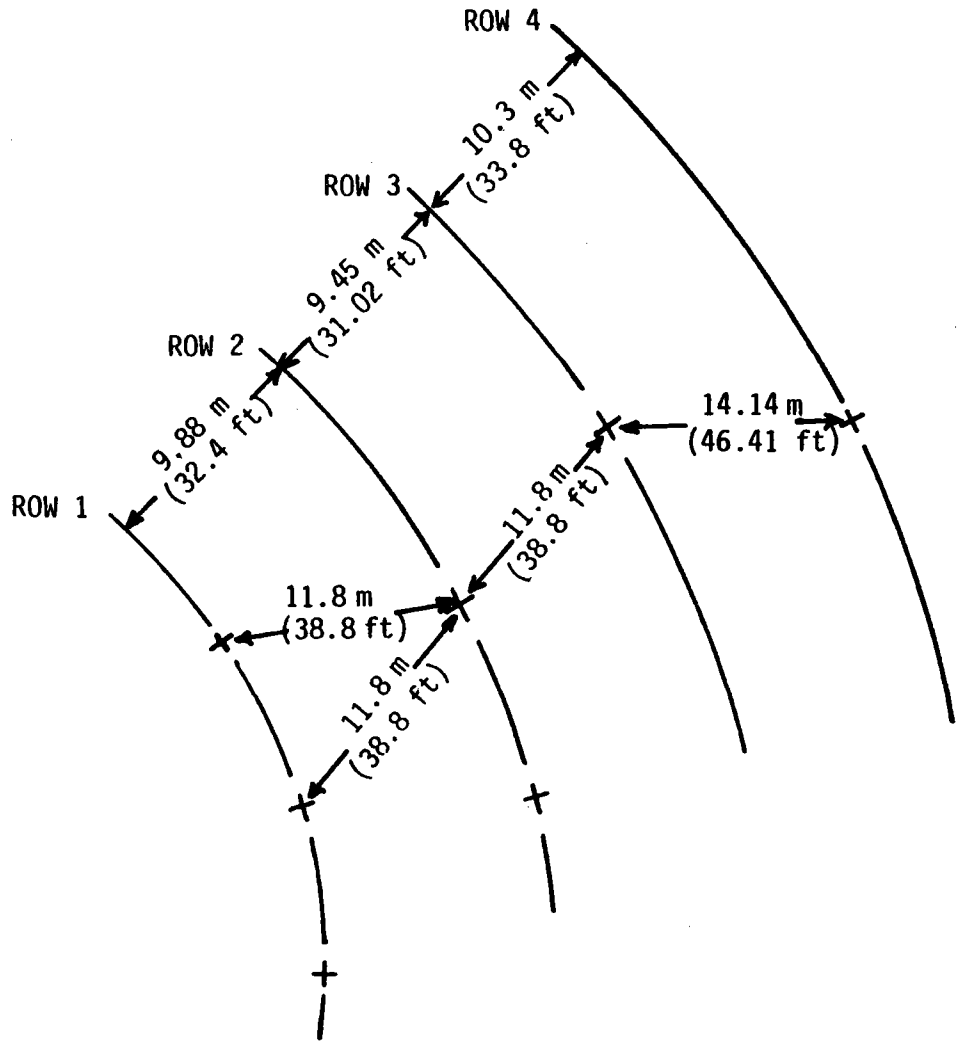

Figure 3.5-3 Access Clearance Between Heliostats (Minimum)

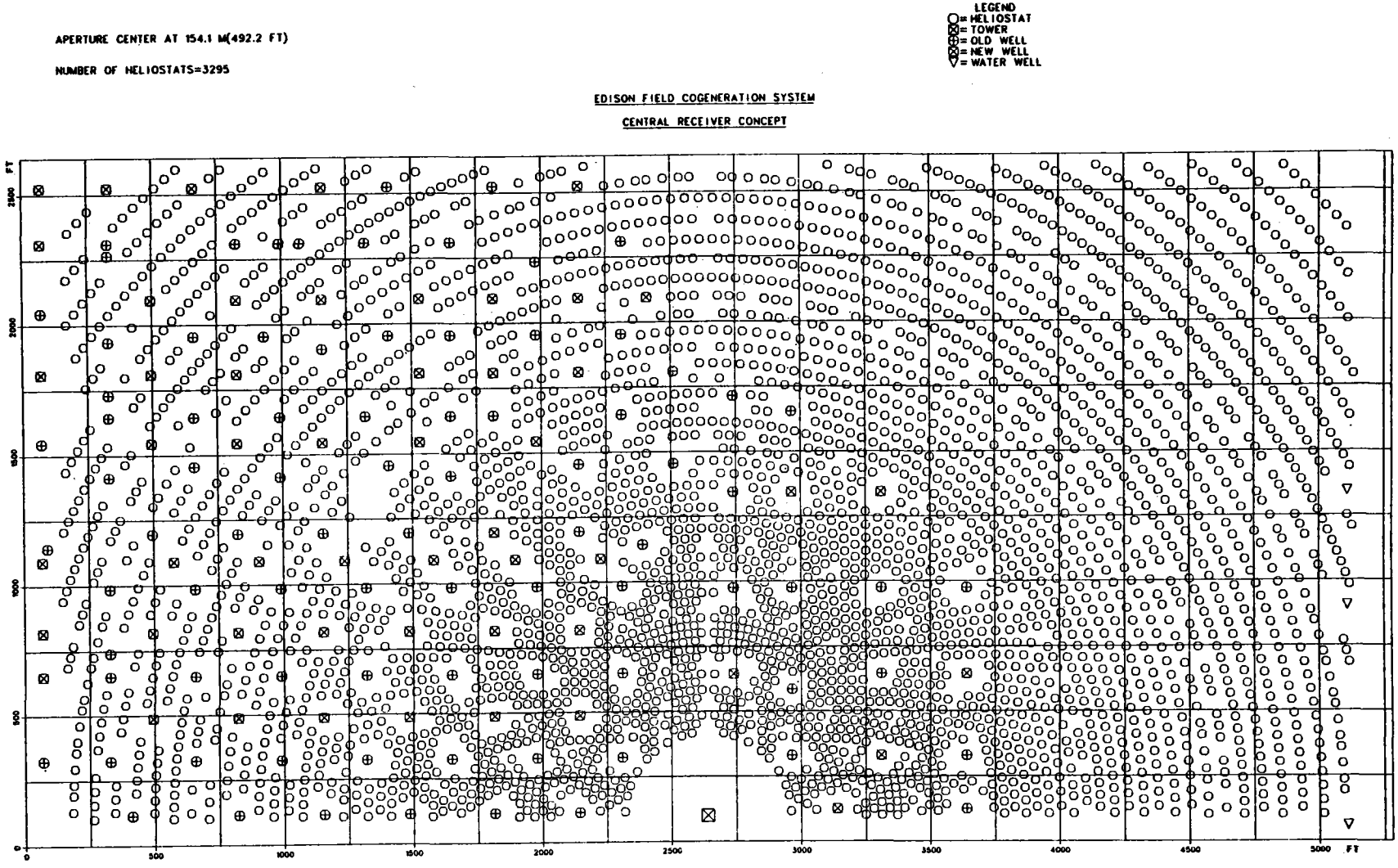

Figure 3.5-4 Collector Field Layout

maximizes the energy absorbed from the collector field. For example, a typical annual thermal efficiency for an exposed receiver is 81%, while that for a while that for a similarly sized cavity receiver is 90%. On this annual basis, the cavity receiver system will deliver 10% more energy than an exposed receiver. As previously stated, Exxon's system sizing analysis shows that it is desireable to maximize the power produced by this tightly constrained collector field. In keeping with this goal of maximum power production, we selected a cavity receiver for the cogeneration facility.

3.6.2 Cavity Arrangement

As explained in Section 3.5, the system power requirements and the rectangular Edison field site limitations dictate the size and shape of the collector field. Possible receiver configurations compatible with this collector field include one, two, three, or four cavity arrangements. A four cavity receiver would require locating the tower north of the southern field boundary to provide room for the south quadrant heliostats. This effectively involves transferring heliostats from the northern boundary of the field to the southern boundary. However, due to cosine effects, the performance of these heliostats is significantly reduced by moving them to the south quadrant. Thus, the power produced by the entire field is reduced. Accordingly, the tower location was fixed at the center of the southern field boundary and the four cavity receiver configuration was rejected.

A single, north facing cavity receiver was then considered. However, heliostats located in the southeast and southwest portions of the field would view the aperture from such an oblique angle that their performance would drop, due to increased spillage. Therefore, this configuration was rejected, as it failed to maximize the power production from this Edison field site.

The remaining two candidate configurations were then compared on the basis of system performance. To determine if any collector field performance advantages existed, the LAYOUT generated heliostat coordinates were input to the TRASYS program (the effects of heliostat displacement by oil wells were neglected in this study) with the candidate three cavity receiver. (For this study, a north aperture of 9x9 m (30 x 30 ft) and east/west apertures of 11x11 m (36 x 36 ft) were used.) The program was run several times at noon, day 81, by varying portions of the field which aimed at the north cavity as shown in Figure 3.6-1. The results of this analysis (shown in Table 3.6-1) indicate that although individual heliostats may perform better depending on which aperture they are aimed at, the field as a whole has the same performance regardless of the receiver configuration. Thus, the choice between a two and three cavity receiver must be made based on receiver performance alone.

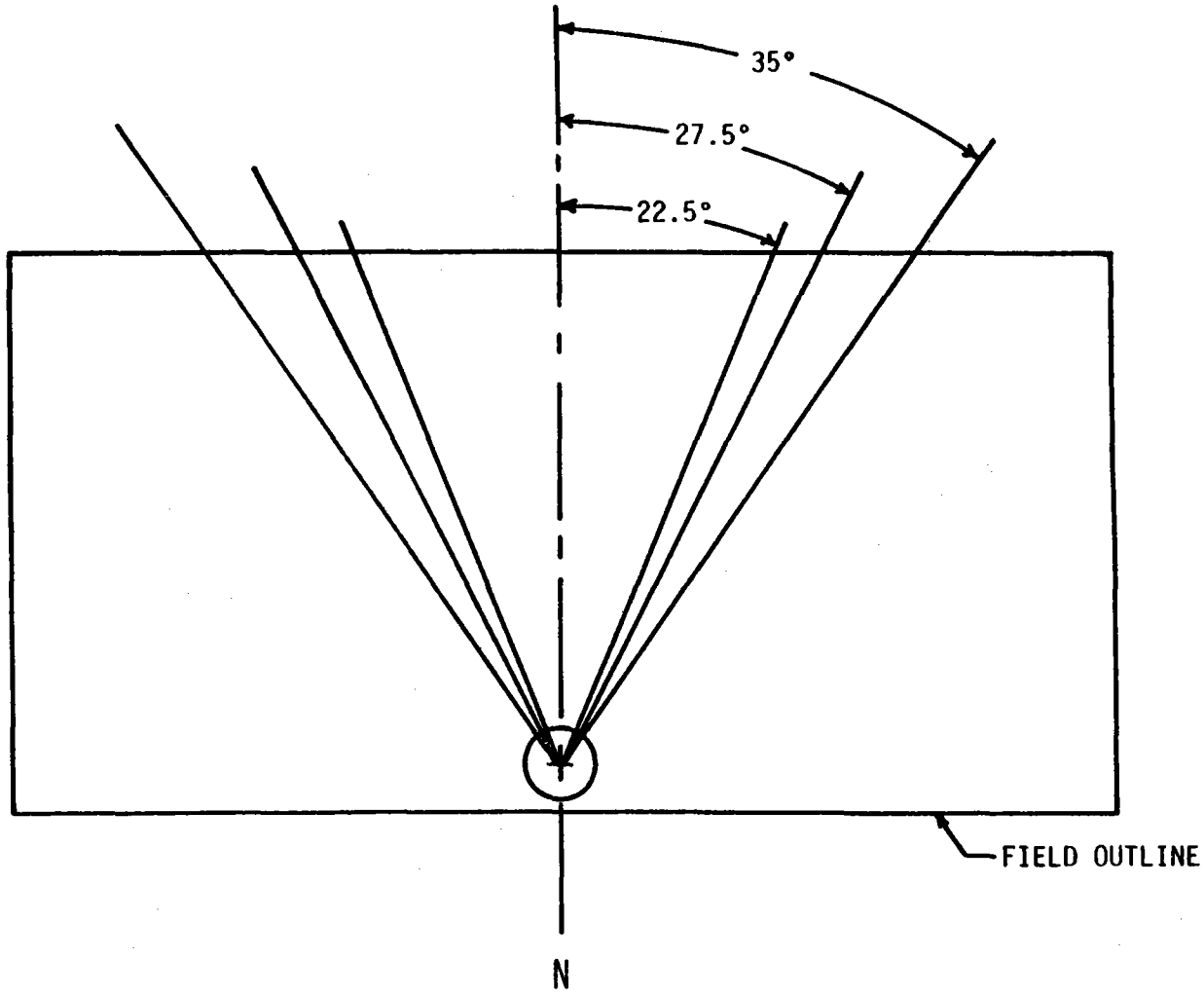

Figure 3.6-1 North Cavity Field of View

Table 3.6-1 Two Cavity vs Three Cavity Field Performance

Included Half Angle	North Cavity Power (MW_t)	East Cavity Power (MW_t)	Total Power (MW_t)
0°	0	73.8	73.8
22.5°	15.7	58.1	73.8
27.5°	21.0	52.8	73.8
35°	29.5	44.2	73.7

In order to fairly evaluate the differences in performance of the two receiver candidates, it was necessary to optimize the apertures for each. Typically, as aperture size increases, spillage losses decrease, but thermal losses increase. Thus, for any given aperture, the optimum size occurs when the sum of cavity thermal losses and spillage is at a minimum. As shown in Figures 3.6-2 through 3.6-4, and in Table 3.6-2, the optimized aperture sizes and the associated thermal performance were determined, using the TRASYS program to calculate spillage.

Table 3.6-2 Receiver Comparisons

	Total Aperture Area	Total Power Losses	Maximum Absorbed Power
Two Cavity	242 m^2	10.8 MW_t	155.8 MW_t
Three Cavity	293 m^2	15.1 MW_t	151 MW_t

As shown, the two cavity receiver design mimimizes both aperture area and thermal losses, thereby absorbing the most power from the collector field. Thus, the two cavity configuration was selected for this application.

3.6.3 Receiver Conceptual Design

3.6.3.1 Aperture Optimization

Realizing that the displacement of heliostats by the various structures located in the field could affect the aperture optimization previously discussed in Section 3.6, the two cavity case was analyzed using the final collector field as shown in Figure 3.5-4. It was found that, although the power delivered to the receiver went down, no reduction in the size of either the east or the west aperture was possible, as there remains a large proportion of heliostats located near the boundaries of the field. These heliostats have larger beam diameters due to their distance from the tower, thus eliminating the possibility of any reduction in the aperture sizes. The optimum aperture size for both the east and west cavities is 11 m x 11 m (36 x 36 ft).

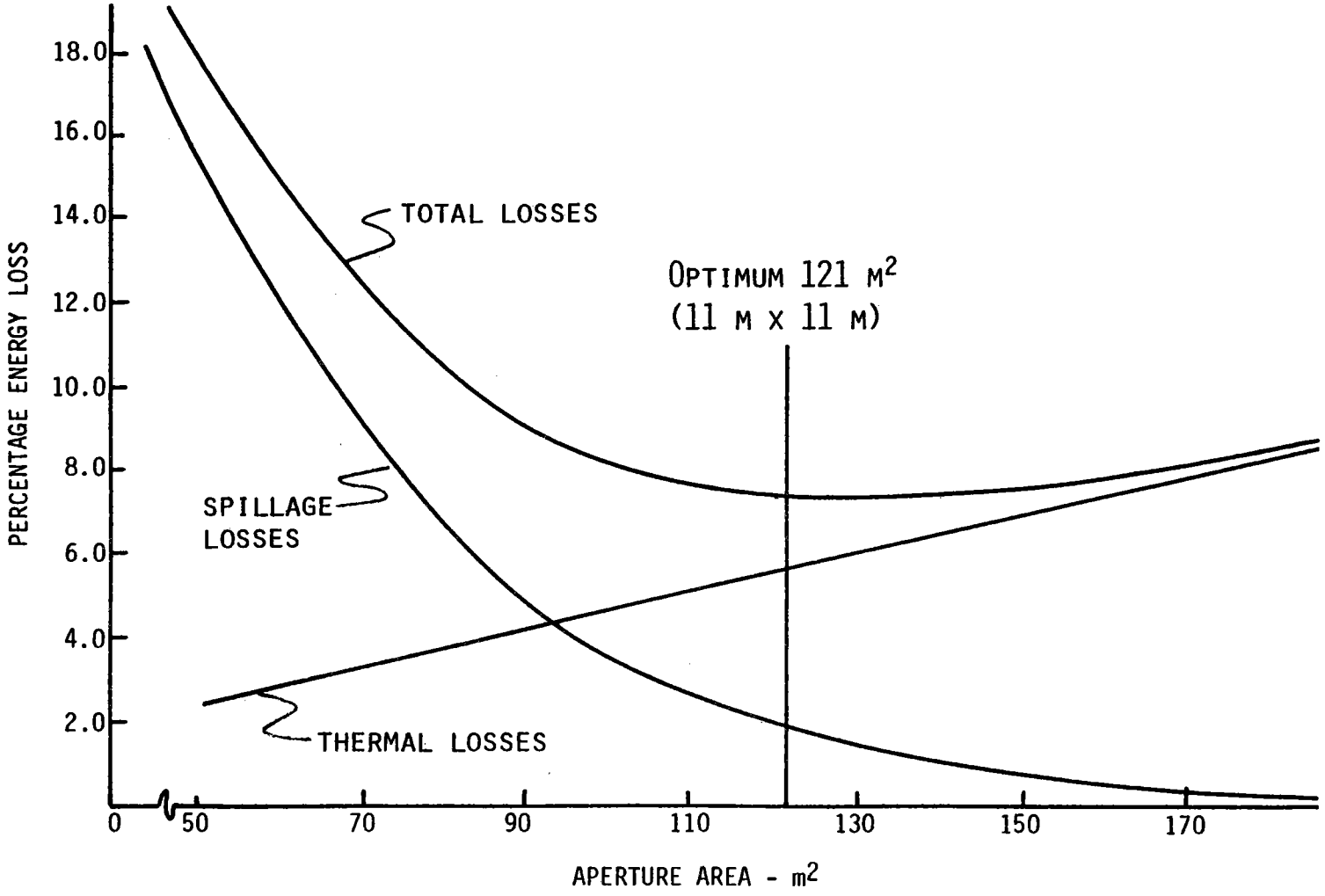

Figure 3.6-2 Two Cavity Aperture Losses

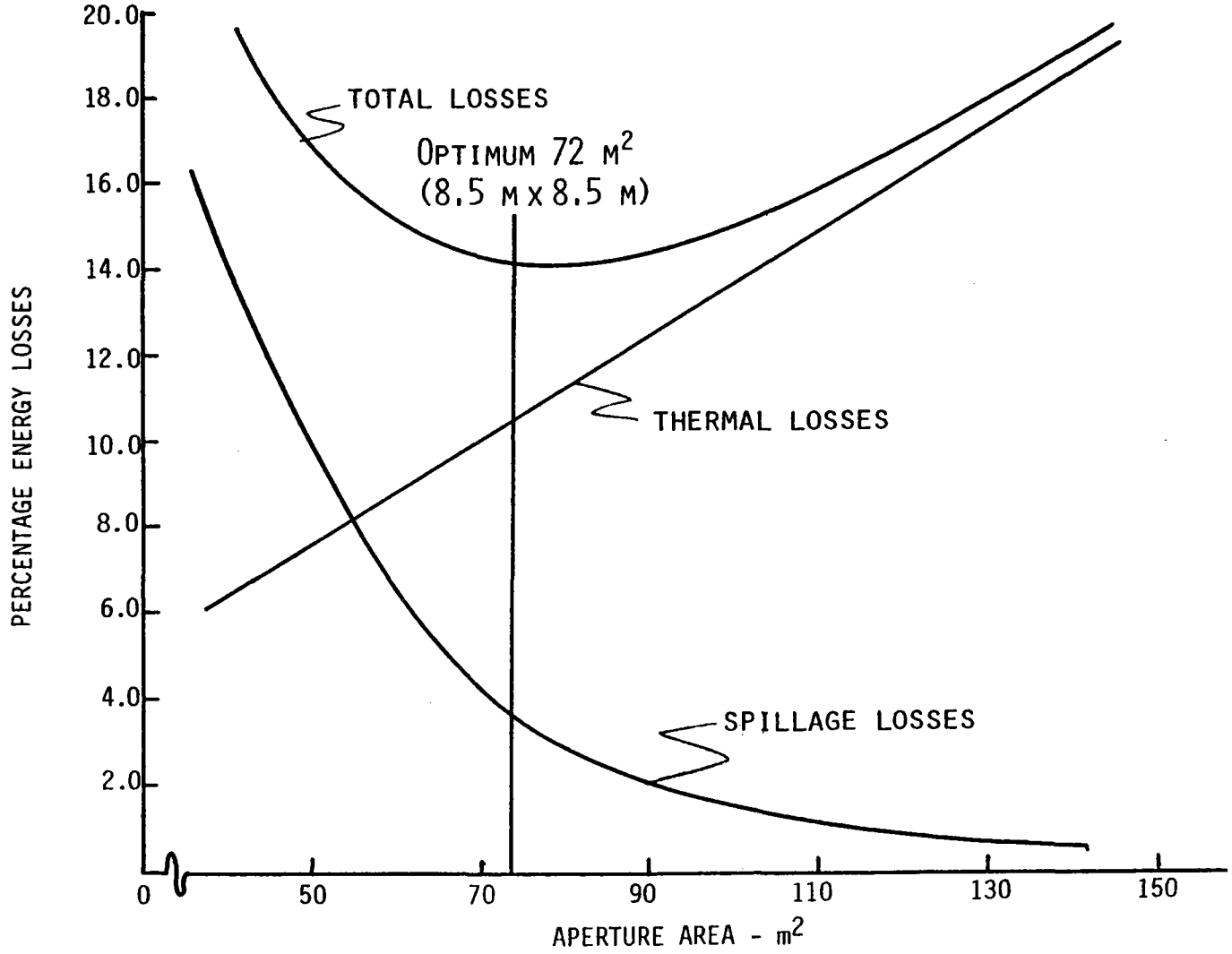

Figure 3.6-3 Three Cavity North Aperture Losses

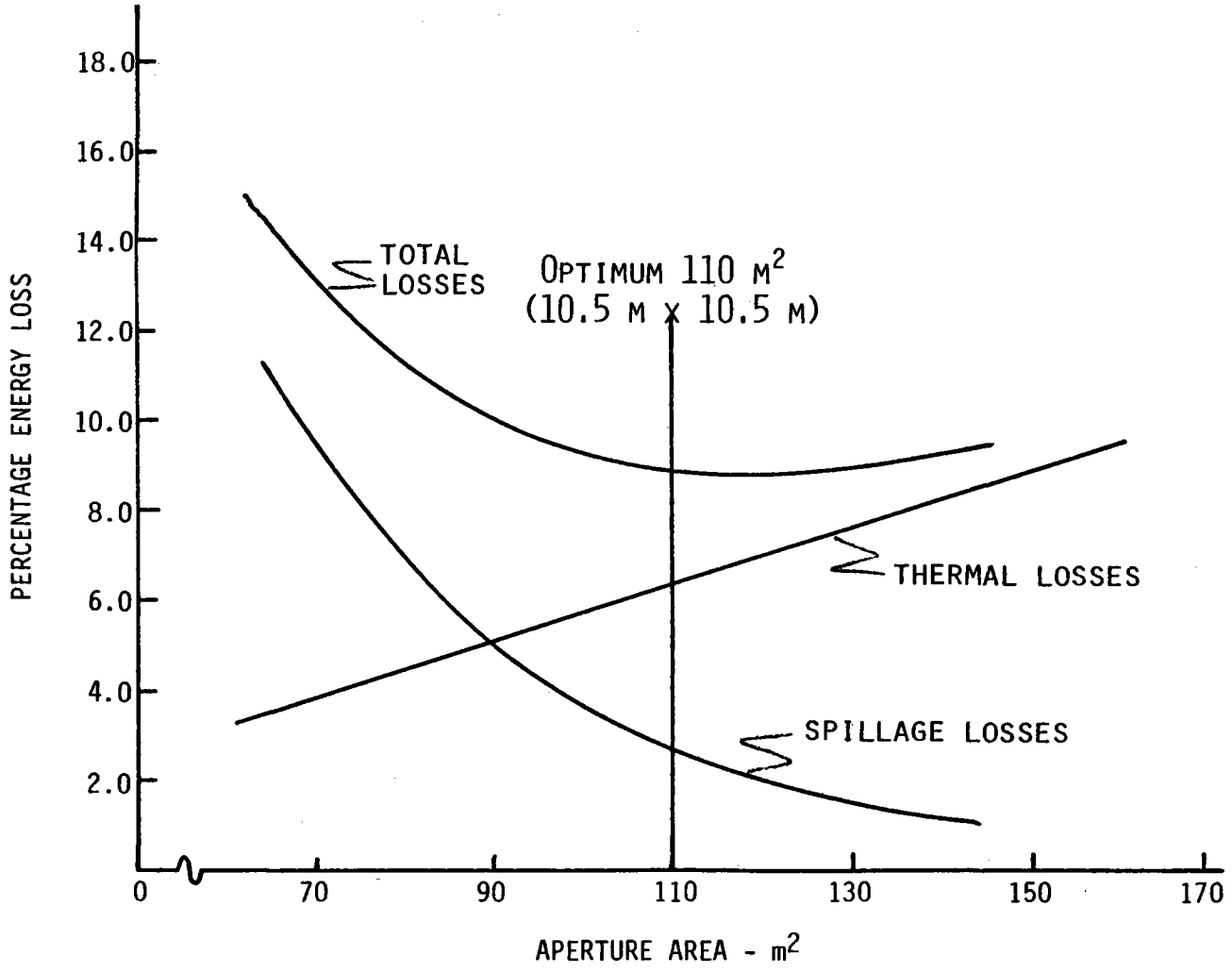

Figure 3.6-4 Three Cavity East Aperture Losses

3.6.3.2 Absorber Configuration

The next step in finalizing the conceptual design of our solar cavity receiver was to determine the optimum cavity depth, i.e., the linear distance from the center of the aperture to the back wall of the receiver. By varying the distance, it is possible to control the peak solar flux on the absorber tubes, thereby keeping the tube temperatures and the associated thermal stresses within acceptable limits. Another method of reducing peak solar fluxes is heliostat aiming. Here, selected rows of heliostats are aimed at some point other than the center of the aperture, thus producing a more uniform flux distribution and allowing for a reduction in cavity depth. In this case, the large aperture dictated by the field layout made any reduction in the cavity depth undesirable, as shallow cavities with large apertures have greater thermal losses than deep cavities with small apertures. The larger the aperture and the shallower the cavity, the more the cavity receiver begins to approximate an exposed receiver. In the interest of maximizing the power production by minimizing thermal losses, we decided not to reduce the cavity depth, thereby eliminating the need for an aiming strategy. If necessary, an aiming strategy can easily be developed for the cogeneration receiver.

The peak incident solar fluxes were reduced to a maximum of 655 kW/m^2 (208,000 $Btu/hr\text{-}ft^2$) with a depth of 9 m (30 ft) in the west cavity and 11 m (36 ft) in the east. The average incident solar power density at noon, day 355 was 15.2 W/cm^2 (48,200 $Btu/hr\text{-}ft^2$) in the west cavity, and 17.1 W/cm^2 (54,200 $Btu/hr\text{-}ft^2$) in the east cavity.

The plan view of the twin cavity receiver (Fig 3.6-5) shows that there are no common tube panels between the two cavities. Although this arrangement slightly increases the overall receiver weight, it allows for a separate control zone for each cavity. This two zone control strategy is necessary for this collector/receiver subsystem due to the uneven power distribution between the two cavities. This also increases the overall system reliability, as each cavity is fully independent of the other. Thus, one cavity could be shut down while the other functions at its design flow.

3.6.3.3 Thermal Hydraulic Studies

With two receiver control zones, and the total absorber area per zone, it was then possible to perform an analysis relating pressure drops and salt heat transfer coefficients to the tube diameter and number of passes. The results of this analysis show for a 3.2 cm O.D. tube that although the salt heat transfer coefficient increases with the number of passes (due to higher salt velocities) the pressure drop through the receiver also increases. (Receiver pressure drops were calculated using friction factor data obtained during the Martin Marietta Alternate Central Receiver Phase II experiment.) Using larger diameter tubes with an increased number of passes will result in acceptable heat transfer coefficients and lower pressure drops, but this requires more drain valves and interconnecting piping, thereby increasing the receiver weight and cost. Separate thermal analyses indicated that for a 3.2 cm (1.25 in.) O.D., 0.17 cm (.065 in.) wall thickness tube, a salt film coefficient of 1.40 $kW/m^2\text{-}°C$

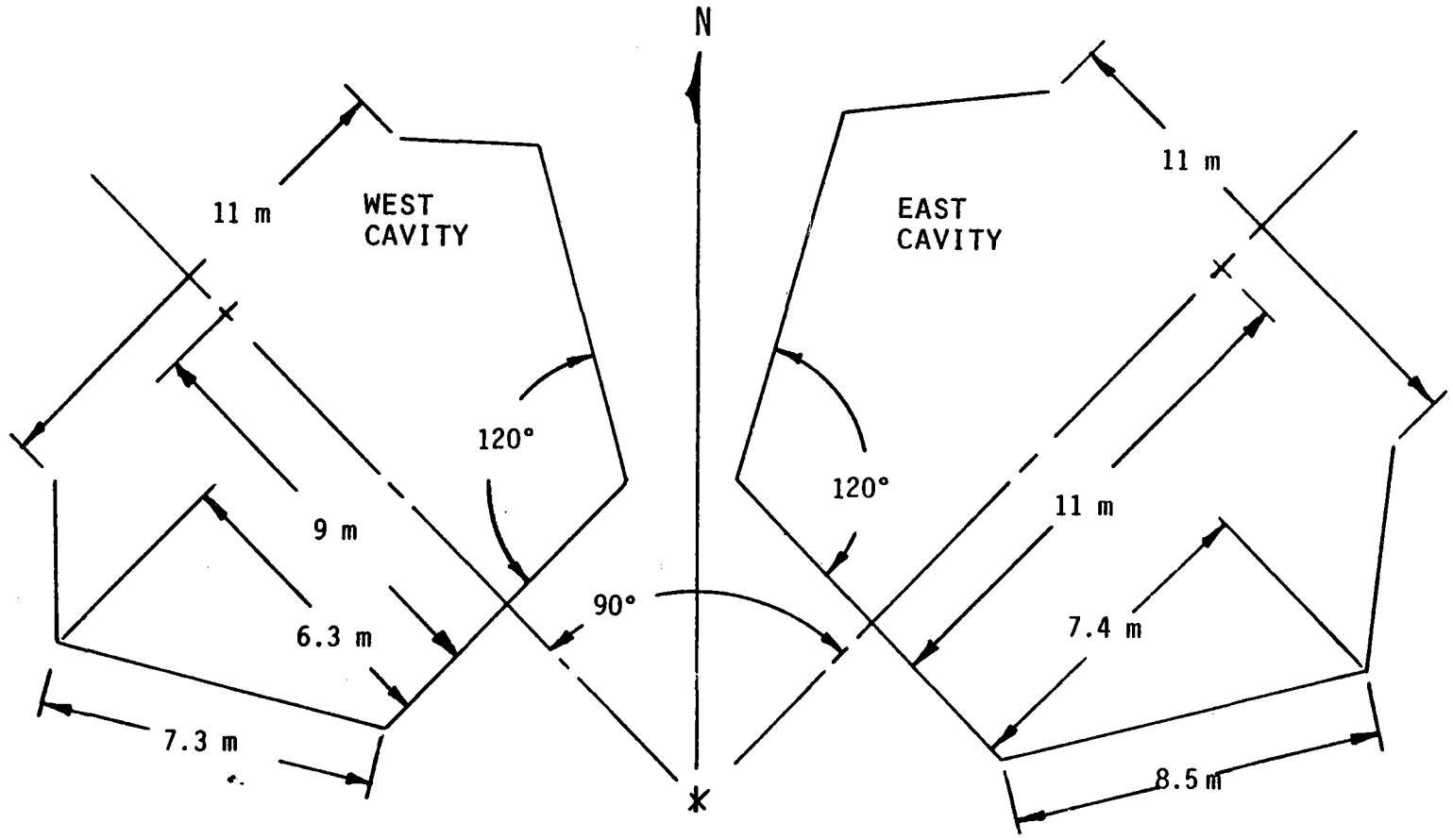

Figure 3.6-5 Plan View of Two Cavity Receiver

(800 Btu/hr-ft^2-°F) was sufficient to limit peak metal temperatures in the receiver to 606°C (1123°F), assuming peak solar flux conditions. This corresponds to a 12 pass flow control zone, and a 1.02 MPa (148 psi) pressure drop through the tubes. This 12 pass arrangement using 3.2 cm O.D. tubes represents a good compromise between sufficiently high heat transfer coefficients, lower pressure drop, and lower receiver weight and cost. Panel width in the east cavity will be 2.1 m (7 ft). Similarly, the west cavity will have 12 - 1.8 m (6 ft) absorber panels and a .874 MPa (127 psi) pressure drop through the tubes. Panel lengths were established based on an analysis of incident flux (see section 5.3). The upper and lower radiation shields are located along a line on the absorber panels where the incident flux drops below 1.5 W/cm^2 (4760 Btu/hr-ft^2). These radiation shields are used to protect headers, valves, interconnecting piping and receiver structure from damaging high intensity solar radiation.

Table 3.6-3 Panel Lengths

East Cavity		West Cavity	
Panel Number	Tube Length	Panel Number	Tube Length
1, 12	15.5 m (50.8 ft)	1, 12	16.1 m (52.8 ft)
2 - 11	18.3 m (60.0 ft)	2 - 11	18.3 m (60.0 ft)

Tube lengths shown in Table 3.6-3 were used to calculate the pressure drops. Considering tube entrance and exit losses, the velocity head loss per pass, losses in the headers and interconnecting piping and valves, and a salt flow velocity of 1.89 m/s (6.2 ft/s), the maximum pressure drop through the receiver due to salt flow is approximately 1.02 MPa (148 psi). The static head of salt in the receiver, the design pressure drop in the flow control valve, and a reasonable margin were added to establish a maximum operating pressure of 2.50 MPa (363 psig) for the receiver.

3.6.3.4 Receiver Panel Ordering

The term "receiver panel ordering" refers to the procedure which establishes the flow path of the liquid salt through the receiver. Investigations into the control of liquid salt cooled solar central receivers have demonstrated that the distribution of absorbed energy along the salt flow path can affect the accuracy and quality of receiver outlet temperature control. While the controllability* aspects dictate a desirable energy distribution along the flow path, the location of peak solar fluxes within the receiver is of prime importance. Generally, the controllability and peak flux considerations in panel ordering do not dictate conflicting requirements. If, however, a conflict does arise, the

* Controllability is defined as the ability of the system to maintain the desired salt outlet temperature under the action of various disturbances in absorbed flux and inlet salt temperature.

the peak flux considerations must take priority, and the control system must be designed to handle the less desirable energy distribution. The relative distribution of absorbed energy over the receiver surface is determined by the receiver and heliostat field configurations. Consequently, the desired absorbed energy distribution along the flow path must be accomplished by directing the liquid salt flow path through the receiver panels in the proper sequence.

3.6.3.5 Peak Flux Aspects in Receiver Panel Ordering

Experience gained during previous receiver designs had indicated that the peak fluxes experienced in the receiver do not necessarily fall on the panels with the largest total energy absorbed. Therefore, care must be taken during panel ordering, such that high peak flux panels do not see high salt temperatures, since the high salt temperatures coupled with high flux can lead to receiver tube overheating.

3.6.3.6 Controllability Aspects in Receiver Panel Ordering

Various flux distribution arrangements with respect to salt flow path were modeled for a typical ten pass receiver. Each configuration was simulated using the Dynamic Receiver Simulation Program (DRSP) developed by Martin Marietta.

The same controller was used for each panel ordering arrangement and the changes in controllability are due solely to the changes in energy distribution along the salt flow path.

Three different power distributions were modeled. These were High-Low, Low-High, and Middle High as shown in Figure 3.6-6. The total power absorbed at each panel location along the salt flow path as a function of panel position number was calculated. The panel position number represents a serpentine flow from panel 1 (inlet) to panel 10 (outlet).

The corresponding closed loop response of the three energy distributions was calculated and is shown typically in Figures 3.6-7 and 3.6-8. The variables TS9 and TS10 represent the salt outlet temperature of panels 9 and 10, respectively, while TW9 and TW10 represent the receiver tube wall temperatures of panel 9 and 10, respectively. Time is represented by T with the dimensions of seconds. The disturbance to the system consists of full flux applied to cold (all parts of the receiver at inlet temperature) receiver and a susequent sinusoidal variation in flux from 100% to 50% power starting at 240 seconds, with a period of 180 seconds. The full flux on a cold receiver transient represents an extreme disturbance which would never be purposefully performed on an actual receiver. However, the controller response provides information concerning possible system temperature overshoots.

Examination of all results demonstrates the superior controllability of the Middle-High energy distribution. The Middle-High arrangement also demonstrates the least temperature overshoot during the startup transient. This arrangement

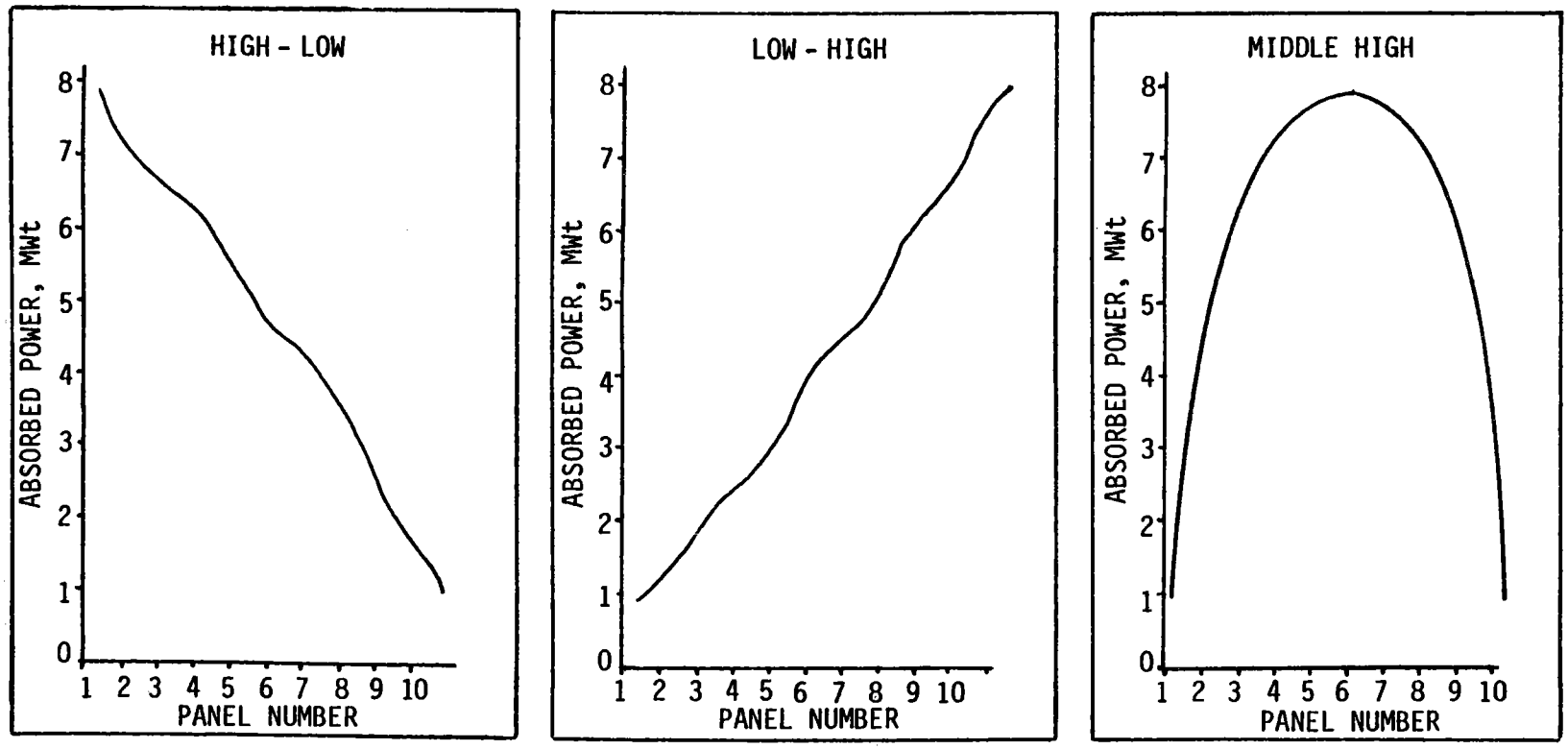

Figure 3.6-6 Receiver Panel Power Distributions

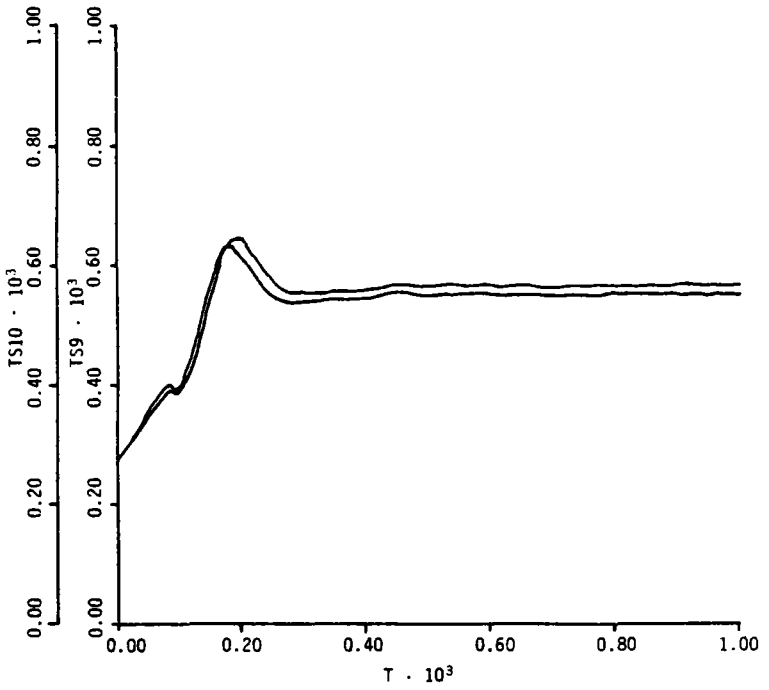

SALT TEMPERATURES FOR HIGH-LOW FLUX DISTRIBUTION

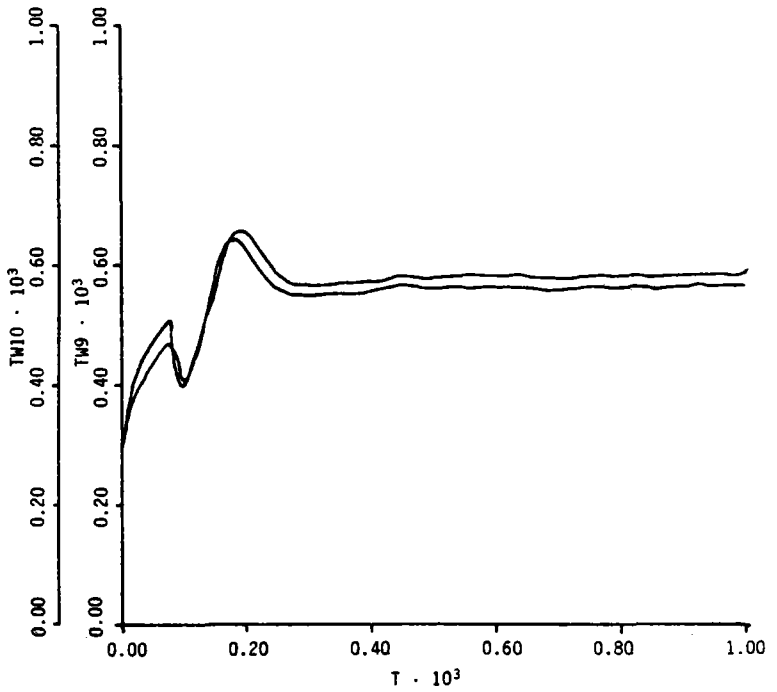

RECEIVER TUBE WALL TEMPERATURES FOR HIGH-LOW FLUX DISTRIBUTION

Figure 3.6-7

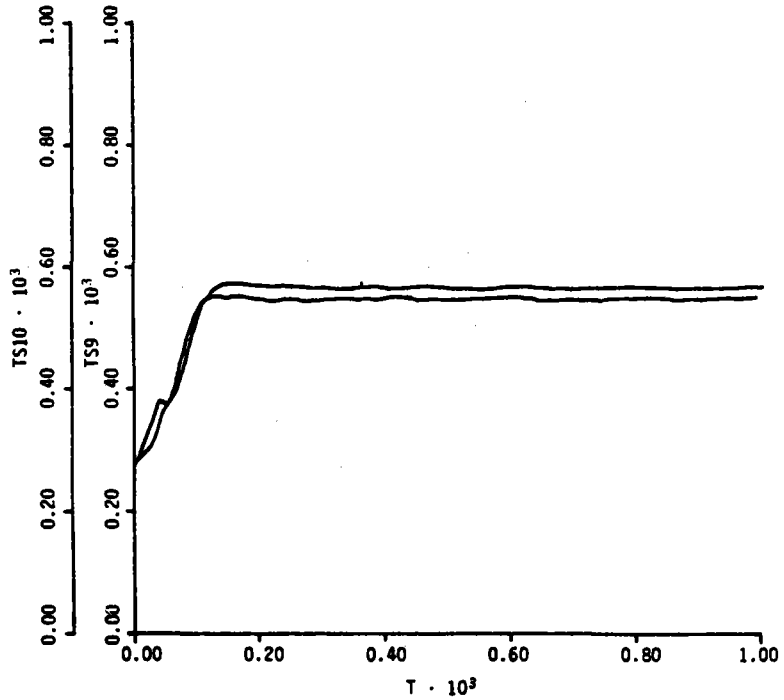

SALT TEMPERATURE FOR MIDDLE-HIGH FLUX DISTRIBUTION

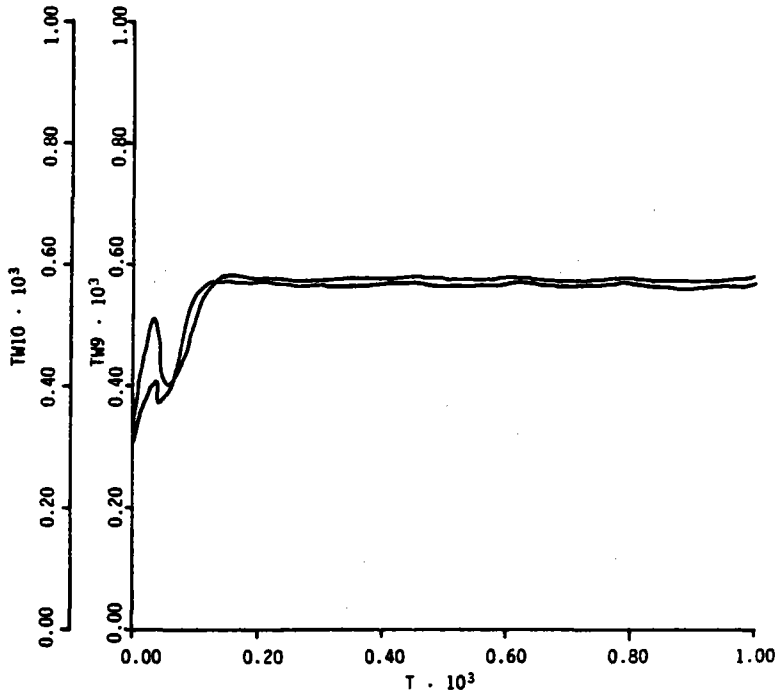

RECEIVER TUBE WALL TEMPERATURE FOR MIDDLE-HIGH FLUX DISTRIBUTION

Figure 3.6-8

does not expose high temperature salt to extreme solar fluxes, thereby avoiding excessive tube metal temperatures. Thus, the middle-high flow configuration represents a good compromise between peak flux and contollability aspects.

3.6.3.7 Panel Ordering

The total energy absorbed at each panel and the peak flux encountered at that panel for east and west cavity are shown in Figure 3.6-9. The peak flux curve in both cavities closely follows the absorbed power curve. Consequently, the panels can be arranged for reasonable tube temperatures and good controllability. The resulting panel ordering is listed in Figure 3.6-10 and results in a simple serpentine flow from panel 12 through 1 for the east cavity and from panel 1 through 12 for the west cavity.

3.6.4 Failure Modes and Effects

It is necessary that both east and west cavities be equipped with the proper controls so that the receiver will fail safe if abnormal conditions develop. The receiver control system (RCS) will have built in redundant alarms and kills that alert the operator in addition to providing automatic protection of the receiver. The operator will be buffered from abnormal conditions by using redundant power supply systems, computer controllers, and pneumatic air systems for emergency valve control. Regardless of the redundancy, receiver protection will be further enhanced by an extensive heliostat defocusing protection system. This system would be used to handle abnormal conditions such as those presented in Table 3.6-4. One advantage of the two zone configuration, is the fact that since the east and west cavities are separately controlled, an abnormal condition for one cavity, may not forbid the operation of the other cavity. This feature would reduce total plant down time and allow operation that would have otherwise been impossible for a receiver with a single control zone.

One severe occurrence that was analyzed is a loss of all electrical power to the system. As a result, the pressure head from the booster pump would be lost. In addition, if the heliostats did not defocus and fail safe, and the ablative coated cavity doors did not shut, there would still be power on the receiver as the aim point drifted east. This normalized incident power in to the east aperature is plotted in Figure 3.6-11 as a function of the time after loss of tracking occurs.

The power at each time step was divided by design power (77 MW_t) to obtain the curve. In addition, the resulting flow caused by the pressure head decay starting from 2.5 MPa (363 psig) in the cold surge tank is also shown. The flow at each time step was normalized to the design flow rate, 0.56 X 10^6 kg/hr (1.23 x 10^6 lbm/hr), at full power. As seen in Figure 3.6-11, the power and flow curves do not match and therefore create an undesirable condition that would damage the receiver tubes. To prevent this condition, a controller would be used to govern the air pressure regulator on the cold surge tank and control the air coming from the 4.14 MPa (600 psig), 5.7 m^3 (200 ft^3) air storage tank. By governing the air supply to the cold surge tank, the proper flow to

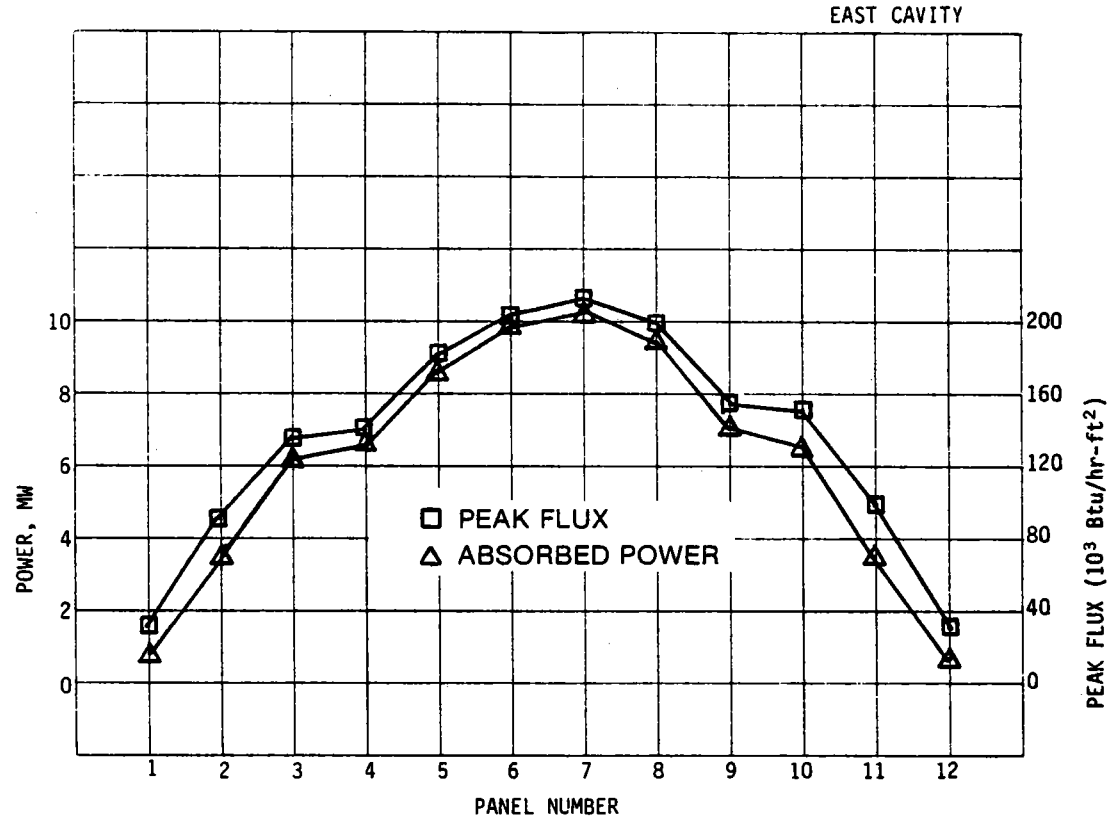

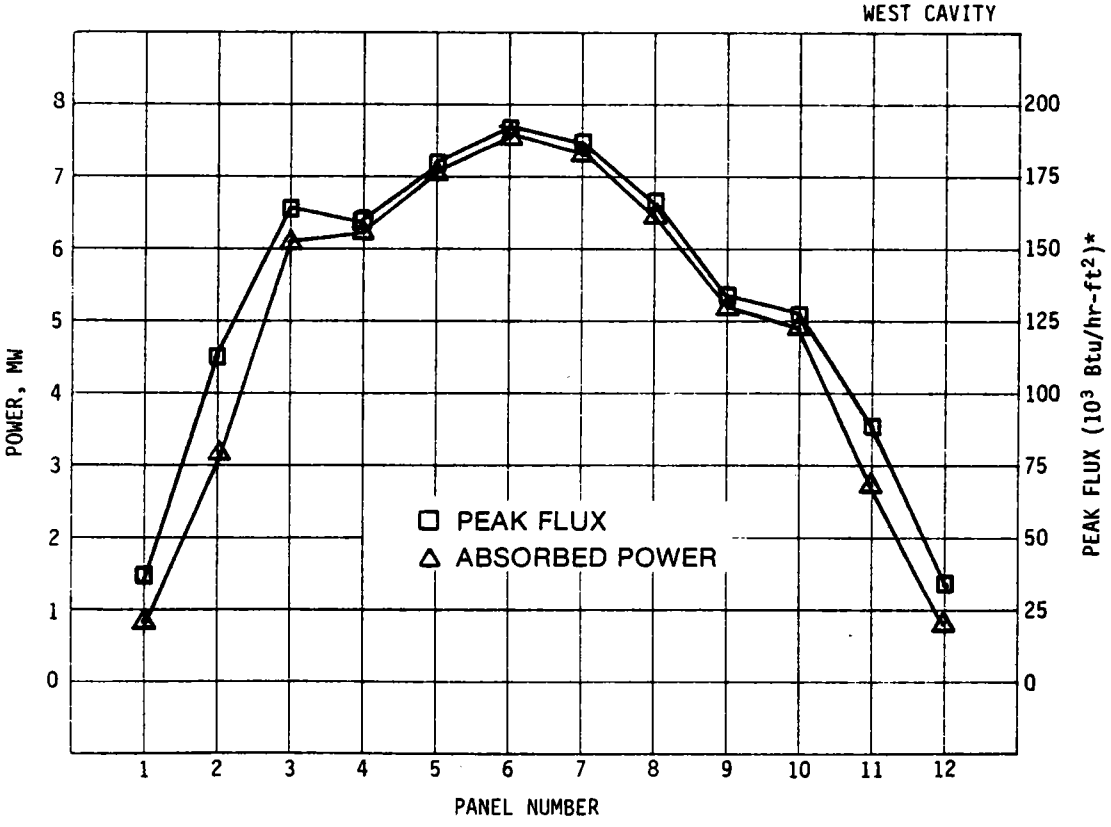

Figure 3.6-9 Peak Flux and Absorbed Power

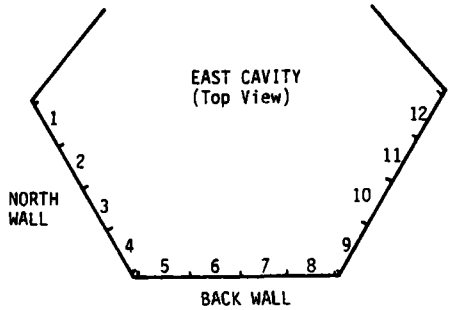

Panel Location Number	Power		PEAK FLUX		Plumb Order 1 = Inlet 2 = Outlet
	MW	Btu/hr x 10^6	kW/m^2	Btu/hr-ft^2(10^3)	
1	0.90	3.08	102	32	12
2	3.53	12.05	291	92	11
3	6.25	21.34	428	136	10
4	6.67	22.75	439	139	9
5	8.79	30.00	579	184	8
6	10.07	34.38	648	206	7
7	10.35	35.32	663	210	6
8	9.44	32.21	629	200	5
9	7.26	24.78	490	155	4
10	6.67	22.73	481	153	3
11	3.60	12.27	317	101	2
12	0.77	2.62	97	31	1

PANEL ORDERING, EAST CAVITY

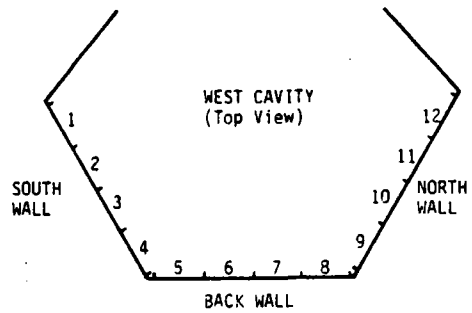

Panel Location Number	Power		Peak Flux		Plumb Order 1 = Inlet 2 = Outlet
	MW	Btu/hr x 10^6	kW/m^2	Btu/hr-ft^2(10^3)	
1	0.80	2.728	113	36	1
2	3.21	10.95	356	113	2
3	6.12	20.88	517	164	3
4	6.24	21.31	504	160	4
5	7.17	24.47	558	177	5
6	7.71	26.34	596	189	6
7	7.35	25.10	586	186	7
8	6.54	22.34	517	164	8
9	5.28	18.02	407	129	9
10	4.89	16.65	400	127	10
11	2.73	9.32	277	88	11
12	0.80	2.73	104	33	12

PANEL ORDERING, WEST CAVITY

Figure 3.6-10 Panel Ordering

Table 3.6-4 Failure Modes and Protection for Receiver

CONDITION	PARAMETER	POSSIBLE CAUSE(S)	PROTECTIVE ACTION
LOW PUMP OUTLET PRESSURE	LOW PRESSURE	LOSS OF RECEIVER BOOSTER PUMP	DEFOCUS OR REDUCE POWER
HIGH FRONT-SIDE TUBE TEMP HIGH RECEIVER OUTLET LAMINAR FLOW	tube T_{max} >649°C (1200°F) out T_{rec} >593°C (1100°F) .1am m_{west} <36,364 kg.hr (80,000 lb/hr) .1am m_{east} <42,273 kg/hr (93,000 lb/hr)	LOSS OF FLOW, LEAK LOSS OF FLOW CONTROL SYSTEM LOSS OF RECEIVER BOOSTER PUMP	DEFOCUS, REDUCE POWER TAKE MANUAL CONTROL DEFOCUS
IMPROPER POWER BALANCE ON RECEIVER	HELIOSTAT CONTROLLER ALARM	LOSS OF HELIOSTAT ARRAY CONTROLLER(S)	DEFOCUS
LOSS OF AIR PRESSURE IN SURGE TANK	LOW TANK AIR PRESSURE	COMPRESSOR MALFUNCTION OR AIR STORAGE LEAK	REDUCE POWER, TAKE MANUAL CONTROL OF SURGE TANK LEVELS
INOPERABLE VALVES	LOW PRESSURE	LOSS OF PNEUMATIC AIR	DEFOCUS, VALVES GO TO PROPER FAIL POSITION
POSSIBLE LINE AND VALVE FREEZING	LINE TEMPERATURE AND FLOW	LOSS OF TRACE HEATERS	DEFOCUS, DRAIN

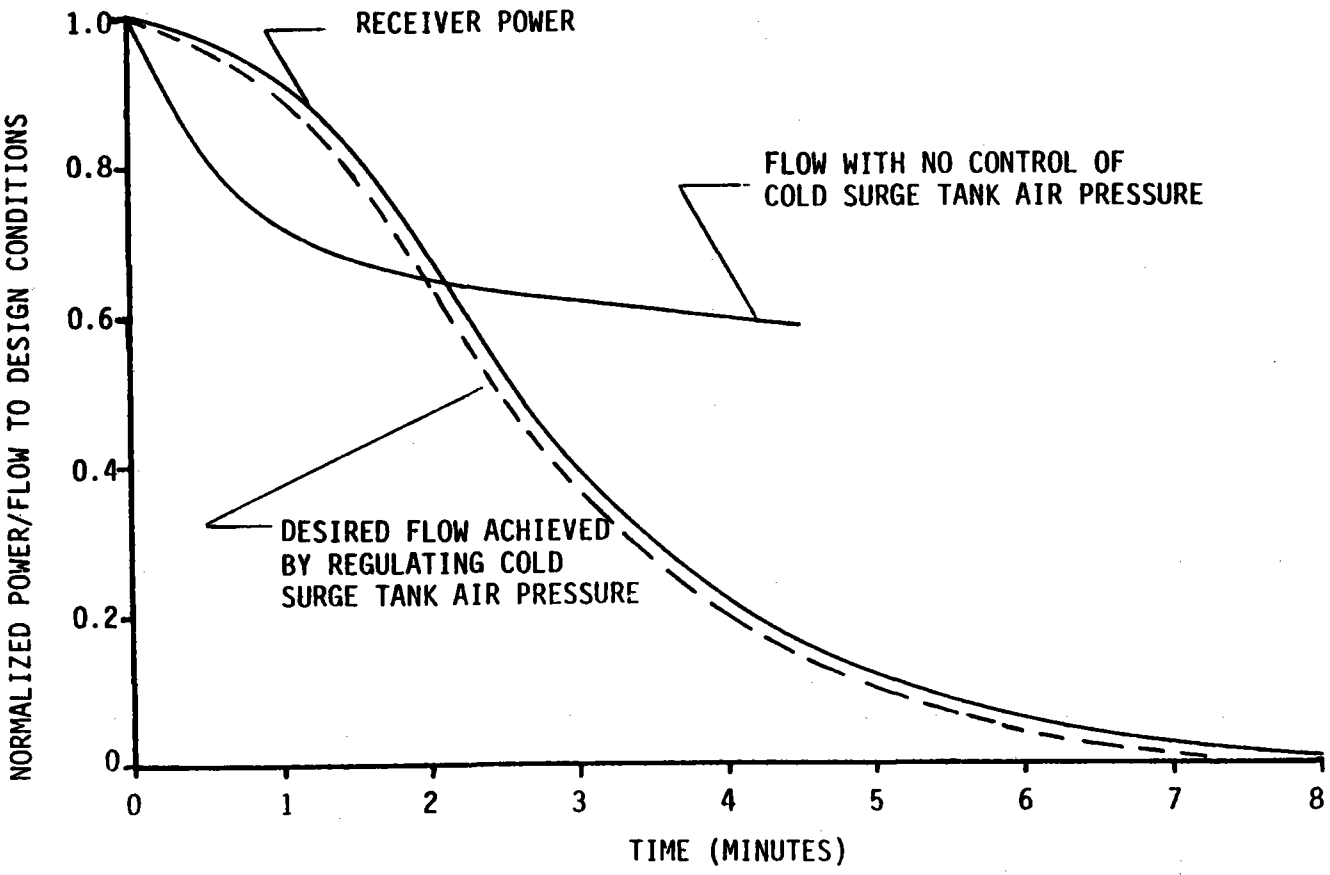

Figure 3.6-11 Receiver Power During Electric Power Loss

the receiver during the incident could be achieved as shown in Figure 3.6-11. Since all site power is lost, the controller for the regulator must be powered by an emergency battery. A computer simulation of this double feature occurrence shows that the salt capacity of the cold surge tank (49,000 kg [108,000 lbs.] during normal operation at 2.5 MPa) is sufficient to provide enough flow for eight minutes to avoid receiver damage. Thus, there is no need for any additional salt storage in the tower to provide flow for this severe accident.

3.6.5 Cogeneration Receiver Control Response

The receiver response to warm-up and transient power level changes has been analyzed with the "Dynamic Receiver Simulation Program" (DRSP). This computer program was developed by Martin Marietta to assist in receiver control development. DRSP can be used for many applications, but in particular, it is an excellent tool for analyzing the temperature/time response for the receiver during transient conditions.

The response of the east cavity of the baseline design receiver was analyzed since it is the peak power cavity. The DRSP inputs include the tube diameter (.032 m [1.25 in.]) tube wall thickness (.065 m [.065 in.]), number of tubes per panel (East 65), and the number of panels per cavity (12). In addition, the interconnecting piping between the panels is utilized to determine accurate time lags for the receiver. Several assumptions were made to perform the computer simulations. These assumptions are:

1) Receiver minimum flow rate is assumed to be 10% of design flowrate (maximum is 110%).

2) Incoming power was assumed to be a linear gradient as a function of heliostat tracking speed.

3) During early morning startup, the solar insolation is half of normal and the heliostat reflective cosine angles also reduce the incoming power by half. Thus, 25% of the incident power of 133 MW_t is available for early morning start-up.

The results of the DRSP simulations of the receiver startup and receiver power step transients are shown in Figures 3.6-12 and 3.6-13. The incoming normalized solar power, the receiver flow rate, and the outlet temperatures are on the ordinate as a function of time. At time zero of this simulation, the solar power is linearly increased from zero to 25% over a 300 second period, with mass flow rate starting at 100% flow. The flow controller then automatically reduces the flow rate to its minimum level (10% of maximum flow). The receiver is near steady conditions at the 25% power level after the first 900 seconds, then the power level is linearly increased to 100% power over the next 300 seconds. The flow controller responds to this transient and the receiver is within the next 300 seconds. In general, the receiver control response is slow at the low power levels and faster at high power levels.

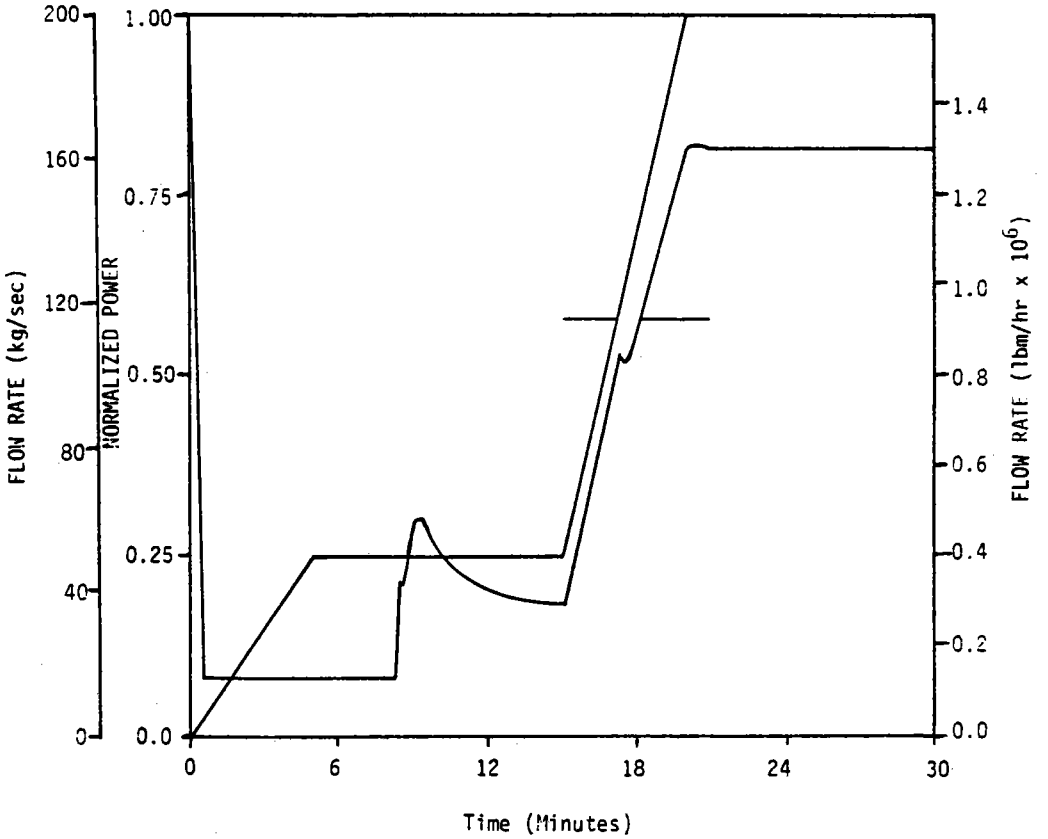

Figure 3.6-12 Receiver Flow Rate and Normalized Absorbed Power vs. Time

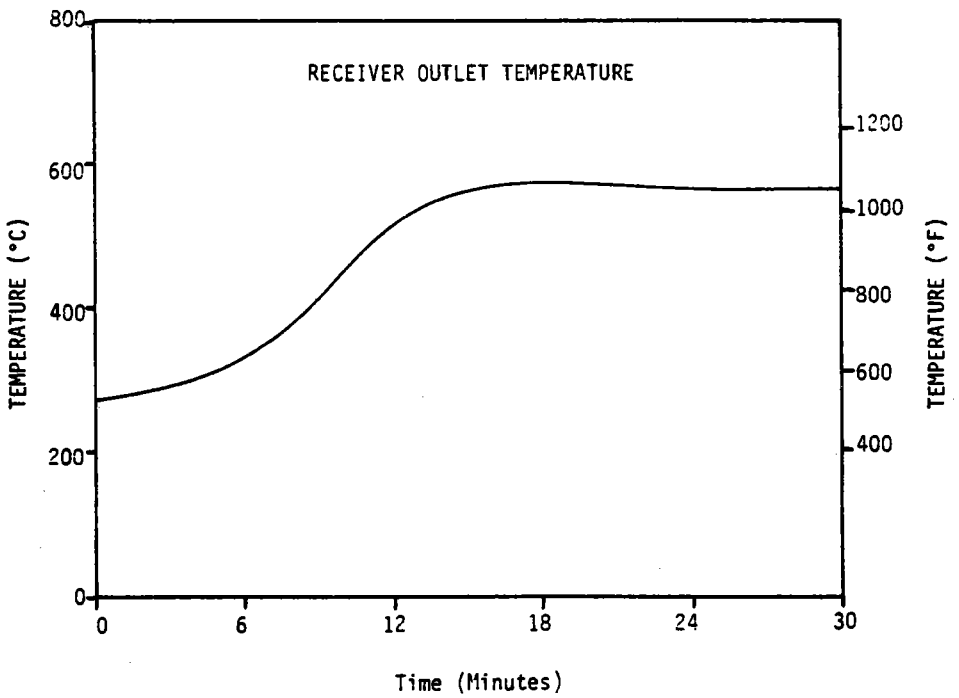

Figure 3.6-13 Receiver Outlet Temperature Response vs. Time

3.7 ELECTRIC POWER GENERATING SYSTEM SELECTION

The selection of the Electric Power Generating System (EPGS) is based on three criteria: compatibilty with the requirements of other systems, performance , and cost. The inlet condition, cycle configuration and exhaust pressure selected by these criteria are summarized in Table 3.7-1 and discussed below.

A high inlet temperature is desirable for high thermodynamic efficiency. The maximum temperature is constrained by the metallurgical limits of the turbine blade material and a practical limit for commercially available machines is 538°C (1000°F). A turbine inlet temperature of 538 C (1000°F) was thus selected to make maximum use of the 566°C (1050°F) hot tank salt temperature and not require excessive heat exchanger surface area.

Table 3.7-1 EPGS Selection Summary

Cycle Configuration	Single Stage Reheat Rankine Cycle
Inlet Condition	538°C, 8.3 MPa (1000°F, 1200 psia)
Reheat Condition	538°C, 2.6 MPa (1000°F, 380 psia)
Exhaust Pressure	6.9 KPa (2 inches Hga)
Heat Rejection	Machanical Draft Wet Cooling Tower
Speed	3600 RPM
Expected Life	26 years

As inlet pressure increases the rankine cycle efficiency of the turbine increases. This effect is offset somewhat by a reduction in the turbine increases. This effect is offset somewhat by a reduction in the turbine wheel efficiency caused by reduced volumetric flow and increased exhaust moisture content. This is shown for machines in the size range in question in tables 3.7-2 and 3.7-3 which show that as the inlet pressure is increased, the cost of salt/steam heat exchanger, associated equipment, and to a lesser extent the turbine itself rises.

The practical limit for currently available standard equipment in the 20000 KW_e size range is 10 MPa (1450 psia). From the baseline system at 8.3 MPa (1200 psia), the increase to 9.7 MPa (1400 psia) will result in performance and cost increases both on the order 1%. A rational choice between the two would therefore require far more accurate cost estimation than was available for this study. The selected baseline inlet pressure of 8.3 MPa (1200 psia) was left unchanged.

Table 3.7-2 Turbine Performance vs. Inlet Pressure

Throttle Pressure MPa (psia)	Heat Rate Btu/Kwh$_e$	Generator KW$_e$
9.7 (1400)	9330	20500
8.3 (1200)	9470	20200
6.9 (1000)	9620	19900
5.5 (800)	9840	19400

Above for: Single reheat machine, heat input of 56 MW$_t$ (191 MBtu/hr) 38°C condenser temperature.

Table 3.7-3 Inlet Pressure vs. Steam System Cost

Throttle Pressure	Approximate Cost ($K)			
MPa (psia)	Heat Exchangers	Steel Drum	Feedwater Pump	Total
12.4 (1800)	750	430	90	1270
7.6 (1100)	410	265	70	745
5.9 (850)	340	245	65	650

Two exhaust pressures, 6.9 and 25.6 KPa (2.0 and 7.5 in. Hg) and two cycle configurations, reheat and non-reheat, were considered. Table 3.7-4 summarizes the performance and cost for these machines. The lower exhaust pressure requires a wet cooling tower, while the higher pressure could be handled with a dry cooling tower. The reheat cycle requires an additional salt/steam heat exchanger, but other heat exchangers would be smaller than for the non-reheat cycle.

Table 3.7-4 Cycle and Exhaust Pressure Comparison

	Reheat Cycle	Non-Reheat Cycle
Heat Input (MW$_t$)	47.8	47.8
Inlet Temperature (C°)	538	538
Inlet Pressure (MPa)	827	827
Reheat Pressure (MPa)	2.76	-
Generator Output MWe (25.6 KPa exhaust)	16.5	15.5
Generator Output MW$_e$ (6.9 KPa exhaust)	18.2	17.0
Approximate Cost	$2.4 x 10^6	$2.2 x 10^6

The lower exhaust pressure increases generator output by 10% and the addition of reheat adds another 7%. The change in cost to achieve these increases is a much smaller fraction of the plant capital cost while the increase in plant revenue is approximately 9%. Thus, the 6.9 KPa exhaust pressure and reheat cycle were selected.

4.0 CONCEPTUAL DESIGN

This section discusses all aspects of the conceptual design for a Solar Cogeneration Facility at the Edison field. The facility will be described, and the functional aspects, requirements, operational characteristics, and performance will be discussed. Capital and operating costs, safety, environmental, regulatory issues and potential limiting considerations for the design are included here.

4.1 SYSTEM DESCRIPTION

The Solar Cogeneration Facility consists of a solar collector subsystem, a receiver subsystem, energy storage subsystem, process and turbine steam subsystems, and an electric power generating subsystem (figure 4.1-1).

The collector subsystem consists of 3295 Martin Marietta second generation heliostats arranged in a north field pattern. These reflect sunlight onto a two cavity molten salt cooled receiver mounted on a 137 m (450 ft) reinforced concrete tower.

The molten salt, a 60% - 40% weight mixture of sodium nitrate and potassium nitrate is heated to 566°C (1050°F) in the receiver. The heated salt flows through the tower downcomer into a hot salt storage tank.

The energy storage subsystem consists of a hot salt storage tank, a cold salt storage tank, piping, hot and cold salt pumps and sumps and associated heat tracing and control equipment. A third tank of the same design as the hot salt storage tank has been included to accomodate emergency system drain requirements and serve as a spare hot or cold tank. The storage system provides a significant degree of decoupling of the solar energy collection, process steam, and turbine steam subsystems. Salt from the hot storage tank is pumped to the process steam and turbine steam subsystems.

The process steam subsystem produces 80% quality steam for injection into the Edison field for enhanced oil recovery operations. Approximately half of the steam is generated by existing crude oil fired steamers, the other half is generated in molten salt/water steam heat exchangers. Some process steam preheat is provided by turbine extraction steam when the turbine is operating. Cold salt from the process steam salt/water heat exchangers returns to the cold salt storage tank at 288°C (550°F).

The turbine steam subsystem produces superheated steam at 538°C (1000°F) and 8.27 MPa (1200 psia) and reheat steam at 538°C (1000°F) and 2.62 MPa (380 psia) for the EPGS. Boiler feedwater at 250°C (480°F) is provided by the turbine extraction feedwater heaters. Cold salt at 288°C (550°F) is returned to the cold salt tank.

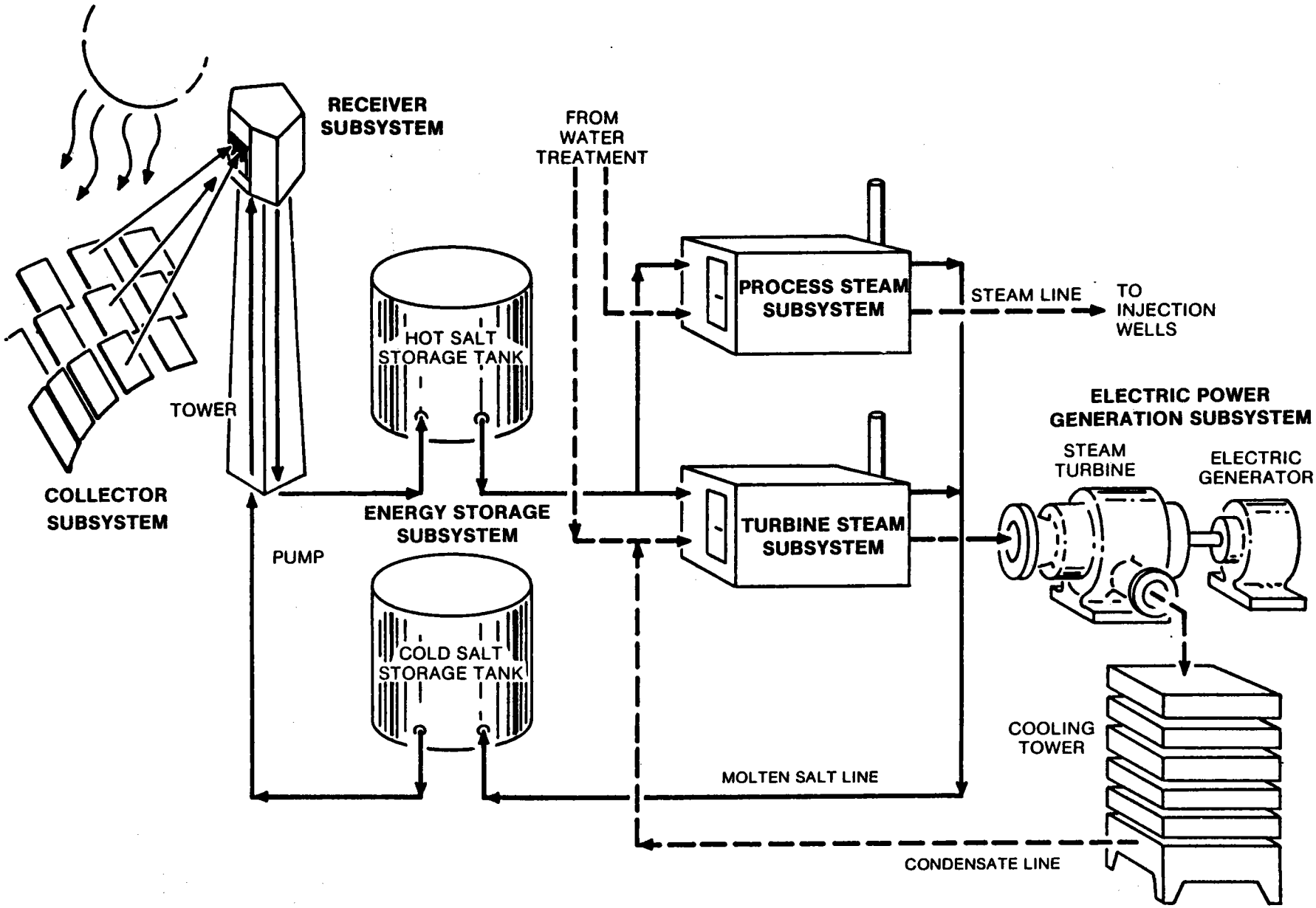

Figure 4.1-1 Facility Diagram

The two steam generation systems share water well storage facilities, but have separate water treatment systems. The process only requires softening while the turbine makeup water must be very clean to prevent damage to the turbine blades.

The turbine generator is a nominal 20.4 MW_e single reheat machine with six stages of regeneration. The electric power produced (18.3 MW_e net after powering the solar field) is sold to PG&E. Transformers, breakers and other protective circuitry on site protects the two systems from electrical faults on the other.

4.2 FUNCTIONAL REQUIREMENTS

Anticipated steam drive operations at the Edison field will require 40,000 kg/hr (88,000 lbm/hr) of 80% quality 293°C (560°F) steam. Two 7.33 MW_t (25 MBtu/hr) crude oil fired steamers will provide about half of this requirement. Production of the remaining 20,000 kg/hr of steam is the principle process operating requirement of the Solar Cogeneration Facility. In addition, the facility will use the energy collected in excess of the process requirements to generate electricity. Most of the electricity will be generated during those periods of the day which will result in the greatest economic return.

The facility will use local ground water for both process and turbine steam makeup. All equipment will be built to survive the climatic and seismic environment at Edison during the expected 26 year facility life.

On the design summer day (day 189 of the SOLMET-TMY weather tape for Fresno, CA) the facility will provide 24 hours of process steam at rated capcity and 14 hours of electric power at rated capacity.

The Solar Cogeneration Facility (with the exception of the fossil steamers) will be monitored and controlled by a master control subsystem that consists of 6 functional subsystems, a data acquisition subsystem, and an emergency control subsystem.

Fossil steamers currently exist at the site and the control hardware is established and operating. These steamers will be manually operated. Indicator lights will be provided in the control room to verify operation of the fossil steamers.

The general design approach for the master control subsystem uses the supervisory control concept. The six plant distributed digital control systems are responsible for first level control functions while the supervisory computer of the operational control subsystem prescribes the proper operating instructions (e.g., set points) so that desired operational objectives can be met. Normal plant control is completely automatic but the human operator may intervene if desired. The emergency control subsystem will intervene to respond to programmed emergency conditions.

The data acquisition subsystem will provide for recording of system variables independent of control system functions and also allow variables to be scanned during operation. This data will be recorded on either disk or magnetic tape and provide a long term record of plant performance.

A complete listing of detailed requirements is contained in the systems specification Appendix A.

4.3 DESIGN AND OPERATING CHARACTERISTICS

The three major facility elements, solar energy collection, the process steam generation and electric power generation, will be capable of independent operation using the energy storage as a buffer.

When not operating, the turbine will be kept warm (blanketed) if the shut down period is for only a few hours or days in order to reduce start up time. When shut down for longer periods the turbine system will not be kept warm.

Each of the subsystems will have the following modes of operation:

(1) Normal Operation
(2) Warm Not Operating
(3) Cold Not Operating
(4) Start Up (from Warm or Cold Not Operating)
(5) Shut Down

Each subsystem will be capable of these modes, independent of the modes of the other subsystems as long as sufficient storage capacity remains available.

The operation of the steamers is completely independent from the Solar Cogeneration Facility.

The system process flow diagrams and system energy balance are shown in Figures 5.6-1, 5.8-1 and 5.7-1 (Section 5) and are discussed respectively in sections 5.6.2.1, 5.8.2.1 and 5.7.

The subsystem design and operating characteristics are summarized in table 4.3-1.

4.4 SITE REQUIREMENTS

The site as it exists is well suited to the installation of the Solar Cogeneration Facility. The flat terrain will require little or no grading. No large structures or trees must be removed. Over head electric power lines can be

Table 4.3-1

Conceptual Design Summary Table

1. Site Location: Exxon Edison field near Bakersfield CA

2. Facility Characteristics:

a.	Turbine type:	Single reheat, condensing turbine generator, 20.4 MW_e gross output.
b.	Turbine inlet condition:	538°C (1,000°F), 8.27 MPa (1,200 psia)
c.	Turbine exhaust condition:	38°C (101°F), 7 kPa (2 in. Hg).
d.	Process fluid and purpose:	80% quality steam for enhanced oil recovery
e.	Process fluid conditions:	293°C (560°F), 7.6 MPa (1,130 psia), 26 MW_t

3. Receiver:

a.	Receiver fluid:	Molten Salt 60% NaNO/40% KNO_3 by weight
b.	Configuration:	Two Cavity
c.	Temperature:	288°C (550°F) inlet, 566°C (1050°F) outlet
d.	Pressure:	2.5 MPa (363 psia)
e.	Tower:	137 m (450 ft) conical concrete

4. Collector Field:

a.	No. of heliostats:	3295
b.	Mirror area per heliostat:	57.4 m^2 (618 ft^2)
c.	Type:	Martin Marietta Second Generation
d.	Field configuration:	3.1 rad (180°) North Field
e.	Total mirror area:	189,133 m^2 (2.03 x 10^6 ft^2)
f.	Total collector field area:	1,300,000 m^2, (320 acres)

5. Storage:

a. 380 MWh_t capacity
b. Molten Salt, 60% $NaNO_3$/40% KNO_3

6. Project Cost, including all capital, startup, and checkout cost but excluding O & M: $120 million.

7. Solar Cogeneration Facility Contribution on Design Day 189:

a. Design Point; Noon, Day 189, 0.95 kW/m^2

1.	Receiver output:	122 MW_t, 460% of process thermal demand
2.	Elecctrical energy:	20.4 MW_e gross, 18.3 MW_e net after 2.1 MW_e plant demand (100%)
3.	Process energy:	13.2 MW_t + 2.55 MW_t preheat to fossil steamers, 60% of process thermal demand

b. Design Day; Day 189 of Fresno, CA, TMY data

1.	Receiver output:	1145 MWh_t, 181% of process thermal demand
2.	Electrical energy:	286 MWh_e gross, 256 MWh_e net after 29.4 MWh_e plant demand (100%) during 14 hours of turbine operation
3.	Process energy:	352 MWh_t, 56% of process thermal energy

7. Solar Cogeneration Facility Contribution on Design Day 189 (Continued)

c. Annual, Based on Fresno, CA, TMY data

1.	Receiver output:	244,000 MWh_t, 116% of process thermal demand
2.	Electrical energy:	47,900 MWh_e gross, 43,000 MWh_e net to grid after 100% of plant electric demand during turbine operation
3.	Process energy:	105,600 MWh_t, 50% of process thermal demand

8. Annual Cogeneration Utilization Efficiency:

$$\frac{\text{Facility Net Electrical and Thermal Energy Production}}{\text{Facility Total Energy Input}}$$

$$= \frac{110{,}000\ MWh_t\ (\text{Fossil}) + 105{,}600\ MWh_t\ (\text{Solar}) + 43{,}000\ MWh_e\ (\text{Solar})}{145{,}000\ MWh_t\ (\text{Fossil}) + 287{,}200\ MWh_t\ (\text{Solar})}$$

$$= 0.60$$

re-routed and re-installed in ground level conduits. The solar collector field as designed accomodates existing and planned oil field operations, including drilling, maintainence and steaming.

Two existing portable steamers will be permanently mounted at the site. These will share a common header with the solar process steam subsystem which is the principle mechanical interface between solar and existing facilities.

New facilities include the collector field, receiver tower, storage tanks, piping, pumps, heat exchangers, turbine generator and two buildings to house the turbine and master controller, and a facility maintenance shop. No existing buildings or structures need be modified or moved to accomodate the Solar Cogeneration Facility.

A plot plan of the site showing the location of the solar facility elements is shown in figure 4.4-1.

4.5 SYSTEM PERFORMANCE

4.5.1 Receiver/Collector Performance

The design point and annual performance of the conceptual design of the Solar Cogeneration Facility was evaluated using three computer models--DELSOL, TRASYS and STEAEC. The performance of the receiver/collector subsystems were modeled separately. These results were input to the STEAEC system simulation program together with typical insolation and weather data to model the annual performance of the system at the Edison field site.

The receiver losses were evaluated using the TRASYS thermal radiation analysis model for the design point and off design point cases. The thermal losses in the receiver downcomer were calculated based on the tower piping and insulation optimization studies.

Resulting system performance stairstep for noon, day 24 is shown in figure 4.5-1 and for noon, day 189 (design point) in figure 4.5-2. The overall solar system efficiency for noon, day 24 is 67%, and for noon, day 189 is 65%.

The annual system performance was evaluated using the STEAEC system model, which simulates the performance of the system using 15-minute time steps and a site weather data tape. For the site weather data (insolation, wind speed and direction, and temperature), the SOLMET typical meteorological year (TMY) for Fresno was used. Fresno is approximately 100 miles northeast of the selected site, but is representative of the San Joaquin Valley Region. This assumption has veen validated for a by total horizontal and direct normal insolation measurements which were taken at the site by Exxon for the entire year 1980 (see Appendix B). The SOLMET data, recorded on the tape at 1-hour intervals, were

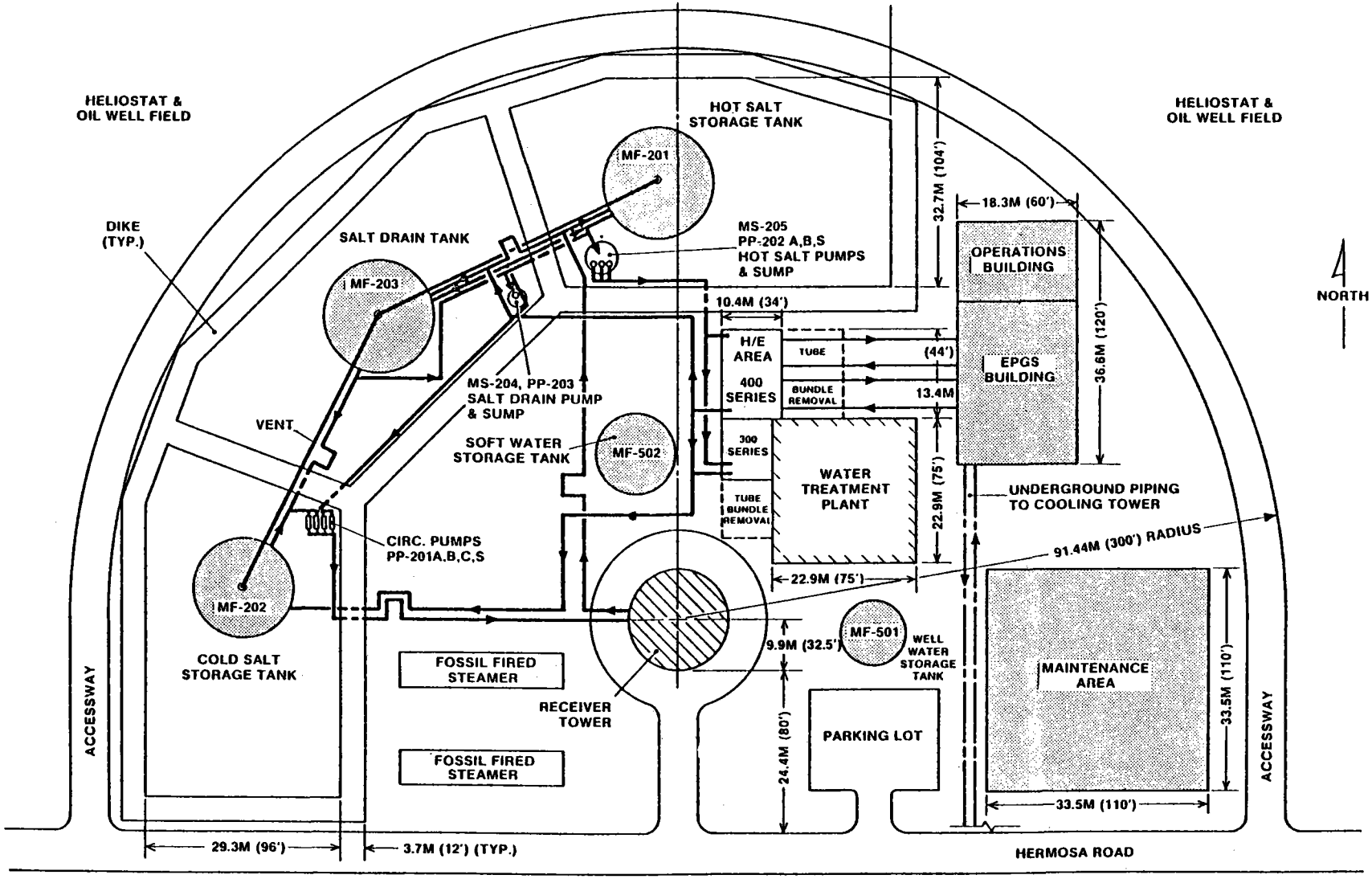

Figure 4.4-1

Plot Plan - Solar Cogeneration Facility
Edison, California

converted to 15-minute interval data using linear interpolation techniques before input to the STEAEC model for a more realistic evaluation of system performance. These SOLMET data yield an average daily direct normal insolation value of 6.21 kWh/m^2-day. The annual solar subsystem performance stairstep is shown in Figure 4.5-3.

The annual energy derived from the solar subsystem and delivered to the bottom of the tower, as shown in the figure, is 244,000 MWh_t (8.29×10^{11} Btu) yielding an annual net solar system efficiency of 57%.

4.5.2 Balance of Facility Performance

The Solar Cogeneration Facility is designed to produce process heat 24 hours day. The remainder of the available energy is used to produce electricity.

The molten salt storage system (380 MWh_t capacity) allows the time of the period of electric operation to be varied somewhat. It is assumed that on-peak power is always produced to the full extent possible with excess energy used for partial peak power. This will maximize electric revenues.

During the low insolation months of December and January so little excess energy is available for production of electricity that the value of the energy used to keep the turbine warm during non-operational periods (turbine blanketing) exceeds the value of electricity produced. Therefore, in our operating plan the EPGS will be shut down during these months. This will provide a fixed time for regular maintenance of the system.

It is necessary to determine the daily energy use pattern in order to properly allocate electrical energy to the peak or off-peak periods. This is essential for a more accurate electric revenue estimate.

Using the solar system efficiencies (for Day 24 and Day 189), the amount of energy collected on each day of the Fresno TMY Data tape was calculated. For each day the available energy was allocated among system losses, process heat, process preheat, turbine, and turbine blanketing. From this the total amount and distribution of power was developed.

The basic energy consuming processes were defined as follows:

Heat to turbine when operating	56.05 MW_t
Gross electric production	20.4 MW_e
Average electric parasitic power	2.1 MW_e
Heat to turbine when not operating (turbine blanketing)	1.6 MW_t
Process heat (with no preheat)	13.21 MW_t
Process heat (with turbine extraction preheat)	10.89 MW_t
Average daily system heat loss (after tower base)	14.2 MWH_t

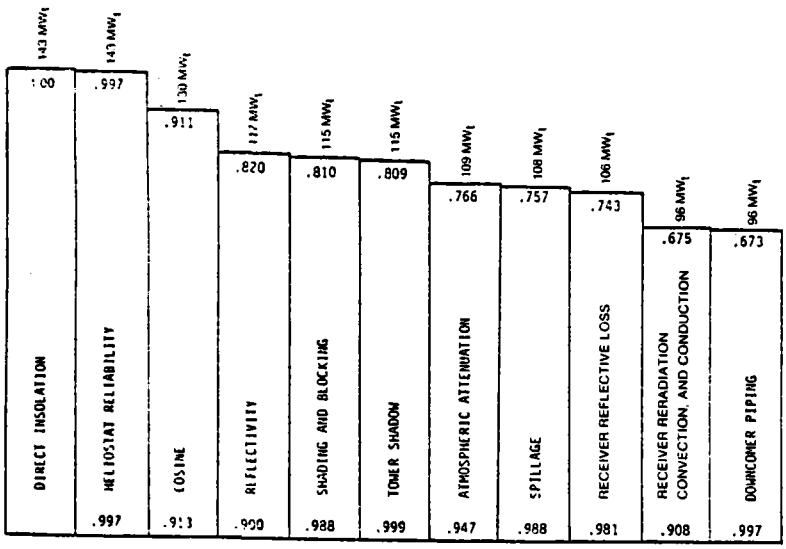

Solar System
Performance Stairstep
Noon, Day 24

Figure 4.5-1

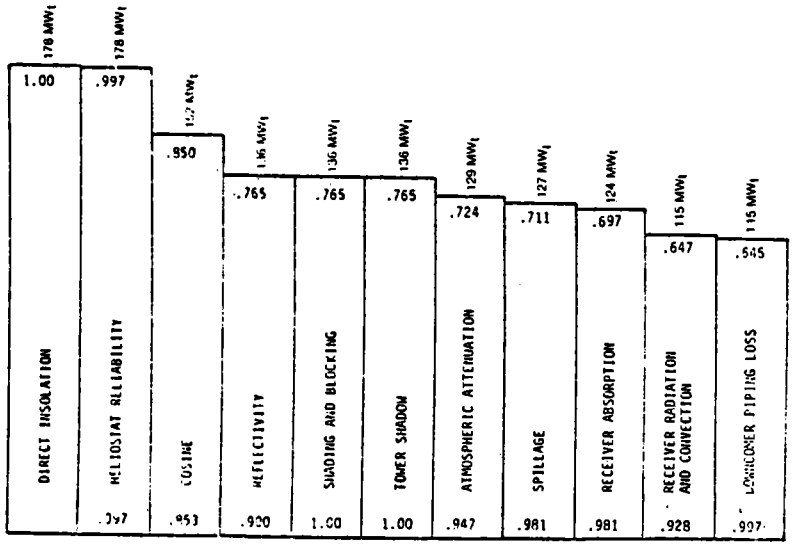

Design Point Solar
System Performance
Stairstep
Noon, Day 189

Figure 4.5-2

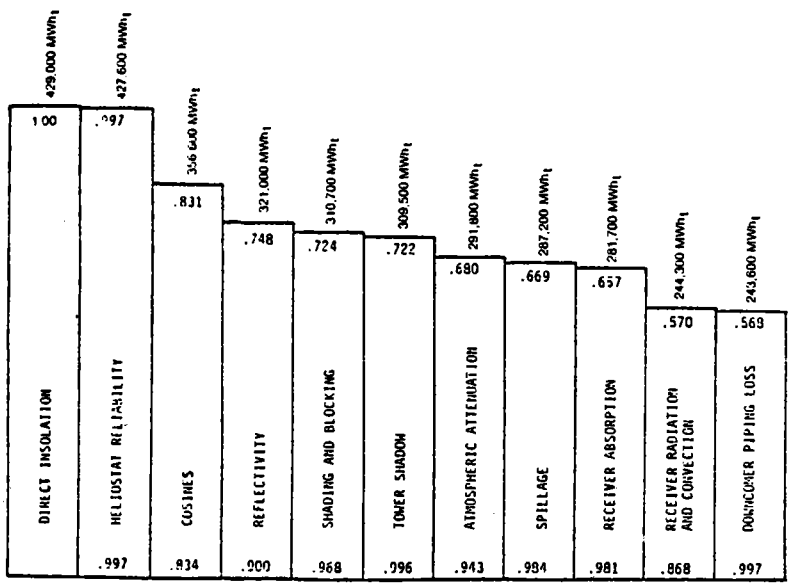

Solar System
Annual Performance

Figure 4.5-3

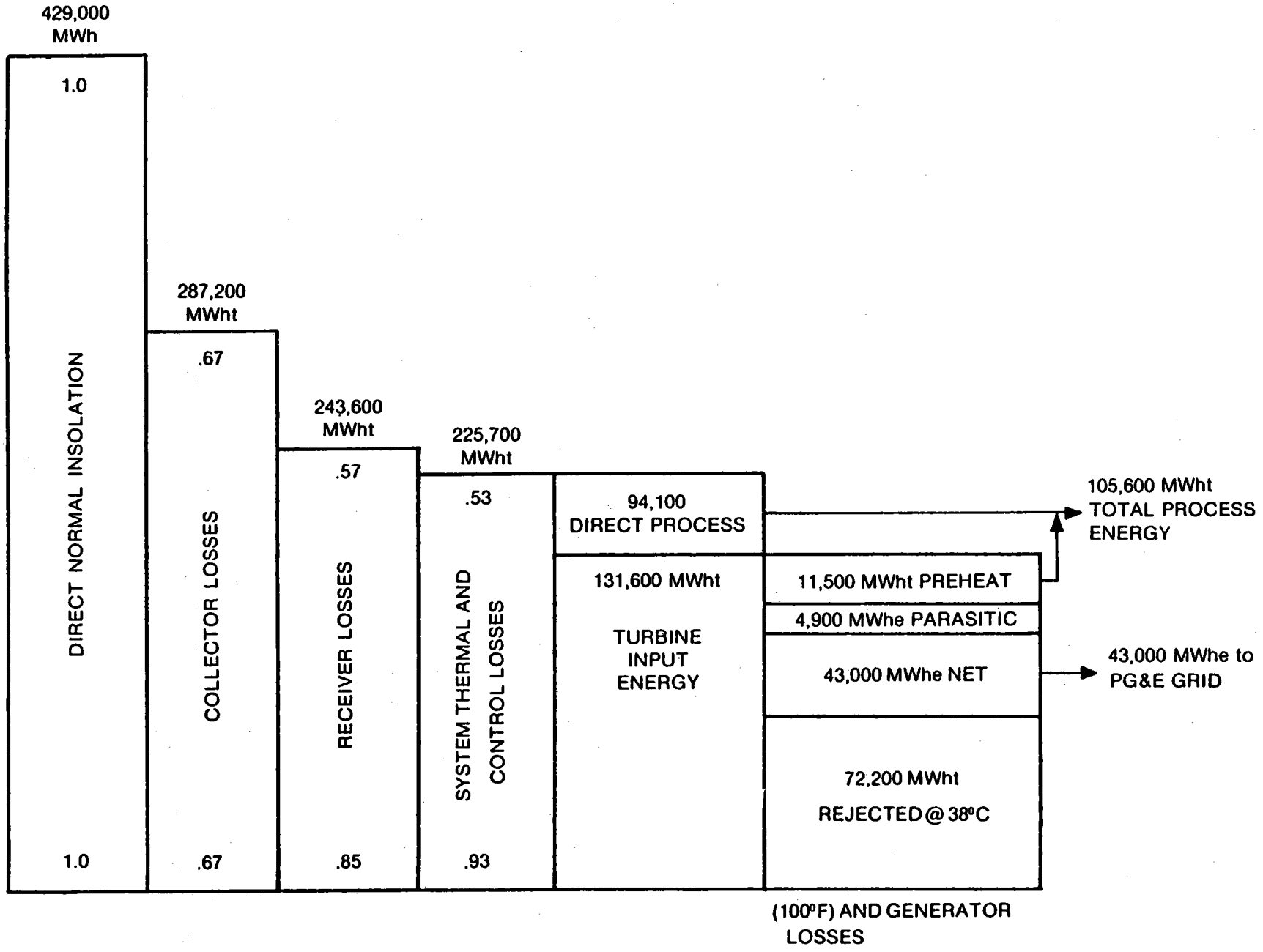

Figure 4.5-4

Solar Cogeneration Facility Annual Performance

Thus for each day if h_t is the number of hours of turbine operation:

Total Collected Energy = (Heat to Turbine x h_t) +
(h_t x process heat, turbine operating) +
((24-h_t) x process heat turbine not operating) +
((24-h_t) x turbine bleed) + Thermal Losses.

Using the above values and re-arranging:

$$\text{Hours of turbine operaton} = h_t = \frac{(\text{Total Collected Energy} - 370\ \text{MWH}_t)}{(52.13)}$$

The hours of turbine operation are allocated to on-peak, partial-peak, and off-peak periods by assuming that the facility is operated to produce as much on-peak electricity as possible with the balance partial-peak. Off-peak electricity is produced only on Sundays and Holidays which were arranged randomly 4 or 5 to each month. This calculation was repeated for each day resulting in the annual energy and power totals in Figure 4.5-4.

The facility would annually produce 237,100 MWh_t (includes turbine inlet energy, direct process energy and process preheat energy) which results in displacing 43,000 MWh_e on the PG&E system, and 105,600 MWh_t at the Edison field. This is equivalent to 139,500 barrels of fuel oil.

The Cogeneration Utilization Efficiency (CUE) is defined as:

$$\frac{\text{Facility Net Electrical and Thermal Energy Production}}{\text{Facility Total Energy Input}}$$

or

$$\frac{MWh_t + MWh_e}{MWh_f + MWh_s}$$

where

MWh_t = Total useful thermal energy, annual
MWh_e = Net useful electric energy, annual
MWh_f = Energy content of fossil fuel to steamers including scrubber, annual
MWh_s = Solar energy incident on the receiver aperture, annual

The CUE for this facility is:

$$CUE = \frac{110{,}000\ MWh_t + 105{,}600\ MWh_t + 43{,}000\ MWh_e}{145{,}000\ MWh_f + 287{,}200\ MWh_s} = 0.60$$

4.6 ENERGY LOAD PROFILE

The nature of this design is such that the dispatch of energy varies literally day to day, depending on the amount of solar energy collected. There are no regular cycles of energy use.

For any given day the two fossil fired steamers produce 13.2 MW_t of steam for 24 hours as they do every day regardless of solar system operation. When the turbine is operating, however, the fuel rate to the steamers decreases because the feedwater is partially preheated by turbine extraction. The balance of the process energy is provided by the solar process heat system if sufficient solar energy is available on the given day, up to the design process requirement of 26.4 MW_t. On days when enough solar energy is not available, the total daily steam injection is reduced. The fossil fired steamers do not have the capacity to make up the deficiency. Thus the solar energy available sets the amount of total injection steam, while demand for the steam remains constant 24 hours a day year round (the demand is not met on cloudy days).

The energy dispatch for the summer design day is shown graphically in Figure 4.6-1.

Most of the bulk of electric power required to operate the facility is generated by the Solar Cogeneration Facility itself (up to 2.1 MW_e). Again in this case the daily solar availability determines electric energy production. Excess power is sold to PG&E on an as available basis.

4.7 CAPITAL COST SUMMARY

The cost account breakdown for the major subsystems in the solar cogeneration facility is shown in Table 4.7-1.

The subsystem cost account boundaries are shown in the facility diagram of figure 4.7-1. Additional information on direct costs for all major equipment and the estimate basis and exclusions is given in section five of Appendix A.

The major assumptions made in estimating the Solar Cogeneration Facility is given in table 4.7-2.

The total erected facility cost estimate is $120 million and the major subsystem costs are shown in Figure 4.7-2, assuming all indirect costs are allocated among the subsystems. As figure 4.7-2 illustrates, the major facility cost elements are the solar collectors (46%), energy storage (16%), electric power generation (13%) and solar receiver (10%), which account for 85% of the facility cost.

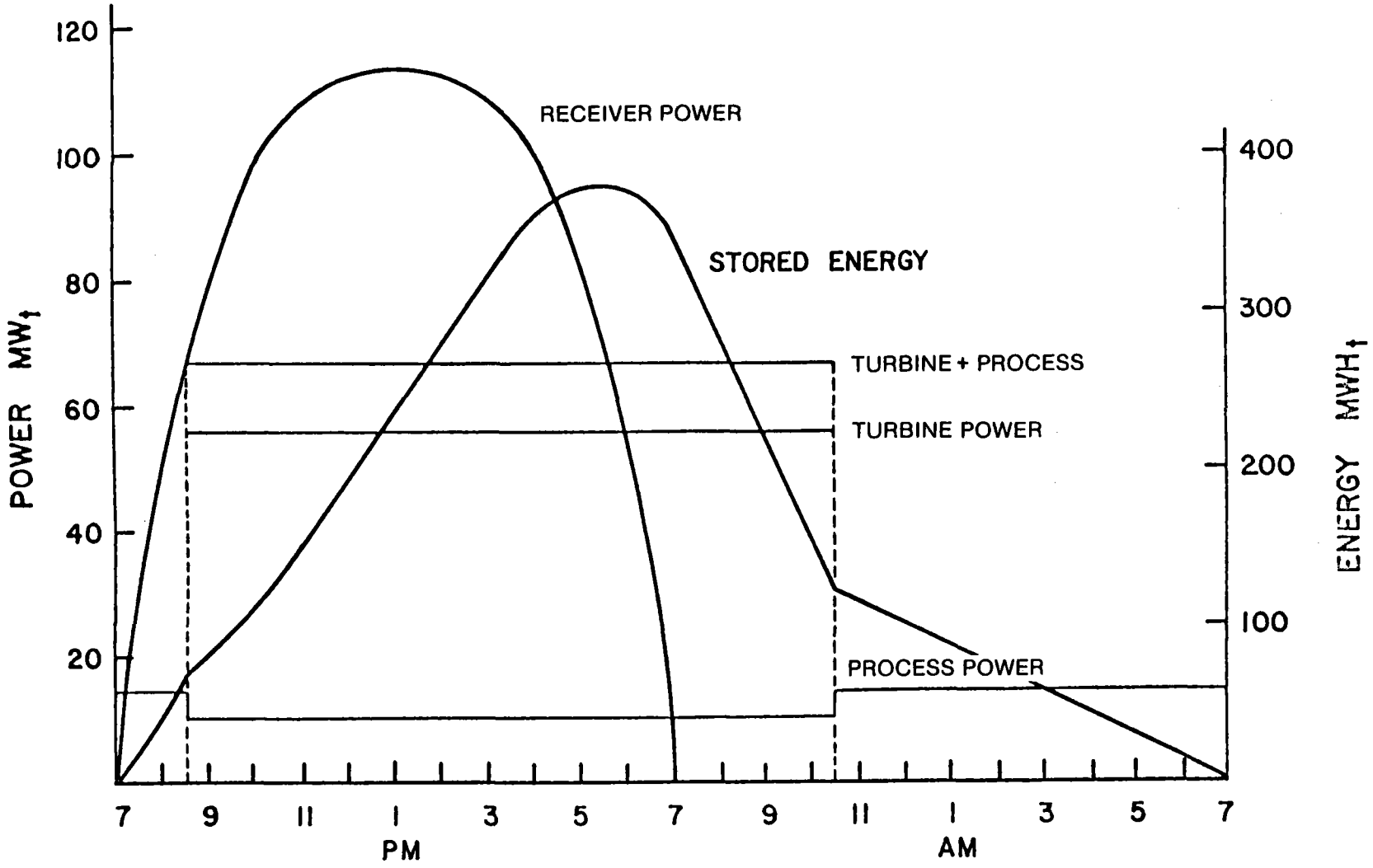

Figure 4.6-1 Energy Dispatch on Design Day

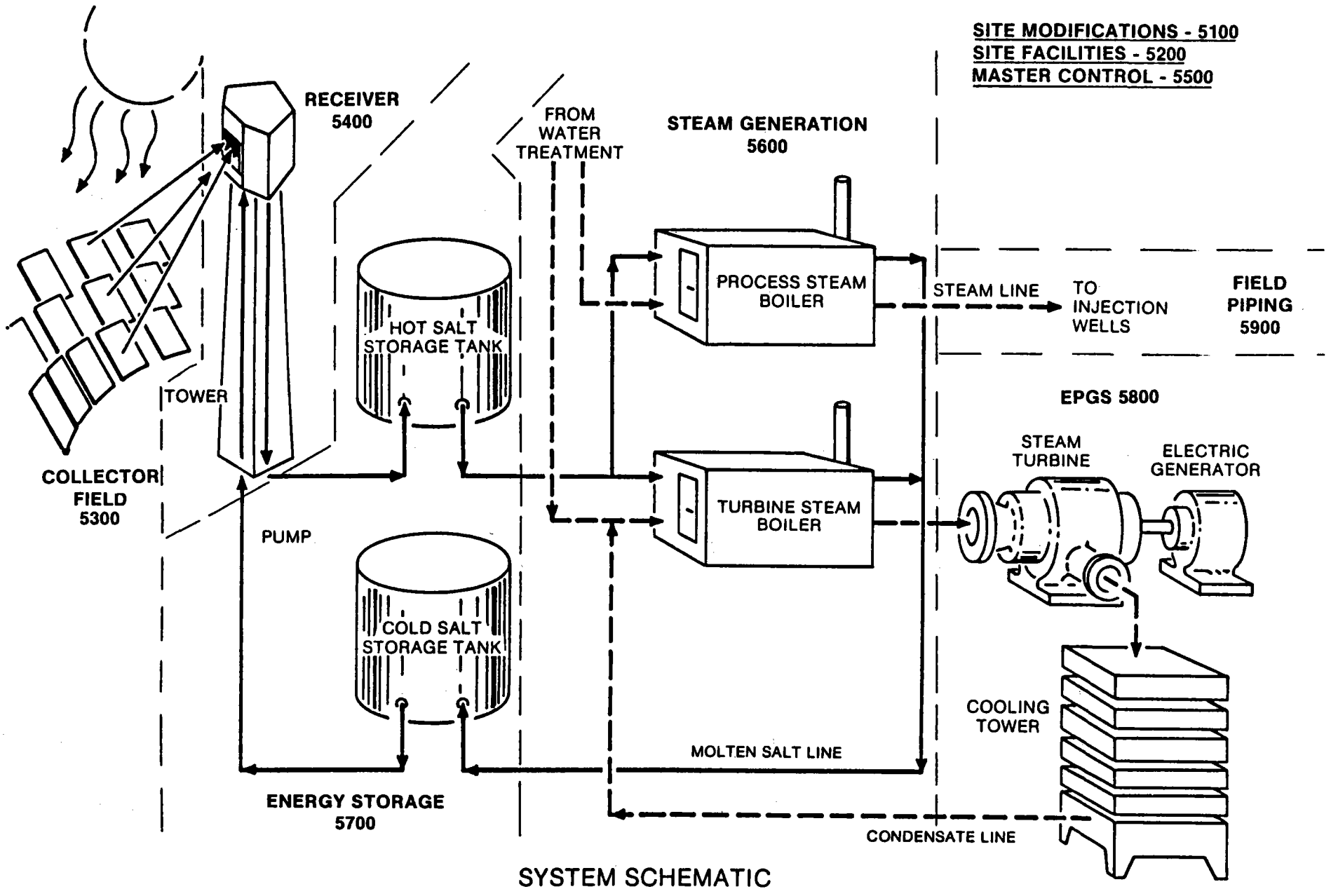

Figure 4.7-1 Cost Account Boundaries

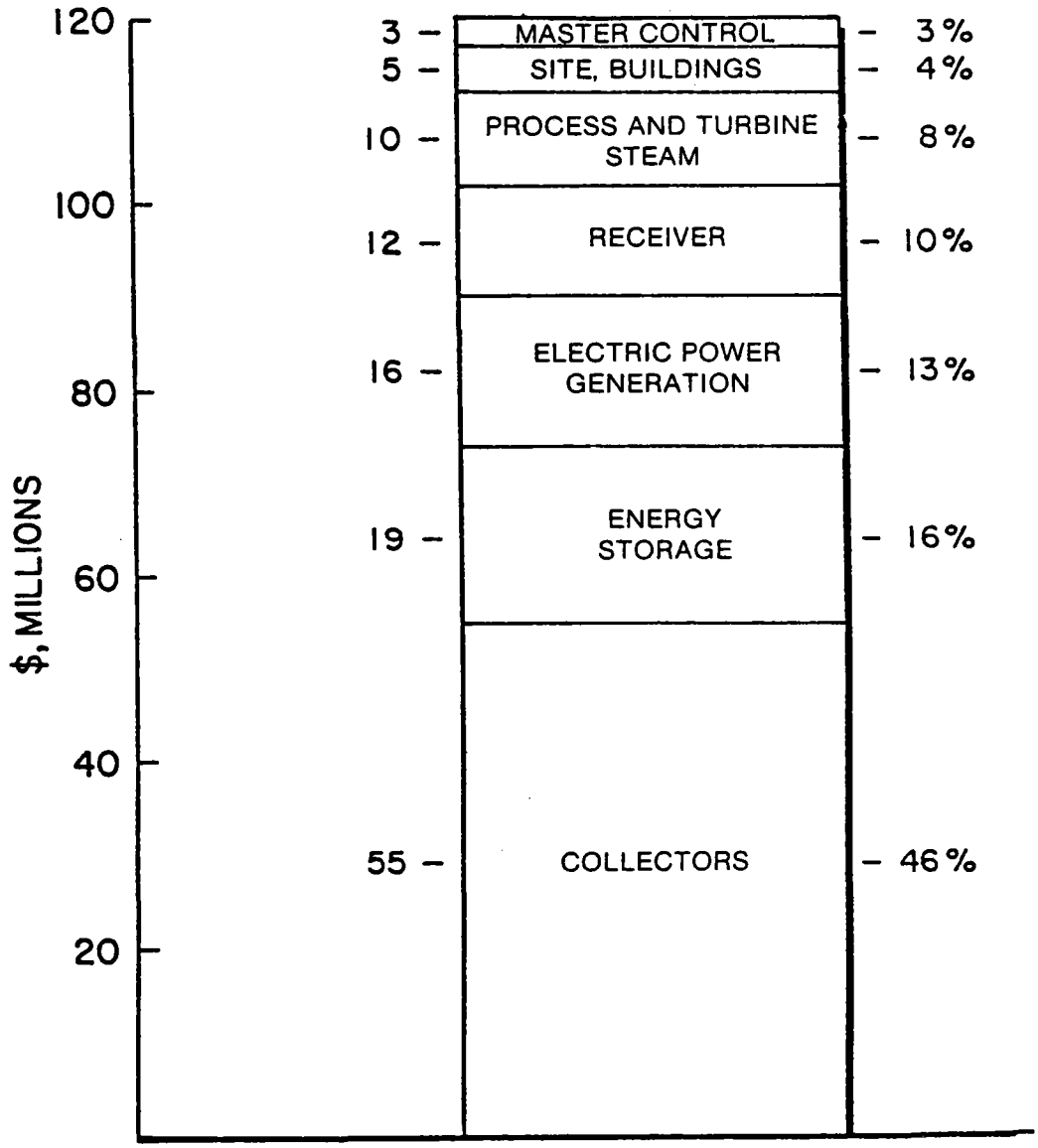

Figure 4.7-2

Facility Cost Breakdown

Table 4.7-1 Cogeneration Cost Accounts

5000	Solar Cogeneration Facility
5100	Site Modifications
5200	Site Facilities
5300	Collector Subsystem
5400	Receiver Subsystem
5500	Master Control Subsystem
5600	Process and Turbine Steam Subsystems
5700	Energy Storage Subsystem
5800	Electric Power Generation Subsystem
5900	Field Piping

Table 4.7-2 Cost Estimate Assumptions

- All costs in mid 1980 $
- Plant location is Bakersfield, CA for material prices and wage rate.
- Estimate includes:

    o installation and check-out
    o indirect costs
    o 25% construction contingency

Estimate Excludes:

    o sales tax, escalcalation
    o design contingency
    o allowance for funds during construction (AFDC)

A facility cost breakdown which reflects the method used to prepare the cost estimate is given in Table 4.7-3 and compared to the standard DOE account structure (column I) in Table 4.7-3. The direct equipment costs are shown according to the account codes and the indirect costs, contingency and owner's project management costs are shown separately (column II). In preparing the cost estimate, the direct costs are totaled first and indirects, contingency and project management costs are added to the direct costs. These "indirect" costs are developed for the entire project and are not normally divided among the major direct cost elements.

Despite the large size of the heliostat field, the heliostat direct costs are only 52% of the total direct costs, due to the requirement to generate electricity which has in turn a strong impact on energy storage and salt/steam heat exchangers.

The heliostat portion of the facility cost estimate was estimated for three cases: The base case, explained previously which uses heliostat direct cost estimates of $\$203/m^2$ installed, a case in which heliostats would be supplied free of charge to the site and cost $\$40/m^2$ to install and the Sandia specified heliostat cost case of $\$260/m^2$ which is taken to be a direct installed cost. Resulting facility cost estimates are shown in Table 4.7-4.

Table 4.7-3 Cogeneration Facility Cost Estimate Breakdown (1980 $)

Account	Item	1980 $ Millions I DOE Format	1980 $ Millions II Separate Costing
5100	Site Improvements	1	0.5
5200	Site Facilities	4	2.5
5300	Collector Subsystem	55	38.5
5400	Receiver Subsystem	12	5.5
5500	Master Control Subsystem	3	2.0
5600	Steam Generation Subsystems	10	5.0
5700	Energy Storage Subsystem	19	11.0
5800	EPGS	16	9.0
5900	Field Piping	0.2	0.2
	Total Direct Cost		74
	Indirect Costs (Field Overheads, Engineering, Fee)		18
	Owner Project Management Service		4
	Subtotal		96
	Construction Contingency @ 25%		24
	Total Project Cost	120	120

Table 4.7-4 Cost Estimate, Three Heliostat Assumptions

Case	Heliostat Costs, $/m^2		Total Facility
	Direct	Including Indirects	Cost $ Million
Base Estimate	203.	290.	120.
Installation Only	20.	40.	75.
Sandia Specified	260.	370.	135.

The impact of facility cost and other economic parameters on project energy costs is discussed in detail in section 6.

4.8 OPERATING AND MAINTENANCE COSTS

The estimated first year operating and maintenance (O&M) costs for the solar cogeneration facility are summarized in this section. Section 6.0 of this report shows how sensitive the facility energy costs are to O&M costs. The O&M first year cost summary is given in Table 4.8-1. The estimated first year maintenance for the facility is $2.4 million/year which is 2% of the baseline capital cost estimate.

The maintenance categories are explained in the following subsections.

4.8.1 Operations

This category includes all subsystem and system operating personnel for three shifts each day of the year. Operating consumables includes water treatment chemicals, and electricity which must be purchased from PG&E when the turbine generator is not operating.

4.8.2 Maintenance Materials

Includes all spare parts for the major facility subsystems. About half of this cost is due to the spare parts requirements of the heliostat field.

4.8.3 Maintenance

Includes fulltime maintenance technicians to service computer, instrument repair, heliostat receiver and turbine equipment. The cost of regularly scheduled maintenance activities such as heliostat washing (twice per year, at $60 per heliostat per year) is also included.

Table 4.8-1 Operating and Maintenance Cost Summary (1980 $ Millions)

OM 100 Operations		0.8
OM 110 Operating Personnel	0.5	
OM 120 Operating Consumables	0.3	
OM 200 Maintenance		0.6
OM 210 Spare Parts and Materials	0.6	
OM 300 Maintenance		1.0
OM 310 Scheduled Maintenance	0.3	
OM 320 Maintenance Personnel	0.7	
Total First Year Operating and Maintenance ($ Million)		2.4

4.9 SUPPORTING SYSTEM ANALYSES

The facility as designed and costed contains significant redundancy which will reduce lost operational time; failure of even a few hundred heliostats would have a small effect on operations, the dual cavities of the receiver can be operated independently so that failure of one does not prevent operations. The storage system drain tank can replace either the hot or cold salt storage tank in normal operations. Redundancy is provided in pumps and control system components.

The intermittent nature of operation provides regular opportunities for maintenance without interrupting operations. The solar collection subsystems, turbine steam and turbine generator are not used at night, the turbine generator and turbine steam subsystem are shut down entirely during the months of December and January during which thorough maintenance activities can be carried out.

Health and Safety

The heliostat field presents hazards of relected sun light to facility personnel and passers by. The entire facility will be surrounded by a fence to protect ground level traffic from mis-directed light.

Heliostat safety provisions are discussed in detail in Appendix D.

The molten salt would present a hazared to personnel in the event of leaks. Diking of the storage tanks and control of personnel access to the site will keep these risks to a minimum. The salt itself does not present a fire hazard, is not highly toxic or reactive and indeed presents many fewer problems than materials routinely handled in chemical and refinery plants. Protective clothing and safety training will be provided all personnel. No safety or health dangers of an unusual or unique type will exist at the plant. The facility will meet or exceed all federal and state safety regulations.

The proposed site is currently in active oil production. The land surface is being used for agricultural purposes.

The primary land use effect would be to remove 320 acres of farmland from production. Ground water currently available and being used for steam stimulation activities at the site is sufficient for the proposed steam drive operations. Displaced agricultural water will be used in the cooling tower.

The use of this solar power system will eliminate the need for two fossil-fueled boilers planned for the site, and not increase air pollution emissions accordingly.

The particulate emissions associated with agricultural operations at the site will be reduced. The only increase in emissions will be water from the cooling tower. Such emissions are currently not regulated.

The chief visual impact will be the receiver tower, which will stand out against the flat landscape and be visible for many miles.

The effect on the local society will be minimal. Bakersfield, a large industrial city, is only a few miles distant and is well able to support the personnel and services the facility would require.

After the construction phase is completed, the system will produce little noise and cause insignificant new traffic.

Accidental release of the receiver fluid would be contained on site and would be disposed of according to accepted procedures.

Waste water from the water treatment plant will be reinjected into the ground in accordance with local regulations.

The regulatory bodies who have authority at the site have been contacted. In addition to those listed, a Federal Environmental Impact Report would be required if government funds were involved:

1) The receiver tower will require a zone variance from the Kern County Planning Department. Two forms are required. The application requires a description of the project, of the property, three copies of a plot plan, and submittal of an Environmental Assessment form;

2) The FAA must approve any construction greater than 61 m (200 ft.) above ground level. FAA form 7460-1 must be filed 30 days before the application to construct is filed. A map showing the relationship of the site to the nearest airport is required;

3) Building permits are required by the Kern County Building Inspection Office for the buildings, heliostat structures and the tower. Two sets of design and plot plans approved by a California registered civil engineer must be included for the heliostat foundation and the tower.

The following agencies do not require permits to be issued:

1) Division of Oil and Gas:
2) Kern County Air Pollution Control Board:
3) California Air Resources Board.

5.0 SUBSYSTEM CHARACTERISTICS

In this section, each of the Solar Cogeneration Facility subsystems is described in detail including a discussion of the functional requirements, design, operating characteristics, performance estimates and a top level cost estimate.

5.1 SITE FACILITIES

The Solar Cogeneration Facility requires several permanent buildings and structures. These buildings and all the cogeneration subsystem elements, except the heliostat field and cooling tower, are shown in the facility plot plan of Figure 5.1-1. This plan shows the major equipment locations in the exclusion area around the base of the receiver tower. This space is bounded on the south by Hermosa Road and extends about 91 meters from the tower base.

Included in the site facilities are the operations building, with 230 m^2 (2,400 ft^2) of space to house the facility master control subsystem and operating personnel; a 1,100 m^2 (12,000 ft^2) maintenance building to service the entire facility; access roads separating the facilities area from the heliostat field and a parking lot and perimeter fencing surrounding the entire heliostat field for security and glare protection.

The estimated direct cost of the site facilities (Account 5200) is $2.5 million, and the site improvements (grading, roads, Account 5100) is $0.5 million.

5.2 COLLECTOR SUBSYSTEM

5.2.1 Overall Design

The cogeneration collector field consists of 3295 Martin Marietta second-generation heliostats. This heliostat design complies with the performance requirements defined by Sandia Laboratory's Requirements Specification A10772, Issue D, as summarized in Table 5.2-1. Any additional improvements resulting from the ongoing development program for this heliostat will be incorporated and the customer will benefit from all of these changes.

The heliostat design, as shown in Figure 5.2-1, incorporates 11 flat or focused and individually canted mirror assemblies mounted on a rigid, lightweight rack assembly structure. The heliostat reflective surface is driven using a two-axis gear drive (azimuth and elevation), with individual two-speed dc motors for each axis. Each of the 10 full-size mirror assembly is approximately 3.6 x 1.5 m (12 x 5 ft). The half size mirror assembly is the same length but only half width.

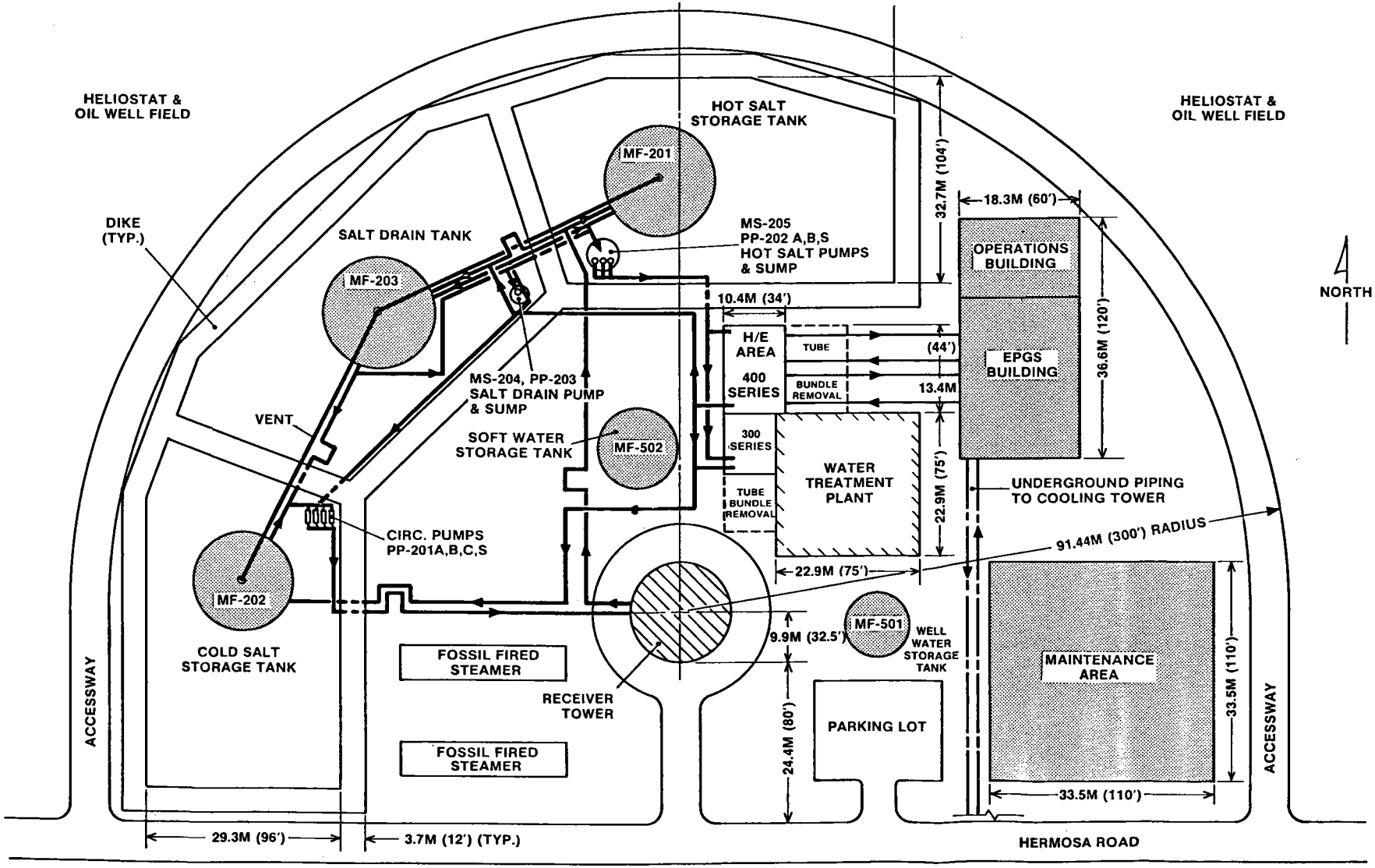

Figure 5.1-1 Plot Plan - Solar Cogeneration Facility

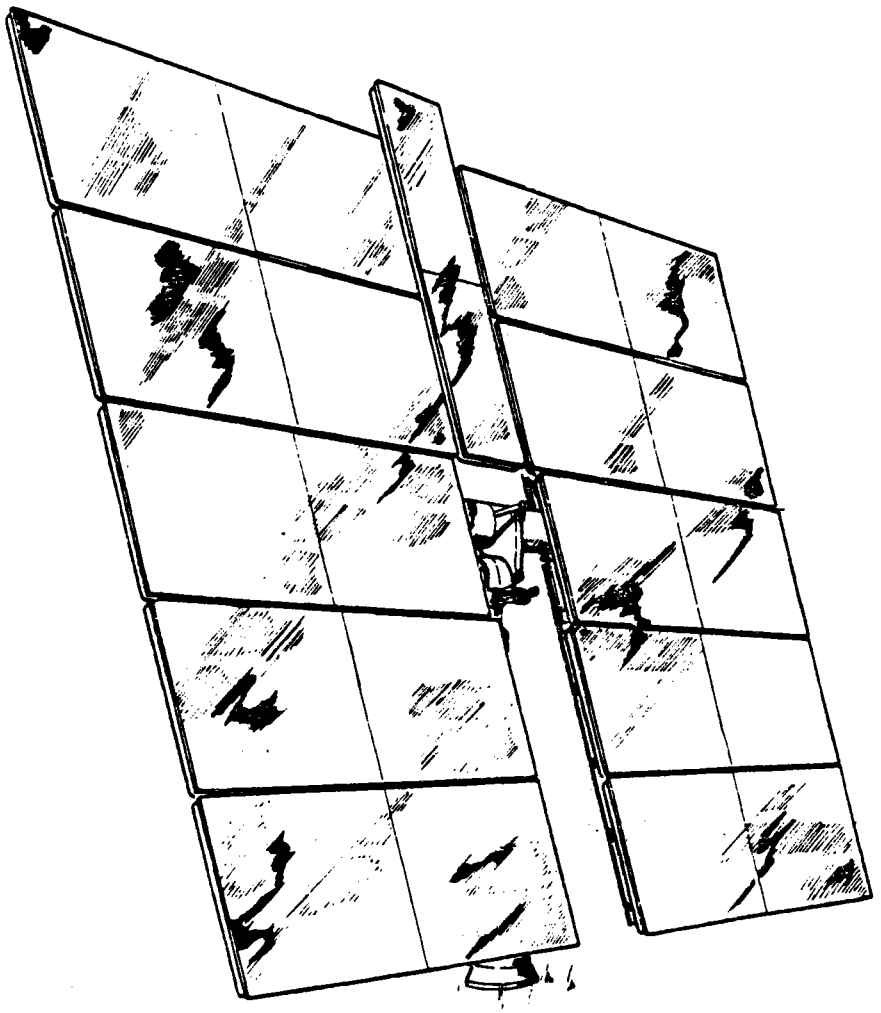

Figure 5.2-1 Second Generation Heliostat - Front View

The mirror assemblies are designed to use 1.5-mm (0.060-inch) fusion glass second surface mirrors that will provide a reflectivity of up to 96%. The mirror-supporting structure is a steel/honeycomb/steel sandwich. To achieve an optimum low-cost design, the honeycomb material is a phenolic impregnated paper. This provides a design with maximum rigidity and minimum weight and cost.

The mirror assemblies are arranged to allow the heliostat to be positioned in a mirror-face-down stow attitude. This important feature gives added protection to the mirrors from adverse weather, particularly frost and wind/rain/dust conditions that could easily dictate an unscheduled mirror washing operation prior to developing full plant power. In addition, although the mirror assemblies have not been tested beyond the 1-in. hail diameter requirements, the face-down mirror assemblies should be able to withstand much larger size hail without damage of the reflective surface because of the shock absorbing characteristics of the steel/honeycomb/steel support structure.

Figure 5.2-2 shows the rear view of the heliostat with the subassemblies and nomenclature identified. The reflective assembly consists of the rack assembly with the 11 mirror assemblies installed.

Table 5.2-1 Performance Summary of Second-Generation Heliostat

Item	Requirement	Baseline System	Remarks
Maximum Beam Pointing Error	1.5-mrad Standard Deviation Each Axis Reflected beam Sun 0.26 rad above horizon Gravity effect included No wind	≤1.5 mrad	Control system is baselined as the Phase I, 10-MWe system. Demonstrated by Sandia test to meet specified requirement.
Beam Quality	2.0-mrad Standard Deviation Each Axis Reflected beam	≤2.0 mrad	Design meets required error budget allocation - See Table 2.1-1.
Reflective Surface	1.7 mrad (1σ) for Normal Operation 12 m/s (27 mph) Any position in field Gravity effect not included	≤1.7 mrad (1σ)	Allocation: 0.5 mrad for foundation 1.2 mrad for structure. Structural deflection analysis using NASTRAN shows design meets requirements.
Structural Strength	No Permanent Set When Subjected to: 12-m/s (27-mph) wind with 50 mm (2 in.) of ice on mirror surface 22-m/s (50-mph) wind with heliostat in any attitude and drives in operating mode 40-m/s (90-mph) wind with heliostat in stow position	Analysis shows that the design meets these requirements with standard safety factors.	At 12-m/s (27-mph) wind, uniformly distributed ice assumed.
Operational Requirements	Function as Appropriate for All Steady-State Modes of Plant Operation 15 min to stowage position No gimbal drift due to environmental loading 15 min over-the-shoulder resolution Heliostat computer control	Software and hardware meet requirements of all modes of operation <15 min. Worm gear design for nonreversibility <15 min. Computer control.	Demonstrated in previous heliostat programs. Nominal slew rate is 23°/min in azimuth and elevation. All specification requirements are readily achievable with our open-loop control system design.
Safety	Emergency Defocussing to 3% Radiation Within 120 s Radiation on Normally Unirradiated Tower Surfaces Limited to 25 kW/m^2 (78800 Btu/ft^2/h) Beam Control Strategy for Personnel/Property Protection	Design provides the capability. Design meets this requirements. Strategy is adequate.	All heliostats can be moving within 2 to 3 seconds. Baseline design includes corridor walk.
Maintainability	Automatic System Malfunction Detection Minimum Routine Field Maintenance	Mirror washing, visual inspection.	Control system includes self-test capability and status and alarm reporting. Environmentally sealed components, self-lubricating bearings, screened parts, all surfaces corrosion protected, etc.
Hail Survivability	Mirror Assemblies Must Survive Impact of 19-mm (0.75-in.) Diameter Hail at 20 m/s (65-fps) Velocity	Design meets the requirements.	Tests have shown survivability at velocities considerably higher than 20 m/s (65 fps).

The rack assembly consists of five basic items--an elevation beam of large-diameter thin-wall tubing, and four open-web bar joists of proven design and economy. The rack assembly is attached to the drive mechanism through two control arms that are mechanically fastened to the elevation shaft. Each mirror assembly is mounted to this rack assembly at three mounting points that provide for ease of canting without warpage of the relective surface. Adjustments correct for all assembly tolerances and allow canting for slant ranges from 300 m to infinity.

The drive mechanism is mounted to the top of the pedestal/foundation. This drive is a conventinal gear-drive unit with both azimuth and elevation drives combined in one integral, cast-iron housing for precise control of the relationship of the gimbal axes. Both elevation and azimuth drive trains are enclosed inside the drive housing and are submerged in an oil bath with dual seals on each output shaft. The result is a sealed drive with an anticipated 30-year life with no scheduled maintenance. The single, compact drive mechanism provides short load paths and thus very high rigidity with relatively low weight.

The heliostat design incorporates a "stow lock" mechanism that minimizes the size of the drive mechanism gears. The addition of this feature effectively isolates the drive mechanism's elevation gear train from wind loads in excess of 22 m/s (50 mph).

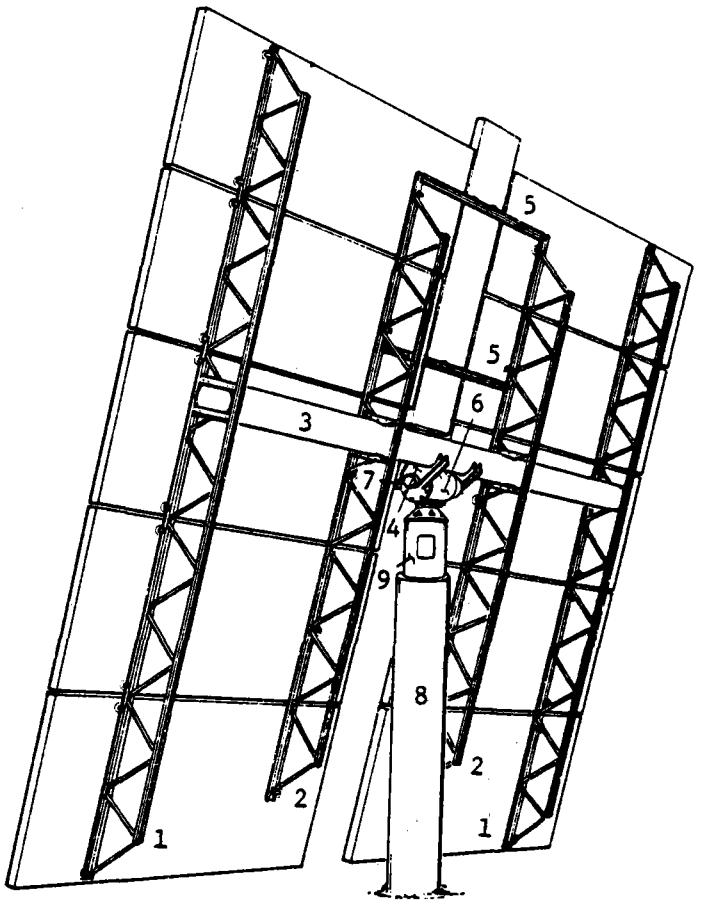

Heliostat Assembly

Reflective Assembly

Mirror Assembly (11 Total)
Mirror Mounting Studs
Rack Assembly
1 - Long Bar Joist with Mirror Support Tabs
2 - Short Bar Joist with Mirror Support Tabs
3 - Elevation Beam
4 - Control Arms
5 - Mirror Support Stringer(s)

Drive Mechanism Assembly

6 - Drive Mechanism
7 - Drive Motors
Encoders
Encoder Couplers
Encoder & Limit Switch

Pedestal/Foundation

8 - Pedestal/Foundation
9 - Pedestal Interface Tube (Electronics Access Cover)

Figure 5.2-2 Heliostat Assembly

The combined pedestal/foundation pier is a continuous, reinforced concrete column extending from below grade level to 3 m (10 ft) above grade. The poured-in-place feature allows the below grade portion to be readily varied to meet the soil conditions of the cogeneration site.

An interface tube is embedded in the upper portion of the pedestal foundation to provide an economical interface with the drive mechanism. This tube has a thin wall and a large diameter to handle the bending loads associated with the large heliostat glass area and the design wind conditions. This interface tube is also used to house the field interface connections, the heliostat electronics, and the cabling. An electronic access door on the interface tube permits easy access to the azimuth encoder and the electronics for maintenance.

Individual heliostats are controlled by a microcomputer-based heliostat controller (HC), drive motors, encoders and an interconnecting cable harness. The microcomputer in the HC receives commands over a data bus, calculates the required gimbal angles, determines actual gimbal angles from the encoder outputs, and turns the drive motors on and off as required. The entire field of heliostats is controlled by a distributed computer control system consisting of a heliostat array controller (HAC) in the control room and heliostat field controllers (HFCs) and HCs located at the heliostats. The computers are inter connected by fiber optic data buses.

Features of the control system include an electronic package installed inside the interface adapter tube for environmental protection, low cost incremental encoders on the output axes, two-speed operation with a single motor per axis, microcomputer that maximize functions on a single chip and therby reduce cost, very low energy consumption, fiber optic data buses, and "computer leveling," i.e., compensation in the control algorithm for pedestal tilt, thus relaxing the accuracy required in pedestal alignment and reducing installation cost.

Figure 5.2-3 shows a dimensional view of the heliostat. The total reflective area of the heliostat is 57.4 m^2 (618 ft^2). When allowance is made for the mirror edge strips, the total heliostat wind load area becomes 58.3 m^2 (628 ft^2).

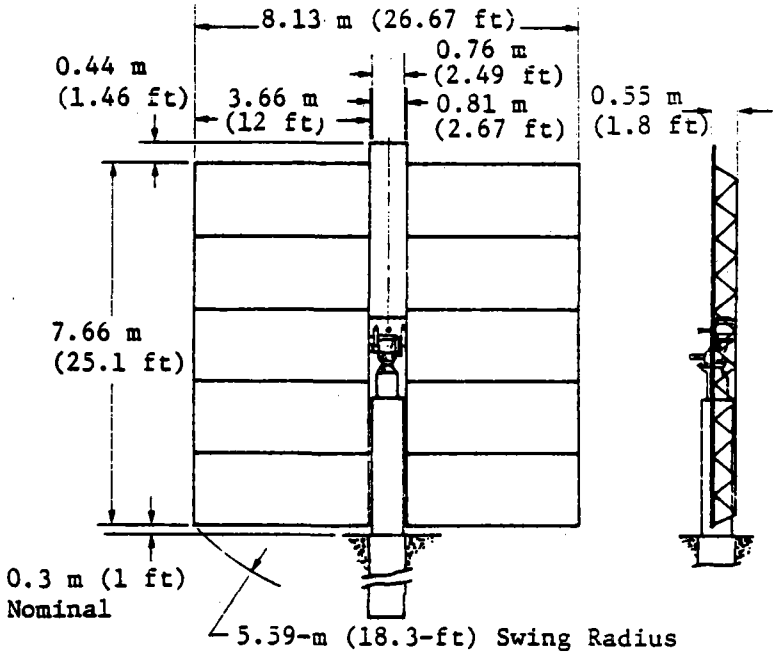

Figure 5.2-3 Heliostat Dimensions

The heliostat weights are as tabulated.

Item	Unit Weight, kg (lb)	Assembly Weight, kg (lb)
Mirror Assembly		1080 (2380)
Large Module	103 (226)	1025 (2260)
Small Module	54 (120)	54 (120)
Rack Assembly		732 (1614)
Long Bar Joist	94 (207)	188 (414)
Short Bar Joist	78 (171)	155 (342)
Mirror Support Stringers	15 (34)	31 (68)
Elevation Beam	298 (658)	298 (658)
Control Arms	30 (66)	60 (132)
Drive Mechanism		549 (1210)
Drive	476 (1050)	476 (1050)
Motors	7 (15)	7 (15)
Interface Tube	59 (130)	59 (130)
Total		2351 (5184)

5.2.2 MIRROR ASSEMBLY DETAILED DESIGN

The mirror assembly uses a sandwich-type mirror assembly construction with thin, second surface, fusion glass mirrors mounted on a rigid steel/paper honeycomb/ steel support structure. The advantages of a bonded mirror/steel/paper honeycomb construction are high strength, low cost, and light weight. The heliostat was designed to survive wind conditions of 40 m/s (90 mph), a limit established by Martin Marietta.

5.2.2.1 Mirror Assembly Description

The mirror asssembly design (Figure 5.2-4) consists of a sandwich support structure 5.2-cm (2.05-in.) thick by 1.52-m (59.75-in.) wide by 3.66-m (144.1-in) long on which two 1.5-mm (0.060-in.)thick by 1.50-m (59.50 in.) x 1.82-m (71.75-in.) fusion glass mirrors are mounted. The sandwich support structure consists of a bondment of two .61 mm (0.024-in.) thick SAE 1010 steel facesheets with a 50.8 mm thick paper honeycomb core between the facesheets. The paper honeycomb core is perforated to allow the core to breathe and is impregnated with phenolic resin to provide dimensional stability and maintain its structural characteristics which used as core material for long life in the outdoor environment. The honeycomb is bonded to the steel with an epoxy adhesive, which cures to handling strength at room temperature in 3 to 5 minutes and thus provides the capability for rapid mass production of mirror assemblies. The thin glass mirrors are mounted to the sandwich support structure

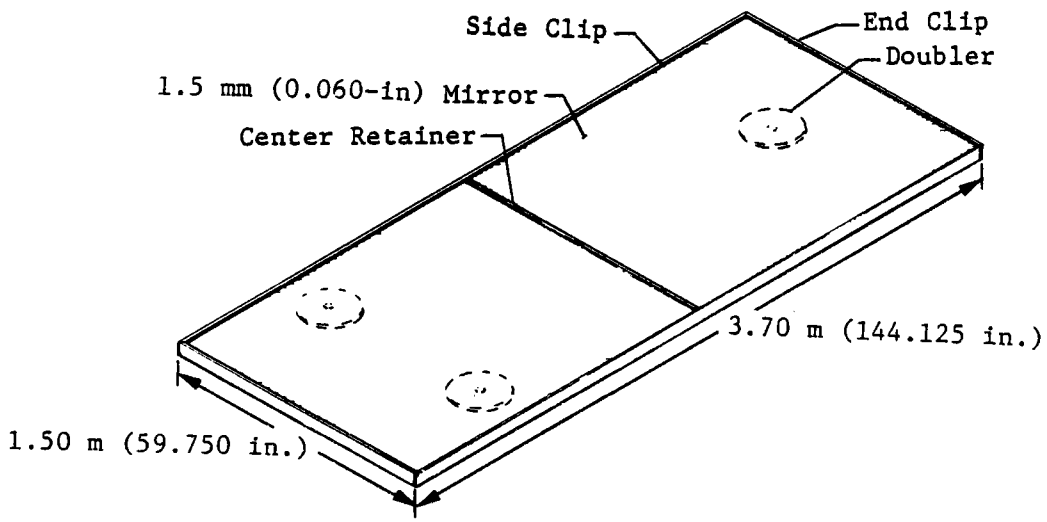

Figure 5.2-4 Mirror Assembly

and ultraviolet radiation. The RTV also provides an elastic, yet structural bond between the steel edge frame and the glass that stabilizes location of the glass. This prevents the glass from sliding as a result of the low shear modulus of the PIB. The center retainer, shown in Figure 5.2-7 holds the two mirrors in place and is mechanically attached to the steel facesheet with five self-drilling and tapping screw fasteners.

The mirror assembly is attached to the rack assembly using a threepoint mounting system. This mounting approach allows rapid mounting and canting of the mirror assemblies without introducing excessive stress or warping of the assemblies. The mounting is achieved by bonding 0.15 m (6 in.) diameter cast iron doublers onto the back of each mirror assembly. Each doubler is drilled and tapped so a 1/2 -13 UNC bolt can be used to mount the mirror assembly to the rack. Cast iron was selected because of its low cost in mass production and its long life properties.

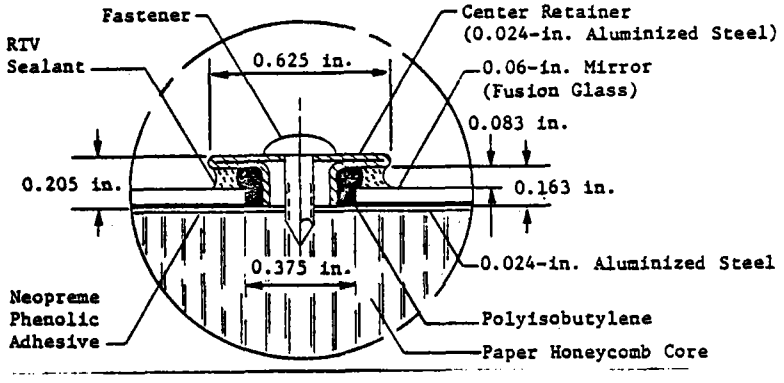

Figure 5.2-7 Center Retainer Seal

5.2.3 Heliostat Rack Assembly Detailed Design

The second generation heliostat rack assembly shown in Figure 5.2-8 consists of five major subassemblies--the elevation beam and four bar joist assemblies--and two additional minor assemblies--the mirror support stringers for the 11th, half-mirror assembly. The rack assembly was designed so all subassemblies can be fully fabricated and finished at the central manufacturing facility, transported to the site in a densely packed configuration and assembled at the site with minimal labor.

5.2.3.1 Rack Assembly Design Description

The elevation beam is a simple fabrication from a 0.41-m (16-in.) OD x 5-mm (3/16-in.) wall tube just under 6 m (20 ft) in total length. For the elevation beam, deflection rather than strength is the designing criterion. Therefore, it may be made by any tube fabricating technique available (i.e., straight seam, spiral weld, either butt-welded or lap seam-welded, etc). Fabrication of the elevation beam from this tube consists only of edge-welding eight 6.4 mm (1/4-in.) plates for the attachment of the four bar joists, welding in a portion of

with a 0.51 mm (0.020-in.) thick layer of polyisobutylene as illustrated in the edge view cross section in Figure 5.2-5. This material has the unique characteristics of (1) sufficient tensile adhesion to support the mirror on the steel face sheet, (2) minimal shear action that removes stresses between the glass and steel, and (3) in concert with the steel sheet, completely seals the mirror back to prevent mirror corrosion. The edges of the mirror assembly are protected by a steel edge guard that doubles as a mirror edge seal clip as shown in Figure 5.2-6. The lower side of the edge frame is bonded to the back steel face sheet with adhesive chosen for its high strength and long life. The upper side of the edge frame is bonded to a support angle with acrylic adhesive and fastened with a series of pop rivets to secure a controlled dimension for the seal next to the front glass surface. An air port is provided in the four corners to ventilate the assembly and allow the honeycomb to breathe. This prevents moisture buildup within the panel. Detailed views of the mirror edge seal for the edge and center retainers are illustrated in Figures 5.2-5 and 5.2-6 respectively. These views show the location of the polyisobutylene (PIB), which provides a positive seal of the mirror edge and the protective outer seal of white RTV. The RTV is applied as a second seal to protect the primary PIB seal from both contamination

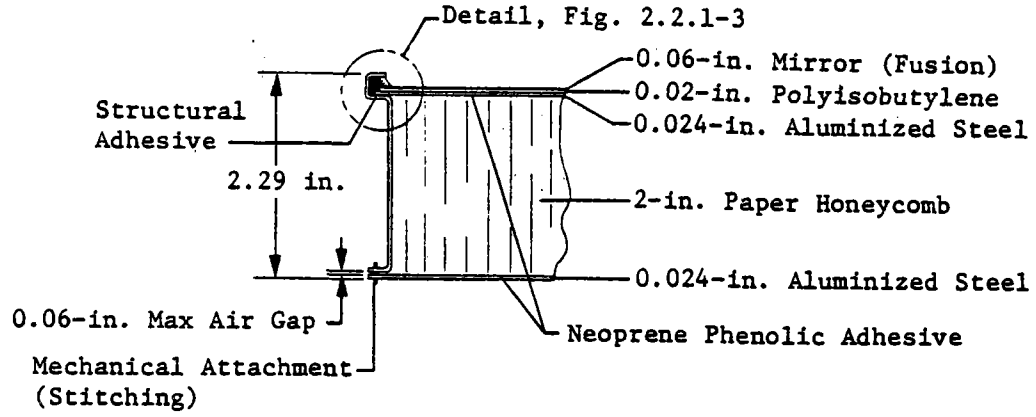

Figure 5.2-5 Edge Cross Section

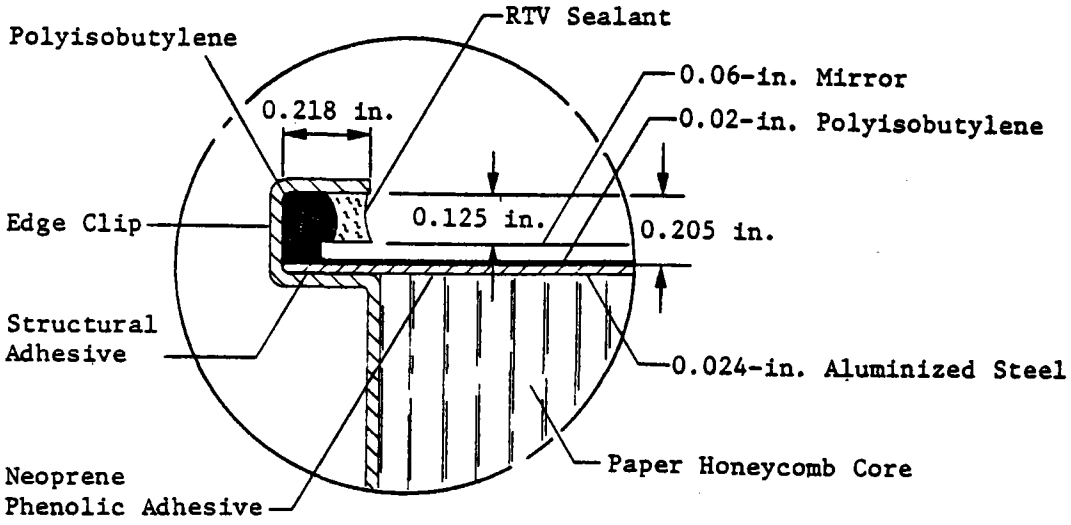

Figure 5.2-6 Detail Edge Seal

configuration shown in Figure 5.2-8 yields a very high strength to weight ratio. The bar joists for this rack assembly vary from commercial bar joist standards and have been uniquely designed to the heliostat requirements. An example is that the pitch of the web bar has been established to suit the support points of the heliostat mirror assemblies.

The 11th mirror support stringers are simply two pieces of the bar joist hat sections placed back to back and resistance-welded together.

Mirror mounting tabs have been added to the bar joist at each of the mirror mount locations. These serve two functions: (1) they stiffen the joist at the load point, and (2) they provide additional material so the mirror mounting hole pattern can be obtained without unnecessarily tight tolerance on the bar joist straightness.

5.2.4 Drive Mechanism Detailed Design

The drive mechanism for the second-generation heliostat (Figure 5.2-9) is a step evolution of drive mechanisms that were and are being produced for Martin Marietta heliostat production contracts.

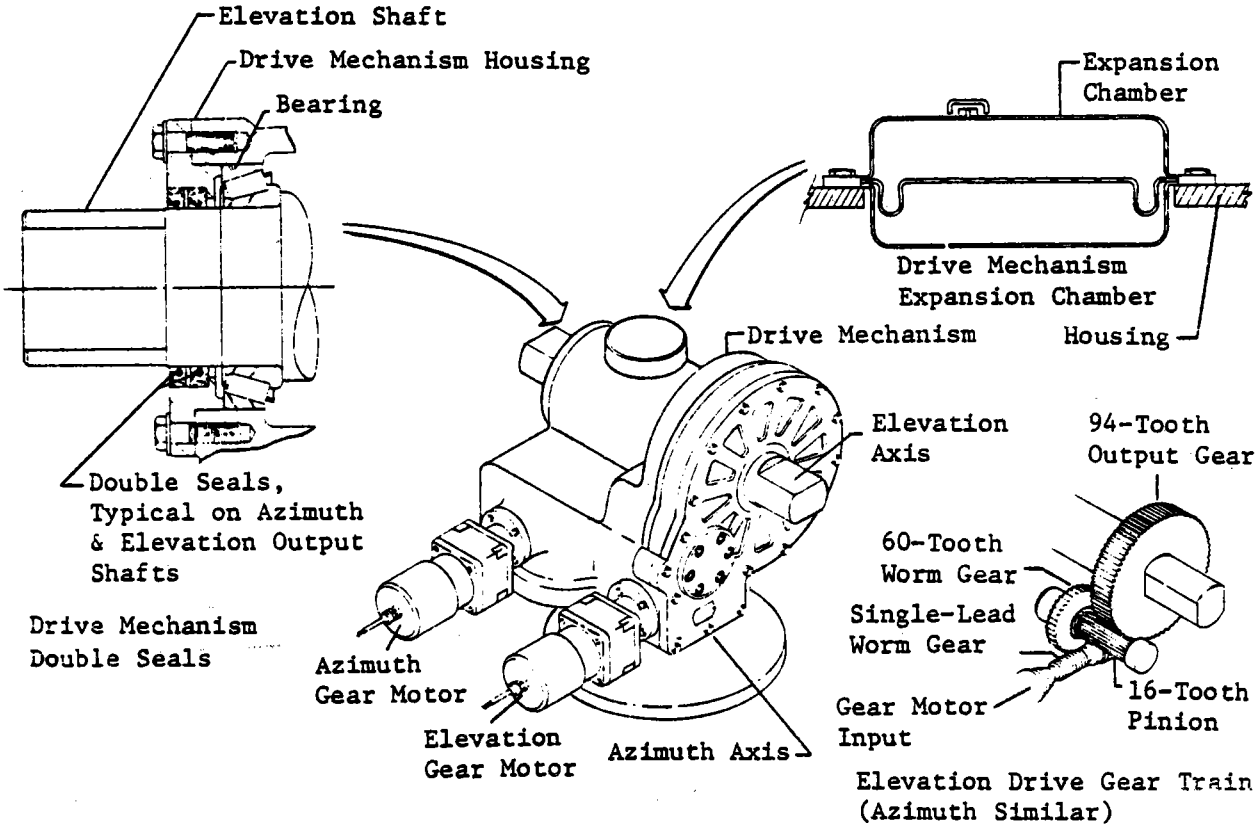

Figure 5.2-9 Heliostat Drive Mechanism

elevation beam from this tube consists only of edge-welding eight 6.4 mm (1/4-in.) plates for the attachment of the four bar joists, welding in a portion of the stow-lock device and welding on two control arms. To preclude the necessity for extremely accurate and/or matched and coordinated tooling for subassembly farication, the design required that the bar joists be aligned to the elevation beam at the site assembly facility (simple fixturing), punching matched holes from pilot holes and using 12.7 mm (1/2-in.) diameter squeeze rivets for the final assembly.

The control arms (Figure 5.2-8), are castings of 80-55-06 ductile iron. Castings of this material were selected for material economy and the ability to easily obtain the proper material shape. The only machining required is the interface to the flats of the drive mechanism elevation shaft. The bar joist or open truss

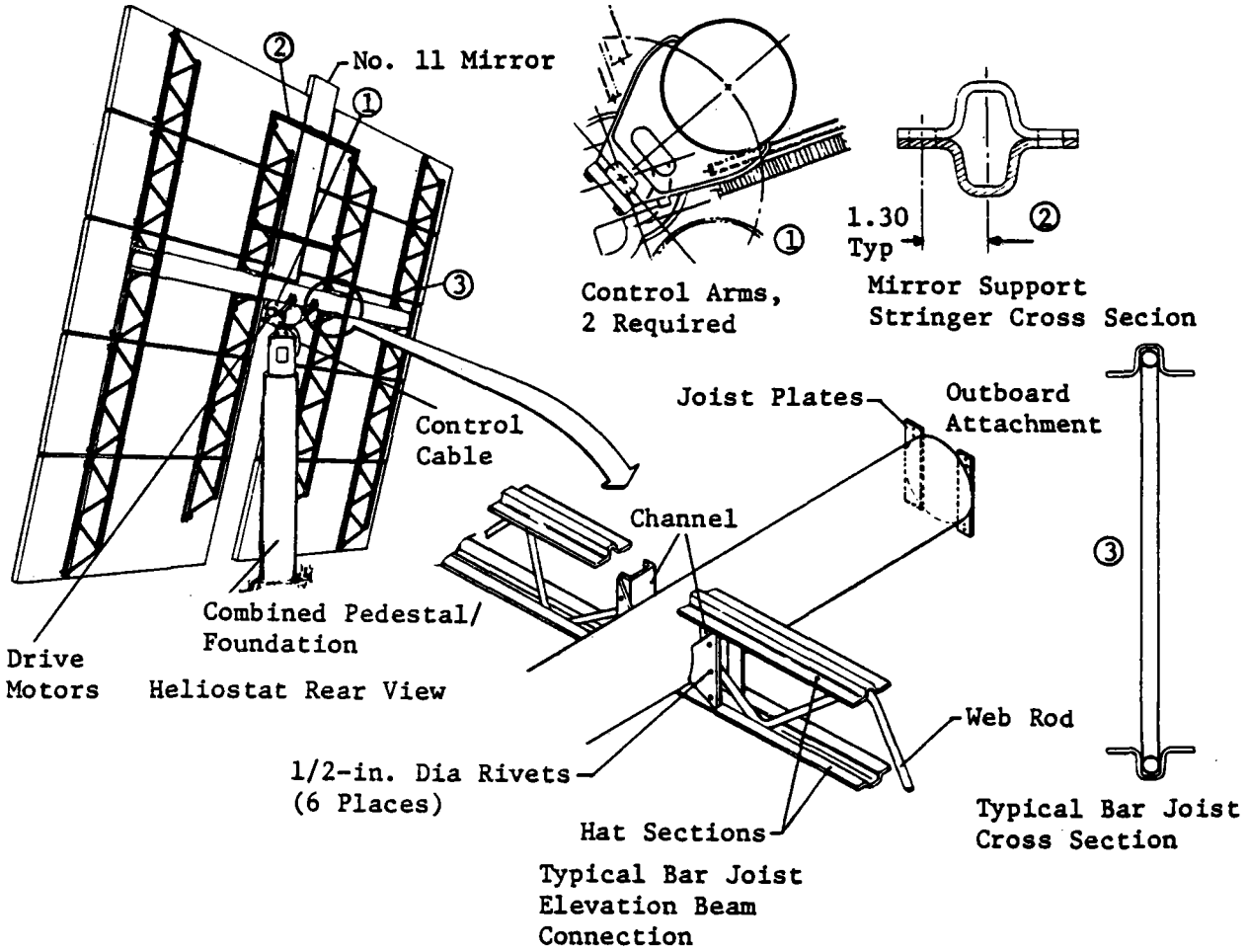

Figure 5.2-8 Rack Assembly Details

The basis for the evolution is the drive mechanisms installed on the 222 heliostats at DOE's CRTF facility at Sandia, Albuquerque. The next evolution step consisted of repackaging these azimuth and elevation gear trains into a common housing for the 10-MW_e pilot plant heliostat prototyping phase.

The second generation design is a further extension of the knowlege gained from the 10-MW_e tests plus a general redesign to provide the same desirable drive mechanism features in a unit better suited for large quantity production at reduced costs.

The drive concept selected was a new single motor, differential drive that incorporated brakes for control.

5.2.5 Pedestal/Foundation Detailed Design

The pedestal/foundation for the second-generation heliostat was designed by Black & Veatch Consulting Engineers of Kansas City, Missouri under subcontract to the second generation heliostat project.

5.2.5.1 Pedestal/Foundation Design Description

As seen in Figure 5.2-10, the pedestal (aboveground portion) foundation (below-ground portion) is a steel-reinforced concrete pier that extends from 3 m (10 ft) below grade to 3 m (10 ft) above grade. The drive mechanism interface tube of 0.45 m (18 in.) OD x 6 mm (0.25 in.) wall steel tubing is embedded 0.37 m (12 in.) in the top of the pedestal at the time of concrete pour. A 25 mm (1 in.) diameter steel electrical conduit is embedded in the pedestal to accommodate the heliostat power and data cables. The upper end of the conduit exits level with the top of the concrete (inside the interface tube) and the lower end exists .15 m (6 in.) below grade.

Foundation - The poured-in-place pier design was selected for the Martin Marietta second-generation heliostat over several other candidate considerations (i.e., pile, post-set, etc) as the result of a tradeoff study that considered these options. It was selected for three basic reasons. First, the foundation portion can accommodate variations in subsurface conditions, including the extremely soft/loose soils, because of the ability to expediently adjust the diameter and length without modifying the pedestal or interface tube. Second, it eliminated the risk and potential extra cost of shattering a pile during driving; and third it was a cost-competitive design.

The rebar cage has been designed to standardized industrywide construction practice with final assembly at the construction site to reduce shipping cubage and cost. Experience has shown this approach to be the most cost effective.

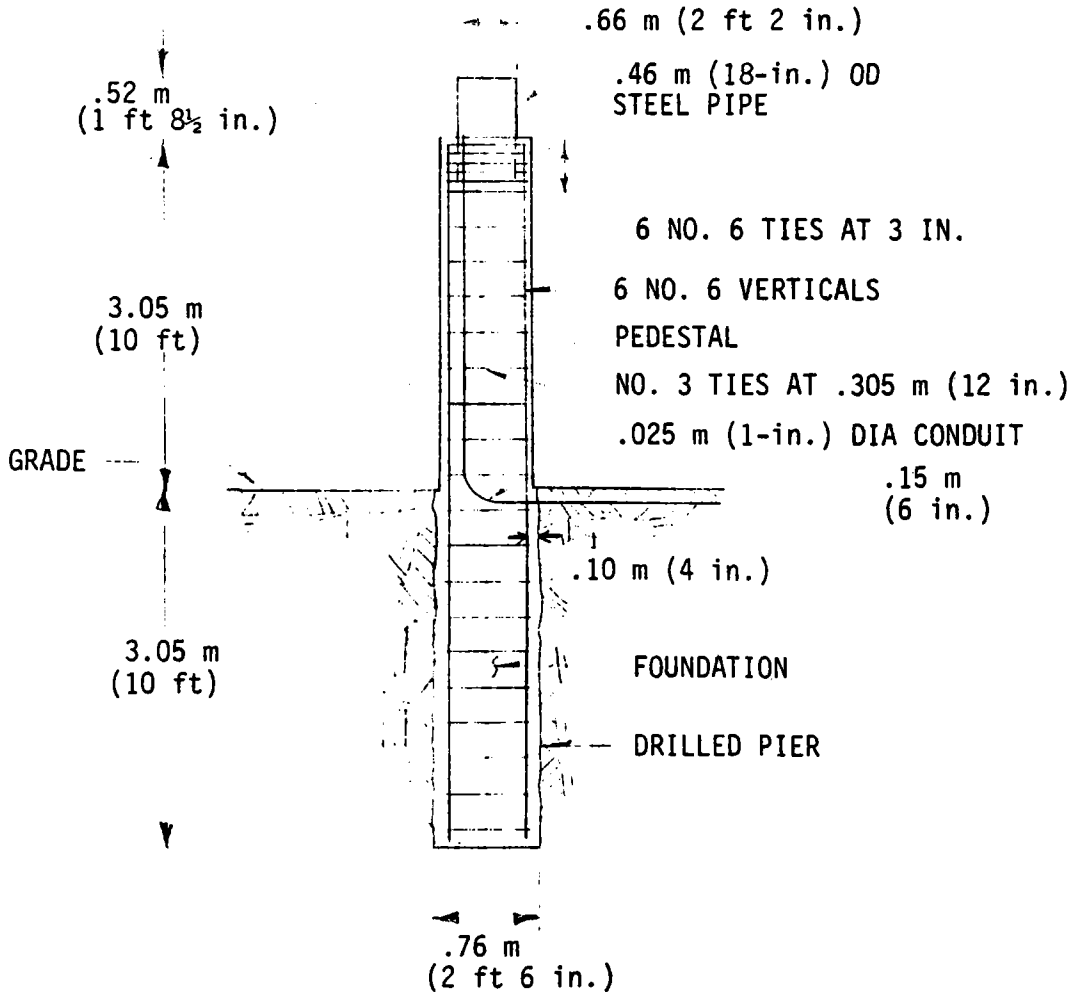

Figure 5.2-10 Heliostat Pedestal/Foundation

Pedestal - The aboveground portion will remain a constant 0.66 m (26 in.) diameter regardless of any variation required of the foundation.

Interface Tube - The interface tube serves two functions: (1) it provides a rapid, bolt-on interface for the drive mechanism, and (2) with the drive mechanism installed, it provides a weathertight enclosure for the heliostat electronics and circuit breaker box. These components will rest on an expanded metal platform to support them above and away from the concrete. An electronics access cover provides access for installation/replacement of these items as well as access to the azimuth axis encoder and limit switches attached to the drive mechanism base.

Although the interface tube is designed to prevent water from getting inside, the conduit also provides a drain for any water that might find its way into the inside of the interface tube.

Six weld studs are provided at the lower end of the interface tube to ensure an adequate shear tie to the pedestal concrete. The drive mechanism interface surface (tube upper end) is machined flat and then leveled to within 1° during installation. Eight 35.4 mm (1-in.) 8 UNC studs are welded to the inside

diameter of the tube to provide a rapid boltdown installation for the drive mechanism. The coarse threaded studs were selected for their ability to sustain substantial abuse and still be serviceable.

5.2.6 Control System

The field of heliostats is controlled by a distributed computer control system consisting of a minicomputer located in the plant control room and a network of data buses and microcomputer-based controllers located at the heliostats (fig. 5.2-11).

The reflective surface on each heliostat is rotated about the azimuth and elevation axes by a gear-drive unit and electric motors. The actual azimuth and elevation angles are determined by incremental optical encoders and a microcomputer. The microcomputer provides the logic to turn the drive motors on and off as required.

The heliostat control system design includes an electronic package installed inside the interface adapter tube for environmental protection, low-cost incremental encoders on the output axes, two-speed operation with a single motor per axis, Motorola 6801 microcomputer that maximize functions on a single chip and thereby reduce cost, and very low energy consumption.

On the basis of experience with the Martin Marietta CRTF heliostats, it has been concluded that the electronics package should be vented rather than sealed and that the package should be protected from rain and spray when the heliostats are washed. The ideal installation location is inside the interface adapter tube because it provides environmental protection and easy access for unscheduled maintencance.

The use of encoders on the output axes to measure the actual gimbal angles eliminates pointing errors that would otherwise be introduced by backlash or lack of stiffness in the drive mechanism.

Two-speed operation is provided by one motor instead of the two motors used on the CRTF heliostats. Low-speed operation is required to provide stable operation in the fine tracking mode; high-speed operation is required to meet the time requirements in slewing from one position to another.

The use of fiber optic data buses provides higher data rate capability, fewer components in the heliostat controller (HC), and complete immunity of the data buses to electrical noise and lightning-induced surges. Fiber optic technology is developing very rapidly, and the cost of fiber optic data systems for the field of heliostats is expected to be less than that of conventional copper wire systems in the second generation heliostat production time frame.

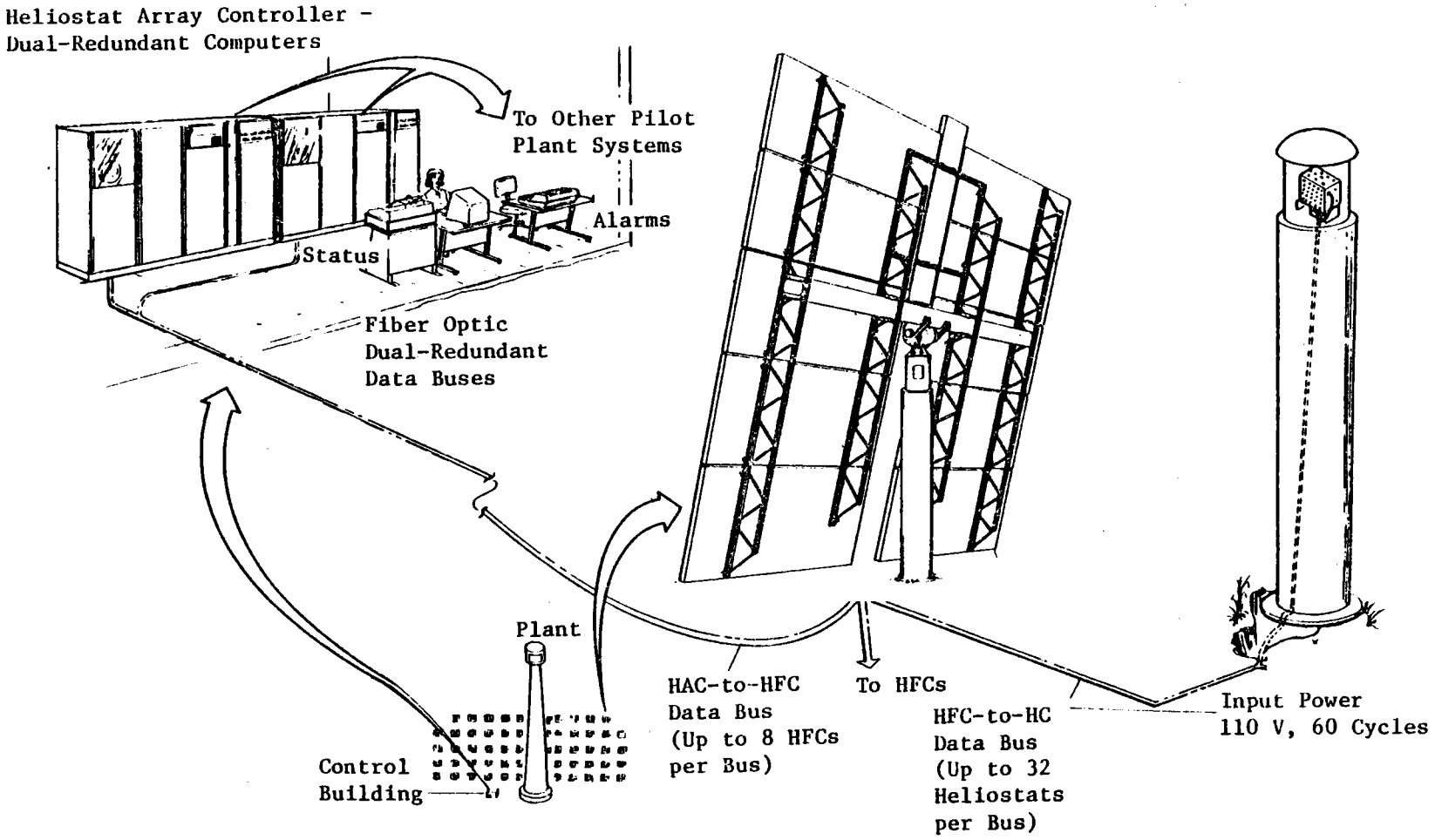

Figure 5.2-11 Control Subsystem

New features of this design are fiber optic data buses, a lower cost HC package with fewer electronic components, and "computer leveling"-- i.e., compensation in the control algorithm for pedestal tilt, thus relaxing the accuracy required for pedestal alignment and reducing installation cost.

The HC package consists of a channel-shaped chassis on which the electronic components are mounted and a cover of perforated metal that is also channel shaped.

All of the control system components on the heliostat are readily accessible for removal and replacement in the event of a failure. Maintenance personnel will use vehicles that include a work platform to provide easy access to the HC, motors and encoders.

A detailed description of the collector control subsystem is presented in Section 5.4 of the Master Control Subsystem.

5.2.7 Collector Field Performance

The performance of the collector field subsystem was analyzed using the MIRVAL computer code, with the following parameters considered:

1) Collector field layout;
2) Heliostat design parameters;
3) Receiver aperture sizes/orientation;
4) Heliostat aiming strategy;
5) Site location.

Receiver aperture sizes of 11.0 x 11.0 (36.1 x 36.1 ft) with aperture normal orientations of 0.79 rad (45°) from due north were internally programmed in the MIRVAL code because the code will not accept cavities that are not oriented due north, south, east, or west as input.

The final collector field efficiency values for various sun azimuth and elevation angles are shown in Table 5.2-2. Field efficiency is defined as the product of tower shadow, average field cosine efficiency, reflectivity (0.90)*, shading and blocking, atmospheric attenuation as calculated using the Martin Marietta atmospheric attenuation model and spillage. The spillage losses include any losses due to heliostat tracking errors and beam quality.

---

*Tests performed on the Martin Marietta Second Generation Heliostat have found the peak reflectivity to be 0.96. It was suggested by Sandia that we use an average reflectivity of 0.90 in our calculations.

Table 5.2-2 Collector Field Efficiencies

Sun Elevation	Sun Azimuth [South = 0 rad (0°)]						
	0 rad (0°)	0.52 rad (30°)	1.05 rad (60°)	1.31 rad (75°)	1.57 rad (90°)	1.92 rad (110°)	2.27 rad (130°)
0.09 rad (5°)	0.320	0.317	0.316	0.312	0.300	0.220	0.190
0.26 rad (15°)	0.610	0.600	0.572	0.545	0.520	0.482	0.440
0.44 rad (25°)	0.720	0.705	0.673	0.650	0.595	0.560	0.515
0.78 rad (45°)	0.763	0.759	0.713	0.696	0.675	0.640	0.590
1.13 rad (65°)	0.728	0.720	0.701	0.685	0.670	0.620	0.580
1.56 rad (89.5°)	0.640	0.640	0.640	0.640	0.630	0.600	0.600

Horizontal = 0 rad (0°)

The collector field performance was also calculated for noon on days 24 and 189, again using MIRVAL and the inputs previously discussed. These efficiencies are shown in Table 5.2-3.

Table 5.2-3 Collector Subsystem Performance

	Noon, Day 24	Noon, Day 189
Tower Shadow	0.9991	1.000
Cosine	0.9133	0.8527
Reflectivity	0.900	0.90
Shading	0.9875	1.000
Blocking	1.000	1.000
Atmospheric Attenuation	0.9467	0.9467
Spillage	0.9880	0.9810
Total Field Efficiency	75.9%	71.3%
Solar Elevation Angle	0.620 rad (35.5°)	1.358 rad (77.798°)
Solar Azimuth Angle	0.0 rad (0.0°)	0.134 rad (7.685°)

Annual field efficiencies were calculated using the STEAEC program with Fresno SOLMET TMY insolation and the field efficiency matrix given in Table 5.2-2. Using the ratio of "yearly energy to receiver" to "yearly energy to collector field," an annual average field efficiency of 66.9% was calculated.

The estimated direct cost of the collector subsystem (Account 5300) is $38.5 million.

5.3 RECEIVER SUBSYSTEM

The receiver subsystem includes the receiver, tower and foundation, vertical salt riser and downcomer, interconnecting piping and valves. The basic function of this subsystem is to effectively intercept radiant solar flux directed from the collector subsystem and efficiently transfer as much of that thermal energy as possible into the molten salt working fluid for subsequent conversion to process steam and electrical power. The two cavity receiver panel layout was determined by the thermal/hydraulic analysis performed in the trade studies. A schematic of the receiver is shown in Figure 5.3-1. The molten salt from the cold storage tank is pumped to the top of the tower and enters panel one in both the east and west cavity. The cold salt surge tank at the top of the tower decouples any pump surges in the risers as well as provides a reservoir of salt to be used in an emergency shutdown operation. The salt flow circulates through the 12 receiver panels arranged in a serpentine flow path increasing in temperature from 288°C (550°F) to 566°C (1050°F). The receiver outlet temperature is controlled by adjusting the flow rate through the receiver. The outlet salt temperature is compared to a set point temperature of 566°C (1050°F) and the flow is adjusted to match the set point temperature. The salt then exits the receiver and travels down the tower to the hot salt storage tank. The liquid level in the hot salt surge tank is above the top of the highest point of the receiver header. This will provide for positive filling of all absorber tubes and interconnecting piping.

5.3.1 Receiver Subsystem Requirements

Design requirements for the receiver are divided into two classifications--the general system requirements including those adapted from the Systems Specification that are applicable to the receiver and the requirements derived during this study. Emphasis was placed on reducing receiver weight and thus reducing receiver and tower cost.

5.3.1.1 General Requirements

In the following discussion, the general requirements imposed on the receiver subsystem design by the general nature of the subsystem and by the Solar Cogeneration Facility Systems Specification (Appendix A) document are summarized. The design shall:

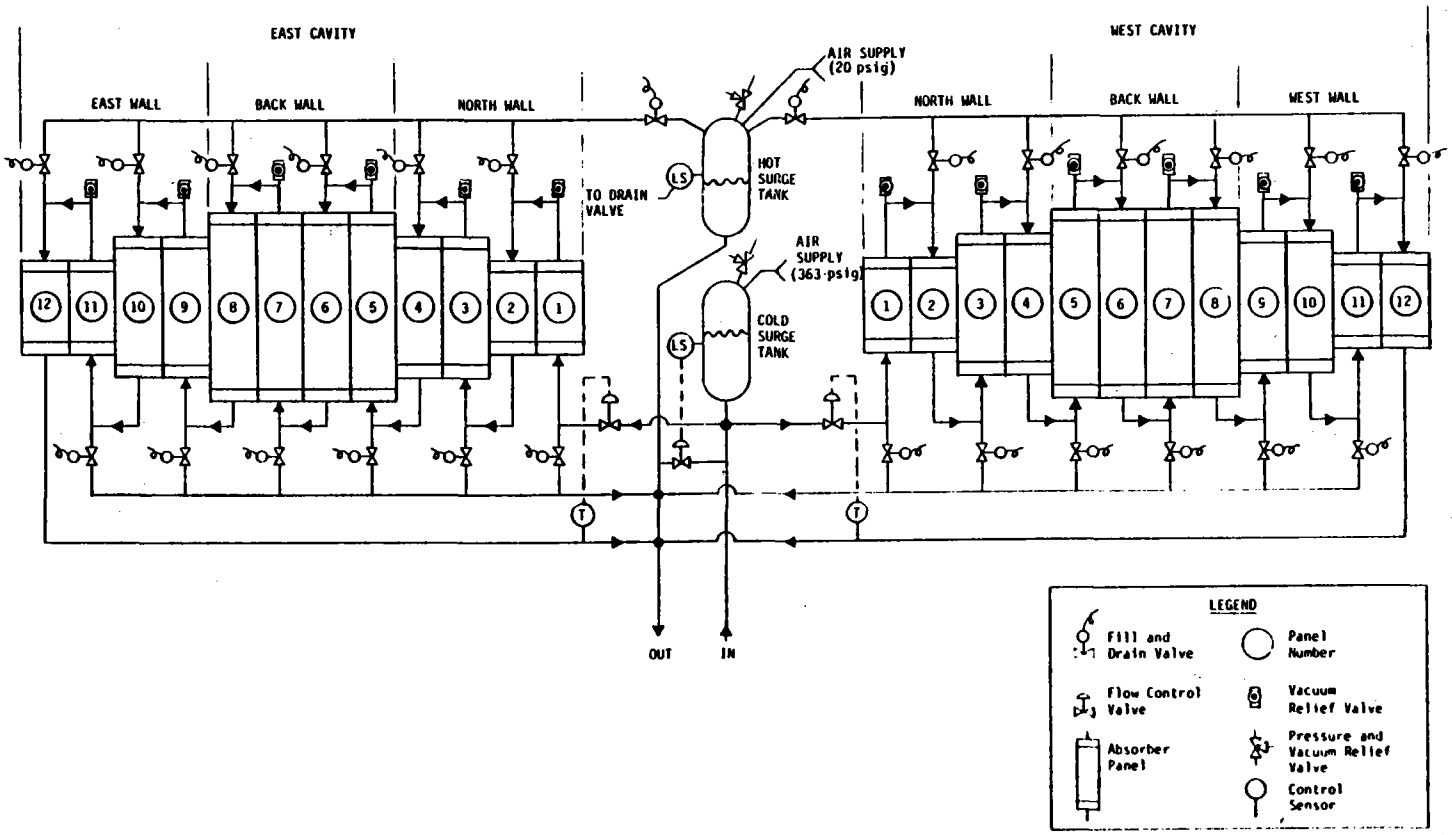

Cogeneration Salt Flow Schematic

Figure 5.3-1

1) Conform to the applicable codes and standards defined in the Systems Specification;

2) Provide thermal control for safe, efficient operation, startup, shutdown, transient and standby modes;

3) Provide access for maintenance and inspection, provide for crew safety, operational safety, and be consistent with the intent of appropriate ASME boiler and other codes;

4) Be designed for a 30-year operating life;

5) Be capable of operating in and surviving appropriate combinations of the environment conditions summarized in Section 4.1.1 of the Systems Specification, and shall be capable of surviving appropriate combinations of the environments specified in Section 4.1.2 of the same document.

5.3.1.2 Derived Requirements

In addition to the general requirements mentioned above, we derived the following requirements for our receiver design:

1) The receiver shall be designed to provide a total solar power of 115.0 MW_t at solar noon on day 189 at the base of the tower. This assumes a solar insolation of 937 W/ m^2 and all 3295 heliostats as described in Collector Subsystem Description, Section 5.2.

2) The receiver shall be capable of transferring 122 MW_t of thermal power into the salt at a nominal peak mass flowrate of 0.995M kg/hr (2.19M lb/hr) with the incident power defined above. At maximum conditions, the receiver shall be capable of transferring 134.5 MW_t into 1.10M kg/hr (2.41 m lb/hr) of salt.

3) The receiver shall be a two cavity receiver with a door over each aperture for survival protection and to decrease overnight cooldown.

4) The working fluid shall be a mixture of 60% $NaNO_3$ and 40% KNO_3 by weight. The salt properties are defined in paragraph 3.5.3 of the Systems Specification.

5) The heat transfer fluid will enter the receiver at 288°C (550°F) and exit the receiver at 566°C (1050°F).

6) Cavity apertures shall be sized for the minimum spillage and minimum thermal losses as described in the trade studies of this report.

7) The receiver absorbing panels shall be designed for 28,000 temperature cycles induced by application and removal of solar flux over a 30 year life.

8) The maximum absorbed flux allowable on the absorber tubes shall be determined by tube material strength at the maximum design mass flowrate and fluid temperature.

9) The receiver shall be capable of gravity draining.

10) The working fluid flow of the receiver shall be decoupled from the horizontal and vertical piping flow through the use of accumulators or surge tanks.

11) In the event of a total power failure to the pumps, heliostats, and cavity doors, the receiver surge tanks and air storage shall be designed for a continuation of working fluid flow that shall absorb the solar flux on the receiver panels as the heliostats defocus due to the natural rotation of the earth. This time period is 480 seconds.

12) The receiver shall be insulated to enhance its thermal efficiency and the cavity apertures shall be covered at night to reduce heat loss.

13) All salt lines, valves, pumps and tanks other than the absorber tubes within the cavity shall be heat traced.

14) The receiver shall be operable from 10% to 110% of design flowrate.

15) The receiver and associated piping equipment shall have provision for fill and drain.

16) The salt supply and return piping system consists of horizontal and vertical pipe to the base of the tower.

17) The tower foundation shall be designed for a soil bearing strength of 71.8 kPa (1500 psf).

18) The tower shall be designed to support the receiver, riser, and downcomer under the applicable environmental conditions.

19) The tower shall be 137.4 m (450.8 ft) high, shall be appropriately lighted, and shall include an elevator.

5.3.2 Structural Design

This section describes the receiver structural design configuration which supports and encloses the absorbing panels and also discusses other analysis influencing the design.

5.3.2.1 Configuration Description

The receiver is 17.1 m (56 ft) wide from north to south and 31.4 m (103 ft) wide from east to west. The two cavity receiver is 24. m (79.4 ft) high from the bottom of the receiver floor to the top structural member. The roof joists extend above the top of the structure by 0.4 m (1.5 ft) to the roof edge. The receiver is supported on a column-type superstructure which is attached to the central tower which supports the hot and cold surge tanks. Figure 5.3-2 shows a projected view of the three separate structures. The top of the tower has a diameter of 12.26 m (40.3 ft) and is shown in Figure 5.3-3, which gives a plan view of the receiver structure. The receiver is supported from the superstructure to the tower top by ten trusses. These trusses are located below the ten vertical receiver columns and pinned connections are used to secure the ends of the trusses.

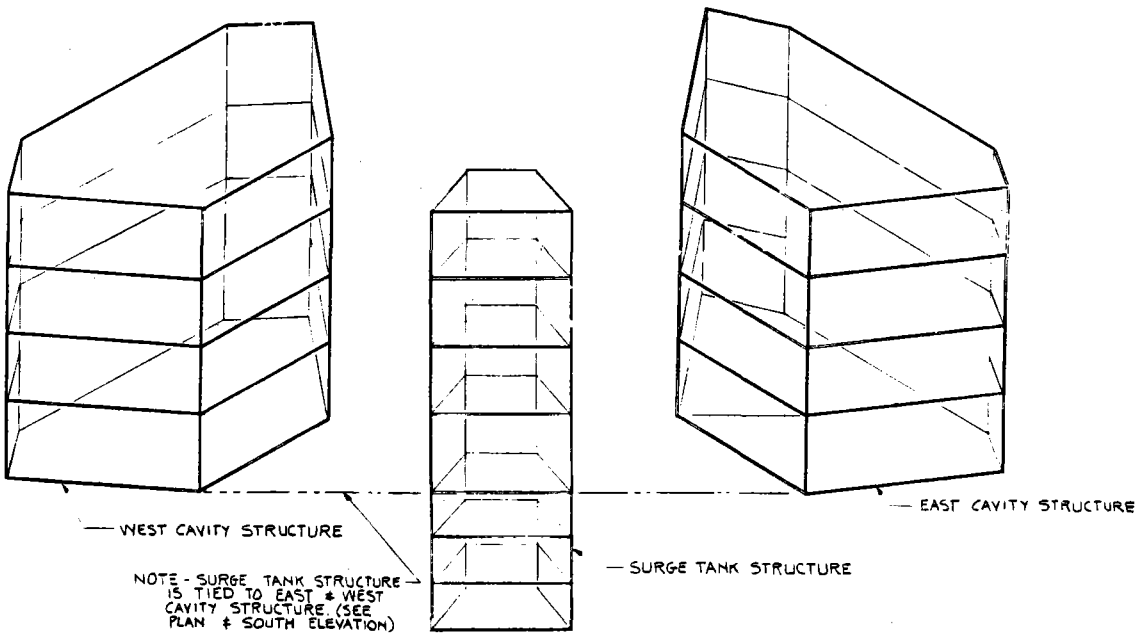

Figure 5.3-2 Receiver Structure

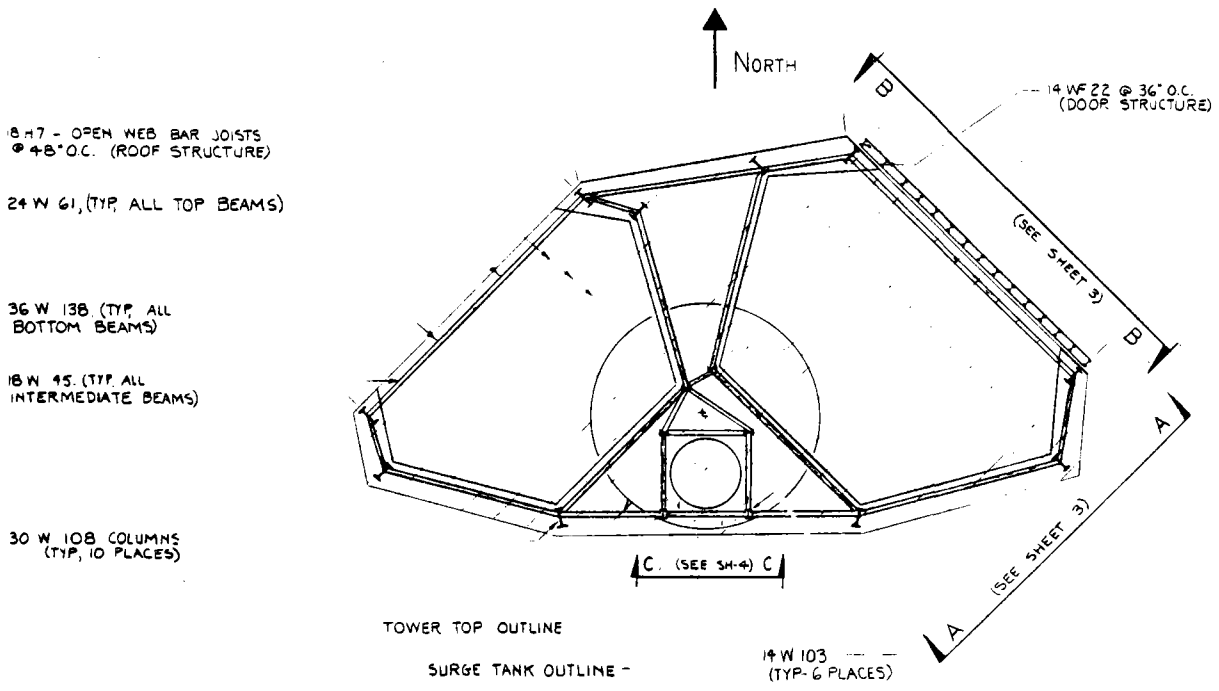

Figure 5.3-3 Plan - Receiver Structure

The centerline location of the east and west apertures is 154.1 m (505.6 ft) from the ground level. Both the east and west cavity aperture are 11 m (36 ft) square. The size and shape were determined by the amount of solar flux directed from the collector field as described in the trade study sections.

Maintenance and personnel safety were considered throughout the conceptual design. Piping and valves are located to allow access for maintenance and removal. Figure 5.3-4 shows the piping arrangement. The valves are between the lower radiation shield and the superstructure. Absorber panels have connections on both the upper and lower supports that allow for complete panel relacement as well as repair-in-place maintenance. Provisions have been made for hoisting equipment to be installed in the top of the receiver structure and for raising and lowering equipment, piping, valves and complete absorber panels. A crane can be installed early in the construction phase atop the surge tank structure and removed when assembly is completed. Additional repair operations can be performed using portable hoists.

Lightning protection is provided by lightning rods installed at the high points of the receiver structure.

5.3.2.2 Structure

A complete set of structural drawings for the receiver conceptual design is given in Appendix A. Figures taken from these drawings are presented in this section to support the structural description.

The main receiver support is the central surge tank tower. It attaches to the top of the tower. A plan view of this attachment is shown in Figure 5.3-5 This view shows a lattice of 30W190 members which form the base for both the vertical 14W130 columns as well as the ten anchor blocks for the trusses. The trusses are light weight compression members which support the portions of the receiver which extend over the tower diameter.

The trusses as shown in Figure 5.3-6 connect the bottom superstructure of the receiver under each of the ten 30W108 columns. Each truss is made from angles 6 x 6 x 1/2 in a four foot square and pin connected at both interfaces to transmit the shear loads to the tower top structure.

The receiver floor is constructed of open steel grating covered by 14 gage sheet steel. Open member-type joists span the girders to support the floor covering. The joists are covered with 1.90 mm (.0747 in.) thick steel plate to accommodate live loads. The outer cover of the receiver is covered with 14-gauge corrugated galvanized steel sheet. The receiver roof is supported with open web 18H7 bar joists on 1.22 m (48 in.) centers.

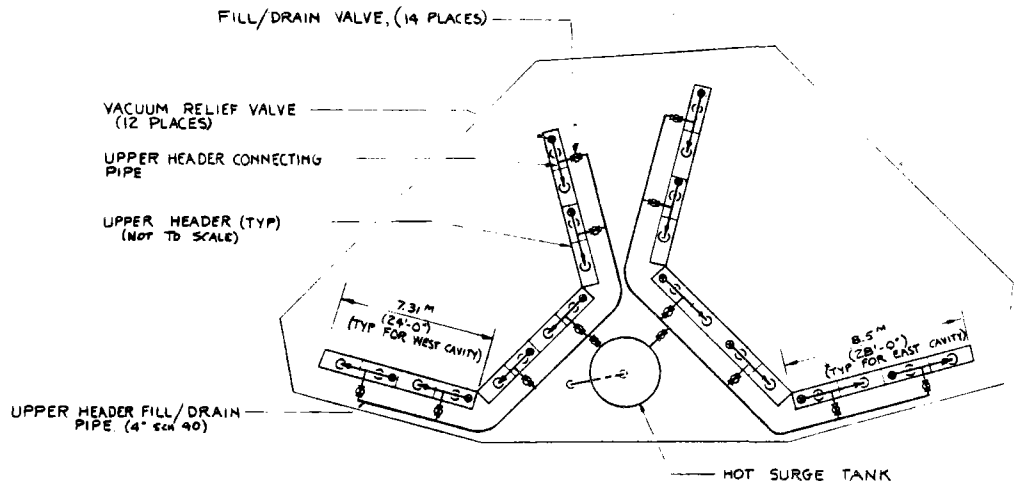

Figure 5.3-4 Plan - Upper Crossover & Vent Piping

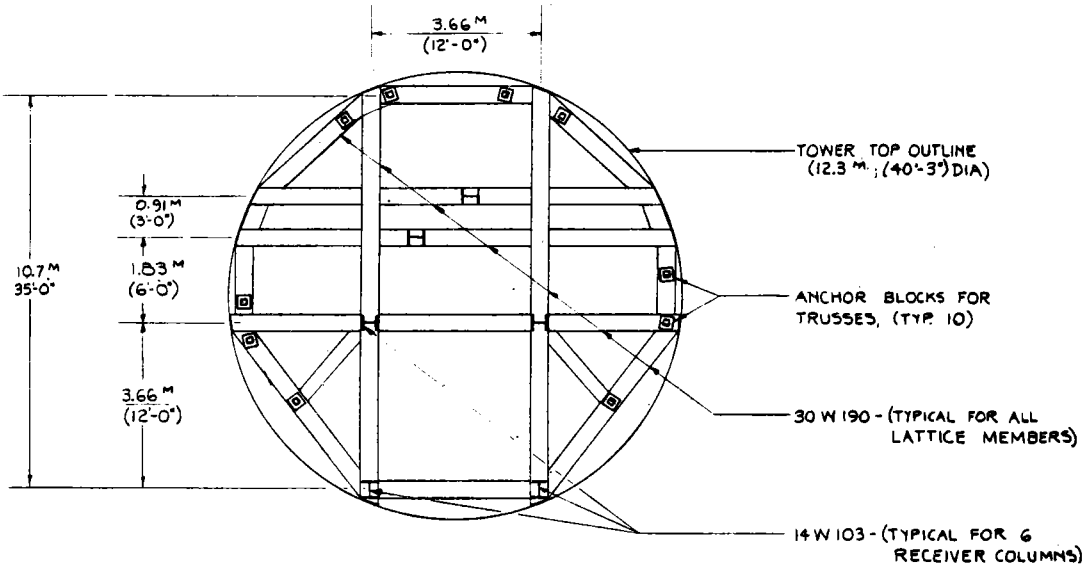

Figure 5.3-5 Plan - Tower Top Structural Lattice

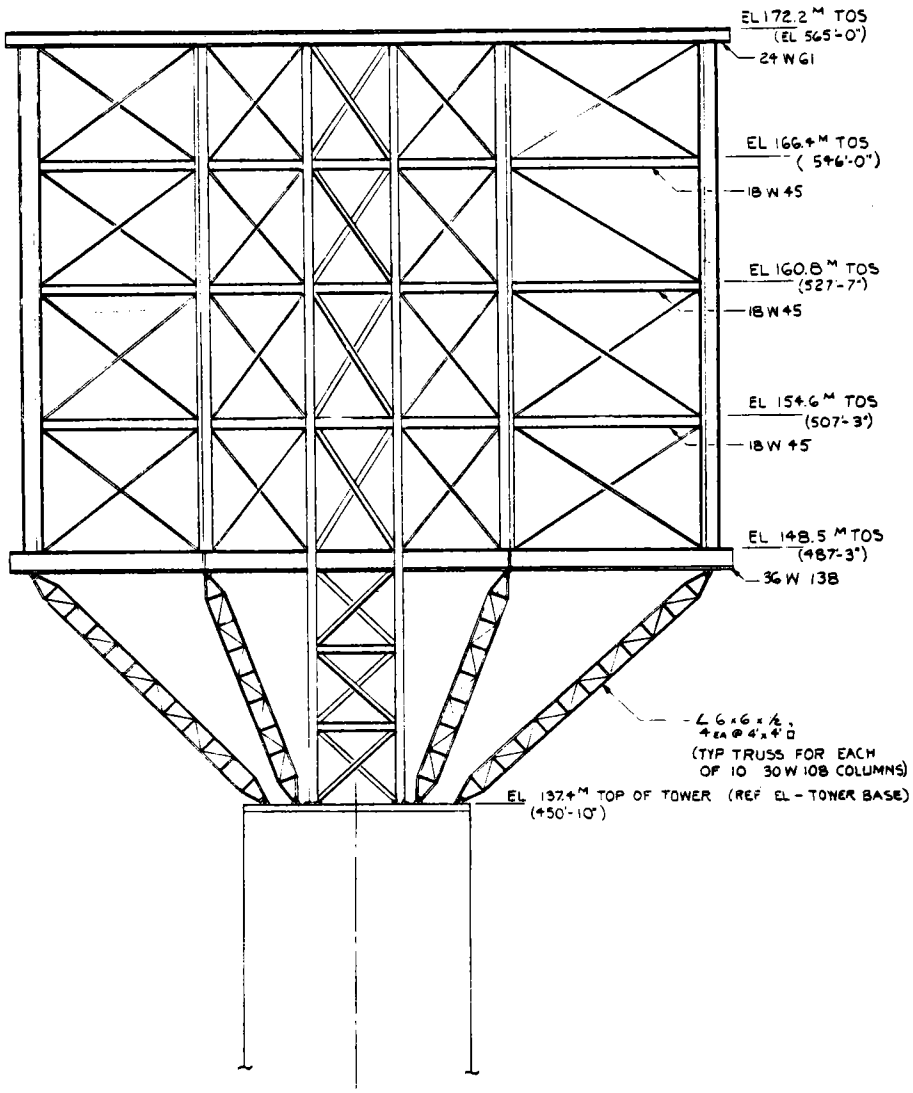

Figure 5.3-6 Receiver Trusses

Each cavity has a door that can be quickly closed during adverse weather conditions, an electrical power system failure, or at night, to reduce convective heat loss. Figure 5.3-7 shows a typical door structure. The side of the door facing outside is covered with 7.62 cm (3 in.) of ablative material. The ablative material fills the cells of the aluminum honeycomb that is faced on each side with 0.82 mm (0.032 in.) aluminum sheet. The aluminum sheet is light weight and protects the ablative material from weather. With the honeycomb, it also forms a rigid panel. These panels carry the ablator weight of 36.6 kg/m^2 (7.5 lb/ft^2) and the wind loads into the door primary structure. The cavity side of the door is formed of 14W22 I-beams on 0.9 m (3 ft) centers.

The inside surface of the door has 0.102 m (4 in.) thickness of insulation faced with stainless steel sheet for protection. No insulation is located between the structural members of the door to reduce thermal warpage due to temperature gradients when the doors are closed and the receiver is in the standby mode. The doors are raised and lowered by a cable drum-type hoist and are guided in tracks and incorporate roller mechanisms that ensure smooth operation. The hoists are fitted with a brake mechanism that will allow the doors to close within 6 seconds after a failure of power to the hoists. The two cavity doors will each fall with 0.1-g acceleration (0.9-g braking force) for 4 seconds and then are decelerated at 0.2-g (1.2-g braking force) for 2 seconds.

The inactive surfaces of each cavity are of stainless steel and painted with solar reflective white paint, Pyromark Series 2500 $a_s = 0.32$, $e_{ir} = 0.84$. The floors and ceilings of the cavities are thin gage stainless steel shields. These stainless steel shields are backed with 10.2 cm (4 in.) of insulation to reduce heat conduction from the cavities to the receiver structure. The shields protect the absorber panel headers and are supported from the receiver structure. The supports have minumum thermal conductance. A fiber insulation of 20.3 cm (8 in.) blackets is used in the receiver to reduce the heat loss and to protect the structural members from high temperature. The basic approach is to insulate the cavities and to allow air to flow up through the receiver around the supporting steel structure. In this way, the temperature of the structural steel can be kept low. All piping and the surge tanks are individually insulated to reduce heat loss and maintain a low temperature environment for valve controls, supports, etc.

The structural steel cavities were designed to accommodate heavy duty hoists for the cavity doors. Each door weighs 10,800 kg (24,000 lb). Provisions were made for a lift crane to be located on the surge tank structure of the receiver. This crane can be used for hauling prefabricated panel sections into place. The construction crane would be removed when construction is completed. However, provisions have been made for rigging and supporting temporary hoists that can be used for component removal and replacement.

All structural elements of the receiver are standard A36 steel sections selected in accordance with AISC specifications. The siding is corrugated 14-gage steel siding and the roof is industrial aluminum, siding 0.8 mm (0.032-in.) thick. Exterior wall siding is carried by double-angle joists varying in size and weight as noted on the drawings in Appendix A. Standard open web bar joists are used on the roof and floor.

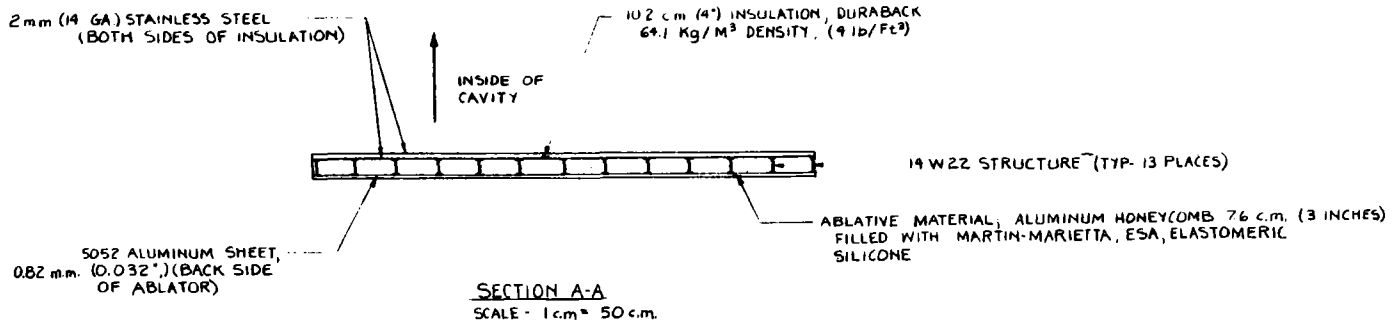

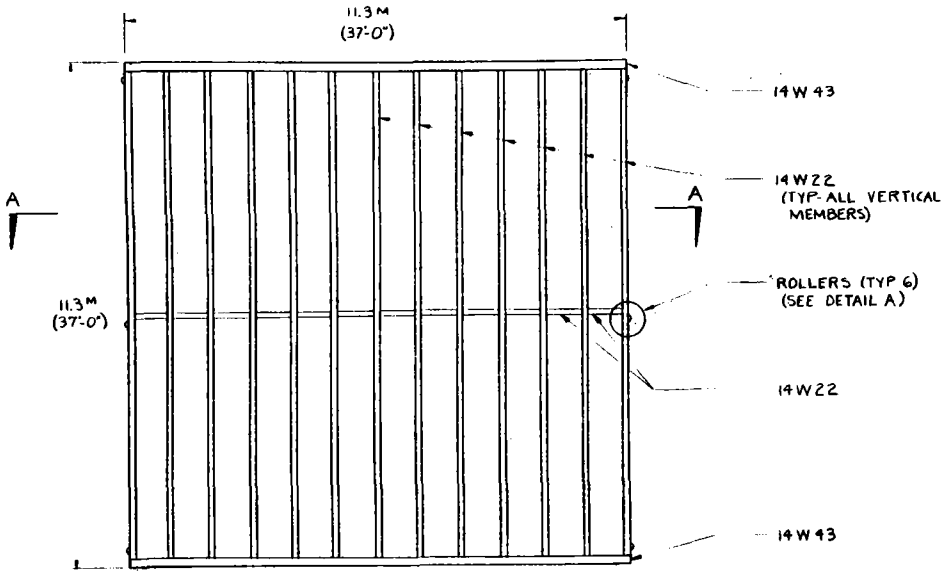

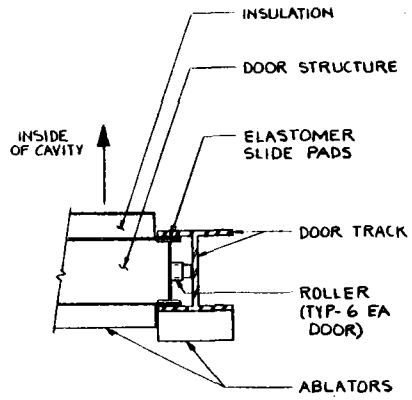

DETAIL A- ROLLERS

Figure 5.3-7 Elevation - Door Structure
(Shown Without Front Ablative Material)

The receiver module deck was designed using open steel grating. Structural trusses and braces are pin attached to the steel lattice at the top of the receiver/tower interface. This design allowed for not only static dead loads but also torsional moments due to the maximum wind loads and accelerations due to earthquakes.

Loading and design criteria have been outlined in Section 4.0 of the Systems Specification. A brief summary of the design factors considered is useful.

1. Snow and ice - These conditions were assumed to include a layer of snow of 3.81 kg/m^2 (0.78 lb/ft^2) and a snow accumulation rate equal to the maximum on record of 0.04 m (1.5 in.). The plant shall survive freezing rain and ice deposits in a layer 50 mm (2 in.) thick.

2. Wind - For analysis a maximum wind condition that assumed winds up to 40 m/s (90 mph) plus dead load was used and found to be the dominant design factor.

3. Earthquake - The facility is located in Kern County, California near Bakersfield and lies in Uniform Building Code (UBC) Zone 4 which identifies a survival ground acceleration of 0.50 g. It was determined that the Nuclear Regulatory Commission dampening requirements that were originally specified were too stringent. An assumed acceleration of .5 g in combination with the relative soil conditions did not dominate the design.

5.3.3 Receiver Absorbing Panels

The absorbing surfaces are divided into an east and a west series of panels as shown in Figure 5.3-8. The flow through the twelve panels is serpentine and is opposite what is shown in the east side. The salt flow through the receiver starts from the riser and divides into the two cavitites in proportion to the flow control valve setting for each cavity. The salt, in each pass, goes through a control valve through the twelve absorber panels and then to the downcomer. This flow for the west cavity is shown in Figure 5.3-8 and was selected based on the trade study discussed in Section 3 of this report. Salt temperature is measured at the outlet of pass twelve and compared to a set point of 566°C (1050°F). A signal is then sent to the control valve adjusting the salt flow to achieve that temperature. Details on receiver control can be found in Section 5.4. A plan view of the east cavity receiver panels is shown in Figure 5.3-9. The absorber tubes in each panel are 31.8 mm (1-1/4 in.) OD Incoloy 800 coated with black Pyromark Series 2500 paint (a = 0.95, e = 0.90). The tubes are connected at the top and bottom into headers that are made from 0.3048 m (12 in.) diameter schedule 20S pipe of Incoloy 800 material. Since there is less solar flux directed toward the west cavity than there is to the east cavity the panel widths in the west cavity are smaller to allow the velocity of the molten salt at 1.85 m/s to match the salt velocity in the east cavity. The panel widths of the east cavity are 2.1 m (7 ft.) wide with 10 panels 18.3 m (60 ft in height) and the number one and twelve panels 15.5 m (51 ft) in hight. The panel widths of the west cavity are 1.8 m (6 ft) wide with ten panels 18.3 m (60 ft) in height and the number one and twelve panels 16.1 m (53 ft) in height.

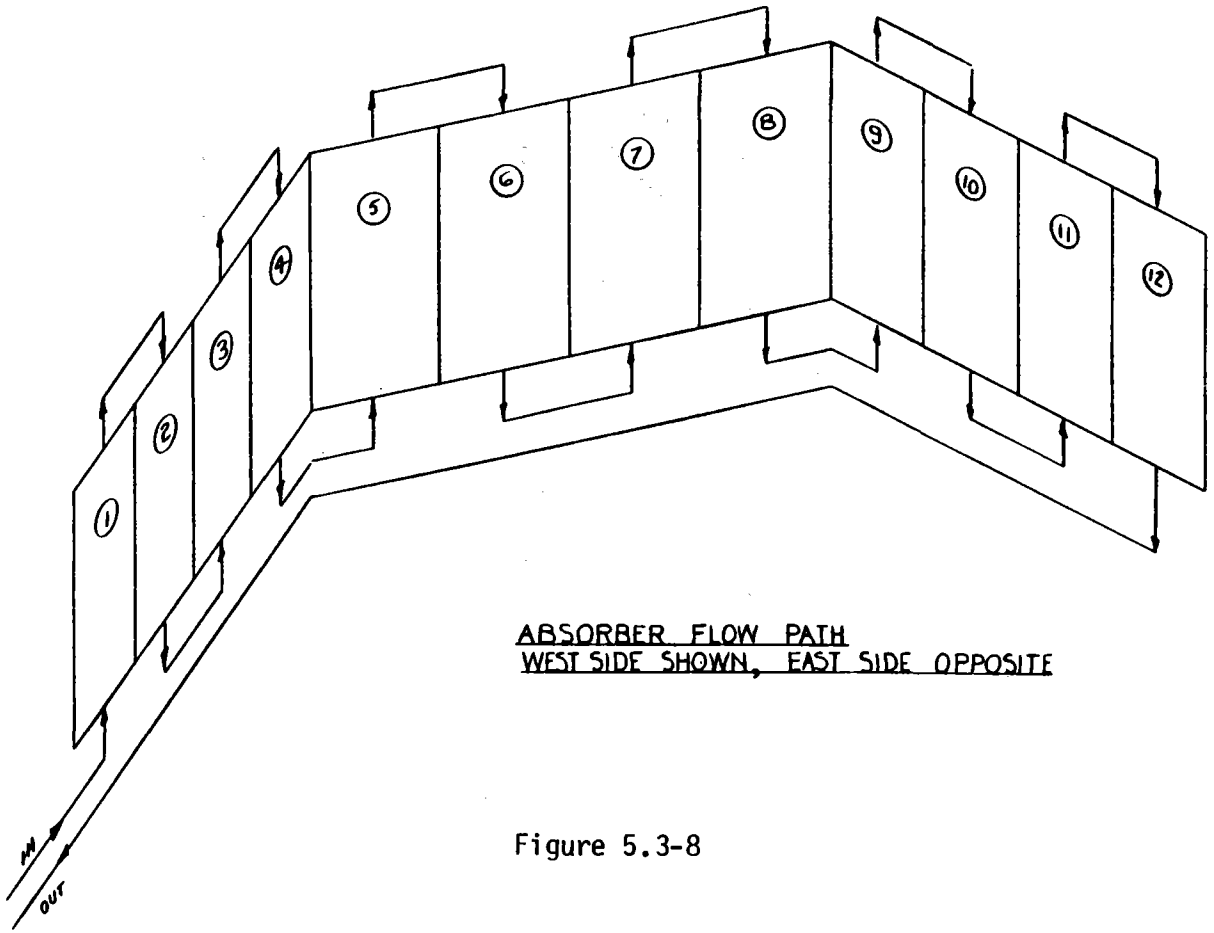

ABSORBER FLOW PATH
WEST SIDE SHOWN, EAST SIDE OPPOSITE

Figure 5.3-8

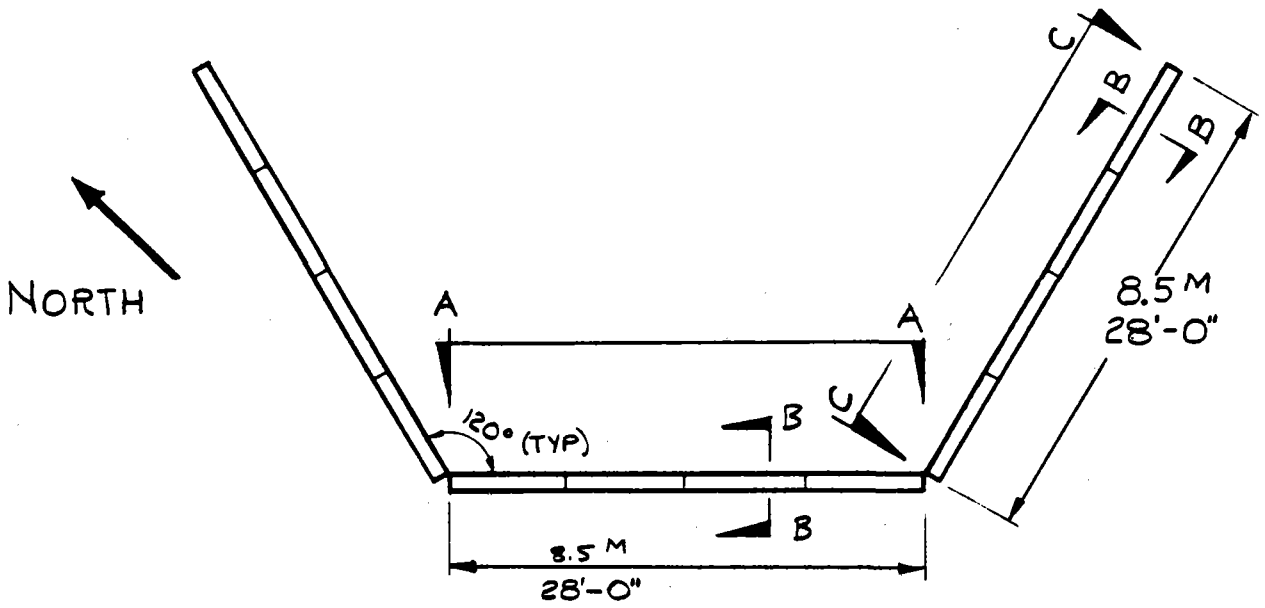

Figure 5.3-9 Plan - Receiver Panels, East Cavity

The panels are arranged and mounted to the cavity structure to allow only one sided heating of the receiver tubes. There is .25 m (10 in.) of insulation behind the receiver panels to protect the structure from any stray solar flux as well as provide a thermal boundary layer to prevent convection losses during the non-solar shutdown periods. The absorber tubes are parallel and attached intermittently to adjacent tubes of the same pass for the entire length to form solid panels. The tubes are attached to the headers by welding every other tube on the vertical centerline and alternate tubes at 30° off the vertical centerline. The panel upper headers are supported from built up beams at the top of each cavity structure. The panels are supported laterally by buckstays to the cavity structure. These buckstays will provide enough support to withstand the dominant earthquake loads. The lower headers are guided to absorb loads perpendicular to the panel faces permitting the headers to thermally expand vertically and horizontally parallel to the panel faces. A projected view of the east cavity panels is shown in Figure 5.3-10. The dashed lines show the outline of the radiation shield and the aperture outline.

5.3.4 Piping

The receiver piping consists primarily of the riser and downcomer attachments, the upper and lower interconnecting header piping, return, vent and drain piping, and the two surge tanks. The receiver inlet, or riser, piping is 0.25 m (10 in.) diameter schedule 20 A516 type carbon steel pipe. The outlet, and downcomer piping is 0.20 m (8 in.) diameter schedule 20S Incoloy 800. The downcomer is designed with a smaller diameter than the riser to help dissipate the potential energy of the salt at the top of the tower. The connections to the surge tanks are 0.25 m (10 in) diameter pipe with the cold line being A516 carbon steel and the hot line being Incoloy 800 pipe. All other receiver piping is Incoloy 800. Supply lines, panel interconnections and return lines are schedule 20S .30 m (12 in.) diameter Incoloy 800 pipes. All connections between valves and interconnecting piping are welded to prevent salt leakage. All drain and vent lines are Schedule 40S 0.201 m (4 in.) diameter Incoloy 800 pipe. The absorber panel upper and lower headers are schedule 20S 0.30 m (12 in.) diameter Incoloy 800 pipe. The drain lines are gathered and connected to the downcomer attachment. Each drain line has a normally closed, remote pneumatically driven drain valve. The vent lines for the east and west passes are separately gathered and connected to the upper part of the hot surge tank. Each line has a normally closed, electrically powered, remotely controlled vent valve as well as a vacuum relief valve to help avoid absorber tube collapse should a vent valve fail to operate.

The cold and hot surge tanks are shown in Figure 5.3-11 along with the inlet and outlet connections. The hot surge tank is mounted at the top of the vertical center structure so that the free liquid level with the tank partially filled will be above the top of the highest headers. This will provide for positive filling of all of the absorber tubes and interconnecting piping. The surge tanks are the same size and will be controlled to maintain their level at the half full point. The receiver inlet, or cold, surge tank is pressurized to 2.50 MPa (363 psig) and the outlet, or hot, surge tank is pressurized to 0.138 MPa (20 psig). The hot surge tank pressure is above the salt vapor pressure and provides a margin to ensure that the tank always has a positive pressure. The cold surge tank pressure was selected to match the conditions at the receiver inlet.

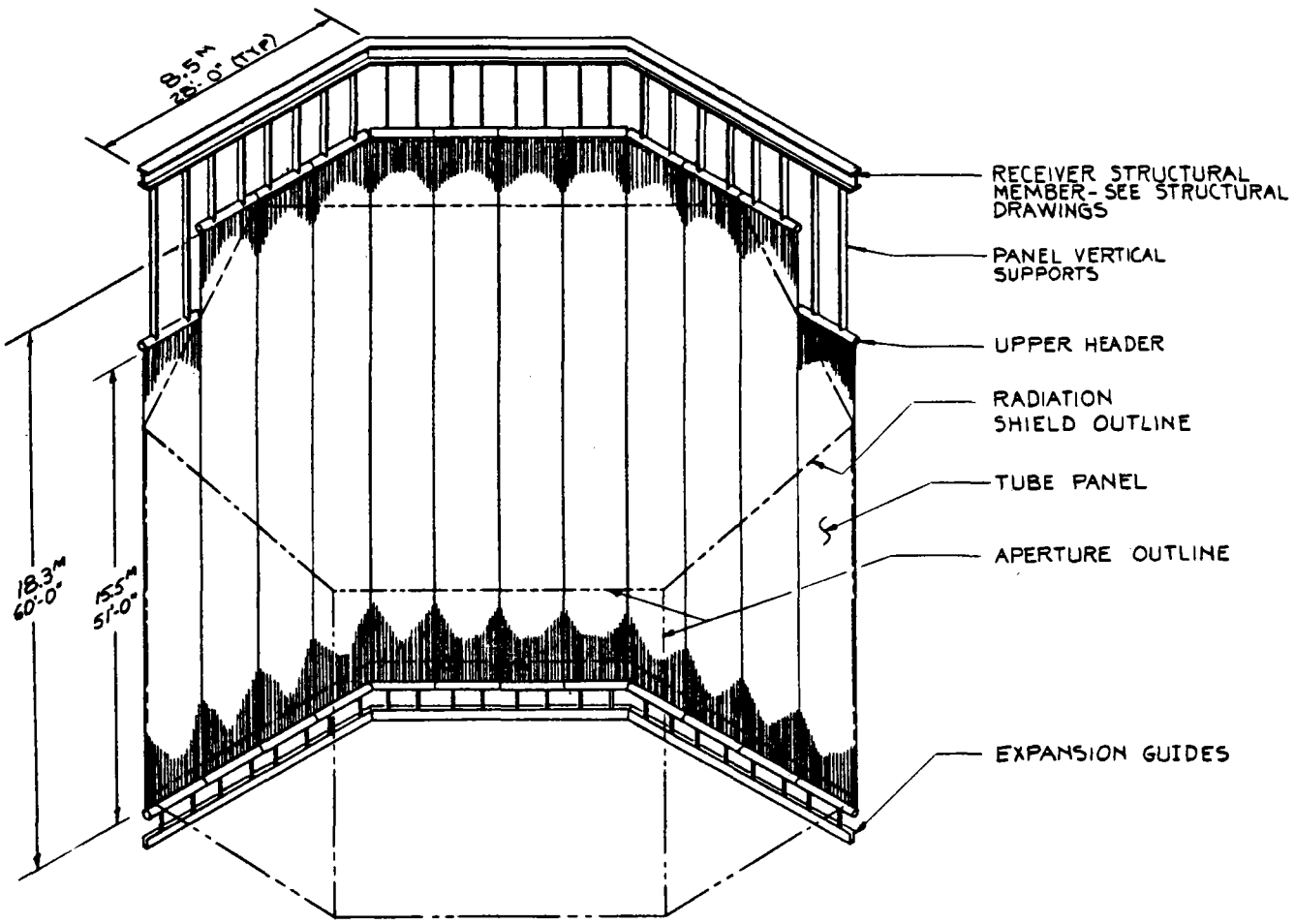

Figure 5.3-10

Projected View of East Cavity Panels

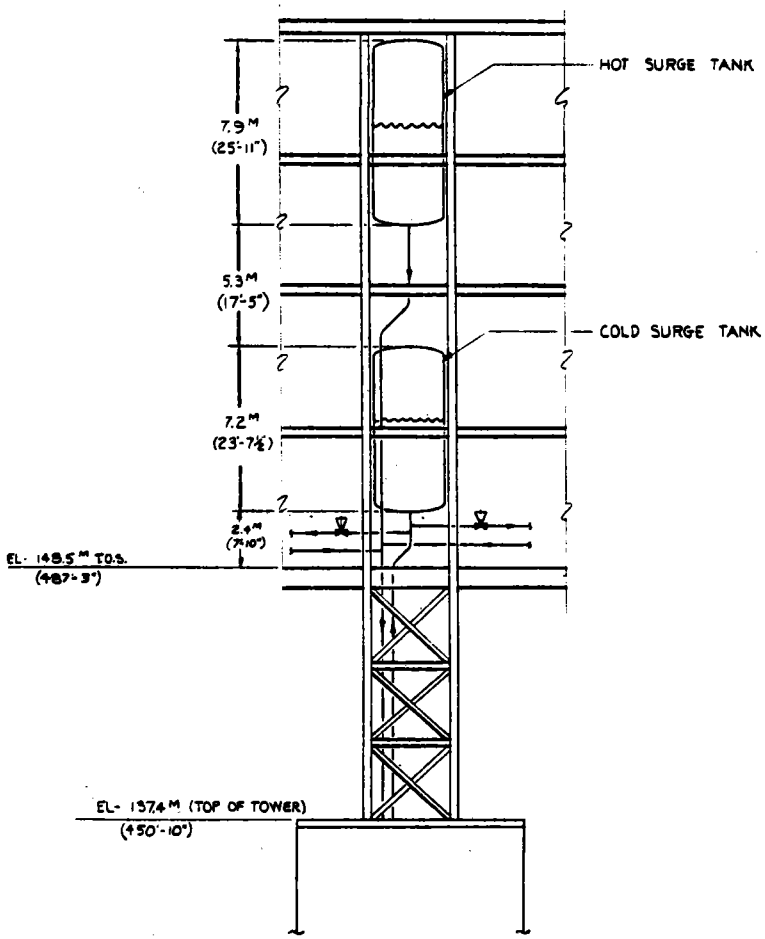

Figure 5.3-11 Section C-C
Surge Tanks Orientation

An air compressor system is provided to supply air to the hot and cold surge tanks. The air compressor will be located in a separate room in the top of the tower so it is not exposed to the higher temperatures in the receiver area and so that it can be readily serviced. The air storage tank will be located near the compressor. This location can be seen in the tower layout drawing, Figure 5.3-12.

The air supply system was sized to permit filling the cold and hot surge tanks from ambient pressure to their design values in approximately 30 minutes using the compressor and stored air together. This resulted in system characteristics shown in Table 5.3-1. The time to fill the air storage tank from ambient is less than 2 hours. When the cold surge tank is being used to force salt through the receiver during an emergency, its air pressure will reduce as the air volume decreases. During this process, the air storage tank will continue to supply air to the surge tank. the result is an average cold surge tank pressure above 2.07 MPa (300 psig) during the blowdown.

Table 5.3-1 Receiver Air Supply System Characteristics

Compressor		
Rating	0.142 Std m^3/min	(300 scf/min.)
Pressure	4.14 MPA	(600 psig)
Motor Power	112 kWe	(150 hp)
Weight of Three Stages with Intercooling	3,629 kg	(8000 lb)
Air Storage Tank		
Pressure	4.14 MPa	(600 psig)
Volume	5.7 m^3	(200 ft^3)
Diameter	1.8 m	(6 ft)
Shell Thickness	38.1 mm	(1.5 in.)
Weight	7,257 kg	(16,000 lb)

An evaluation of the pressure drops in the receiver at the design point was made with the results shown in Table 5.3-2. Most of the pressure drop occurs in the absorber tubes and the static head above the tower top. The control valve was taken as a percentage of the dynamic head and the margin was taken as a percentage of the first five items in the table.

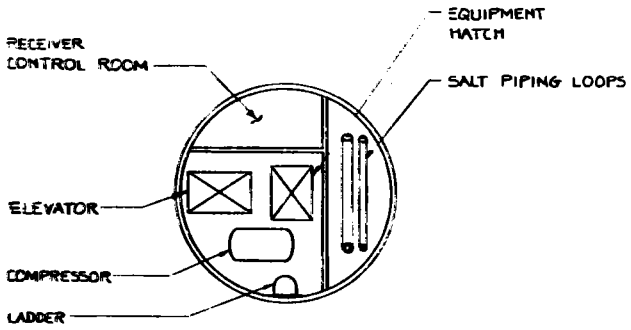

PLAN AT 137M (449'-6")

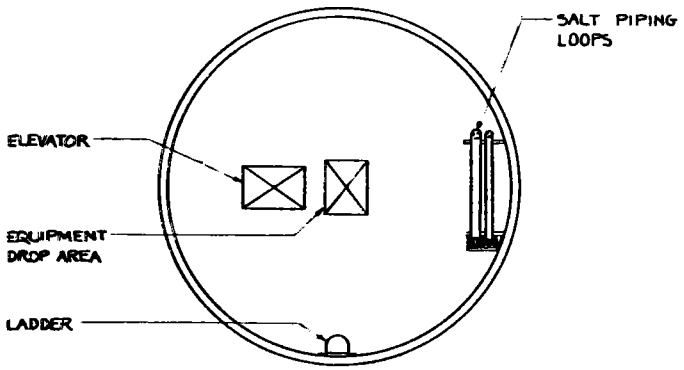

PLAN AT 1.5M (5'-0")

Figure 5.3-12 Tower Layout

Table 5.3-2 Receiver Pressure Drop Summary

Item	Equivalent Head of Salt, m (ft)
Absorber Tubes	54 m (178 ft)
Interconnecting Pipe	15 m (48 ft)
Headers	7 m (24 ft)
Valves	19 m (63 ft)
Surge Tank	7 m (24 ft)
Static Head of Receiver	20 m (66 ft)
Margin	10 m (34 ft)
Total Operating Head	132 m (437 ft)

5.3.5 Receiver Thermal Protection Considerations

Thermal protection methods were examined to (1) insulate the structure of the receiver from high temperatures, (2) minimize the cooldown of the receiver during overnight shutdown, and (3) protect absorber tubes when a pump or power failure occures with solar flux directed into the receiver. The first two items require the use of radiation shields within the receiver cavity to both redirect radiation within the receiver and also protect nonabsorber materials (structure, headers, instrumentation). Insulated doors on the receiver apertures are used to minimize cooldown during nonoperation.

Protection of the absorber tubes during an unexpected salt flow stoppage required consideration of the potential causes of such a failure and methods to shield the absorber tubes from high energy flux.

Calculations were first performed to determine the absorber tube metal temperature rise rate with a salt flow stoppage and energy from the collector field into the receiver. Such an occurrence might happen due to one of the following:

1) Failure of the cold salt pumps;
2) Downcomer valve closure;
3) Salt piping blockage;
4) Receiver salt control valve failure in a closed position;
5) Electrical power failure.

If such a salt flow stoppage should occur and power is available to the collector field, heliostats will be defocused to reduce energy flux into the receiver. However a finite time period is involved in detecting the failure, deciding what action to take, and then acting. Therefore, in our evaluation the first step was to determine the time required to heat the absorber tubes to an upper temperature limit with complete salt flow stoppage. This temperature was determinined to be approximately 649°C (1200°F) for Incoloy 800.

A two-dimensional heat transfer computer model was formulated using the MITAS code. The nodal network developed for the Incoloy 800 tube is shown in Figure 5.3-13, which shows Node 1 on front side and centerline of the tube where it

receives peak incident power from the collector field. Node 19 is on the back side of the tube and receives no solar energy from the heliostats. Thus, Nodes 1 through 19 represent the outer surface of half the tube, Nodes 101 through 119 represent the inner surface of the tube, Nodes 301 through 319 represent the salt boundary layer, and Node 200 represents the salt bulk temperature.

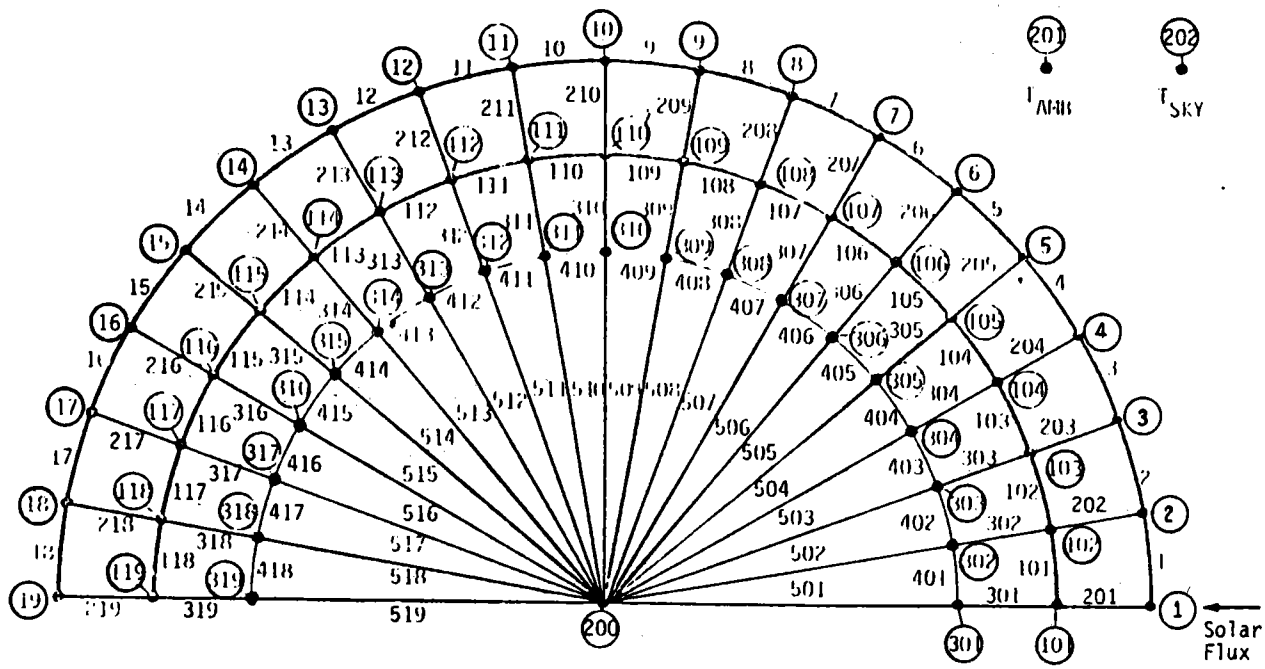

Figure 5.3-13 Sudden Flow Stoppage Model, Node and Conductor Numbers

Two failure modes were examined; the first assumes that a flow stoppage occurs in the tube with an incident power level of 640 kW_t/m^2 (203,000 Btu/hr-ft^2) on the front side of the tube for 5 seconds. Initial temperature of salt is 433°C (830°F). After 5 seconds, the power level on the tube immediately drops to zero. The resulting temperatures in the tube and salt at 5 seconds after a flow stoppage are shown in Figure 5.3-14. Results indicate that the tube temperature are quite high--936°C (1716°F)--and the temperature gradient from the front to the back side of the tube is excessive--486°C (875°F). Figure 5.3-15 shows the time-dependent tube surface temperature.

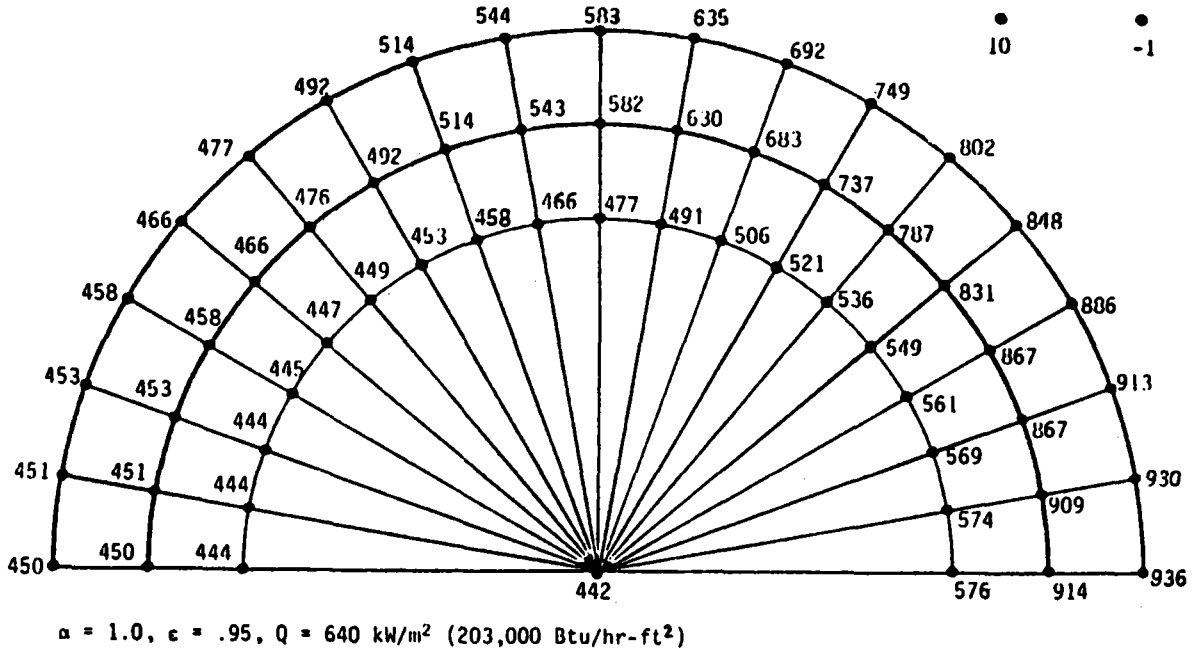

Figure 5.3-14 Sudden Flow Stoppage, Temperatures at 5 Seconds (°C)

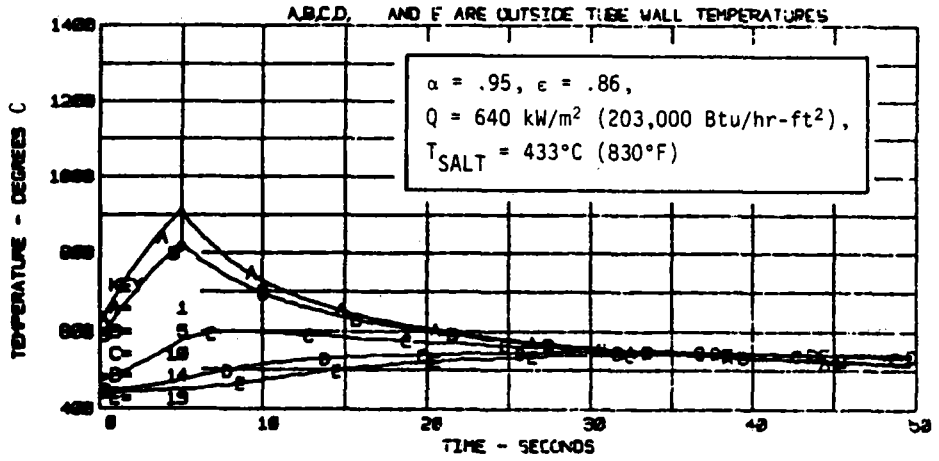

Figure 5.3-15 Sudden Flow Stoppage, Temperatures Around the Tube (°C)

The second failure mode assumed salt flow stoppage, 640 kWt/m^2 (203,000 Btu/hr-ft^2) power on the tube for 2.5 seconds, and then a declining straight-line decrease in power to zero at 5 seconds.

The time-dependent tube surface temperatures are shown in Figure 5.3-16. Again, high tube temperatures and temperature gradients result which cannot be tolerated.

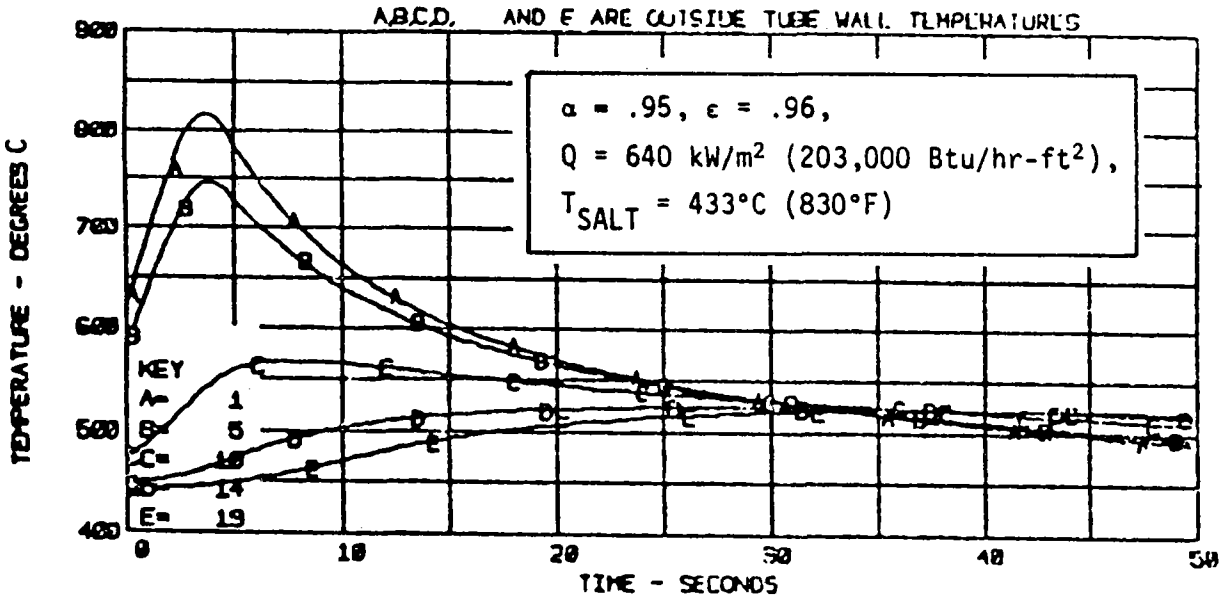

Figure 5.3-16 Sudden Flow Stoppage, Temperatures Around the Tube (°C)

Results of these analyses clearly indicate that even a short duration flow stoppage cannot be tolerated in a salt receiver with high solar flux levels on the receiver. Such an occurrence would lead to either absorber tube failure, tube warpage, or reduction of tube life. Therefore, in the receiver design, we have incorporated additional features that will ensure salt flow through the receiver (cold surge tank) and protection of absorber tube surfaces once salt flow through the receiver is exhausted (ablative covered door). A backup diesel generator will also be available that can provide 600 kW_e with 30 seconds from start which will actuate the collector field scram.

It is expected that any loss of cold salt surge tank pressure would be gradual. At the first sign of pressure loss, the heliostats would be defocused. If salt flow dropped below a set limit before the cavity solar flux had dropped sufficiently, then the cavity door closing function would be exercised. Designing the door closure with 0.1 g gravity assist requires 6 seconds to complete the cavity door closure. Once the door closes, the face of the door intercepts the incoming flux. Without thermal protection, the solar flux may damage the door by either creating thermal stresses that will warp it or burning a hole through the thin metal sheets. Therefore, various thermal protective systems were evaluated to protect the door.

Our evaluation of thermal protection methods considered the use of typical schemes for high-temperature applications. These methods include ablative, radiative, transpiration cooling, and heat-sink concepts. The concept selected for receiver door application was the use of an ablative material. The ablative provides the lowest cost and lowest weight of the options considered. The properties of the selected ablative material are given in Table 5.3-3.

Table 5.3-3 Material Properties of Martin Marietta ESA-3560 Ablator

Density	481±32 kg/m^3 (30±2 lb/ft^3)
Thermal Conductivity	0.098 W/m-°C (0.68 Btu-in/hr-ft^2-°F)
Specific Heat at 24°C	1.55 J/kg°C (0.37 Btu/lb-°F)
Emissivity	0.85
Ablation Temperature	443°C (830°F)
Effective Heat of Ablation	13491 kJ/kg (5800 Btu/lb) for 50 sec at 681 kWt/m^2 (60 Btu/ft^2-sec)
Storage Life	Indefinite below 66°C (150°F)

This ablative material has been used on flight test vehicles and the Viking spacecraft. A 0.076 m (3 in.) thickness of this ablative material was estimated to be sufficient to accept the peak solar flux and carry heat away from the receiver door as the material ablates. The material will be installed in small easily handled panels on the receiver door to minimize the expense of replacement.

It now appears that such power failures leading to salt pump outages or collector field in operation would occur infrequently, thus minimizing the need for replacement of ablative surfaces. However, the use of low cost thermal protection schemes alleviates the concern for absorber tube replacements due to excessive temperatures during potential failure modes.

5.3.6 Receiver Weight

The results of the receiver weight study are summarized in Table 5.3-4 While the distribution of weights is somewhat different than previous molten salt receivers, the center of gravity for this cogeneration conceptual design falls approximately over the centerline of the tower.

Table 5.3-4 Receiver Weight Summary

Structure	273,516 kg (603,000 lb)
Surge Tanks	48,081 kg (106,000 lb)
Siding	60,600 kg (133,600 lb)
Insulation	45,509 kg (100,330 lb)
Panel Tubing	32,568 kg (71,800 lb)
Piping, Valves	22,544 kg (49,700 lb)
Door Hoists	2,722 kg (6,000 lb)
Subtotal Dry Weight	485,540 kg (1,070,430 lb)
Molten Salt Weight	154,221 kg (340,000 lb)
Total Operating Weight	639,761 kg (1,410,430 lb)

5.3.7 Thermal Stress Analysis and Creep-Fatigue Evaluations

The design guidelines for creep-fatigue damage on the tubes are based on the ASME Boiler Code, Code Case 1592. The total creep-fatigue damage criterion is expressed as:

$$\sum_{j=1}^{P}\left(\frac{n}{N_d}\right)_j+\sum_{k=1}^{P}\left(\frac{t}{T_d}\right)_k \leq 1$$

Where:

n - number of applied cycles
N_d - number of design allowable cycles;
t - time duration of load condition, k;
T_d - allowable time at a given stress intensity;
P - number of time intervals used for analysis.

The life of the receiver tubes is to be 30 years. The tube must therefore survive nearly 28,000 temperature cycles and avoid creep fatigue damage.

Fatigue damage on the receiver tube is based on the equivalent strain range which is defined in code case 1592 as:

$$\Delta\varepsilon_{equiv} = \frac{\sqrt{2}}{3}\left\{\left[\Delta(\varepsilon_1 - \varepsilon_2)\right]^2 + \left[\Delta(\varepsilon_2 - \varepsilon_3)\right]^2 + \left[\Delta(\varepsilon_3 - \varepsilon_1)\right]^2\right\}^{\frac{1}{2}}$$

where:

$\Delta\varepsilon_{equiv}$ = equivalent strain range

ε_1 - Linear strain in longitudinal direction of the tube

ε_2 - linear strain in tangential direction of the tube

ε_3 - liner strain in radial direction of the tube

Design allowable fatigue cycles, ND, is found using Figure 1420-1c of code case 1592-10 and T_d values for creep damage is found using Figure I-14.6c of code case 1592-10.

As shown in the creep-fatigue damage equation, the creep-damage is defined as follows:

$$\Delta_c = \int_0^t \frac{dt}{T_d} = \sum \frac{\Delta t}{T_d}$$

where: t = time

T_d = allowable time at a given stress intensity

Δ_c = creep damage

Following a rationale suggested by the Power Piping Code, ANSI B31.1, reliance is placed on the previous analysis and the similarities between the two projects. A duplicate analysis has not been done at this stage.

5.3.8 Receiver Riser and Downcomer Piping

The receiver riser and downcomer piping delivers molten salt to the receiver and returns it to the molten salt storage area. Based on Martin Marietta's materials compatibility tests, the selection of Incoloy 800 for hot salt piping represent low risks for installation at the facility. Discussed below are the requirements, design description, and performance and cost of this molten salt piping subsystem.

5.3.8.1 Requirements

The receiver riser and downcomer piping as well as the pumps required to circulate molten salt through the receiver will be required to deliver molten salt at a flow rate which will allow a normal peak thermal rating of 122 MWt (417 MBtu/hr) at the base of the tower with a temperature differential of 277°C (500°F). The design salt flow will therefore be 0.995M kg/sec (2.19 M lb/hr) or 0.144 m^3/sec (2285 gpm) of cold salt. The system of pumps, piping and controls will be capable of delivering molten salt at all flwo rates from 10 to 110% of design. In every case, the pumps will need to overcome the static head of salt up to the liquid level in the cold surge tank plus the pressure in that drum above the liquid level as well as friction losses in the line. Downcomer piping is designed to use the available pressure in the hot salt surge tank as well as the static head of salt from the hot salt surge drum liquid level to the hot salt storage tank liquid inlet.

Provisions are made for temporary retention of salt that is too hot for return to the cold storage tank and too cold for storage in the hot tank. The piping is designed to accommodate thermal expansion without exceeding allowable design stress limits. The piping is also designed to be drained to a tank provided for that pupose.

Vertical piping will include conventional expansion loops. Loop sizing and stress analysis are based on methods outlined in Grinnell, "Piping Design and Engineerng," Fifth Edition.

Downcomer piping carries hot salt 566°C (1050°F); Incoloy 800, Schedule 20 has been selected for this service. Riser piping carries cold salt at 288°C (550°F); carbon steel, A516, Sch 40, has been selected for this service.

Allowable stresses for carbon steel are taken from ANSI B31.1, Power Piping Code. Allowable stresses for Incoloy 800 are taken from the ASME Boiler and Pressure Vessel Code, Code Case 1325-9. Sketches of tower piping loop configuration are based on these calculations and shown in Figure 5.3-17.

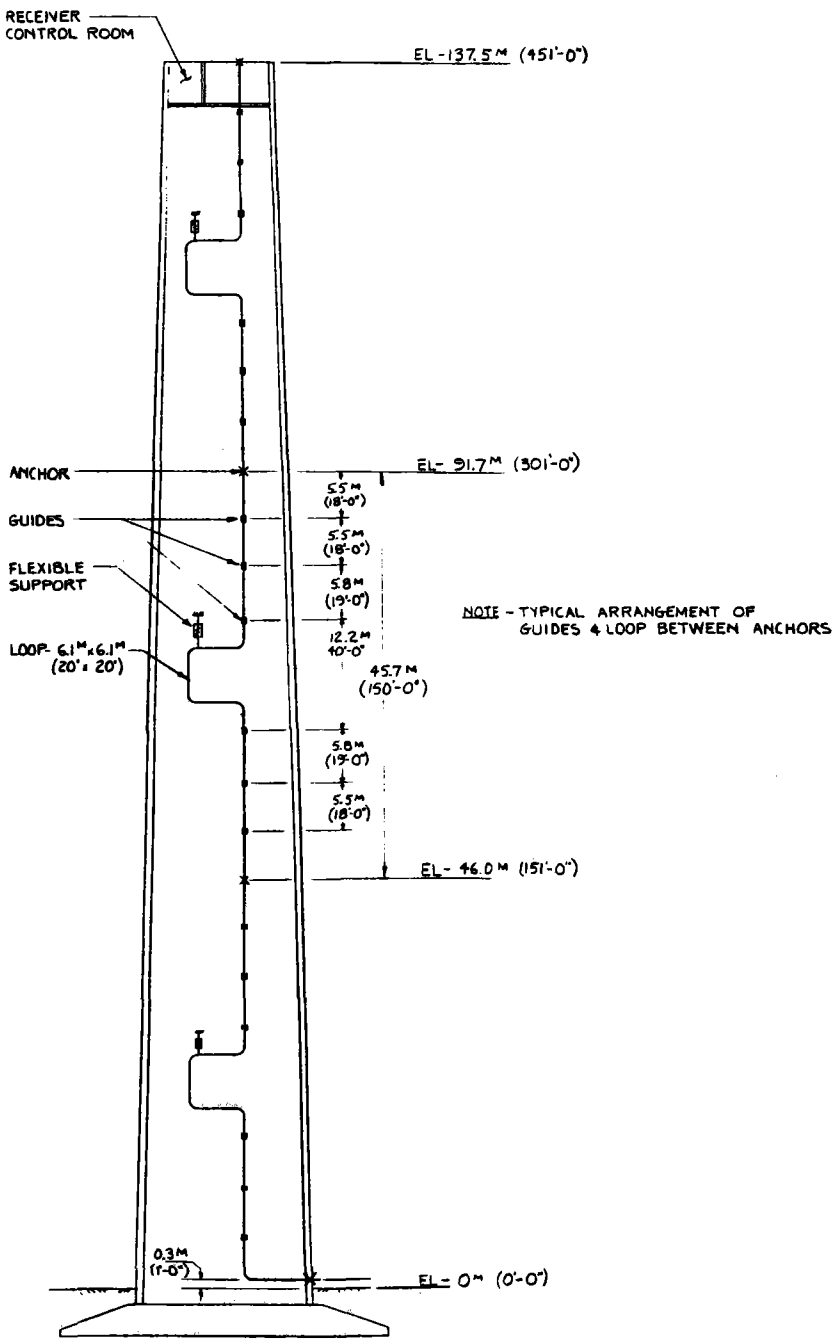

Figure 5.3-17 Tower Elevation-Piping Configuration

Materials testing has been performed on various candidate metals for use with molten salts. Detailed results of this testing are reported in Martin Marietta Corporation Document No. MCR-81-1707, March 1981, "Final Draft Report; Alternate Central Receiver Power System Phase II; Volume II, Molten Salt Materials Tests."

Of specific interest for piping design is Table 5.3-5, reproduced in part (for Incoloy 800), as follows.

Table 5.3-5 Extrapolated 30 year Weight Loss - Metal Reduction Values for I800 as a Function of Temperature in Dynamic Molten Salt Loop

MATERIAL	TEMPERATURE °C (°F)	WEIGHT LOSS (30 Years) mg/cm^2	METAL (30 Years) mm (x 10^{-2})	MILS
I800	357 (675)	5.8	7.6	0.3
	440 (825)	191.7	23.9	9.4
	482 (900)	32.9	4.1	1.6
	566 (1050)	105.2	13.2	5.2

This is a report of "dynamic" testing, including influence of flow in the pipe, which results in a combined corrosion-erosion metal loss.

An allowance must be provided in the pipe wall thickness to accommodate this corrosion and erosion. The test report indicates a maximum corrosion-erosion of 9.4 mils at 440°C (825°F) for 30 years (extrapolated), and a salt velocity of 3.4 m/s (11 ft/sec). An allowance of 12 mils would therefore be conservative.

The allowance is included by the use of Schedule 20 pipe (wall thickness, 0.64 cm [0.25 in.]) which includes 0.25 cm (0.10 in.) excess material over that dictated by pressure/temperature ratings and other stress requirements.

5.3.8.2 Performance and Cost

The pumping and piping system has been designed with adequate controls and instrumentation to handle all flow rates between 10 and 110% of design capacity while minimizing operating costs. No difficulty is anticipated in meeting these requirements.

The estimated installed cost of the receiver circulating equipment and piping including instrumentation and controls, heat tracing, insulation and engineering is included in the supporting data of Appendix A.

5.3.9 Tower Design

This section describes the receiver tower design and discusses the supporting analyses influencing the tower design.

5.3.9.1 Tower Description

The reinforced concrete tower that supports the receiver weight of 639,806 kg (1,408 kips) with salt in the tubes, headers and surge tanks consists of a hollow truncated conical shaft integral with an octagonal shaped mat foundation as shown in Figure 5.3-18. The conical shaft extends 137.4 meters (450.8 ft) above the top of the foundation. Outside diameter of the slip formed concrete shaft is 19.8 m (65 ft) at the base and 12.26 m (40.25 ft) at the top. Wall thickness of the concrete shaft at the base is 46 cm (18 in.) and it tapers uniformly to a thickness of 25 cm (10 in.) at the top (Figure 5.3-19). A large reinforced concrete ring beam which is integral with the shaft is provided at the top of the shaft in order to provide a base for the receiver's steel support structure and base plates. A reinforced concrete slab is provided at the top of the shaft.

Tower Design Consideration - The receiver tower is designed to withstand the following lateral loads:

1. Wind loads corresponding to a maximum wind speed including gusts of 40 m/s (90 mph). Wind loads are calculated in accordance with the requirements of ANSI A58.1-1972.

2. Seismic loads corresponding to the UBC Zone 4 seismic loads are calculated in accordance with the procedure described in the 1979 edition of the Uniform Building code (UBC).

The tower bottom diameter, wall thickness and the mat plan dimensions and thicknesses are adequate to resist the maximum wind or seismic loads together with the gravity loads on the structure.

The size of the ring beam of the tower top is selected to suit the receiver support structure dimensions and to provide sufficient space for the elevator, piping and equipment and equipment hatch.

The calculated bearing pressure on the soil due to dead loads is approximately 0.143 kPa (2.98 lb/ft^2). Under the lateral wind load corresponding to 40 m/s (90 mph) wind, and the dead load, the calculated soil pressure varied from 0.245 kPa (5.12 lb/ft^2) on one edge of the mat to 0.04 kPa (0.84 lb/ft^2) on the opposite edge of the mat. From the site soil information and assumptions, it appears that the soil bearing capacity is adequate to support the tower loads.

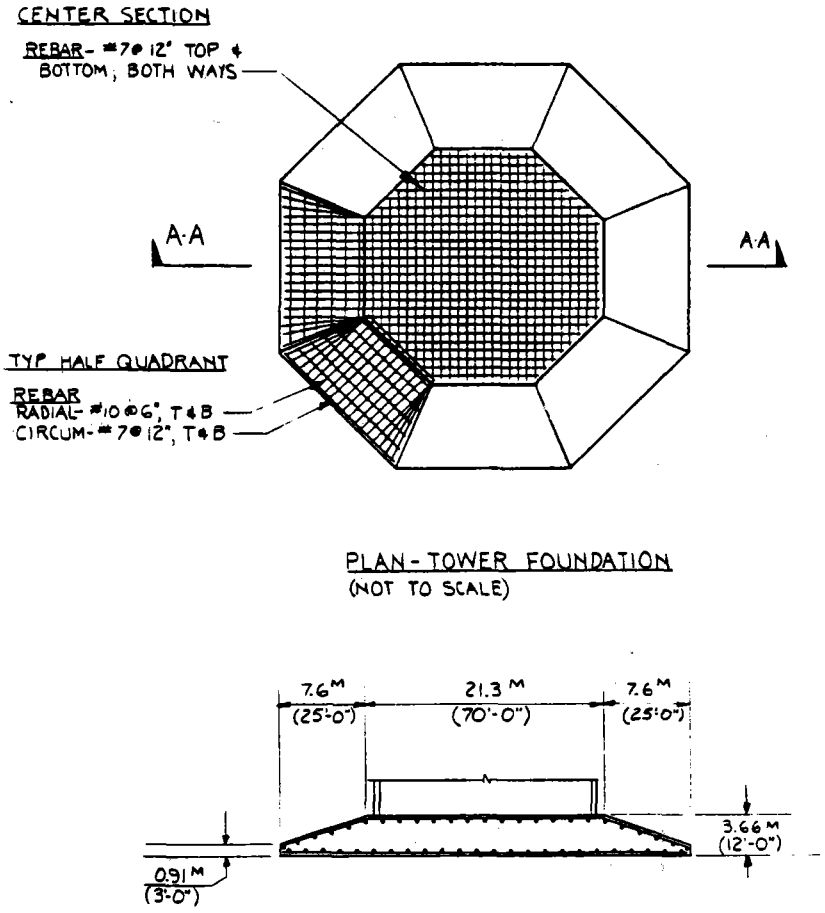

Figure 5.3-18 Section A-A - Tower Foundation

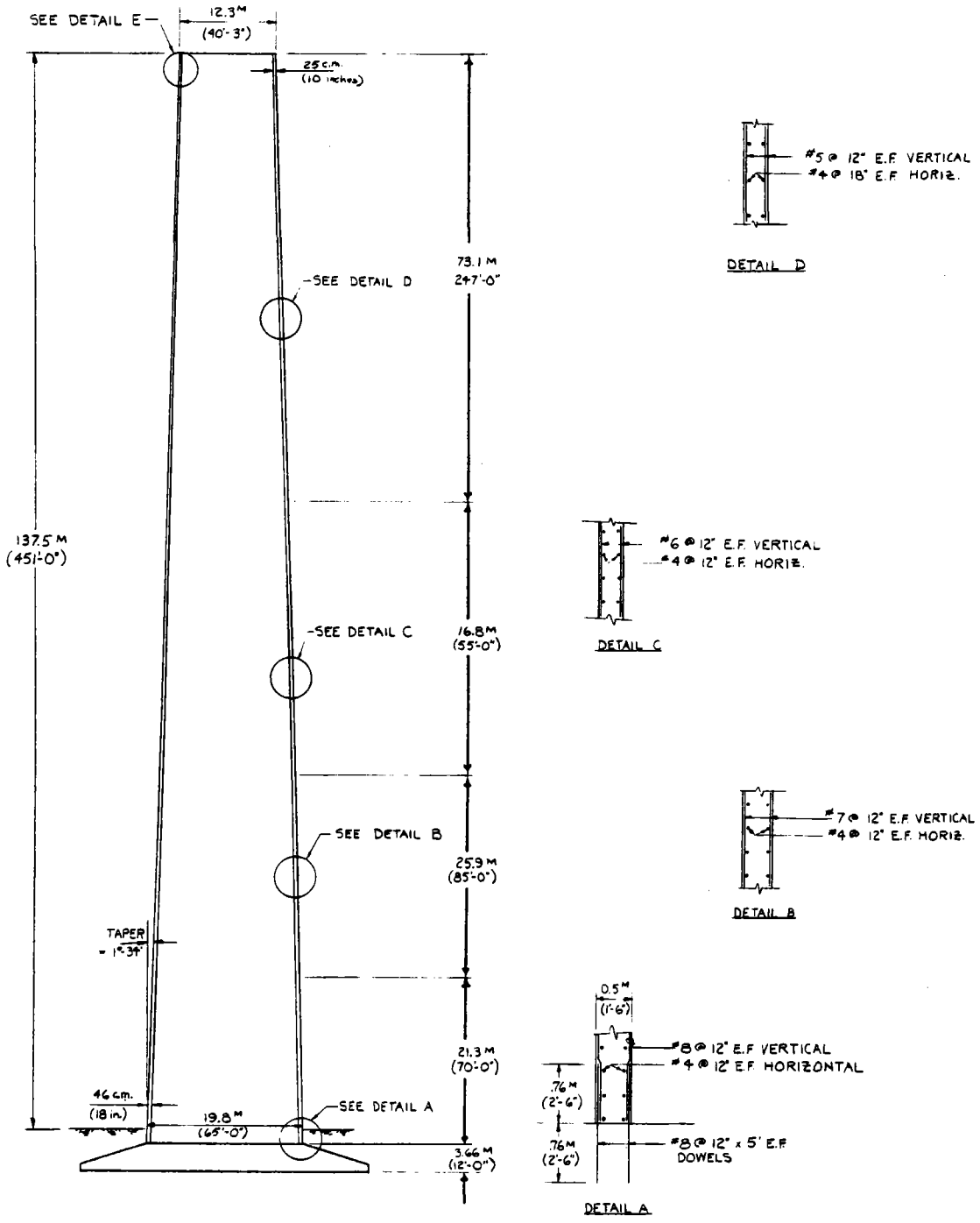

Figure 5.3-19 Elevation-Tower Structure

The tower weight is 6,181,557 kg (13,628 kips) and the foundation weight is 8,482,177 kg (18,700 kips) for total of 14,663,734 kg (32,328 kips). The receiver weight of 639,658 kg (1408 kips) would bring the total to 15,302,392 kg (33,736 kips).

A room has been provided at the top of the tower for the air compressor for the receiver hot and cold surge tanks and for the receiver control system air compressor and storage tank. A smaller room at this level will contain the electronic equipment racks for the receiver controllers. The tower will be fitted with the appropriate lighting per Federal Aviation Administration requirements. An elevator has been provided for personnel and carrying smaller equipment to the top of the tower. The central area of the tower (near the vertical centerline) has been reserved for lowering and raising the larger receiver parts during repair operations.

5.3.9.2 Receiver Cost Summary

The direct costs of the various elements of the receiver subsystem are listed in Table 5.3-6. Further costs details may be found in Appendix A.

Table 5.3-6 Receiver Direct Costs

WBS Number	Element	Cost, 1980 $
5410	Receiver Unit	4,114,154
5421	Riser/Downcomer	462,030
5430	Heat Transport Fluid	58,966
5440	Tower	1,728,888
5450	Tower Foundation	852,273
5400	Receiver Subsystem	7,216,311

5.3.10 Receiver Performance

5.3.10.1 Flux Determination

Martin Marietta's TRASYS program was used to develop aiming strategies and flux distributions on the receiver surfaces. TRASYS is a computer program developed by Martin Marietta with the generalized capability to solve the radiation related aspects of thermal analysis problems. In the past, it has provided valuable, accurate data to support thermal analyses of a variety of space systems. The program has been expanded over several years to handle radiation problems associated with heliostat fields and solar central receivers by the addition of a "Mirror Field" library of subroutines. TRASYS-generated heliostat flux data have been compared with actual heliostat test data several times, most recently in the Martin Marietta Alternate Central Receiver Power System Phase II project (Ref 5.3-5). These comparisons indicated that TRASYS is fully capable of reproducing experimental measurements within a reasonable level of accuracy. Its particular advantage lies in its ability to determine radiant thermal interactions within a cavity receiver.

To calculate this information, TRASYS requires a geometric cavity surface description, along with the size and location of all the heliostats, the desired date, time, and solar beam strength. Each heliostat is aimed directly at the aperture center unless otherwise specified, and the combined flux from all the heliostats is then totaled for each surface node. (Detailed computer generated plots of the breakdown for each cavity are presented in Appendix A.)

Information calculated by TRASYS for each heliostat includes: the solar flux incident on that mirror, the flux reflected to the receiver (after allowing for atmospheric attenuation), the cosine of the half bounce angle, and the aperture and overall efficiencies. Results given for the entire field include the total power entering the aperature, the incident and absorbed fluxes on each receiver node, the average field cosine of angle of incidence, aperture efficiencies, and average atmospheric attenuation.

The individual coordinates of the optimized heliostat field listed in Appendix A were used in the TRASYS model for the cogeneration receiver. Two independent models were constructed by dividing the collector field into east and west quadrants, then constructing separate geometric descriptions of each cavity. TRASYS runs were then made which calculated the incident flux on each receiver node for a given time of day and year. Flux data for each cavity for days 81, 172 and 355, for 0900, 1200 and 1500 hours were run. Figure 5.3-20 is a typical flux map for day 81. These TRASYS incident flux calculations were orignally made with the intention of extrapolating absorbed flux data from them. Typically, our high efficiency cavity receivers reflect less than 2.0% of the incident solar energy. However, to verify this, it was subsequently decided to calculate the absorbed fluxes. This flux information, presented in Appendix A, agrees well with the incident flux information presented here.

As explained in Section 3.6, a properly optimized aperture allows some spillage of the incident solar energy. This energy which does not enter the cavity is either reflected or absorbed by the white painted radiation shields located around each aperture. However, if the absorbed solar fluxes around the apertures are too high, damage to the receiver may result.

Figure 5.3-21 shows the results of a TRASYS analysis pinpointing the yearly peak absorbed solar fluxes around the apertures. Complete flux diagrams for the peak conditions around each aperture are shown in Figure 5.3-22 and 5.3-23. Previous Martin Marietta studies (Ref 5.3-4) have shown that stainless steel with a low absorptivity paint (white pyromark Series 2500) can tolerate an absorbed heat flux of 6.31 W/CM^2, while our maximum absorbed heat flux is only 1.64 W/cm^2. Thus, high temperature white painted stainless steel is an acceptable protective material for use around our apertures.

5.3.10.2 Thermal/Hydraulic Performance

A MITAS thermal math model was constructed to calculate the salt and absorber tube steady-state temperature profiles in the receiver panels. One absorber tube was modeled to represent all of the tubes in a panel. This tube is divided into ten segments containing front and back outside tube surface nodes, front and back inside tube surface nodes and salt nodes. A typical tube segment is shown in Figure 5.3-24.

TIME: 1200

DAY: 81

INSOLATION: .950 kW/m^2

APERTURE EFF: 0.978

AVG. COSINE: 0.8951

INCIDENT POWER: 77.08 MW
(AT APERTURE)

EAST CAVITY
INCIDENT FLUXES - W/cm^2

($1 \frac{W}{cm^2} = 3.17 \times 10^3 \frac{Btu}{hr\text{-}ft^2}$)

0.0	.707	2.51	2.90	3.18	2.65	1.63	1.97	2.44	2.11	.740	.002
0.0	1.22	3.29	3.65	4.31	4.07	4.01	4.09	3.59	2.77	.813	.003
0.0	1.71	3.72	5.07	6.24	6.23	7.69	7.15	5.30	4.27	1.12	.010
.004	2.90	6.99	9.98	12.4	12.3	13.2	12.6	9.31	8.33	3.03	.122
.242	7.87	20.4	25.5	33.1	33.9	32.8	30.9	23.8	21.2	9.59	.846
2.50	18.2	37.6	41.7	53.3	56.8	54.2	48.9	37.9	34.7	18.7	3.66
5.57	25.1	45.0	47.3	60.0	65.6	63.0	54.8	42.5	40.1	23.6	6.33
6.47	23.8	39.2	39.8	51.3	57.7	56.0	47.2	35.9	35.0	22.0	6.95
5.01	1.62	25.5	25.9	34.7	40.3	39.3	32.4	23.8	23.6	15.6	5.32
2.68	8.38	13.0	13.4	19.0	22.8	22.3	18.0	12.5	12.4	8.30	2.92
.836	3.01	4.94	5.16	8.21	10.4	10.3	7.97	5.05	4.93	3.21	1.07
.049	.353	.712	.665	1.31	1.89	1.86	1.27	.605	.733	.510	.132

1.52 m (5 ft)

SOUTH WALL | BACK WALL | NORTH WALL

2.13 m (7 ft)

Figure 5.3-20 Typical Receiver Incident Flux Map

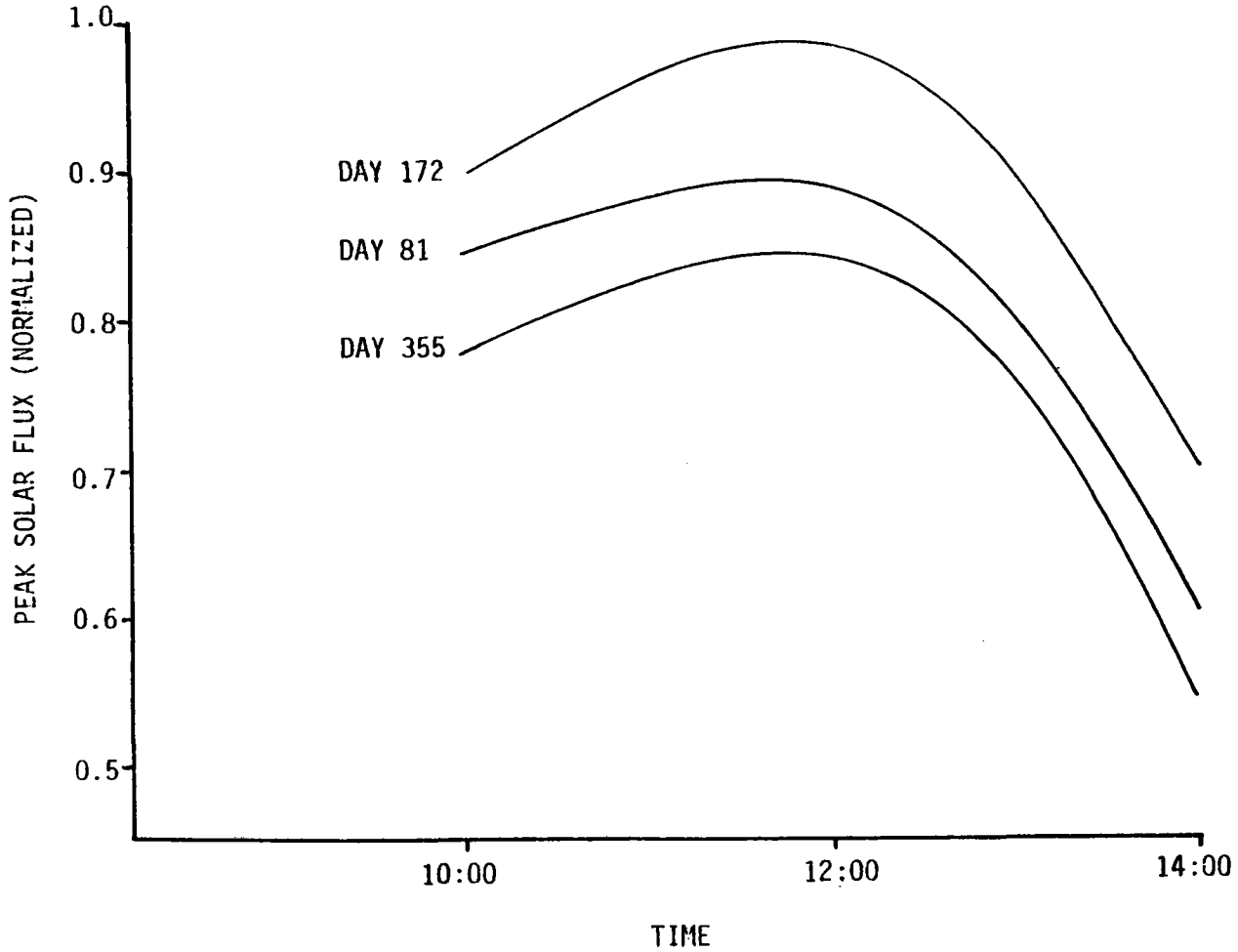

Figure 5.3-21 Peak Solar Flux on Area Around Aperture

TIME: 1200
DAY: 172
INSOLATION: 950 kW/m^2

WEST APERTURE FRAME
ABSORBED FLUXES, W/cm^2

0.	0.	0.	.006	.027	.046	.028	.006	0.	0.	0.
0.	.001	.050	.271	.584	.735	.581	.260	.044	0.	0.
.001	.074								.061	0.
.025	.449								.448	.016
.077	1.02								1.03	.068
.102	1.30								1.30	.102
.064	1.02								1.01	.070
.012	.430								.435	.020
0.	.054								.069	.001
0.	0.	.042	.253	.572	.723	.570	.262	0.	0.	0.
0.	0.	0.	.005	.027	.041	.026	.006	0.	0.	0.

Figure 5.3-22

TIME: 1200
DAY: 172
INSOLATION: 950 kW/m^2

EAST APERTURE FRAME
ABSORBED FLUXES, W/cm^2

0.	0.	0.	.008	.037	.059	.038	.009	.001	0.	0.
0.	0.	.057	.342	.768	.981	.778	.352	.062	.001	0.
0.	.073								.088	.001
.019	.538								.564	.027
.075	1.27								1.30	.086
.116	1.64								1.64	.117
.080	1.28								1.26	.071
.022	.543								.514	.014
0.	.080								.066	0.
0.	.001	.060	.342	.760	.965	.754	.332	.055	.001	0.
0.	0.	0.	.008	.035	.053	.035	.008	0.	0.	0.

Figure 5.3-23

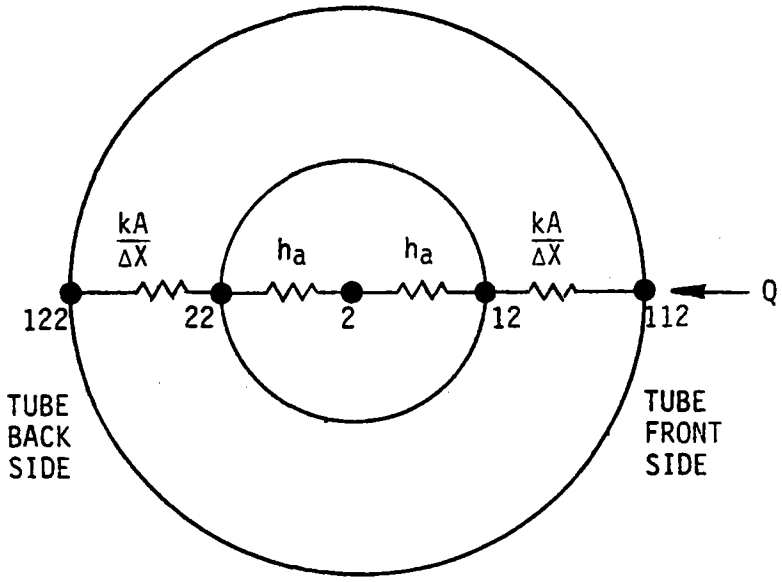

Figure 5.3-24 MITAS Model Type Segment

The complete node and conductor diagram is shown in Figure 3.8-24. Fluid enters the tube at boundary temperature T_1, receives heat inputs through the tube walls as it flows through the tube and exits at temperature T_{11}. By stacking MITAS runs, using the exit temperature from the preceeding panel as the inlet tmeperature for the succeeding panel and applying the appropriate energy (Q) inputs for each panel, one can establish the receiver temperature profiles.

The MITAS model calculates the heat transfer coefficient between the fluid and tube inside surface nodes based on the node temperatures and fluid velocity. The salt velocity is also calculated at each ode using a constant mass flowrate through the tube and the fluid temperature. The salt film coefficient is calculated by MITAS using the following equation from W. H. McAdams (Ref 5.3-6).

$$h = 0.023 \frac{K}{d} (Re)^{0.8} (Pr)^{0.4}$$

where:

h = convective heat transfer coefficient of salt, W/m^2-C° (Btu/h-ft^2-F),
K = salt thermal conductivity, W/m °C (Btu/hr-ft °F),
d = tube ID, m (ft),
$R_e = \frac{Pvd}{H}$
$Pr = \frac{CpH}{K}$
v = flow velocity, m/s (fps),
P = salt density, kg/m^3 (lbm/ft^3),
C_p = specific heat of salt, J/Kg-°C (Btu/lbm-°F),
H = salt viscosity, kg/s-m (lbm/s-ft)

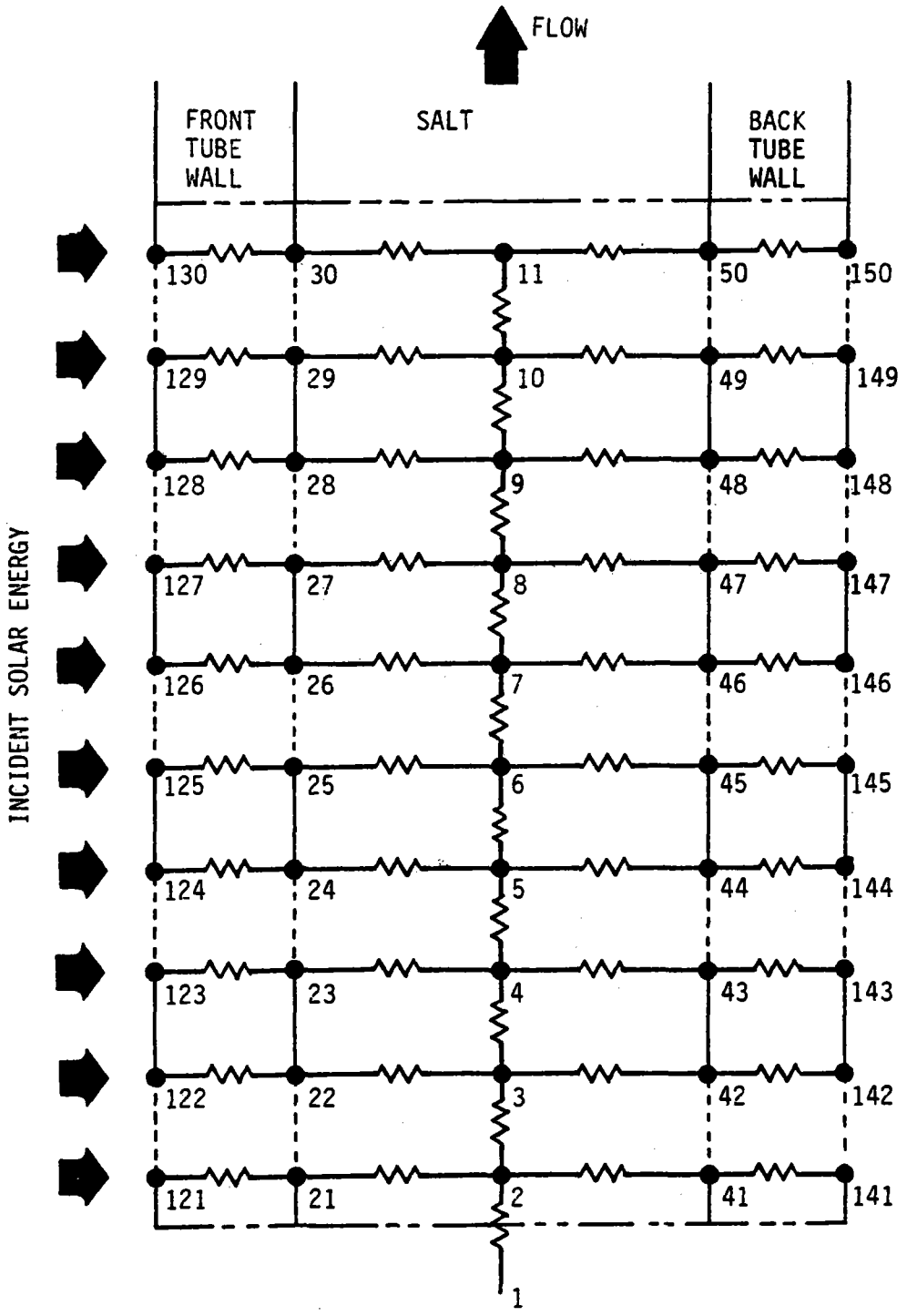

Figure 5.3-25 MITAS Model Node Diagram

Test results reported in the Martin Marietta Alternate Central Receiver Phase II report (Ref 5.3-5) indicate that tempertures calculated using this correlation were in close agreement with measured temperatures.

Heat inputs to the MITAS program were taken from the incident flux maps (an example is shown in Figure 5.3-25). The program further reduces these fluxes by a loss fraction to represent convection, reflection, and radiation losses. Thus, the actual heat flux absorbed by each node is fused to generate the temperature profiles.

The tube and salt temperature profiles for incident power levels and salt flow rates of 10% above the design conditions previously were computed and show maximum panel temperatures for this extreme case only a few degrees higher than those experienced during design conditions. Figure 5.3.26 shows the salt film coefficients and velocity profile through the receiver also calculated by MITAS for the peak conditions and design salt flow rates.

5.3.10.3 Thermal Losses

Thermal losses from the solar central receivers consist of spillage, solar reflection, infrared radiation, convection, and conduction. The cavity receiver concept was selected primarily to minimize receiver thermal losses during operation and overnight or cloudy-day shutdown periods. Solar reflection, infrared radiation, and convection losses are minimized by the cavity enclosure during operation and are eliminated entirely by the aperture doors during shutdown. Conduction is limited by a 0.2 m (8 in.) thick ceramic fiber insulation (manufactured by the Carborundum Company of Niagara Falls, New York).

Spillage is defined as the amount of energy reaching the aperture plane that does not enter the cavity. Spillage losses depend on several factors including aperture size, aiming strategy, field configuration, and heliostat tracking errors. MIRVAL was used to calculate spillage, as this program considers more of the factors which affect spillage than does TRASYS and is, therefore, more realistic. For this cavity design, spillage losses were calculated to be 1.60% of the incident energy at peak conditions (noon, day 355). Reflective losses are minimized by the cavity receiver concept because a large protion of the solar energy reflected from one panel is absorbed by the other panels and reflected by the inactive surfaces. Only that portion reflected directly back out the aperture is lost. This results in an effective cavity absorptivity of .981, using an absorber surface absorptivitity of 0.950. Similarly, the infrared losses are also reduced by the cavity geometry. This reduction occurs because the aperture area is significantly less than the high temperature absorber area. These infrared losses were found to be 3.49% of the power incident on the receiver at peak conditions. Table 5.3-7 summarizes the receiver the map losses under peak operating condition.

Convective heat losses for any type of a solar receiver are difficult to accuarately calculate. The large physical dimensions of the heated surfaces as well as the high surface temperatures result in very high Reynolds and Grashof numbers, for which virtually no heat transfer data are available. A detailed

ALL TEMPERATURES ARE IN °C

(°F = 9/5 °C + 32)

292	292	326	326	381	381	453	453	517	517	562	562
292	292	326	327	381	382	452	453	517	518	562	562
292	292	324	327	379	382	451	454	516	518	562	562
292	292	323	328	377	383	448	456	513	519	561	562
291	293	319	331	371	386	442	458	507	522	559	562
291	294	314	335	364	392	433	464	500	527	555	562
289	297	309	340	358	400	426	472	494	534	551	562
288	301	307	345	354	407	420	479	490	540	549	562
288	302	304	348	351	412	417	484	488	544	547	562
288	304	304	350	350	415	416	487	487	547	547	562

INLET

OUTLET

Figure 5.3-26 West Cavity Salt Temperature Profile, Design Conditions

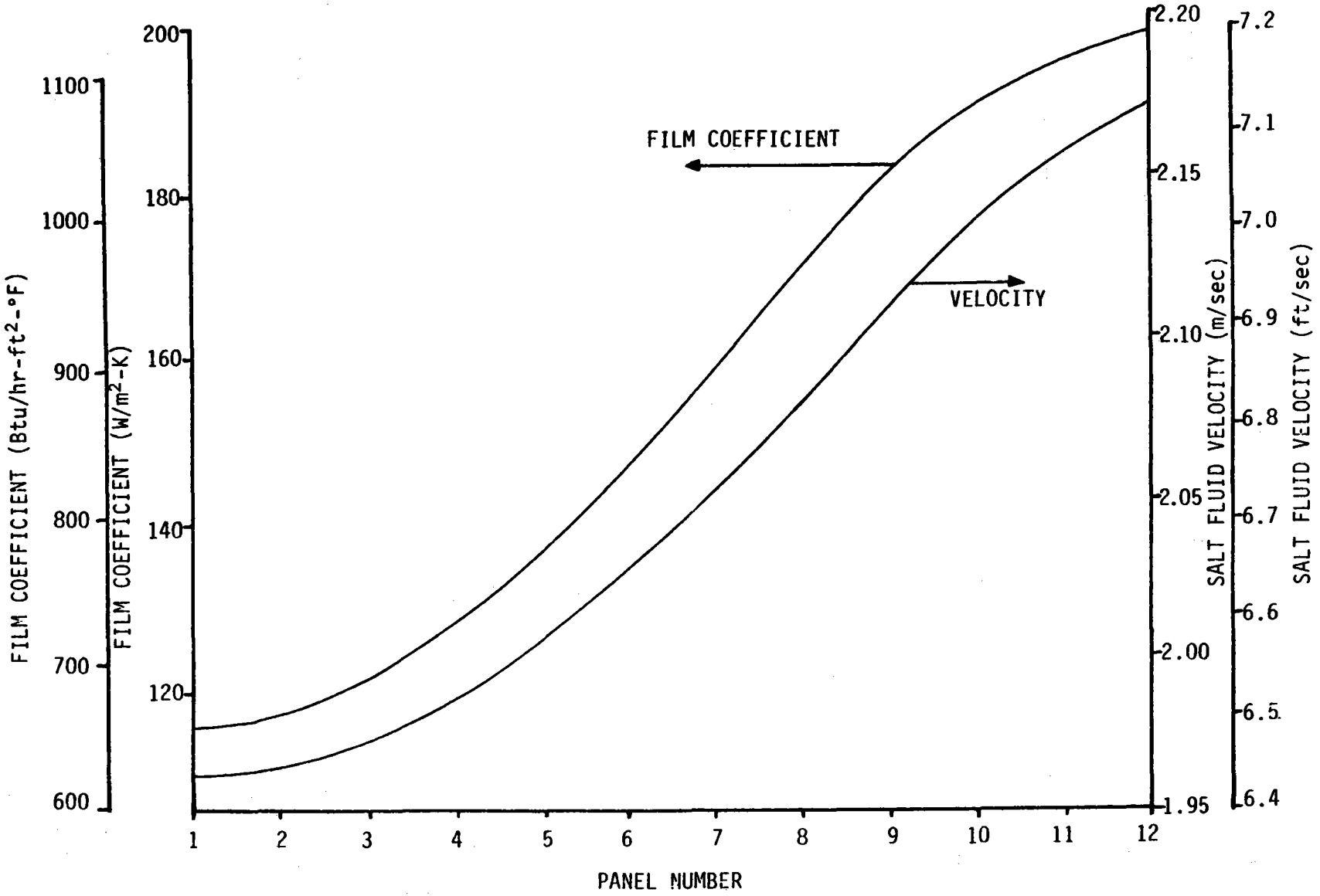

Figure 5.3-26 Absorber Tube Heat Transfer Coefficient and Salt Velocity Profiles

MITAS nodal model of a cavity receiver was constructed for both the Martin Marietta Advanced Water Steam Phase I receiver (Ref 5.3-2), and for the Martin Marietta Hybrid Phase I receiver (Ref 5.3-3) to calculate convective losses. The results of these programs agree well with subsequent test results reported by the Martin Marietta Advanced Central Receiver Phase II report (Ref 5.3-5). Correlations derived from this MITAS model make use of an "effective heat transfer coefficient" relating absorber area, aperture area, and receiver temperature to predict convective energy losses. For this twin cavity receiver, thermal losses due to convection are 2.8% of the peak incident power.

Conduction losses from the twin cavity receiver were found to be 0.60% of the peak incident power. for this calculation, we assumed that the receiver interior was at the average salt temperature of 427°C (800°F), and that the exterior receiver temperature was at 19°C (86°F). A 25% additional loss was assumed to account for structural penetrations of the insulation.

Table 5.3-7 Receiver Thermal Losses, Peak Operating Conditions

	Percentage of Peak Incident
Convection	2.8%
Conduction	0.6%
Radiation	3.5%
Reflection	1.9%
Spillage	1.6%
Total	10.3%

Nonoperating receiver cooldown was calculated assuming that the aperture doors were in place, thereby limiting heat leakage to that due to conduction. Also, to account for any air leakage around the aperture door seals, an extra heat loss corresponding to 5.0% of the open door convective losses was added. As shown in Figure 5.3-28 the salt will cool to 288°C (550°F) after 14.8 hours of shutdown. At this point, the receiver will be drained to eliminate any possibility of damage to the receiver from salt solidification. When doing this calculation, we assumed an ambient temperature of -17.8°C (0.°F), which is much lower than normal for the Bakersfield, California area. To bound the problem, we assumed a 15.6°C (60°F) ambient temperature, and recalculated the cooldown. The results of this analysis show that the receiver will reach the minimum allowable temperature after 16.4 hours.

5.3.11 Overall Solar Subsystem Performance

Using the results of the performance analyses discussed above as input to the STEAEC program (along with the SOLMET weather tape for Fresno, California), the daily and annual performance of the solar collector/receiver subsystem was determined. As previously explained, the collector subsystem performance was evaluated using the MIRVAL Monte Carlo computer code. The collector field performance as defined by the ratio of solar radiation entering the receiver to

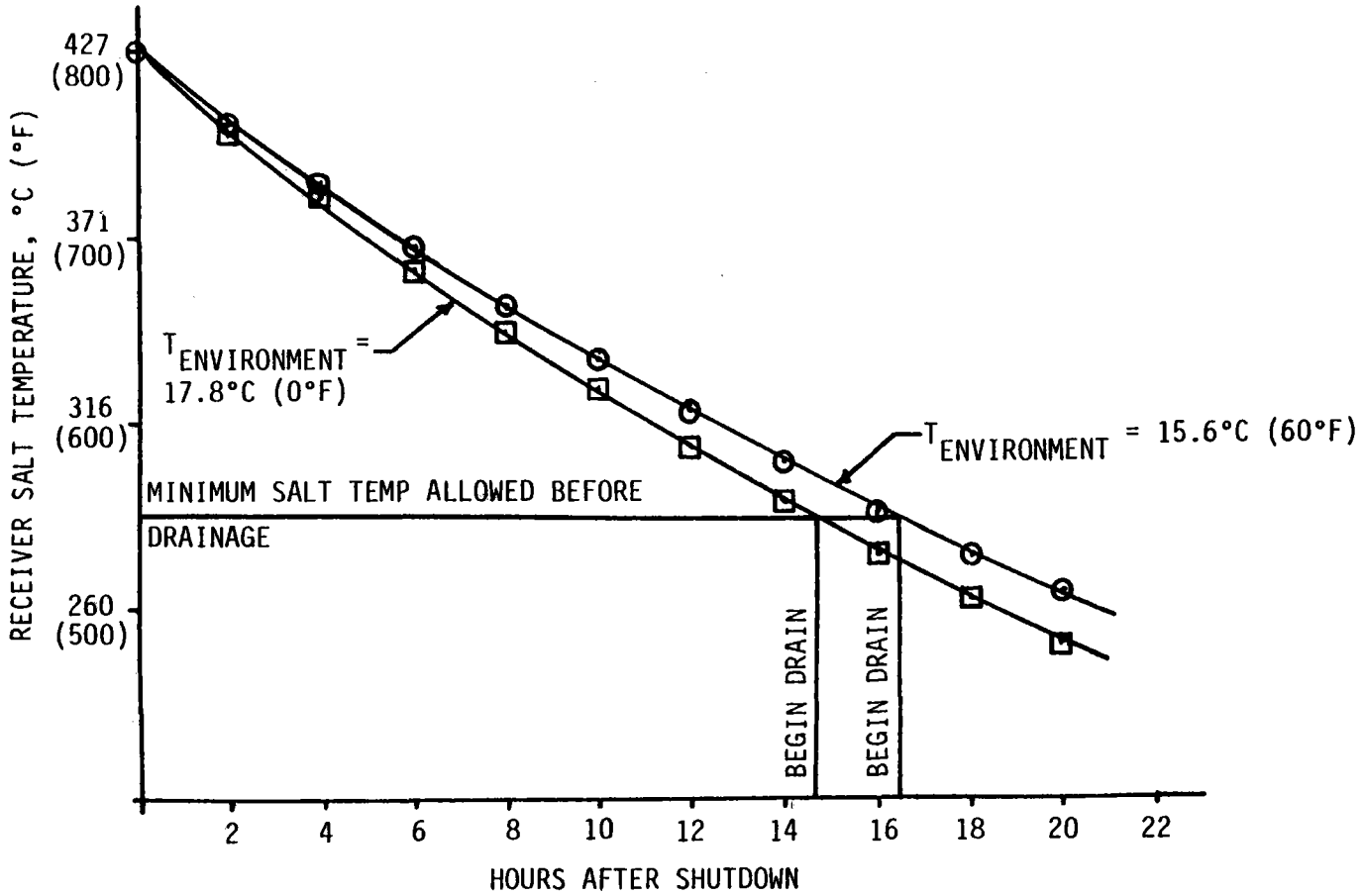

Figure 5.3-28 Receiver Cooldown

the total available insolation incident on the collector area, was calculated for a matrix of seven solar azimuth angles and six elvation angles, as well for the sun positions at noon, day 24, and noon, day 189 (see Table 5.2-2). The receiver thermal losses were evaluated for a matrix of five ambient wind speeds and five ambient temperatures.

The annual system performance was then evaluated using the STEAEC system model, which simulates the performance of the system using 15-minute time steps and a site weather data tape. For the site weather data (insolation, wind speed and direction, temperature and pressure), the SOLMET typical meteorological year (TMY) weather data base was chosen. Because no TMY exists for the Bakersfield, CA area, the TMY data type for Fresno, CA was used. Fresno is approximately 100 miles northeast of the selected cogeneration site, but is nontheless representative of the San Joaquin Valley region. This assumption has been validated for a single year using total horizontal and direct normal insolation measurements taken at the site by Exxon. For a typical clear day (2/2/80), the daily direct normal insolation was measured at 6.24 kWh/m^2, as compared with a SOLMET TMY clear February day value of 6.14 kWh/m^2. The SOLMET data, recorded on the tape at 1-hour intervals, were converted to 15-minute interval data using linear interpolation techniques before input to the STEAEC model for a more realistic evaluation of system performance. These SOLMET data yield an average daily direct normal insolation value of 6.21 kWh/m^2/day. The annual system performance stairstep is shown in Figure 5.3-28 Daily system performance stairsteps are shown in Figures 5.3-29,30, and 31 for days 24, 89 and 189 respectively.

The estimated direct cost of the receiver subsystem (Account 5400) is $5.5 million.

REFERENCES

5.3-1 "Saguaro Power Plant Solar Repowering Project" Final Report, Vol I, DOE-SF-10739-2, Arizona Public Service Company, Phoenix, Arizona, July 1980.

5.3-2 "Advanced Water/Steam Receiver Phase I Conceptual Design" Final Report, SAND79-8175, Martin Marietta Aerospace, Denver, Co, January 1980.

5.3-3 "Solar Central Receiver Hybrid Power System" Final Report, Vol II, DOE-ET-21038-1, Martin Marietta Aerospace, Denver, Co, September 1979.

5.3-4 "Solar Repowering/Industrial Retrofit Systems, Category B: Solar Thermal Enhanced Oil Recovery System" Final Report, MCR-80-1353, Martin Marietta Aerospace, Denver, Co, July 1980.

5.3-5 "Alternate Central Receiver Power System, Phase II" Final Report Draft, MCR-81-1707, Martin Marietta Aerospace, Denver, Co, March 1981.

5.3-6 W. H. McAdams, Heat Transmission, 3rd Ed., McGraw-Hill, New York, 1954.

5.3-7 "Alternate Central Receiver Power System, Phase II, Midterm Topical Report, DOE-SF-10534-1, Martin Marietta Aerospace, Denver, Co, March 1980.

Figure 5.3-29

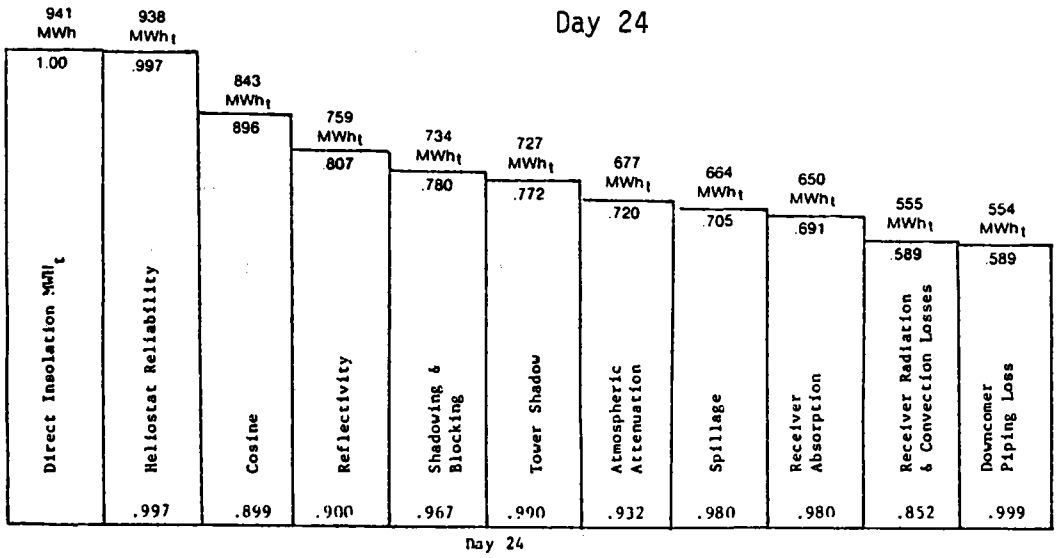

Figure 5.3-30

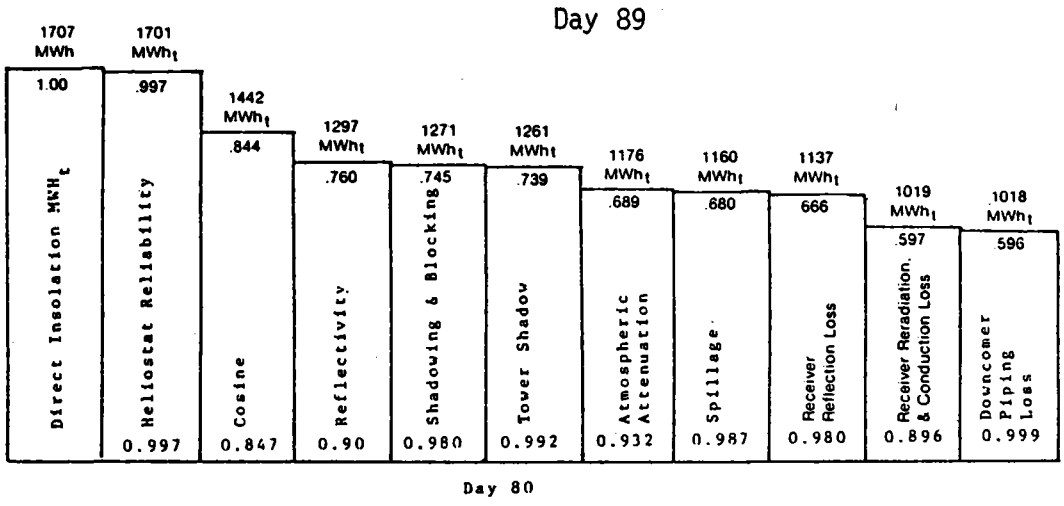

Figure 5.3-31

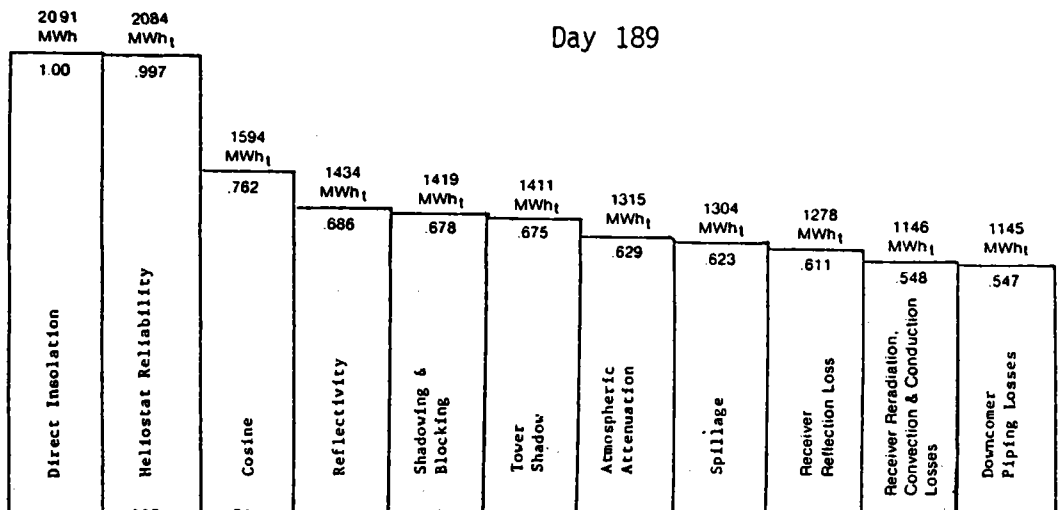

Figure 5.3-32 Solar System Annual Performance

5.4 MASTER CONTROL SUBSYSTEM

The master control subsystem (MCS) consists of an operational control subsystem, data acquisition subsystem and a control subsystem for each of the major subsystems -- collector, receiver, energy storage, process steam, electric power generation, and turbine steam subsystems. The existing fossil fuel boilers will be a separate subsystem but will remain as a standalone system not integrated into the new master control subsystem. The general relationship between the major components of the MCS is shown in Table 5.4-1. The man-machine interface consists of rack mounted controls at remote locations and CRT/Keyboard controls at the OCS console. The Data Bus consists of redundant communication links between the supervisory Operational Control System (OCS), Data Acquisition System (DAS), and the subsystem distributed controllers.

The basic function of the master control subsystem is to sense, direct, monitor and control all system and subsystem parameters necessary to ensure safe and proper operation of the cogeneration facility. The MCS will provide for completely automatic operation of the cogeneration including the process steam, turbine steam and electric power generation subsystems. An operator may supervise plant operation or exercise manual control through the OCS, or for individual subsystems, through the control racks located at each remote subsystem controller location. The master control system is arranged so that it will fail safely and has redundancy. Emergency reactions are built into each of the subsystem control systems. Each valve and actuator will have a selected fail safe position which will protect the receiver and subsystems in the event of a control or power system failure.

Each control subsystem will consist of valves and actuators, sensors, communication lines, control elements, displays, operator input devices, interfaces with the equipments, and power supplies. The control elements for the solar system will be microprocessor based and will contain control logic, signal checking, transfer control (manual/automatic), output limiting, signal scaling,and signal conversion. Most valve actuators will be pneumatic. The operator interface, the OCS console, will be located in the new operations building and in the form of a CRT/Keyboard display shown conceptually in figure 5.4-1. The collector subsystem computer and displays and the CRT displays paralleling the solar system displays will also be in the control room. There will be separate subsystem control racks located near the sensors and actuators for the salt/steam heat exchangers and for the energy storage subsystem. The distributed nature of the receiver subsystem requires the use of three control racks -- near the main circulation pumps, near the receiver cold salt pumps and in an area at the top of the tower adjacent to the receiver.

5.4.1 Master Control Subsystem Requirements

Requirements for the master control subsystem are divided into two classifications: (1) the general system requirements including those adapted from the contract form of the Systems Specification, and (2) those requirements derived during the course of the study. All of the requirements can be met by the general master control subsystem configuration identified below. Emphasis has been placed on operability of the cogeneration facility and on maximizing the success of the operation.

Table 5.4-1 Control Subsystem Descriptions

SUBSYSTEM	FUNCTION BEING CONTROLLED	INTERFACES	COMPUTATION TECHNIQUES	COMM. METHOD	DISPLAY/ CONTROL APPROACH	DATA RECORDING METHOD
Operational Control Subsystem (OCS)	Coordinates all other subsystem controls	All other control subsystems	Digital	Data Bus (electronic or fiber optic)	CRT display, keyboard input	Hard copy display printer
Collector Control Subsystem (CCS)	Controls heliostats including activation, stow, washing, beam characterization	OCS DAS	Digital	Data Bus (fiber optic)	CRT displays, keyboard inputs	DAS
Receiver Control Subsystem (RCS)	Main circulation pumps Booster pumps, receiver drag valve, salt return, receiver control valves	OCS DAS	Digital	Data Bus (electronic or fiber optic)	CRT display, keyboard inputs	DAS
Energy Storage Control Subsystem (ESCS)	Foundation coolant flow, salt reprocessing, salt melting, tank fluid level	OCS DAS	Digital	Data Bus (electronic or fiber optic)	CRT display, keyboard inputs	DAS
Electric Power Generation Control Subsystem (EPGCS)	Turbine bearing temperatures, steam admission, circulating water flow, condensate flow	OCS DAS	Digital	Data Bus (electronic or fiber optic)	CRT display, keyboard inputs	DAS
Turbine Steam Control Subsystem (TSCS)	Hot salt pump, feedwater pump, steam flow, salt recirculation pump, water recirculation pump	OCS DAS	Digital	Data Bus (electronic or fiber optic)	CRT displays, keyboard	DAS
Process Steam Control Subsystem (PSCS)	Hot salt pump, feedwater pump, steam flow	OCS DAS	Digital	Data Bus (electronic or fiber optic)	CRT displays, keyboard	DAS
Data Acquisition Subsystem (DAS)	Data collection and processing	OCS ESCS CCS TSCS RCS PSCS EPGS	Digital	Data Bus (electronic or fiber optic)	CRT displays, keyboard inputs	Stripchart recorder hard copy display

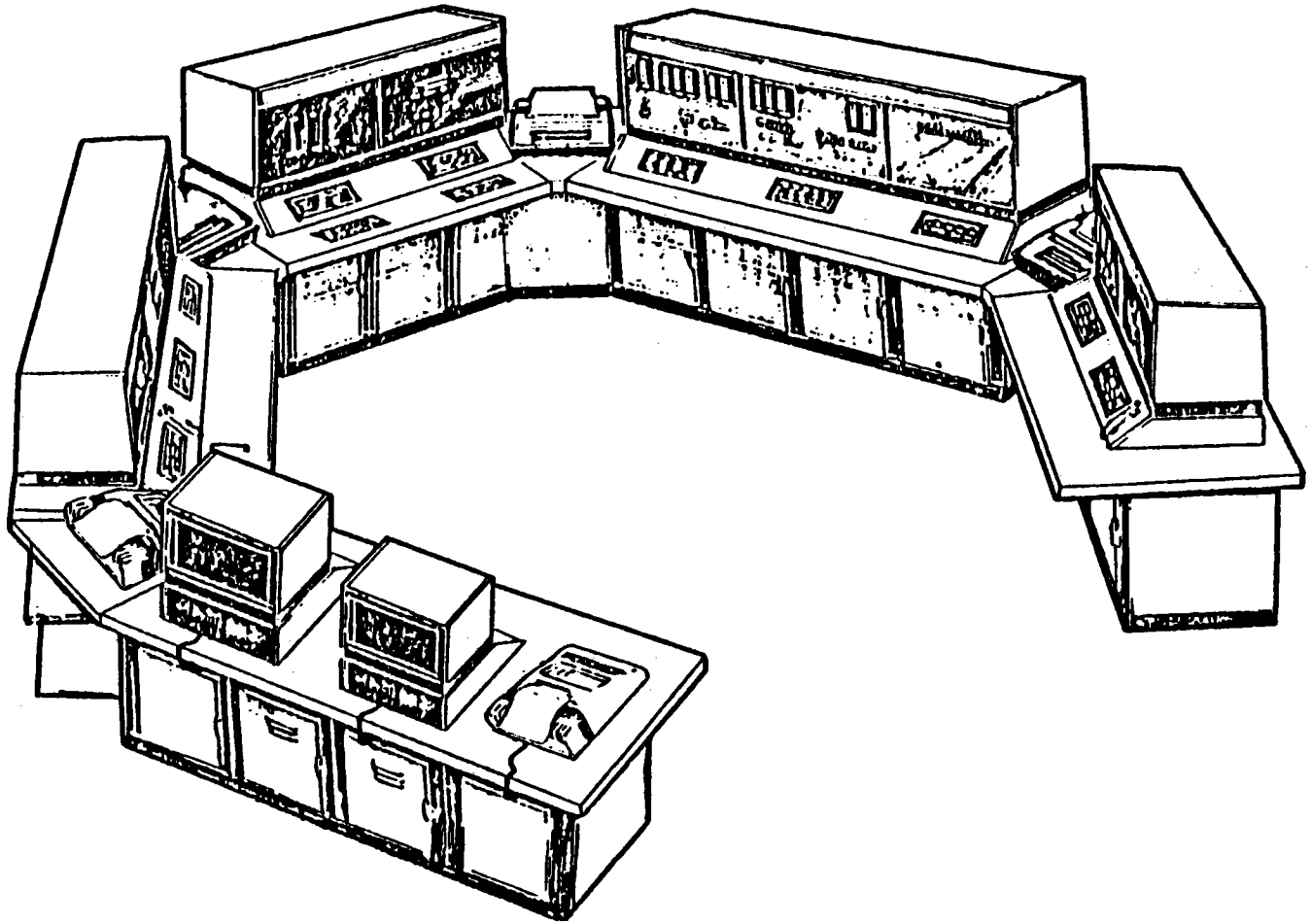

Figure 5.4-1 Conceptual Control Room Configuration

5.4.1.1 General Requirements

These general requirements were established by the nature of the Systems Specification.

1. Shall conform to the applicable codes and standards defined in of the Systems Specification (see Appendix A).

2. Shall provide safe and effective operation for all steady-state modes, transitions between modes, and emergency shutdowns.

3. Shall provide access for maintenance and inspection and shall provide for crew safety.

4. Shall be designed for a 30 year operating life.

5. Shall have design simplicity, and the receiver, energy storage, turbine and salt/steam heat exchangers control systems shall resemble standard power plant or process heat control systems by use of:

   a) Standard control practices;
   b) Simple, well defined interfaces between the operational control subsystem and the other plant subsystem controls.

6. Shall have operational simplicity using the supervisory control philosophy (primary operation to be automatic with operator override capability) and have:

   a) Centrally located control consoles for both automatic and manual operations;
   b) Easily read displays;
   b) Easily operated manual inputs.

7. Shall incorporate design reliability by:

   a) Use of proven designs;
   b) Elimination of single point failures through redundant elements whenever it is cost effective to do so.

8) The design shall be cost-effective based on:

   a) Selection of off-the-shelf equipment;
   b) Use of modularity among the major subsystems of the master control subsystem;
   c) Use of generically similar equipment in the control systems for the receiver, energy storage, and salt/steam heat exchanger subsystems.

5.4.1.2 Derived Requirements

The following requirements were derived in the course of the study for the master control subsystem:

1) Sense, detect, monitor and control all applicable system and subsystem parameters.

2) Control all parts of the cogeneration plant in all steady state operating modes and all transistions between modes.

3) Provide for steam generation from both the salt/process steam heat exchanger and salt/turbine heat exchanger using molten salt from storage as a source.

4) Control of the collector subsystem shall use the same philosophy as the system being developed for Barstow 10 MW_e Pilot Plant.

5) The existing fossil fuel boilers will operate continuously for twenty four hours per day. The only interfaces with the master control system will be an indication of steam conditions to show that the system is in operation.

6) Control of the collection and storage of solar energy shall be decoupled from the control of the use of the stored thermal energy.

7) Provide the necessary sensors, communications, annunciators, and logic for proper and effective corrective actions.

8) Provide a graphic CRT display of the subsystem fluid flow schematic.

9) CRT or video displays with keyboard controls shall be included for all subsystem controllers as well as the OCS and DAS. These controls will be located within a central control room. Remote, manual or supervisory control of each of the distributed subsystem controllers shall be accomplished at the control racks located near each of the respective subsystems or through the OCS console (i.e., receiver can be controlled from the control rack located within the tower; likewise for ES, PSS, TSS, and EPGS). The collector system control racks may be located in the same building as the control room.

5.4.2 Design Description

The master control subsystem is composed of six subsystem control systems. The specific subsystems being controlled are:

1. Collector (CS)
2. Receiver (RS)
3. Energy Storage (ES)
4. Process Steam (PSS)
5. Turbine Steam (TSS)
6. Electric Power Generation (EPGS)

The operation of the subsystems is coordinated and interrelated by the Operational Control System (OCS) (with the exception of the ESCS). Data which is required to be collected and stored for the evaluation of plant operation is gathered via the control system data bus and recorded by the Data Acquisition System (DAS).

The existing fossil fuel boiler units which are in continuous 24 hour operation are monitored only to ensure steam is being generated. A failure in the fossil fuel boiler system will be flagged to the master control subsystem, but no other action will be initiated.

5.4.3 Control Philosophy

The master control system will utilize Distributed Digital Control (DDC) technology. DDC technology has a proven record of superior performance and reliability. This is achieved by distributing the control hardware such that each major subsystem is controlled by an independently operating controller. These distributed controllers continue to operate in spite of failures in other subsystem control elements. Each of the subsystem controllers communicate over a common data bus with a supervisory Operational Control Subsystem (OCS). The OCS coordinates the action of the subsystem controllers in the required manner to achieve the desired plant operation. A block diagram of master control system configuration is shown in Figure 5.4-2.

The master control subsystem will provide for three basic modes of control. These are:

- Completely automatic control of total plant operation.
- Supervisory control by control operator of any or all subsystems.
- Manual operation of any or all subsystems.

Any of these three modes of control operation can be performed at the OCS control console located in the control room. Manual control can also be initiated and executed at any of the distributed subsystem controller locations.

The master control system data bus consists of electrical or fiber optic communication links. Currently available DDC hardware utilizes multiple redundant data highways. The information transmitted on the information links is constantly checked to assure data bus integrity. If an error is detected in the data highway, an error condition is flagged and another redundant data highway is used.

Operational integrity of the master control system is maintained through the use of redundant systems. Commercially available DDC systems utilize redundant power supplies, controllers, data highways, sensors, and displays. An advantage of DDC technology is that the control hardware is distributed in such a manner that single point failures are minimized. All information concerning plant operation resides on several redundant data highways. If for example, the CRT display for the receiver subsystem should fail, any of the other available subsystem CRTs could be used to display the receiver system information while the original was being repaired. Thus, the operational integrity of the plant is much less sensitive to individual component failures.

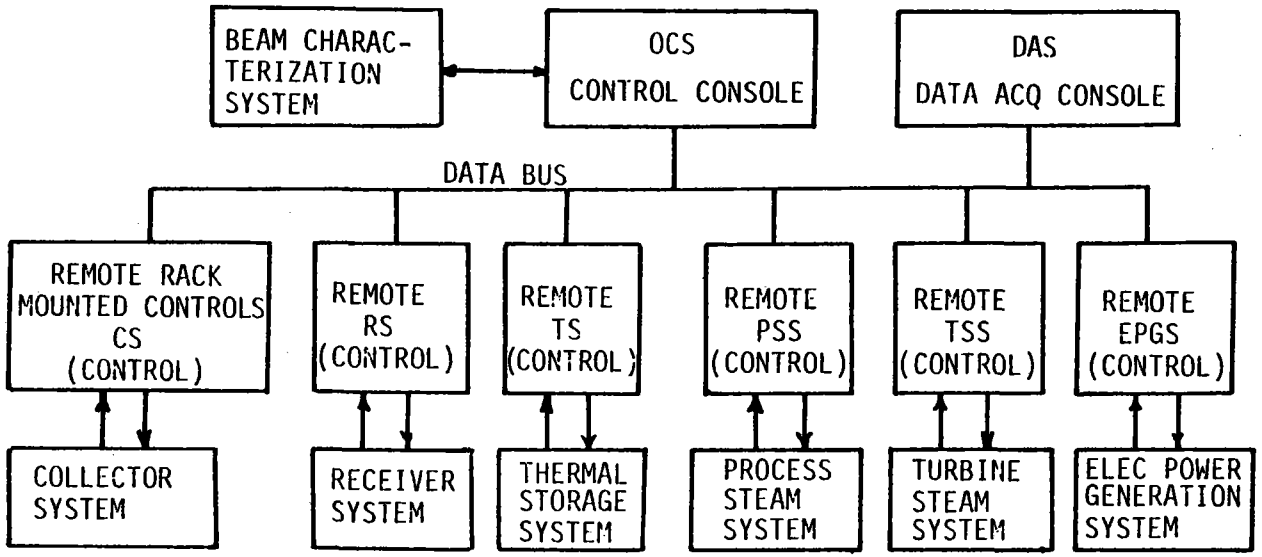

NOTE: Emergency control functions are part of each subsystem control system

Figure 5.4-2 Master Control System Configuration

In the event of any system failure, an automatic failure event sequence record is automatically recorded by the OCS for easy analysis of the original source of failure. Hard copy of this report will be available from the OCS system.

All major manufacturers of control systems provide a complete line of off-the-shelf DDC hardware. Each of the subsystem controllers will be identical and thus minimize the stock of spare parts. DDC technology also allows easy expansion and improvement at a future date due to its building block approach.

The basic functions, computation techniques, interfacing systems, and input/output of each subsystem control system is shown in Table 5.4-1. The main data recording/evaluation function is performed by the Data Acquisition System (DAS). Secondary hard copy is provided from the OCS display.

5.4.4 Operational Control Subsystem

The operational control subsystem (OCS) interconnects and interrelates all of the other control subsystems as noted in Figure 5.4-2. The major characteristics of the OCS are as shown in Table 5.4-2.

Table 5.4-2 Operational Control Subsystem Characteristics

1. Controls subsystem interaction
2. Determines Operating Modes/transitions for each Subsystem
3. Contains Rules/Algorithms for Mode/Transition Selection
4. Defines Steady State Operation criteria for each subsystem based on the plant operation objective.
5. Contains Procedures for all Transitions between Modes, Startup and Shutdown.
6. Monitors total system for abnormal conditions.
7. Responds to emergencies and notifies of system failures.

Each of the individual subsystem controllers are responsible for only its respective system. For example, the responsibility of the receiver subsystem controller is to maintain the salt outlet temperature at the value specified by the OCS. The OCS deterimes this value by considering the mode of plant operating as dictated by a set of rules which were established to define the priorities of plant operation. The OCS system will contain an extensive list of these rules which are expressed in the form of boolean equations. The OCS minicomputer continuously solves the set of operating equations relative to the dynamic operating environment of the plant and resolves the proper interaction of such subsystem.

The OCS also contains a set of rules which govern safety aspects of plant operation. An example of such safety rules is shown in Table 5.4-3.

Table 5.4-3 OCS Plant Safety Rules

1.	If the wind velocity exceeds 15.6 m/sec (35 mph), then stow heliostats, close receiver doors, and place receiver in warm standby position.
2.	If receiver outlet temperature exceeds 585°C (1085°F), defocus all heliostats to standby position.
3.	If receiver pump fails, defocus heliostats to standby, close receiver doors.

5.4.5 Collector Control System

The collector control system for the congeneration plant is a distributed computer control system (Figure 5.4-3) consisting of a heliostat array controller (HAC), heliostat field controllers (HFC, and heliostat controllers (HC). The HAC, HFCs, and HCs are connected by data buses as shown. The HAC is a dual-redundant minicomputer located in the control room. The HFC is installed in the electronics package that houses the HC. One HC (or a combination of HC/HFC) is installed inside the interface adapter tube of each heliostat.

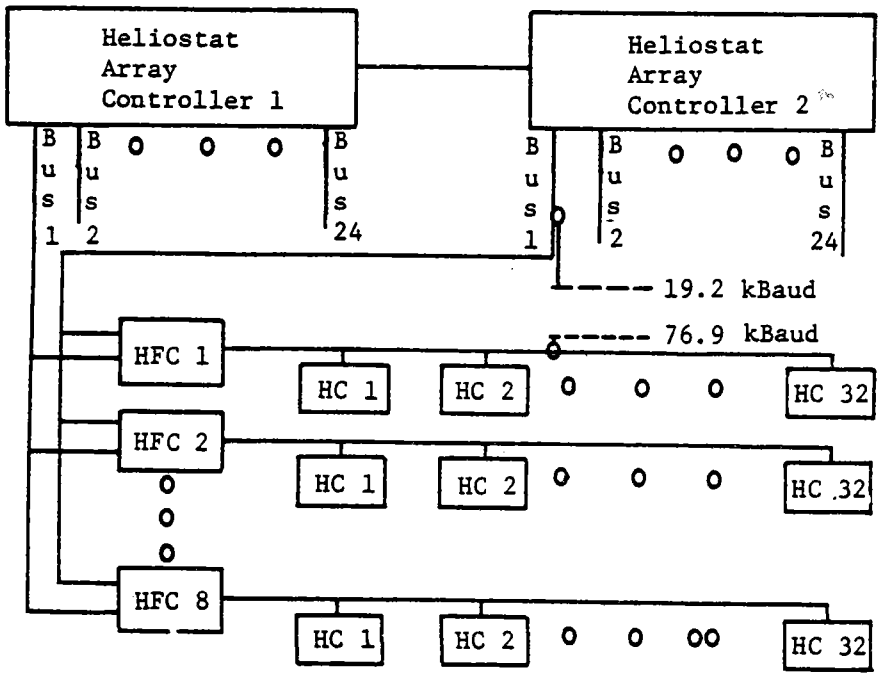

Figure 5.4-3 Collector Control Subsystem (Production)

The HAC consists of two identical minicomputers with automatic switchover to the backup computer should the prime computer fail. Each computer has 512k words of memory with the shadow memory option used for simultaneous memory operations. Peripheral equipment includes three 10-Mbyte disks (one associated with each computer and one shared by both computers), a color CRT terminal, a status printer, an alarm printer, two color graphic CRTs, and a magnetic tape unit. A WWV receiver is used to provide the accurate time base required for calculating sun position.

The plant operator controls the field of heliostats by typing commands into the CRT console. A capability is also provided for complete automatic control using time-sequenced commands stored on the disk.

Color graphic displays allow the operator to display the status of either the complete field or selected segments of the heliostat field. Each heliostat is represented by a small symbol on the screen and different colors are used to indicate the operating mode of that heliostat, e.g., track, standby, or stow.

The HFC provides the interface between the HAC and the HC. It receives commands from the HAC and transmits commands to the HCs, receives status information from the HCs, and transmits status to the HAC. Once each second, the HAC transmits the current sun vector to all HFCs. These data are transmitted to the HCs for use in the pointing algorithm to determine the necessary encoder positions for each heliostat to direct its reflected beam at the desired target. The HFC also calculates a new target once each second during a corridor walk, and transmits the target to the HC.

The HC consists of a minicomputer, data bus input/out circuits, motor control circuits, and power supplies.

The collector control subsystem provides a "computer leveling" capability -- that is, the control subsystem compensates for pedestal tilt. The purpose is to relax the requirements for pedestal alignment and consequently reduce the cost of heliostat installation. This technique can also be used to compensate for small permanent deflections of the heliostat or foundation that may be caused by large wind torques during the life of the power plant. A computer program has been written to simulate the entire computer leveling operation. Results concerning parameter calculation accuracy and computer leveling correction accuracy as functions of the number of measurements, the number of samples per measurement, and the heliostat position in the field indicate that about three measurements times with from two to five samples per measurement are needed to achieve the desired computer leveling correction accuracy.

The computer leveling algorithm consists of two parts: (1) correction of the commanded azimuth and elevation from determined tilt coefficients and encoder biases, and (2) determination of the tilt coefficients and encoder biases from measurements of the beam centroid using the beam characterization system (BCS) pattern on the target. The correction of the commanded azimuth and elevation will take place in the microprocessor in the HC. The tilt coefficients and encoder biases will be calculated off line in the HAC computer.

Correction of the commanded azimuth and elevation is implemented in two phases: (1) a corrected heliostat normal vector is computed from the commanded heliostat normal vector obtained from the sum of the normalized target vector and normalized sun vector and the tilt coefficients, and (2) the encoder bias angles for azimuth and elevation are then subtracted from the azimuth and elevation commands to give the corrected azimuth and elevation.

The measured horizontal and vertical offsets of the centroid of the reflectecd beam are used, along with the normalized sun vector, normalized target vector, BCS position and orientation, heliostat position, and commanded heliostat normal vector, to obtain the two tilt coefficients and the encoder bias angles. The tilt coefficients and encoder biases are solved numerically by an iterative nonlinear least squares schemes that finds the best set of quantities to minimize an error criterion.

Use of the "computer leveling" system will reduce costs and improve performance. The cost reduction will result from a reduction in heliostat installation time because accurate leveling is not required. Analysis of data from the Sandia tests of Martin Marietta heliostats at the CRTF indicates that part of the tracking error could be caused by pedestal tilt. "Computer leveling" should eliminate these error components.

Figure 5.4-4 is a block diagram of the collector control system for the heliostats. The system is basically the same as the collector control system for a 50-MWe plant except that the HAC is significantly scaled down.

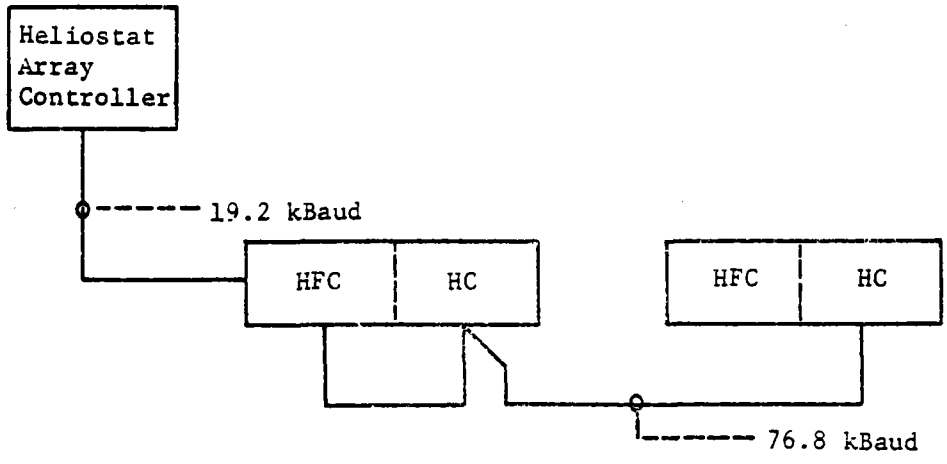

Figure 5.4-4 Collector Control Subsystem (Prototype)

5.4.6 Individual Heliostat Control System

Figure 5.4-5 is a block diagram of the control system for an individual heliostat. The minicomputer calculates the required gimbal angles based on sun vector and target vector data received from the heliostat field controller. The required gimbal angles are compared to the actual gimbal angles; if there is a difference, the minicomputer sends an output to turn on the appropriate drive motor. The microcomputer determines actual gimbal angles by counting changes in the state of the encoder outputs.

The heliostat control system is an on-off system that operates at two different speeds -- slew and track. The motors are turned on at slew speed if the error is large, or track speed for small errors. Slew speed is approximately 20°/min and is required to meet time requirements on positioning the heliostat. Track speed is about 2°/min.

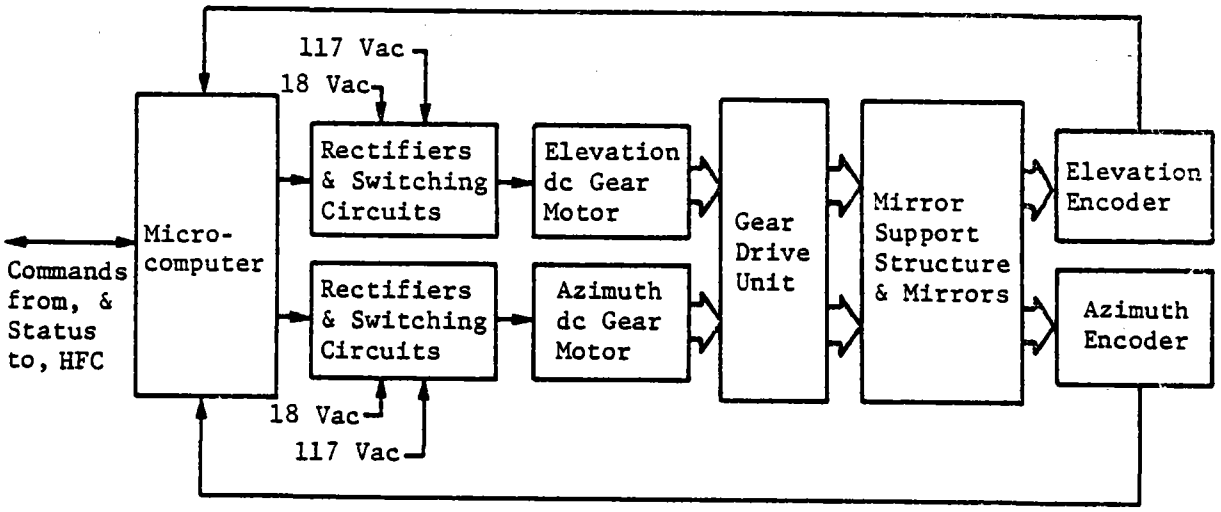

Figure 5.4-5 Control System for Individual Heliostat

5.4.7 Control System Components and Subsystems

This section of the report provides a more detailed description of the HAC, HFC, HC heliostat electrical installation and cabling, gear motors, encoders, field power distribution system, data buses and control support equipment.

5.4.7.1 Heliostat Array Controller - Production

The configuration of the HAC computer system is shown in Figure 5.4-6. The HAC computer system consists of a set of identical, dual-redundant MODCOMP CLASSIC computers, with a set of peripheral and input/output equipment needed to satisfy the HAC computer system requirements.

The HAC computer system includes two identically configured MODCOMP CLASSIC 7870 CPUs and 512k words of memory and the shadow memory option for simultaneous memory operations. Each computer has the MODCOMP 3109 communications processor option and a 3771 dual-bus memory processor. One of the dual buses is dedicated to input/ output of the CPU (e.g., disk, graphic displays). The HAC has a dedicated 10-Mbyte disk unit on each computer, along with a TI-820 KSR terminal for the computer console.

A single set of peripheral equipment is connected to MODCOMP 4906 peripheral control switch units. With the switch under software control and with a manual control override, this concept allows one set of peripheral equipment to be used and switched to the backup computer if the prime computer fails. The HAC console is an Intelligent Systems Corporation 8001G color CRT terminal. To provide emergency backup to this unit, command input can be switched to the computer console. A hardcopy log of commands entered and alarms generated is furnished through a MODCOMP 4228 serial matrix printer capable of 150 characters per second printing. This is sufficient for the low-volume traffic of commands and alarms. To achieve the higher volume capability required for status requests, a MODCOMP 4227 serial matrix line printer capable of output up to 280 lines per minute is provided. In case of failure of either printer, its output is automatically rerouted to the other printer. To provide the color graphics required, two Intelligent Systems Chromatics 1999 terminals are interfaced with the computers. These terminals have integral keyboards for interactive requests of display formats. They are also equipped with function keys for emergency field command entry. To maintain the accuracy of the time base, a Tru-Time Model 60 dc WWVB receiver/clock is interfaced with the computers.

For a long-term data storage capability and transportability of software programs and data to/from other computer systems, a nine-track magnetic tape unit (MODCOMP 4148) is included in the system.

The HAC computers must communicate with the field of heliostats, with the external subsystems, and with each other. To communicate with the field, two MODCOMP 1930 universal communications chassis are used. Each unit is equipped with 12 MODCOMP 1931 asynchronous line interface modules to communicate over the 24 data buses to the field through a special Martin Marietta-designed and built interface. These 1931 universal communications chassis are dual-ported so either computer can communicate to the field through either unit. Thus switchover of communications from the "prime" to "backup" unit is software-controlled and does not require a full computer switchover. Communications between prime and backup HAC computers is over two MODCOMP 4824 highspeed serial coax link controllers. In addition, both computers share a 10-Mbyte dual-ported disk.

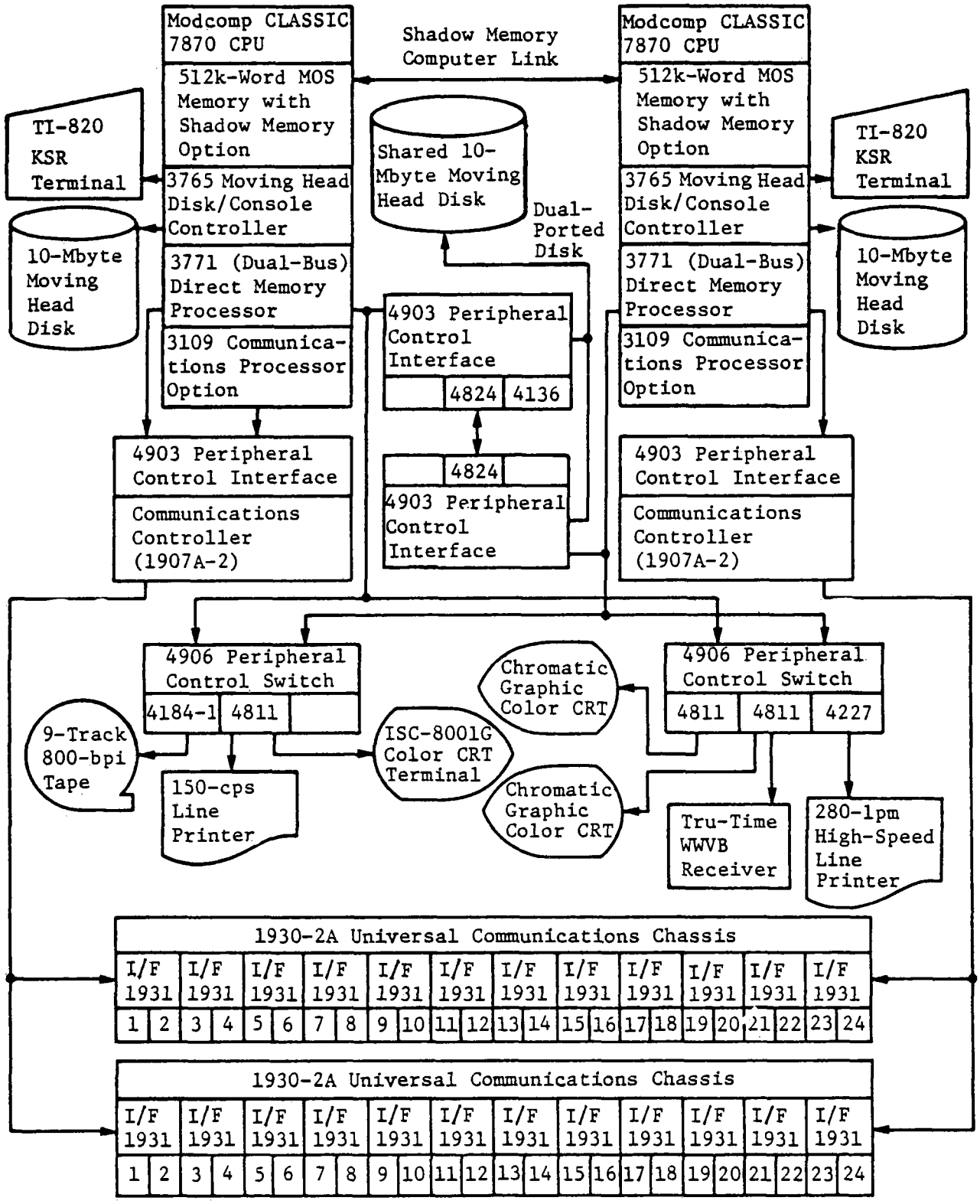

Figure 5.4-6 HAC Computer System - Production

The HAC software system provides the capability to control the field of heliostats in the required operational phases as described:

1) Initialization - This phase prepares the HFCs and HCs for heliostat control. The HFCs are automatically loaded at system initialization and any time the HFC status indicates a need from the HFC for a new download, e.g., a power loss reset. The downloaded data include the corridor values (corridor upper limit point, corridor rate for wire walk, and corridor assignments for HCs controlled by the HFC). Data are also downloaded to the HCs although they are downloaded on operator command. The LOAD command downloads data to installed HCs in the field. The download data consist of heliostat position, current heliostat orientation, and heliostat biases. In both microprocessors, the downloaded data are stored in RAM and must be downloaded whenever the microprocessors are powered up. Before any heliostat positioning commands are issued, the affected heliostat's position must be accurately determined. This is done by issuing the MARK command that causes the heliostats to be driven to the reference marks. When the heliostats have reached the reference marks, which are within a few degrees of the stow position, this information is combined with the bias information to produce accurate encoder position information. A STOW command is issued to return the heliostat to the stow position, which is the reference point for further sequences;

2) Prepower - This phase covers the movement of selected heliostats from their stow position called the corridor upper limit point (CULP). The UNSTOW command initiates this phase, which results in an automatic sequence of operational commands to be sent to the selected heliostats to move to the corridor lower limit point (CLLP), and move up the corridor in a coordinated fashion to the power standby position (CULP). This coordinated movement is called a corridor walk. For a more detailed description of this movement, refer to item 7) in this listing;

3) Power - The power phase causes selected heliostats, at their CULP, to be positioned so their reflected beams strike a target, normally on the receiver. In this mode, corrections for sun motion are made continuously and automatically to keep each reflected beam on its target. Each heliostat is capable of independent targeting from every other heliostat, to permit a uniform flux distribution on the receiver. Target tracking is initiated by either a TRACK command, which causes an absolute number of heliostats to track their targets, or the INCREASE command, which causes an incremental number of heliostats to be added to the heliostats in the power phase;

4) Postpower - The postpower phase causes the heliostats in the power phase to return to the power standby point (CULP). This phase is initiated by the DECREASE command, which causes an incremental number of heliostats selected to go to the CULP. An emergency postpower phase will cause all heliostats tracking the target to return to their CULPs. This phase is initiated by a DEFOCUS command or is automatically initiated by a trip signal from the receiver subsystem;

5) Shutdown - The normal shutdown phase consists of returning the heliostats to their stowed positions. The STOW command to the selected heliostats will bring heliostats from their CULP to the CLLP, through the coordinated corridor walk, then to the stowed positions. The lock command is used to move the heliostats to the locked position if high winds are expected;

6) Maintenance - This phase is intended for heliostat performance checkout, heliostat repair, or mirror modules washing. It allows the heliostats to be positioned at absolute encoder positions. The POSITION command will direct the heliostat to the specified azimuth and elevation encoder positions. The WASH command will direct the heliostat to a prestored azimuth and elevation encoder position for mirror module washing;

7) Corridor Walk - Based on previous heliostat control experience with the CRTF, a beam movement method has been derived to safely bring the heliostats from the stowed position to an adjacent collector target standby position and, conversely, to return heliostats from the standby position to the stow position. The safety constraints identified are based on similar constraints developed at the CRTF. Up to eight imaginary corridors will be defined on the sides of the receiver support tower figure 5.4-7 shows two such imaginary corridors. Two points, the corridor lower limit point (CLLP) and the corridor upper limit point (CULP) will define a linear, single-element segment called the corridor centerline (CCL). This centerline may be vertical or slanted as required. During heliostat movement from the stowed position to the standby position in response to the UNSTOW command, all heliostats affected by the command will move so their beams converge on and track the CLLP. After a suffic ient time has elapsed to allow the heliostat with the largest angular change to reach and track the CLLP, all heliostats affected by the command will automatically be directed to move their beams up the corridor in a coordinated fashion so the concentrated beam moves up the centerline until the beam reaches and tracks the CULP. Likewise to stow the heliostats, beams will be collected at the CULP and moved down the centerline in a coordinated fashion to the CLLP, where each heliostat will be directed to the stowed position. Corridor "slides" will be defined so heliostat beams will be within corridor limits during normal operations.

The HAC software has the capability to command a heliostat or group of heliostats as follows:

1) Single Heliostat - The capability to command a specific heliostat by its number;

2) Heliostat Field Controller - The capability to command all heliostats controlled by a single heliostat field controller as a group;

3) Segment - The capability to command a group of heliostats in an arc segment around the tower;

4) Ring - The capability to command a complete set of segments that forms a circle approximately on the same circular rows from the tower;

5) Wedge - The capability to command a complete set of segments that form a pie-shaped wedge centered on the tower.

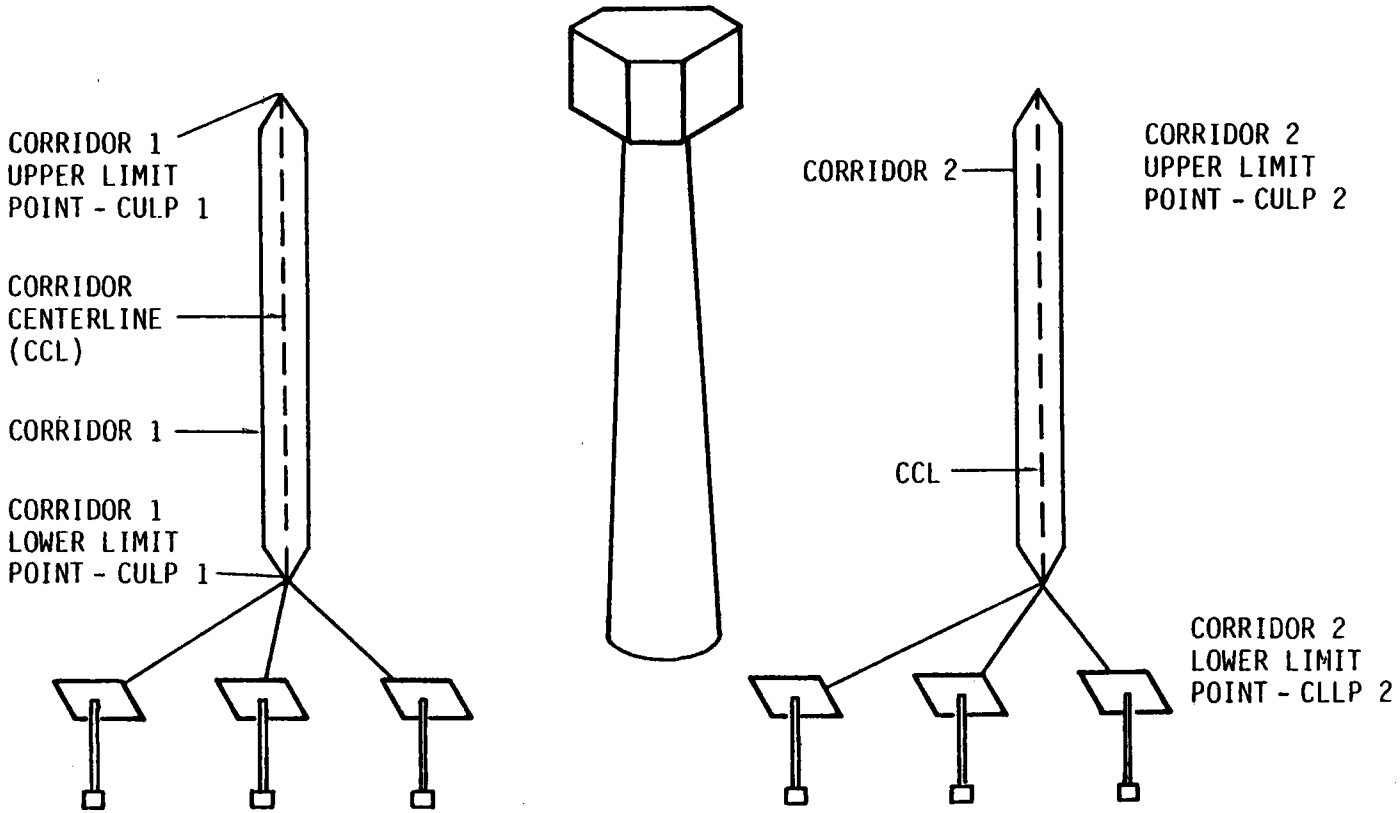

Figure 5.4-7 Corridor Walk Diagram

5.4.7.2 Heliostat Field Controllers

The HFC provides the interface between the HAC and the HC. It receives commands from the HAC and transmits commands to the HCs, receives status information from the HCs, and transmits status to the HAC. Once each second, the HAC transmits the current sun vector to all HFCs. These data are transmitted to the HCs for use in the pointing algorithm to determine the necessary encoder positions for each heliostat to direct its reflected beam at the desired target. The HFC also calculates a new target once each second during a corridor walk and transmits the target to the HC.

The HFC performs an emergency corridor walk of all HCs on the receiver, or on the corridors, if communications from the HAC are interrupted for an extended length of time (approximately 20 seconds).

Figure 5.4-8 is a block diagram of the HFC. The HFC includes a microcomputer, input/output electronics and fiber optic transmitters and receiver. Although the fiber optic link to the HAC is dual-redundant in the production system, redundancy is not included in the prototype. The watchdog timer provides an automatic reset if the microcomputer fails.

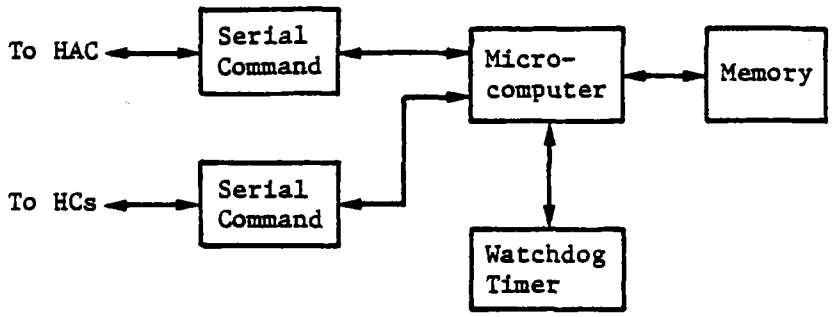

Figure 5.4-8 Heliostat Field Controller

The HFC has 4096 bytes of read-only memory (ROM) and 1152 bytes of random-access memory (RAM).

5.4.7.3 Heliostat Controller

Figure 5.4-9 is a block diagram of the HC, which is positioned at each heliostat, receives commands, and controls beam position with a digital control system. The heliostat can be manually controlled through the HC by connecting a manual control unit. The HC has a self-check system and can automatically signal the control room in case of failure. These functions are implemented by a microcomputer controller in the HC. The microcomputer receives data from the bus, transmits data back when required, calculates gimbal angle commands, determines actual gimbal angles from encoder outpus, and services the motor control loop.

Motor control is set up by the microcomputer software that provides slew, track, or off commands to the motor control circuit.

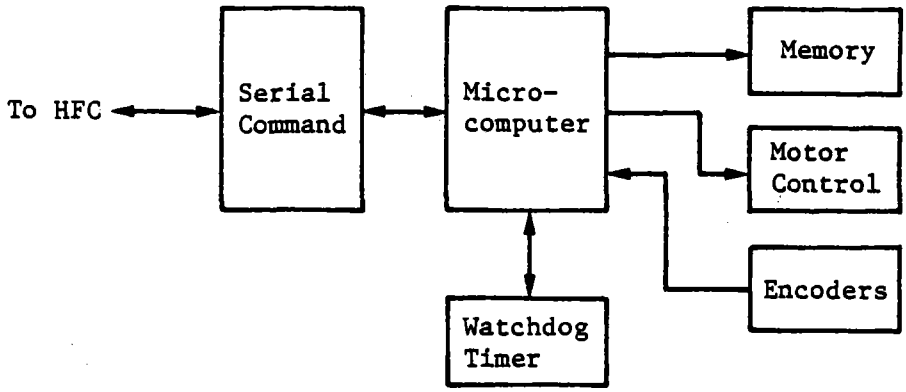

Figure 5.4-9 Heliostat Controller

The microcomputer performs the necessary functions based on commands supplied by the HFC. It provides motor control based on comparison of the commanded position and gimbal position, and formats the data for status information.

The microcomputer provides automatic reset during power-up, an the clock section provides the crystal-controlled operating frequencies for the system. The timer section serves as a watchdog, giving automatic reset and initialization during any error.

The HC has 4096 bytes of ROM and 256 bytes of RAM.

The HC/HFC power supplies is a high-efficiency switching power supply. This type of power supply is smaller in size and generates less heat than a linear power supply with the same rated output power.

The HC or combination HFC/HC is packaged in a sheet metal enclosure consisting of a channel-shaped chassis on which is mounted the electronic components and a cover of perforated metal that is also channel-shaped (Figure 5.4-10). These two channels are combined to form the 4.00 x 9.25 x 10.25-in. enclosure. This approach has been selected to minimize the cost of a separate electronics mounting plate installed within an enclosure. This is also a very basic sheet metal fabrication.

The I/O connectors and the ac power cord are mounted on one leg of the chassis channel. The solid-state relays, three-phase bridge rectifiers, and low-speed transformer are mounted on the far leg of the chassis channel. The 5-V switching power supply and the microprocessor printed wiring boards (wirewrap boards in the prototype) are located on the base of the channel. For economy, the printed wiring board is double-sized and designed for flow soldering. The printed wiring board is installed with nylon snap-in standoffs. All wiring will use either mass terminations or crimp terminations as applicable.

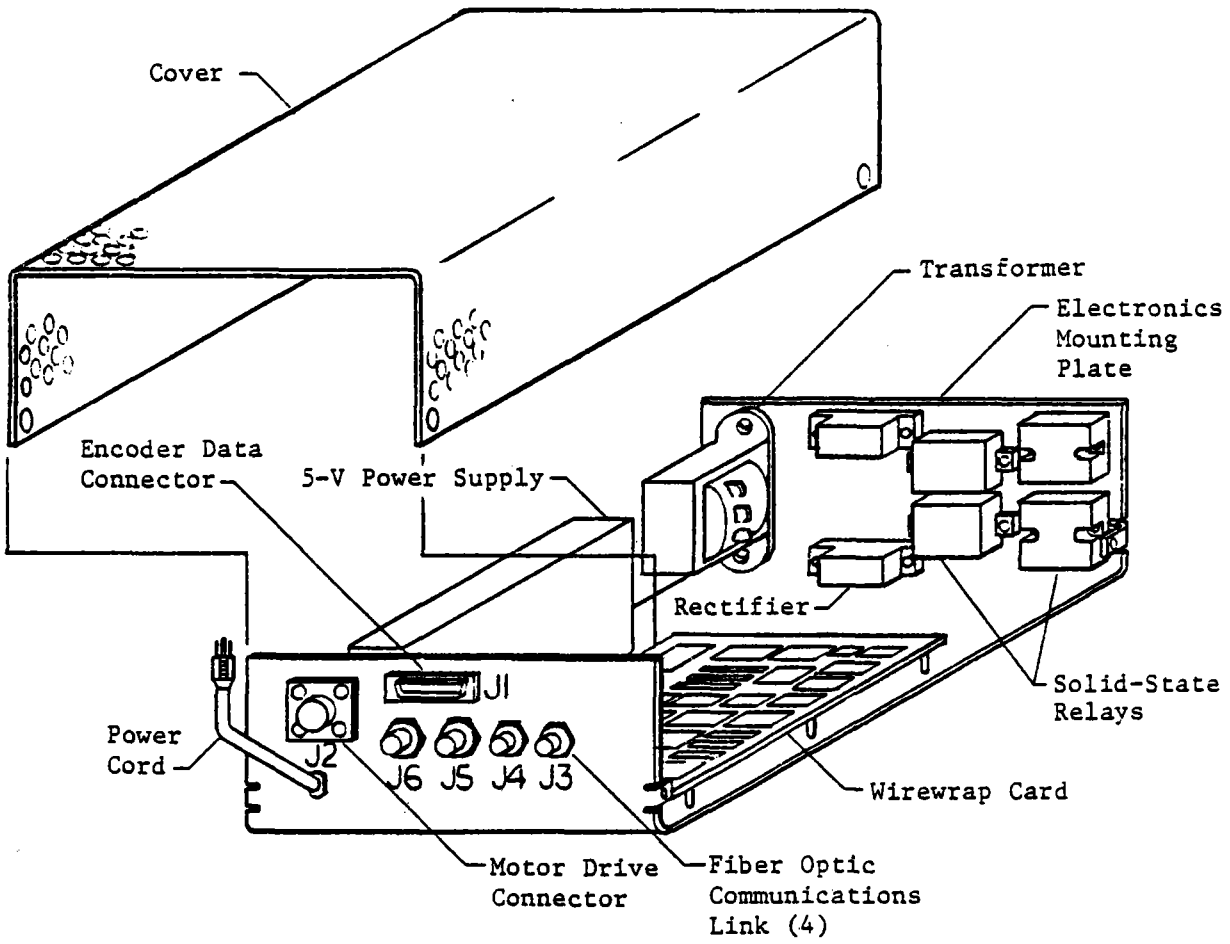

Figure 5.4-10 HC/HFC Packaging Concept

The perforated metal cover is a one-piece channel with a pattern of 1.6 mm (0.062-in.) holes staggered on 3.6 mm (0.14-in.) centers providing a 30% opening. The cover serves to protect personnel as well as the electronics while acting as an insect screen and allowing ventilation for cooling. The cover is fastened to the electronics chassis with four self-threading fasteners.

The HC or combination HFC/HC is installed in the pedestal with the connector panel facing the door. The unit will rest on its narrow dimension with the power supply at the top. This will position the PC board, power supply, and solid-state relays for the most efficient cooling and allow convection flow using the cover perforations.

In the production design, the HC and HFC will be separate printed wiring boards.

5.4.7.4 Heliostat Electrical Installation and Control Cabling

Figure 5.4-11 illustrates installation of the electrical/electronic components on the heliostat and the control cable that interconnects those components.

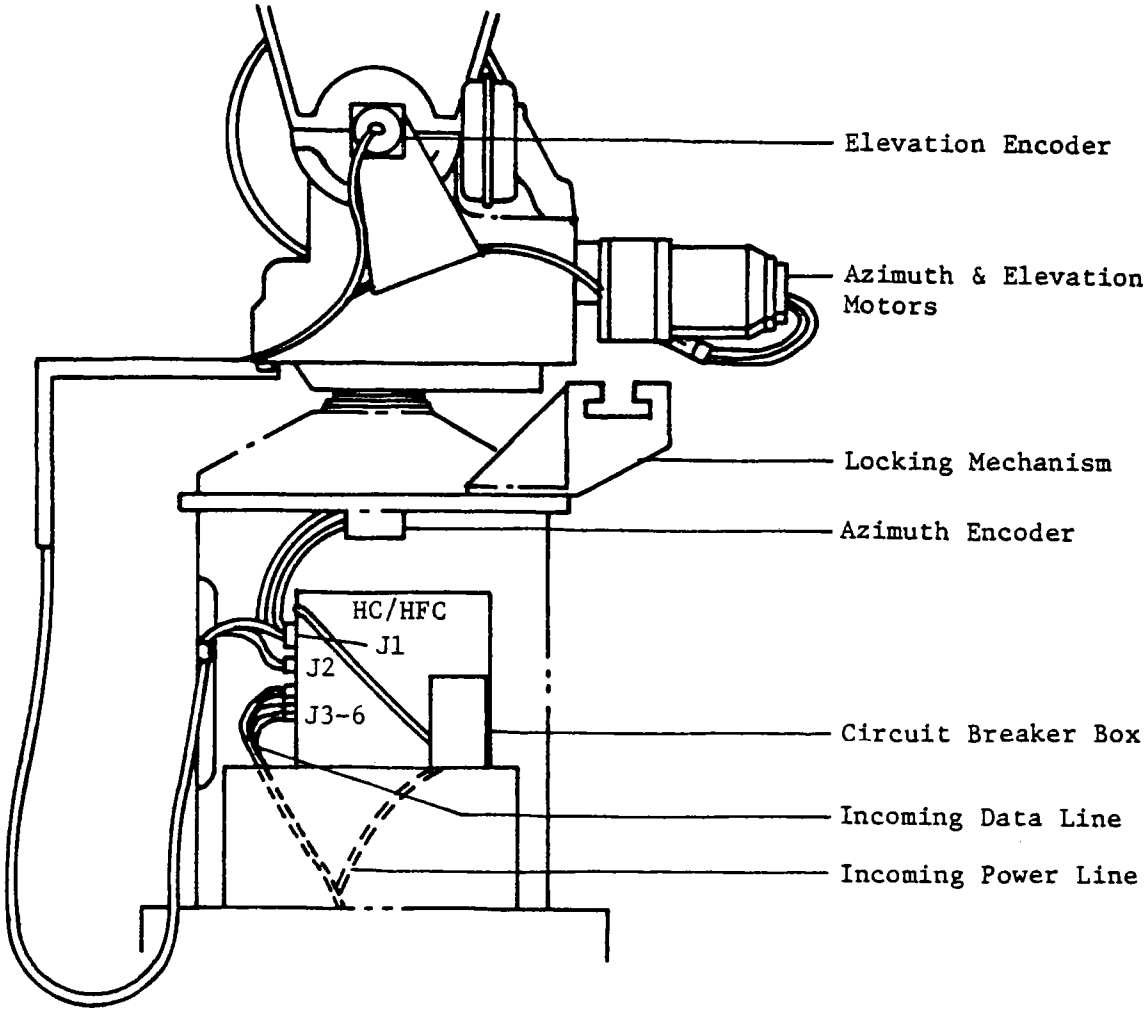

Figure 5.4-11 Heliostat Electrical Installation

Incoming 120-Vac power is brought up through the pedestal through a conduit and connected to an individual circuit breaker box in each heliostat. The box provides power for the HC/HFC and an additional convenience outlet for maintenance equipment.

Fiber optic data lines are brought up through the pedestal through the same conduit used for the power lines and are connected into the HC/HFC. The multiconductor cable connects the HC/HFC to the limit switches, motors, and encoders. The service loop allows for cable movement as the drive mechanism turns.

The multiconductor cable consists of single conductors and twisted, shielded, jacketed pairs encased in an ultraviolet-stabilized thermoplastic rubber jacket. One multiconductor cable runs from the HC/HFC to the appropriate equipment, but the interior pedestal connections are made with twisted, shielded pairs to provide a substantial cost reduction in cable.

5.4.7.5 Gear Motors and Motor Control

Bodine Electric Company 1/6 horsepower dc gear motors are used to drive the heliostat. The gear motors operate at two significantly different speeds -- slew and track. The slew speed is necessary to meet time requirements for stowing the heliostats and for resolving the south-field singularity. The track speed is required to provide stable operation when the heliostat is in the fine-track mode.

Slew or fast operation is obtained by applying voltage (rectified) to the motor. Track or slow operation is obtained by supplying a reduced voltage to the motor. Figure 5.4-12 is a block diagram of the motor controller. Solid-state relays are used to turn the motor on and off at either slew or track speed. The solid-state relays turn on as the voltage waveform is going through zero, and turn off as the current waveform is going through zero. This type of operation minimizes switching transients and noise generation.

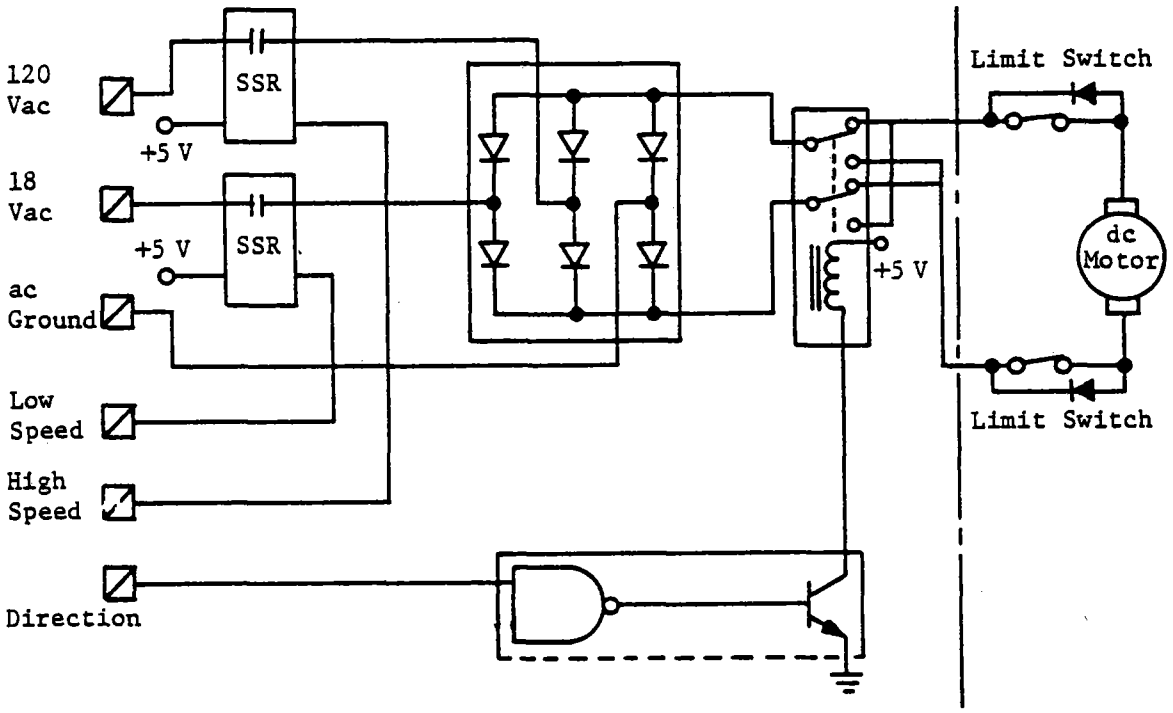

Figure 5.4-12 Motor Control Circuit

The mechanical relay is used to change the direction of motor rotation. Logic in the microcomputer permits operation of the mechanical relay only when the motor is turned off so the mechanical relay never breaks the motor current.

The limit switches are mechanically actuated at the limits of gimbal travel (approximately ±270° in azimuth and ±95° in elevation) to prevent any damage of the heliostat that could result from driving it too far.

The diodes around the limit switches provide the capability of driving the heliostat back in the opposite direction after it has been driven into the limit switches.

5.4.2.6 Gimbal Angle Encoders

BEI Electronics, Inc. optical encoders are used to determine the heliostat gimbal angles. The gimbal-angle encoders are 11-bit, self-contained, totally enclosed optical encoders for each axis, directly coupled to the azimuth and elevation output shafts. The encoders have two optical tracks with outputs that are 90° out of phase and provide 13-bit resolution. The encoder outputs are fed into the microcomputer in the heliostat controller; the microcomputer detects all incremental changes in the encoder output and stores a count that is the gimbal angle position. This approach eliminates 22 electronic components and provides improved noise immunity over an earlier design in which the electronics in the encoder provided the 13-bit output. This improved encoder was developed for the production heliostat for the Barstow 10-MW_e pilot plant.

5.4.7.7 Field Power Distribution System

The field power distribution system consists of primary feeders, transformers, distribution panels, and secondary feeders. The power required at each heliostat is 120-V single-phased ac.

A specific design for the field power distribution system was not a part of this contract. The cost estimate for the field power distribution system was based on scaling up the cost of the system being installed at Barstow.

5.4.7.8 Data Bus Communications

Communications between the HAC minicomputer and the HFC micro computer, as well as the communications between the HFC and the HC microcomputer are maintained over fiber optic data buses.

The HAC minicomputer maintains communications with the 103 HFCs over 24 data buses, with eight HFCs connected to each data bus. Each HFC maintains communication with up to 32 HCs over a single data bus.

The data transmitted over the HAC/HFC data buses include sun position, status poll requests to each of the HFCs, status response from each of the HFCs, and operational commands to the HFCs as required. The data transmitted over the HFC/HC data buses include sun positon, operational commands, status poll requests, and status poll responses.

Commands issued from the HAC are transmitted by the HAC interface fiber optic transmitter to the first HFC on the link. The HFC receiver accepts the command to the HFC transmitter for transmission to the next HFC on the link, as well as to the microprocessor located in the first HFC. This assures that all HFCs receive the command at the same time, allowing for the short propagation delay of the fiber optic transmitters and receivers.

If a status response is required from the HFC, internal logic controlled by the microprocessor gates the response data to the HFC's transmitter for transmission to the next HFC in the link, and ultimately to the HAC interface receiver. Firmware residing in the HFC rejects any commands or status requests not specifically intended for that HFC. Nevertheless, the command or status request, or possibly a status response, is always sent to the next HFC on the link; from the last HFC, the messages are transmitted back to the HAC over a separate fiber.

Operation of the HFC/HC data link is almost identical to the HAC/HFC link, with the following exception. The HFC does not issue any status requests to the HCs; rather HCs respond in order, based on their address, after the acceptance of a valid HFC command.

The HAC-to-HFC data buses are dual redundant in the production system; if a failure makes a bus inoperable, the HAC and HFCs will automatically switch over to the backup bus.

Fiber optic communications offers several advantages over conventional communications systems. One of the primary advantages is the high data rates that can be achieved. As heliostat fields increase in size, real-time field status and control requirements will increase. This will require higher communication rates with no loss of data integrity. Fiber optic communications offers this capability.

Another major advantage is the low noise susceptibility inherent to fiber optics. Total electrical isolation provides enhanced reliability as well as increased lightning protection. Another important consideration is the reduced parts count over conventional long-distance data bus systems. Fiber optic systems do not require special voltages or the isolated power supply required for differential current MOS systems. They also eliminate the optical isolators, drivers and receivers, and transient suppressor. Because the fiber optic transmitters and receivers mount to the controller chassis directly, printed circuit board space and the time required to lay out the parts are decreased.

Fiber optic systems (receiver, transmitter and optical cable) are rapidly decreasing in cost. Vendor target prices for transmitter/receiver pairs will approach the $30.00 cost level in the very near future. Fiber optic cable costs, which are currently lower than conventional RG-22 twin axial cable, are also decreasing in price. Larger diameter plastic cable, designed for shorter distances, is also available. This cable, coupled with compatible low cost transmitters and receivers, offers a cost effective high-speed approach for heliostat-to-heliostat communications.

5.4.7.9 Control Support Equipment

Control support equipment being supplied with the heliostat includes a manual control box, and a motor drive tool. The manual control box plugs into the HC and provides the capability to turn on the azimuth and elevation drive motors at either slew or track speed. The motor drive tool bypasses the HC and plugs directly into the azimuth and elevation motors; it provides the capability to turn the motors on in either direction in either a continuous or momentary mode at slew speed. Both the manual control box and motor drive tool are indispensable tools for heliostat installation, checkout and maintenance.

5.4.7.10 Basis for Collector Control Subsystem Cost Estimates

Cost estimates for the gear motors, encoders and HAC were based on vendor quotes. cost estimates for the HC, HFC and heliostat control cable were based on vendor quotes for the componednts and labor cost estimates that were scaled from the 10-MW_e Pilot Plant heliostat design. The cost of the field power system was scaled from cost data for the 10-MW_e Pilot Plant. Fiber optics costs were based on vendor data.

5.4.8. Receiver Control Subsystem

The steady state operation of the receiver control subsystem (RCS) involves control of the salt booster flow, salt flow through the receiver, and pressure dissipation in the drag valve. The system is normally in an insolation following mode such that the salt flow will be controlled to maximize the amount of energy reflected into the receiver cavities and the receiver will be controlled to absorb the incident energy safely and to maintain the outlet salt temperature at the setpoint.

The operation of the receiver must be coordinated with the operation of the collector system through the OCS. Coordination is particularly important during start up when the receiver is brought from a cold standby to normal operation. This is accomplished by slowly bringing heliostats on target in a specified manner, such that even, controlled warming of the receiver to operating temperatures is achieved. Coordination with the collector system is also required in emergency situations such as pump failures, where the incident energy must be quickly removed from the receiver.

A schematic of the domain of the receiver control system which starts with supply of cold salt to the receiver and ends with the return of hot salt to energy storage is shown in Figure 5.4-13. Separate cold and hot surge tanks are provided for the receiver. The cold salt surge tank decouples the supply of cold salt from the receiver. The hot salt surge tank decouples the return of salt to energy storage from the flow of salt through the receiver. As the cold surge tank is charged to 2503 kPa (363 psig) and the hot salt surge tank is charged to 138 kPa(20 psig) a relatively constant pressure difference has been established for control of salt flow through the receiver. This configuration

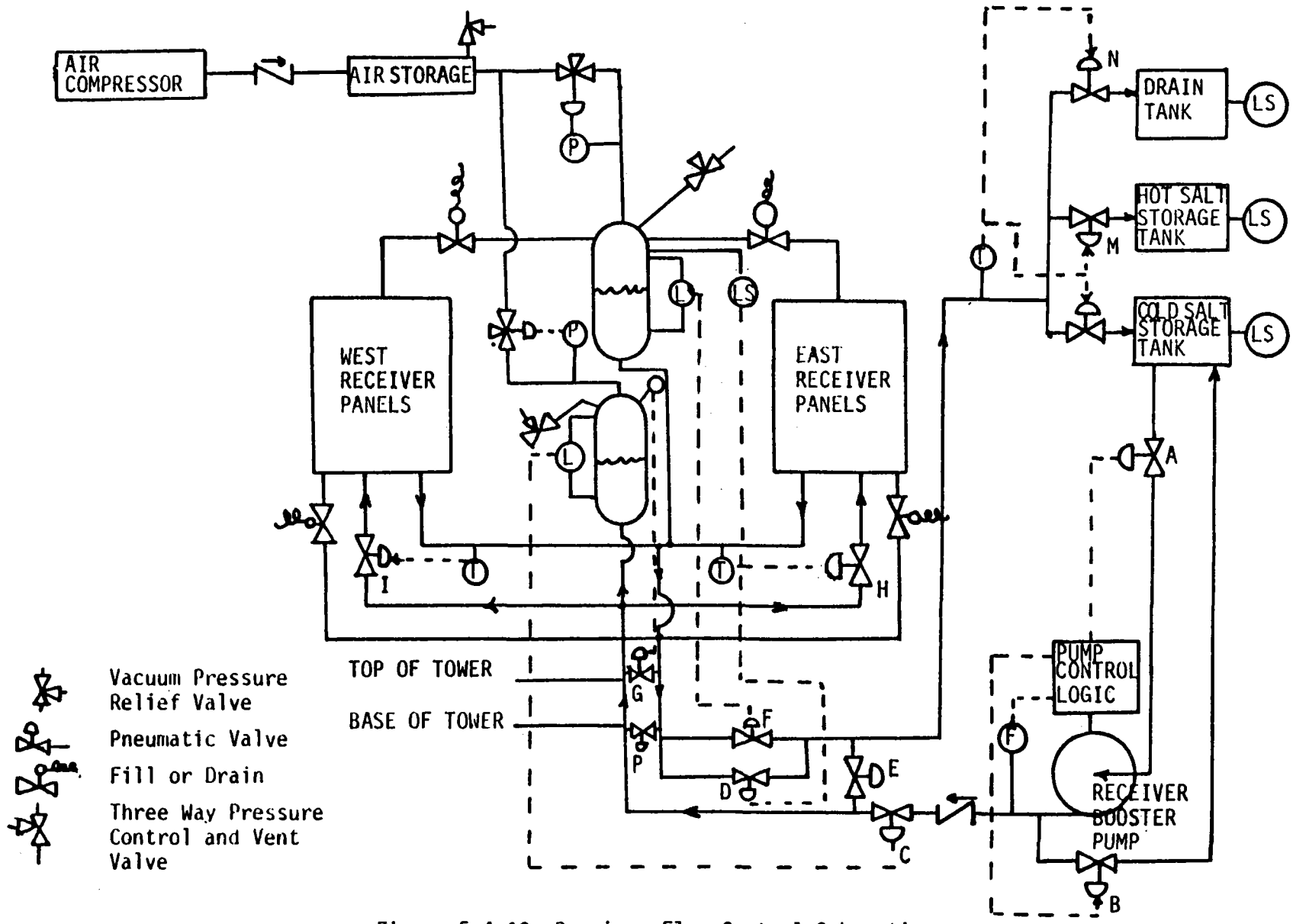

Figure 5.4-13 Receiver Flow Control Schematic

also allows the receiver subsystem to maintain continuous salt flow through the receiver in the event of a pump or electrical failure. This safety flow maintains receiver cooling while the receiver doors are closing and the heliostats are being redirected from the receiver cavity.

Supply of salt to the receiver from the cold salt storage tank is accomplished by three pumps operating in parallel. These pumps are located near the cold salt storage tank.

Control of the cold salt pumps is accomplished by the level of the salt in the cold salt surge tank. This level signal is used in a feedback control loop to adjust the valve located near the booster pumps which throttles the flow from the booster pumps. A series control valve approach is recommended for the pumps because the dynamic head (flow effects) and the control valve pressure head is a small part of the total pump head. System flow is measured after flow control valve D is used to control the number of pumps operating.

Flow of salt from the receiver is controlled by valve F. The salt returning to the energy storage area is directed to the hot or cold storage tanks depending on its temperature. Valves L and M are used for this function. The intermediate temperature salt which flows from the receiver panel during startup and shutdown will be directed to the cold tank after a temperature <700°F is reached. This will ensure that the inner carbon steel walls will not be exposed to the corrosive salt at temperatures greater than 750°F.

The flow of salt through the receiver is controlled by one control valve for each zone of the receiver. A schematic representation of the receiver as seen in Figure 5.4-13 illustrates the two control zones. Due to the pressurized cold and hot salt surge tanks, the actual control of the salt through the receiver is decoupled from the remainder of the receiver subsystem.

Investigations into the dynamic aspects of receiver control has resulted in the development of specialized digital control algorithms. A block diagram of a receiver cntrol scheme is shown in Figure 5.4-14. The algorithm is based on a hybrid combination of feed-back/feed-forward control. The actual algorithm is receiver design dependent and must be developed to take receiver flux distributions into account.

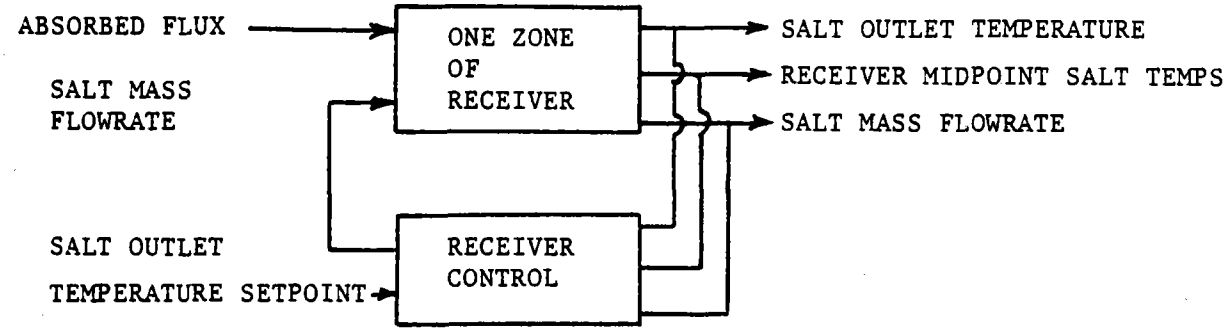

Figure 5.4-14 Receiver Flow Control Configuration

5.4.9 Energy Storage Control Subystem

The center of the cogeneration facility is the energy storage subsystem with three separate operating functions stemming from this point. One mode is to put hot salt into the hot salt storage tanks. Salt from the cold storage tank is circulated through the receiver and solar insolation is directed to the receiver panel to heat the salt to the design point temperature. The second mode of operation is to generate steam for injection into the oil field. Salt from the hot salt storage tank would be circulated through the salt/process steam heat exchanger and returned to the cold salt storage tank. The third mode of operation is to generate electricity. Salt from the hot salt storage tank will be circulated through the salt/turbine steam heat exchanger. This steam would be directed to the turbine for generation of electrical power.

All interactions with the energy storage subsystem (ESS) is the responsibility of the subsystem which is utilizing or providing the energy. For example, the receiver control subsystem is responsible for control from the moment salt leaves the cold tank until it enters the hot tank. Thus, the energy storage control subsystem (ESCS) is responsible for only the ancillary hardware associated with the storage tanks. It does not control the flow of salt from the hot salt tank. The ancillary hardware included in the ESCS control is as follows: 1) control of storage tank foundation temperatures, 2) control of salt melter when used for reheating, and 3) control of salt reprocessing.

A diagram of the ESCS is shown in Figure 5.4-15. The foundation cooling control is shown on the lower part of the diagram. A single pump is used to provide cooling water from the cooling tower sump. Each tank foundation has its own outlet water temperature sensor for control of the cooling water control valve.

The salt reprocessor will contain its own controls. If the salt reprocessor operated in a batch mode, then a pump will not be necessary. However, if salt reprocessing is continuous then a salt pump will be required. Salt will be taken from the cold salt tank, conditioned to the proper purity and returned to the cold salt tank. The salt melter will also contain its own pumps and controls. The melter will be connected so it can be used in two ways:

1) To melt granular salt using a fossil fuel and transferring the melted salt to the cold salt tank.

2) To add heat using fossil fuel, to salt from the cold salt tank and returning the warmer salt to the cold salt tank.

5.4.10 Heat Exchanger Control Subsystems

There are two separate heat exchanger (steam generator) subsystems. These are the Process Steam Subsystem (PSS) and the Turbine Steam Subsystem (TSS). The PSS conrol system is responsible for the conversion of energy from storage into steam which is used in the oil recovery process. The TSS control system is responsible for the conversion of energy from storage into steam which is used to generate electricity in the EPGS.

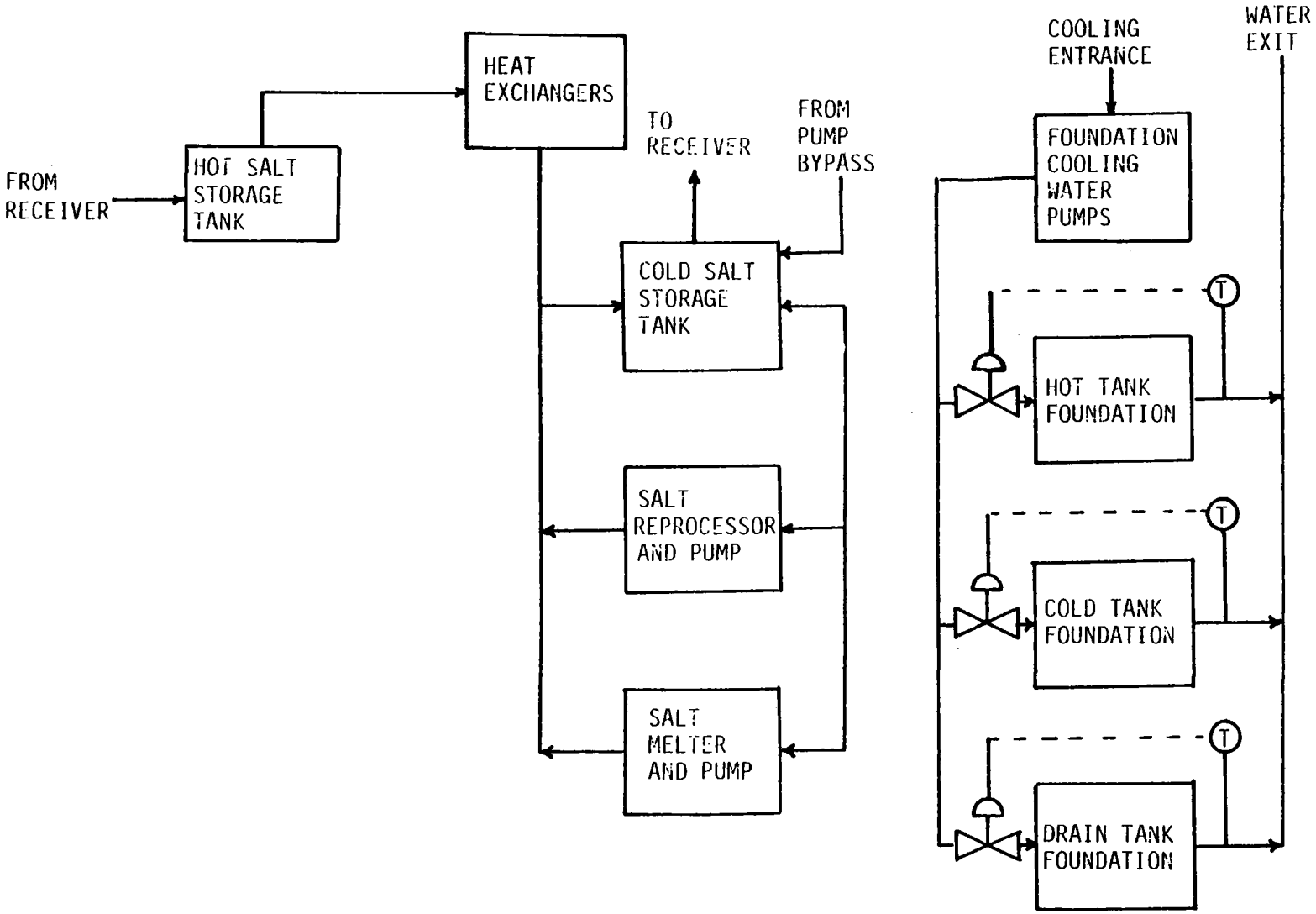

Figure 5.4-15 ESCS Diagram

The remainder of this section will deal with the TSS control subsystem. The PSS control subsystem will be identical with the exception of the superheat requirements and the additional turbine steam reheat heat exchanger in the TSS. The salt/steam heat exchanger control configuration is shown in Figures 5.4-16 and 5.4-17. The temperature of the molten salt streams entering the Steam Generator TT-304 and leaving the preheater TS-303 are also used as inputs to the computer which then modulates salt flow to generate the desired pressure of steam. A signal from this salt flow controller is also fed back to the hot salt pump control logic for summation with the EPGS salt flow to ensure sufficient pumping capacity.

This equilibrium is maintained through the utilization of control logic and various sensed temperatures, pressures, liquid levels, and mass flow rates, as seen in Figure 5.4-18. The control subsystem will also monitor critical pump and motor bearing temperatures, and any other aspects of system operation which are required to assure safe and efficient operation. Critical parameters will be monitored by the OCS through red line units (RLUs). The RLUs provide for direct hardwired trip functions, in the event that any critical parameter exceeds the predetermined limits.

The region of control authority for the PSS, TSS, and EPGS control subsystems relative to the entire plant is shown in Figure 5.4-18.

5.4.11 Electric Power Generating Control Subsystem (EPGCS)

The domain of the EPGCS relative to the entire plant was shown in the last section on Figure 5.4-18. The main function of the EPGCS is to ensure safe turbine operation. This requires the monitoring of many bearing temperatures as well as steam pressures and temperatures. Critical parameters will be hardwired for direct OCS monitoring through red line units.

The EPGCS is also responsible for the control feedwater and condensate pumps, as well as makeup and blowdown water. A block diagram representation of the EPGCS is shown in Figure 5.4-19.

The EPGCS will provide sychronization of the generated electrical power with the local grid and will monitor phase and voltage to assure compliance with minimum requirements. The EPGCS will also be responsible for the safe shutdown of the turbine in the event of generator or steam supply failure. In the event of an EPGS failure, the control subsystem will go to the predetermined standby position, and will present a failure sequence record to the OCS. The failure sequence record will provide a record of the sequence of events which resulted in the trip condition, facilitating a restart or repair.

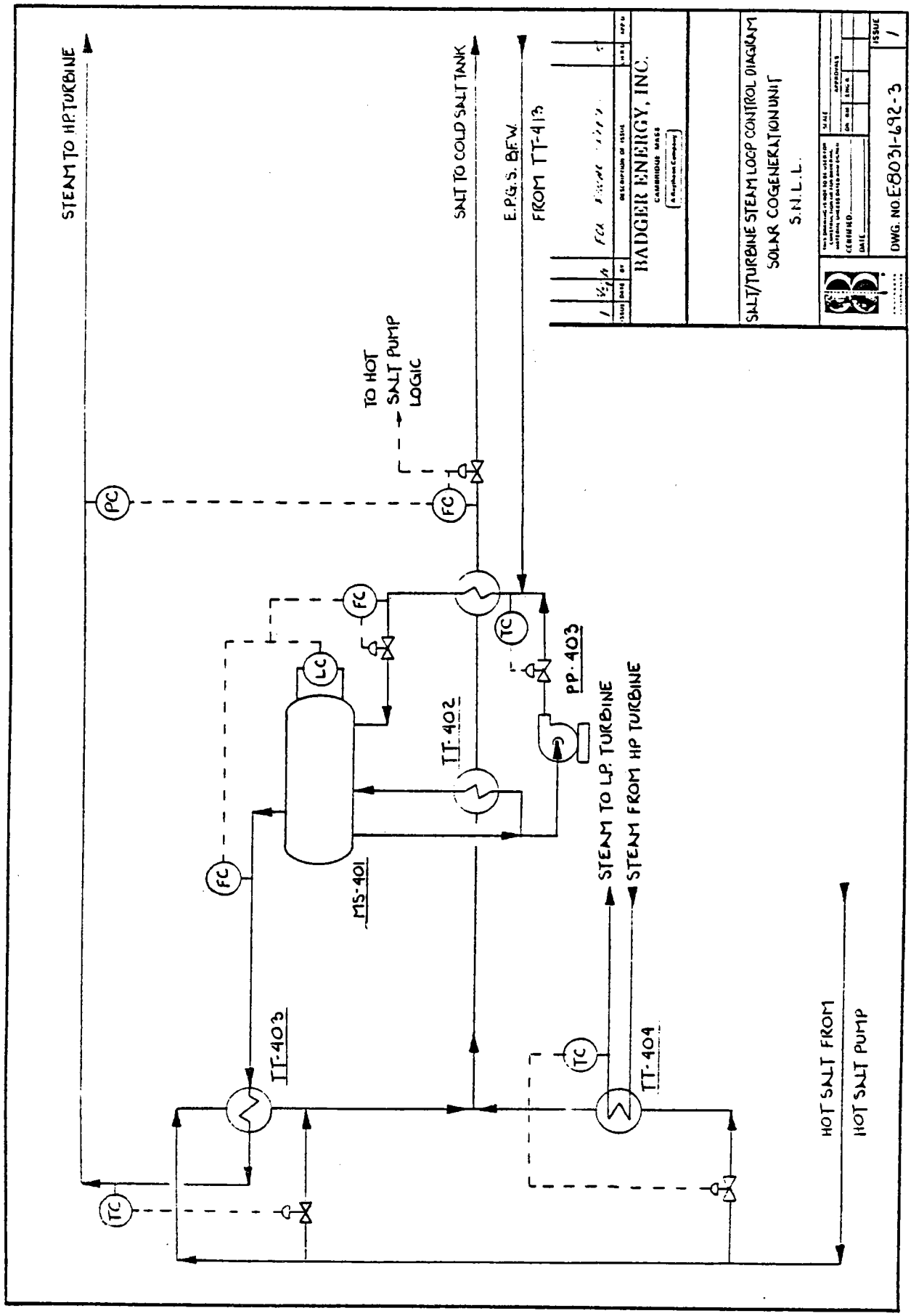
STEAM TO HP TURBINE
SALT TO COLD SALT TANK
E.P.G.S. B.F.W.
FROM TT-413
TO HOT SALT PUMP LOGIC
PC
FC
LC
TC
TT-402
TT-403
TT-404
MS-401
PP-403
STEAM TO LP TURBINE
STEAM FROM HP TURBINE
HOT SALT FROM
HOT SALT PUMP
BADGER ENERGY, INC.
CAMBRIDGE, MASS.
SALT/TURBINE STEAM LOOP CONTROL DIAGRAM
SOLAR COGENERATION UNIT
S.N.L.L.
DWG. NO E8031-692-3
ISSUE 1

Figure 5.4-16

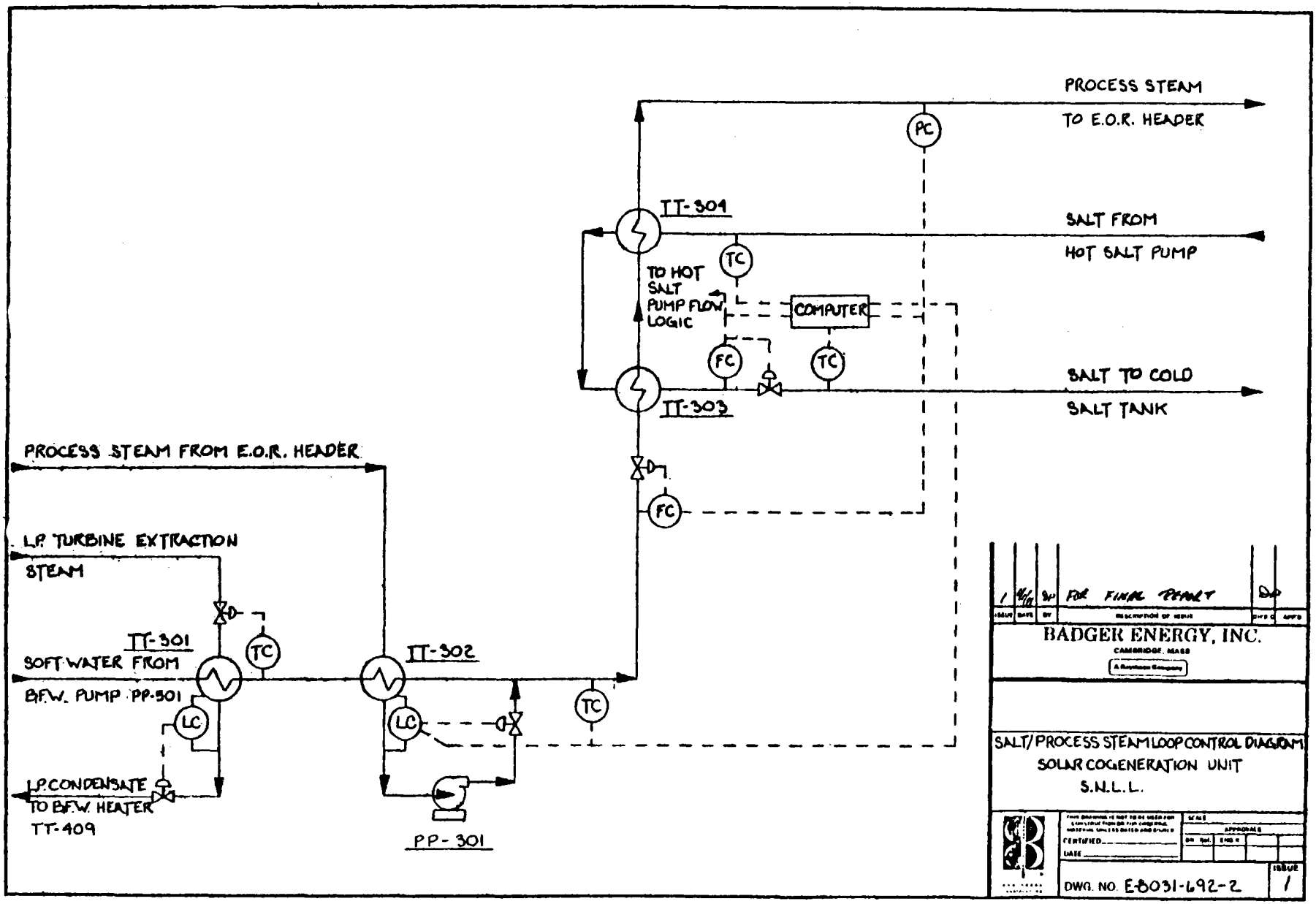
PROCESS STEAM
TO E.O.R. HEADER
PC
IT-304
SALT FROM
HOT SALT PUMP
TC
TO HOT SALT PUMP FLOW LOGIC
COMPUTER
FC
TC
IT-303
SALT TO COLD
SALT TANK
PROCESS STEAM FROM E.O.R. HEADER
FC
L.P. TURBINE EXTRACTION STEAM
IT-301
SOFT WATER FROM B.F.W. PUMP PP-501
TC
IT-302
LC
LC
TC
L.P. CONDENSATE TO B.F.W. HEATER TT-409
PP-301
1
FOR FINAL PRINT
BADGER ENERGY, INC.
CAMBRIDGE, MASS
SALT/PROCESS STEAM LOOP CONTROL DIAGRAM
SOLAR COGENERATION UNIT
S.N.L.L.
DWG. NO. E-8031-692-2
ISSUE 1

Figure 5.4-17

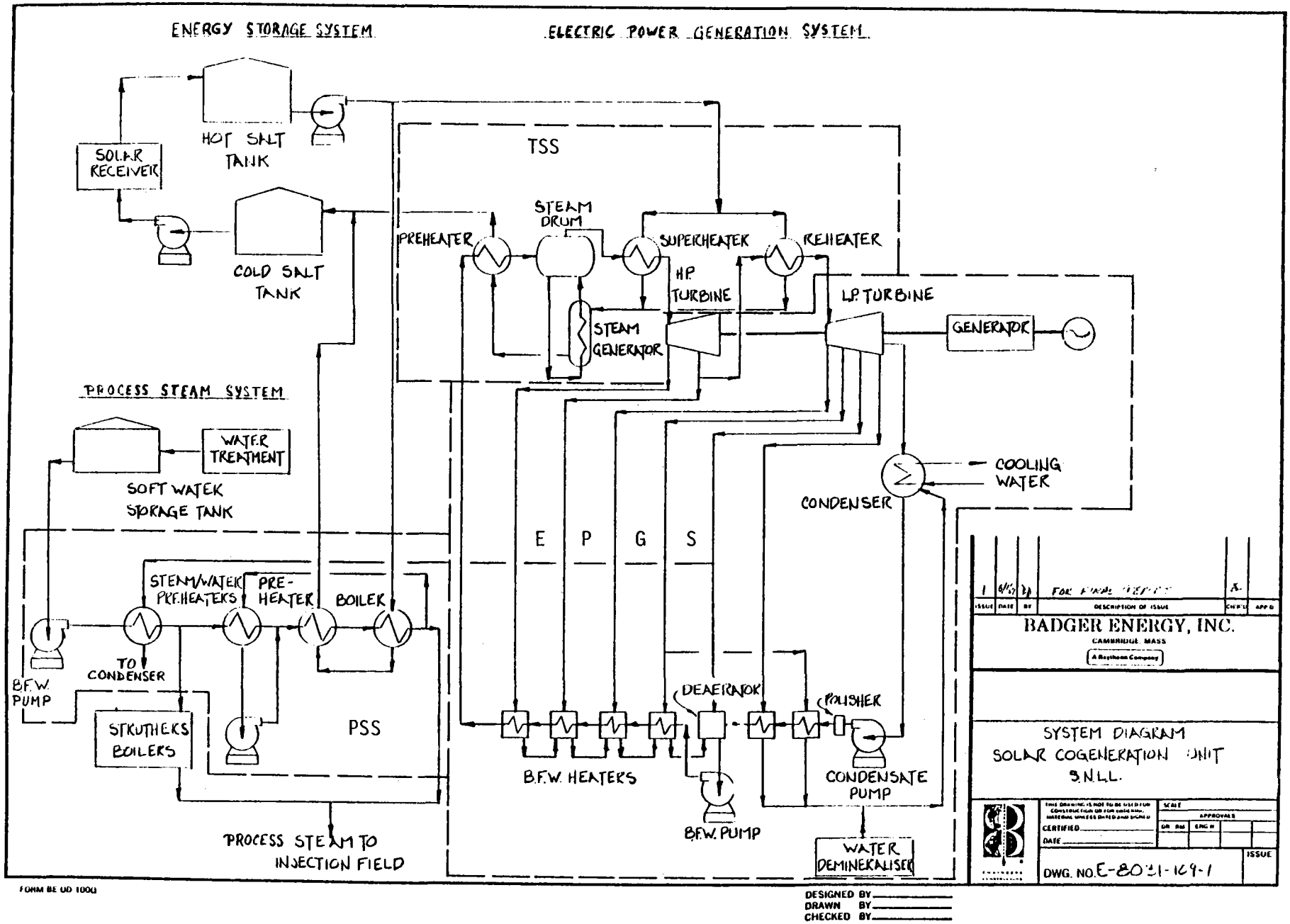

Figure 5.4-18 Control Subsystem Domains

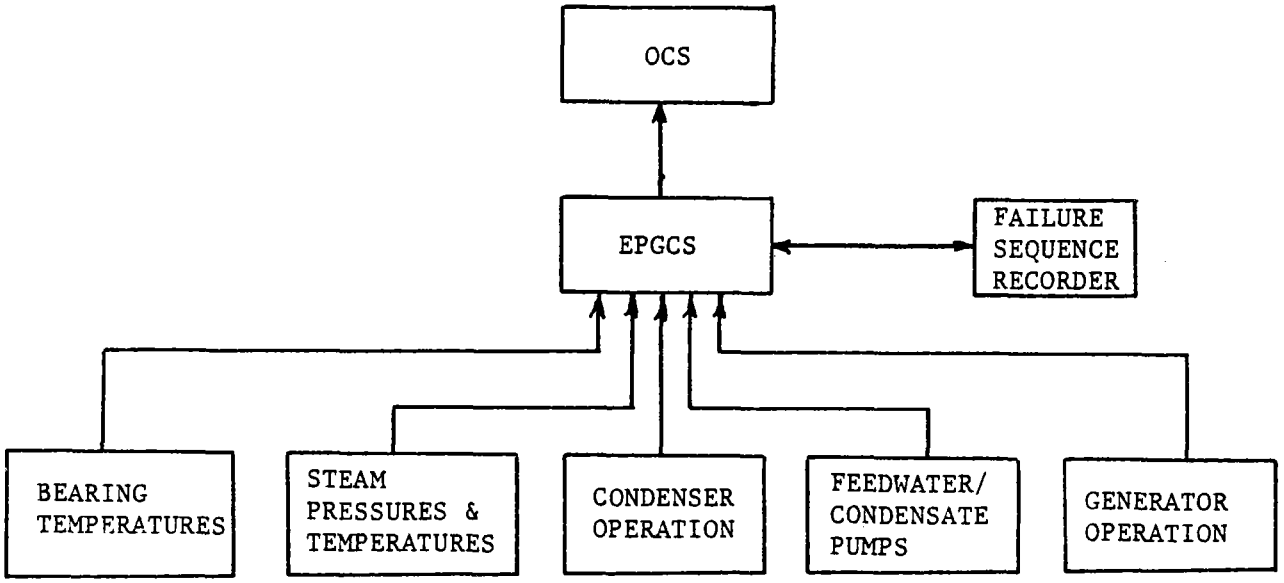

Figure 5.4-19 Block Diagram Representation of the EPGCS

5.4.12 Data Acquisition Subsystem (DAS)

Due to the nature of the distributed digital control (DDC) hardware, all variables measured for control purposes by any of the control subsystems are available to the DAS through the data bus. The DAS system will provide for recording of system variables independent of control system functions. Those variables selected for long term storage will be either written to a disk or magnetic tape, depending upon the final system configuration.

The purpose of the DAS system is to provide a long term record of plant performance. The variables recorded at any specific time can be changed at the DAS console. The operator has complete freedom in deciding which variable and how many are recorded at any specific time. The system will allow rapidly changing variables to be scanned at a faster rate than more stable variables. The freedom of data recording is only limited by the minimum scan time and the maximum number of variables which can be recorded at any one time. Both of these limitations are hardware dependent and will be designed to not interfere with anticipated DAS requirements.

A block diagram representation of the DAS is shown in Figure 5.4-20. All DAS interfaces, such as the CRT display, keybord, display hardcopier, and strip chart recorders are located a the DAS console.

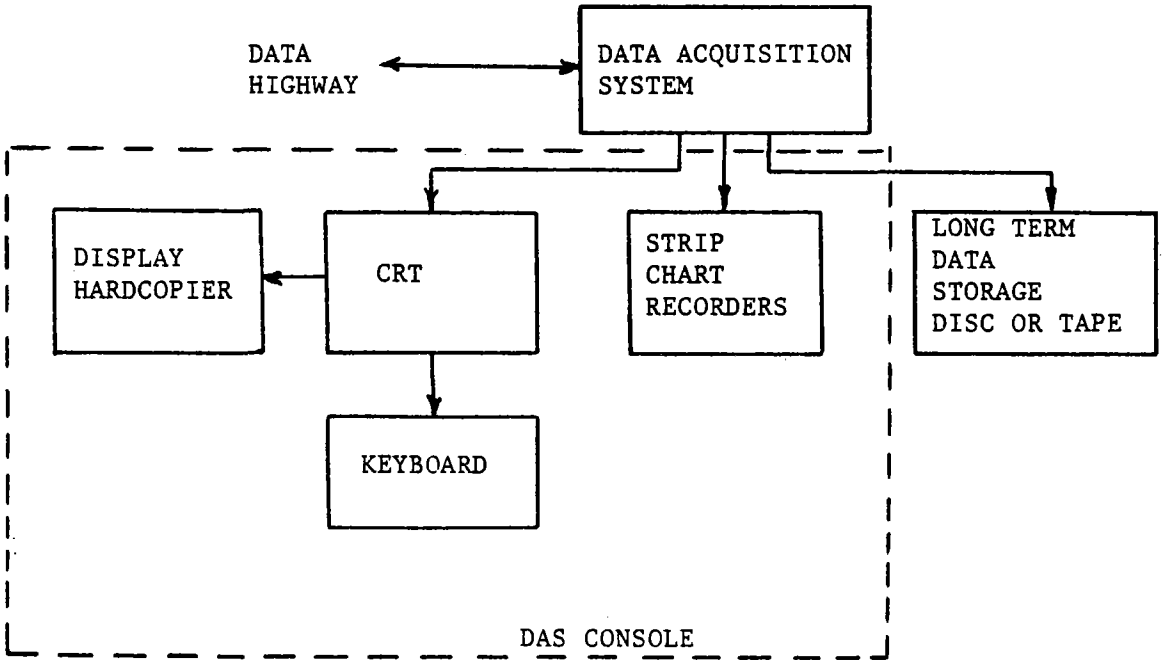

Figure 5.4-20 Data Acquisition Subsystem (DAS) Configuration

5.4.13 Emergency Control Functions

The emergency control functions which protect the plant from damage during equipment or other failures are built into each respective control subsystem through red line units (RLUs).

The status of all RLUs is reported via the Operational Control Subsystem. Any RLU which has entered a trip mode is annuciated at the OCS console and the OCS automatically records a failure event sequence record for future analysis and system repair if necessary.

The OCS monitors the status of all RLUs and coordinates the trip cascade in the event of a failure. For example, if the receiver subsystem should lose salt mass flow through the receiver (due to pump failure, line failure, etc.) an RLU which is monitoring receiver salt mass flow rate would enter the trip mode. This would immediately result in the closing of the receiver doors and a trip message sent to the OCS. The OCS would then instigate a trip in the collector subsystem RLU which would defocus the heliostats from the receiver.

Similar emergency functions are built into each control subsystem. Together, they interact to form the emergency protection system for the entire plant. The emergency functions, although independent of the control functions, are integral parts of each subsystem control system.

5.4.13.1 Control System Emergency Condition Considerations

Each of the six subsystem control systems will have built-in emergency condition responses. The OCS will have built-in emergency condition coordination schemes for failures in any of the six subsystem control systems. The control subsystems and their responsibilities for emergency conditions are shown in Table 5.4-4 More detail concerning emergency condition response is included in the following sections.

Table 5.4-4 Control Subsystems and Emergency Condition Responsibilities

Control Subsystem	Emergency Responsibilities
Operational Control	Coordination of all emergency upsets.
Collector Control	Respond to receiver failures, defocus heliostats
Receiver Control	Protect receiver, initiate maximum flow, close doors
Energy Storage Control	Storage tank foundation over heating. Salt reprocessing/melting system failures.
Process Steam Control	Heat exchanger failures
Turbine Steam Control	Heat exchanger failures
Electric Power Generation Control	Turbine/generator/cooling failures

5.4.13.2 Operational Control Subsystem (OCS)

The responsibilities of the OCS during emergency conditions are to:

1. Direct the proper action by each subsystem to protect plant security.
2. Provide a detailed failure event sequence record for later analysis to determine cause of failure.
3. Notify responsible parties of plant failure and current status.

The actions required to coordinate the proper interactions between each subsystem are controlled by built in control algorithm rules. For example, consider a receiver pump failure. The receiver control subsystem (RCS) would sense a pump failure and simultaneously enact its built in receiver protection logic and notify the OCS of the failure. The OCS, using its emergency condition logic would immediately request a defocus of heliostats from the collector control subsystem (CCS). The CCS would then execute the heliostat scram. In the meantime, the RCS has started to close the receiver cavity doors and has opened the flow control valves for maximum coolant through the receiver (the flow is maintained by the pressurized cold salt surge tank). The receiver and collector subsystems would move to a standby status and a failure event sequence record would be printed by the OCS to facilitate repair. The remainder of the plant would continue to operate until the thermal energy in storage was exhausted.

The OCS would have similar failure coordination schemes for all conceivable failure modes and an overall failsafe scheme which would address any problem which occurred which did not fall into a previously defined category.

5.4.13.3 Collector Control Subsystem (CCS)

The CCS responds to two different classes of failures.

1. Collector field failures - individual or group heliostat failure.
2. Emergency field scram due to receiver failure alarm.

The CCS will have built-in responses to individual or group heliostat failures. These procedures will provide for the safe defocusing of the heliostat and the placement in the stow position.

The CCS response to a receiver failure alarm will be immediate defocusing of the heliostat beam from the receiver to the standby position.

5.4.13.4 Receiver Control Subsystem (RCS)

The responsibility of the RCS is the safety of the receiver. In the event of an emergency condition, the RCS will:

1. Increase the salt flow rate through the receiver to maximum.
2. Send receiver failure alarm to OCS (OCS to command heliostat defocus, backup capability directly to CCS if OCS fails).
3. Close receiver doors.

5.4.13.5 Energy Storage Control Subsystem (ESCS)

The ESCS is responsible for the detection and alarm of failures in the thermal storage tank foundation cooling system and the salt melting/reprocessing systems. The ESCS will also be responsible for the sensing of storage tank leaks and the liquid salt level in the tank.

5.4.13.6 Process and Turbine Steam Control Subsystems (PSCS and TSCS)

The responsibility of the PSCS and TSCS is the protection of the safety of the PSS and TSS systems. The TSCS is also responsible for responding to emergency situations resulting from occurances within the region of the electric power generation subsystem (EPGS). In these situations the TSGS would be commanded by the OCS in response to failure alarms produced inside the EPGS domain.

5.4.13.7 Electric Power Generation Control Subsystem (EPGCS)

The EPGCS is responsible for the safety of the turbine, electric generator and turbine water cooling systems. For example, in the case of an electrical generator trip due to outlet phase or over/under voltage, the EPGCS will automatically place the turbine in a standby position and send a failure alarm to the OCS. The OCS will command a decrease in steam output from the TSCS.

5.4.14 Master Control Subsystem Cost Estimate

The estimated direct cost of the master control subsystem (Account 5500) is $2.0 million.

5.5 FOSSIL ENERGY SUBSYSTEM

The existing fossil energy subsystem at the Edison field consists of two portable oil fired 7.33 MW capacity steamers used for enhanced oil recovery operations. The existing steamers and EOR process is described in section 2.6 and 2.7. As part of the solar cogeneration facility, it is planned to permanently mount the two existing steamers near the solar receiver tower base (Figure 5.1-1) and join the steam output lines of the fossil steamers with the steam header from the solar steam. The fossil steamers would share a common feedwater treatment facility with the solar boiler. A low pressure turbine extraction line would provide feedwater preheating to both fossil and solar boilers during turbine operation. The interfaces between the fossil and solar boilers can be seen in Figure 5.4-18.

The fossil subsystem also includes about 800 meters of steam distribution piping to transfer process steam from the cogeneration facility to the injection wells. The direct cost of mounting the steamers and running steam distribution piping (account 5900) is about $200,000 or less than 0.2% of the estimated facility cost.

5.6 ENERGY STORAGE SUBSYSTEM

The energy storage subsystem is the interface between the receiver subsystem and the steam generation subsystems. The storage capacity is sufficient to decouple energy supply and demand. This surge capacity permits the receiver and steam subsystems to operate independently of each other. This mode of operation is necessary during night-time operations and prevents transient variations in insolation from affecting production capability.

5.6.1 Functional Requirements

The primary requirement of the energy storage subsystem is to store and distribute 380 MWh_t of thermal energy. The energy storage medium is molten salt, a mixture comprised of 40% potassium nitrate/60% sodium nitrate by weight. In addition to the storage requirement, the subsystems perform the following: deliver molten cold salt to and receive molten hot salt from the receiver subsystem; deliver molten hot salt to and receive molten cold salt from the steam subsystems; store molten salt at varying temperatures whenever it proves necessary to drain the interfacing salt subsystems; make up the molten salt inventory from solid salt storage; maintain the salt in the molten state during a prolonged shutdown.

The piping and equipment in this subsystem is designed to minimize thermal losses and to minimize excess heliostat costs. It is to be located in an individual area on the site for which the environmental design parameters are:

- o Wind Velocity: 40 m/s (90 mph.)
- o Seismic Zone 4
- o Snow Load: 3.81 Kg/m^2 (0.78 lb/ft^2)
- o Max Foundation Loading: 220 KPa (4,500 lb/ft^2)

The energy storage subsystem includes all equipment piping, equipment, instrumentation controls, electrical, civil and any other work necessary to meet these requirements. It will be designed to meet all statuatory codes and regulations currently in force and to provide safe and reasonable access for all operating and maintenance requirements.

5.6.2 Design Description

The operational and economic optimum configuration for a salt storage system of this size (380 MWh_t) is a dual hot and cold tank pair. Hot salt at 566°C (1,050°F) is stored in one tank and a second tank is used to store the cold salt at 288°C (550°F) after the thermal energy has been extracted. A third tank, the salt drain tank is provided for storage of any off-temperature specification salt prior to its consumption in the system. The salt drain tank also acts as a spare hot and cold salt tank should this be required. Distribution of the molten salt to the interfacing subsystems is provided by hot and cold salt pumps.

This subsystem includes the molten salt storage and pumping equipment and the ancilliary salt melting equipment and salt relief separation equipment.

5.6.2.1 Flow Description

The schematic flow diagram for this subsystem is shown in Figure 5.6-1. Equipment included in this subsystem is the cold salt tank MF-201 from which the cold salt pumps PP-201 A/B/C take molten salt at 288°C (550°F) for discharge through the receiver subsystem. After absorbing solar energy, the heated salt at 566°C (1,050°F) returns to the hot salt tank MF-202. Hot salt is then discharged through the heat exchangers by vertical hot salt pumps P-202 A/B which take suction from hot salt sump MS-205. After heat exchange in the subsystems, the salt returns to the cold salt tank MF-201 at 288°C (550°F). A salt drain tank MF-203 is provided to accummulate off-temperature salt or to act as a drain tank in event of an emergency plant shutdown. This salt may be returned to the process by salt drain sump pump PP-203 which takes suction from the salt drain sump MS-204. The salt drain tank acts as a spare cold or hot salt tank. The salt tanks and sumps are provided with water cooling coils in their foundations for intermittent heat removal from the foundation substructures.

The salt melter G-201 and relief effluent separator MS-206 equipment is included in this subsystem. The salt melter is used to melt solid salt for addition to the molten salt inventory and acts as a molten salt heat source in the event of prolonged shutdown. The relief effluent separator MS-206 permits recovery of molten salt in the event of a salt heat exchanger tube rupture. Salt separated from the steam will be pumped to storage by sump pump PP-205 located in the effluent separator sump while the steam is vented.

5.6.2.2 Control Description

The instrumentation and controls for this subsystem are shown in Figure 5.6-1 and Figure 5.6-2. Controlling functions of this subsystem involve the following parameters: salt levels in the hot salt and salt drain sumps, and salt drain injection temperature control. There are auxiliary control functions associated with this subsystem:

- Salt storage tank and sump foundation temperature;
- Salt melter controllers which will be provided as part of a package unit.

Energy storage subsystem controls do not involve primary control of the salt flow through either the receiver or the steam generation subsystems. Rather, the flows are monitored and applied to the salt pump flow logic controllers to ensure sufficient pumping capacity.

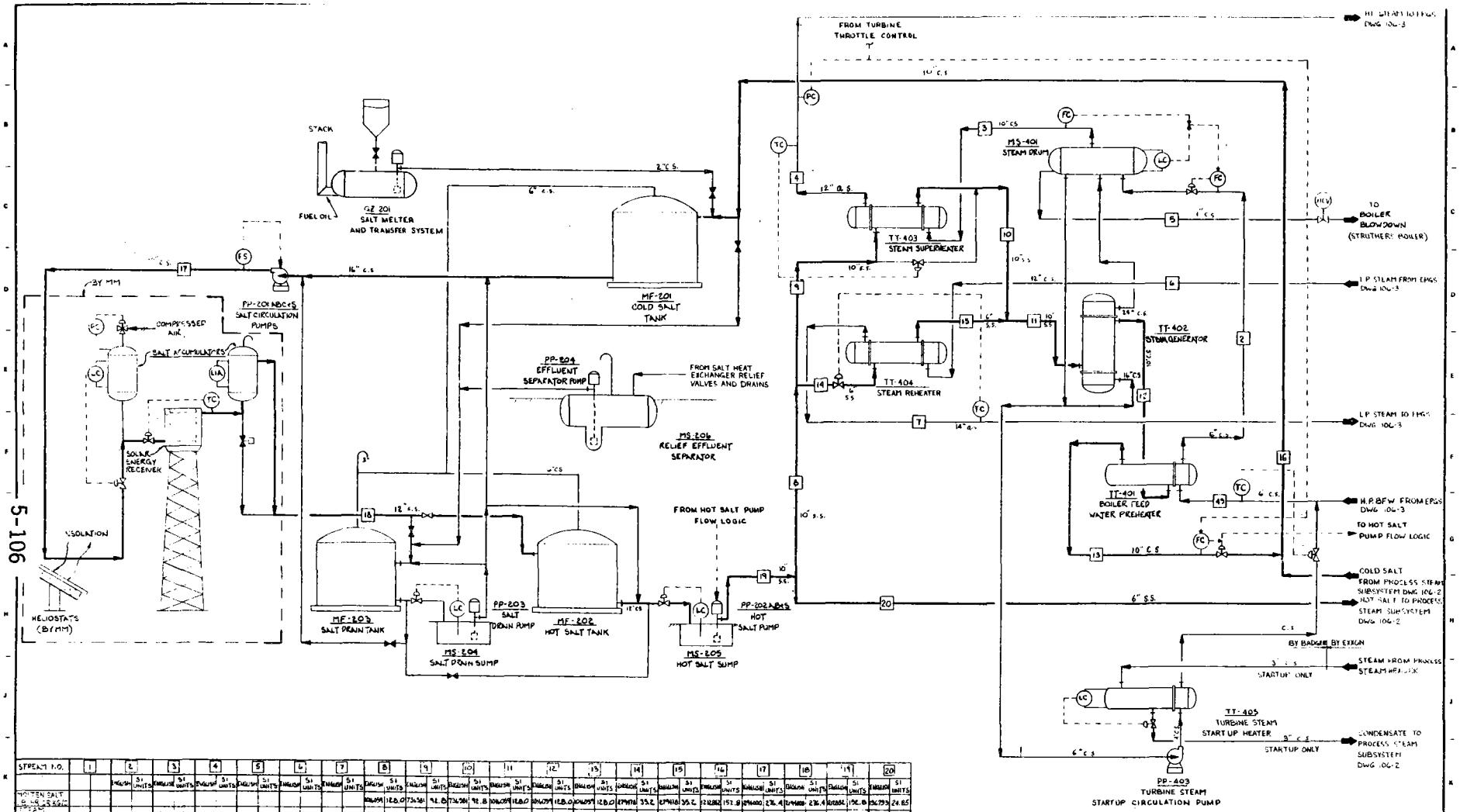

STREAM NO.	1	2		3		4		5		6		7		8		9		10		11		12		13		14		15		16		17		18		19		20	
		ENGLISH	SI UNITS	ENGLISH	SI UNITS	ENGLISH	SI UNITS	ENGLISH	SI UNITS	ENGLISH	SI UNITS	ENGLISH	SI UNITS	ENGLISH	SI UNITS	ENGLISH	SI UNITS	ENGLISH	SI UNITS	ENGLISH	SI UNITS	ENGLISH	SI UNITS	ENGLISH	SI UNITS	ENGLISH	SI UNITS	ENGLISH	SI UNITS	ENGLISH	SI UNITS	ENGLISH	SI UNITS	ENGLISH	SI UNITS	ENGLISH	SI UNITS	ENGLISH	SI UNITS
MOLTEN SALT FLOW				45758	20.9	45758	20.9			45586	18.4	45586	18.4	106059	12.8.0	734581	92.8	734581	92.8	106059	12.8.0	106059	12.8.0	106059	12.8.0	279478	35.2	279478	35.2	221882	157.8	279480	27.6.4	279480	27.6.4	221882	157.8	736793	24.85
WATER FLOW		46588	21.0					850	0.10																														
TOTAL FLOW GPM OR M3/HR		46588	21.0	45758	20.9	45758	20.9	850	0.10	45586	18.4	45586	18.4	106059	12.8.0	734581	92.8	734581	92.8	106059	12.8.0	106059	12.8.0	106059	12.8.0	279478	35.2	279478	35.2	221882	157.8	279480	27.6.4	279480	27.6.4	221882	157.8	736793	24.85
TEMPERATURE °F OR °C		550	560.8	571	572.4	1000	810.8	571	572.4	750	671.9	1000	810.8	1050	838.4	1050	838.4	654.5	729.9	654.5	729.9	584.0	580.8	550	560.8	1050	838.4	1050	838.4	550	560.8	550	560.8	1050	838.4	1050	838.4	1050	838.4
PRESSURE PSIA OR KPa		1295	8919	1258	8936	1200	8204	1238	8536	900	6758	380	2620	102	703.3	101	696.4	98	675.7	92	634.3	88	606.7	82	565.4	97	668.8	94	648.1	69	441.3	1000	6895	95	303	108	744.6	99	682.6
FLOW GPM OR M3/HR		466.6	29.99					2.35	0.15					106.5	24.54	106.5	24.0	106.3	52.3	1148.1	72.4	1086.7	48.54	1092.2	67.84	32.5	20.5	95.8	19.93	1283.4	81.0	132.7	14.5	1359.2	141.0	1460.3	89.0	2788.8	14.39
SPECIFIC GRAVITY		1.714	1.0.714					0.714	0.714					1.72	1.72	1.72	1.72	1.77	1.77	1.77	1.77	1.87	1.87	1.89	1.89	1.72	1.72	1.77	1.77	1.89	1.89	1.89	1.89	1.72	1.72	1.72	1.72	1.72	1.72
ENTHALPY BTU/LB OR KJ/KG		594.5	1238.1	1183.1	2751.9	1494.1	3482.6	577.1	1342.3	1387.4	3223.1	523.6	1214.9	188.6	438.7	188.4	438.7	117.9	273.1	117.9	273.1	143	33.3	0	0	188.6	438.7	117.4	273.1	0	0	0	0	188.6	438.7	188.6	438.7	188.6	438.7

LEGEND:
□ = STREAM NUMBER
C.S. = CARBON STEEL
S.S. = STAINLESS STEEL
A.S. = ALLOY STEEL

NOTE:
MOLTEN SALT ENTHALPY IS TAKEN AS 0 AT 550°F (560.8K)

FIGURE 5.6-1
PROCESS FLOW DIAGRAM
HEAT AND MATERIAL BALANCE
ENERGY STORAGE & SALT/TURBINE STEAM SUBSYSTEMS
SOLAR COGENERATION FACILITY
SANDIA NATIONAL LABORATORIES
LIVERMORE CA.

BADGER ENERGY, INC.
CAMBRIDGE, MASS.

DWG NO E8031-106-1

5-106

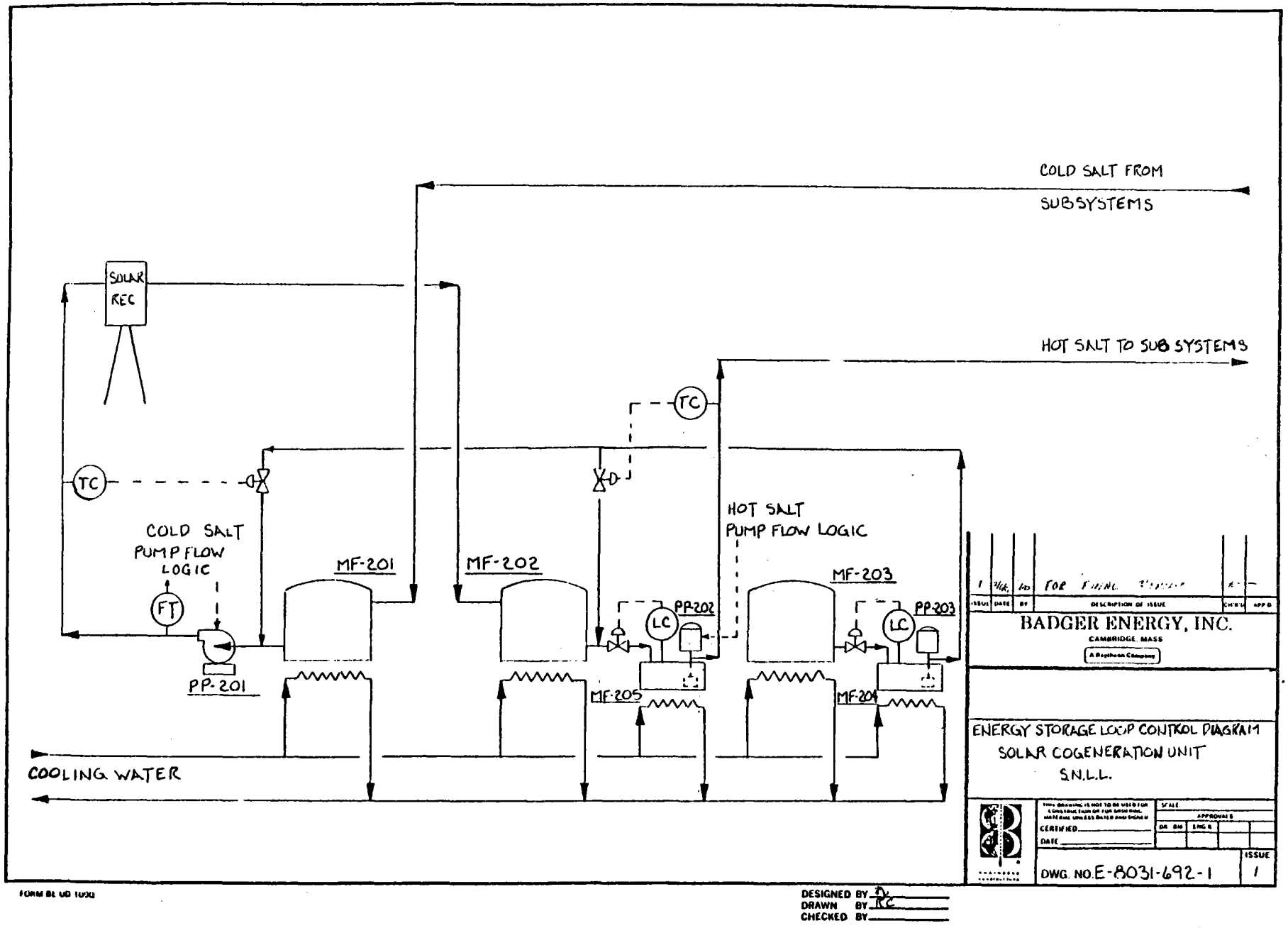
COLD SALT FROM
SUBSYSTEMS
SOLAR REC
HOT SALT TO SUB SYSTEMS
TC
TC
COLD SALT
PUMP FLOW
LOGIC
FT
MF-201
MF-202
MF-203
HOT SALT
PUMP FLOW LOGIC
PP-202
PP-203
LC
LC
PP-201
MF-205
MF-204
COOLING WATER
BADGER ENERGY, INC.
CAMBRIDGE, MASS
ENERGY STORAGE LOOP CONTROL DIAGRAM
SOLAR COGENERATION UNIT
S.N.L.L.
DWG. NO. E-8031-692-1
ISSUE 1
DESIGNED BY
DRAWN BY
CHECKED BY

Figure 5.6-2

Salt Flow

Cold salt flow rate is measured at the discharge of the cold salt pumps. The output from the flow transmitter is applied to the pump control logic. This has predetermined set points to ensure start-up and shut-down of the three working pumps as flow demands require. This demand is dictated by the solar insolation and receiver characteristics. The process design is based upon a constant molten salt temperature of 566°C (1,050°F) from the receiver. This temperature is maintained by controls within the receiver subsystem. Due to the wide variation in solar insolation, a wide variation of salt flow rates are required. This is provided by means of the three cold salt pumps. The output from each of the hot salt flow transmitters located on the respective turbine steam and process steam subsystems is fed to a summator, the output of which is applied to the hot salt pump control logic. Two hot salt pumps are provided to accommodate the flow variations in the steam generation subsystems, the second of which is automatically started or stopped as flow demands require.

Salt Sump Levels

Level controllers in the hot salt and salt drain sumps vary salt flow from the respective salt tank. Salt tank levels themselves are not controlled, but monitored.

Foundation Temperatures

Cooling water coils for the salt tank and sump foundations will be provided. The foundation temperatures will be controlled by the MCS.

Drain Salt Injection Temperature

Off specification temperature salt accummulated in the salt drain tank is pumped into the hot salt sump or the cold salt pump suction line. To prevent a significant salt temperature variation of the stream into which injection occurs, the drain salt injection rate is controlled by monitoring the salt temperature as discharged from the hot or cold salt pumps.

5.6.2.3 Design Features

Salt Storage Tanks

The most economical design for this size of salt storage system is the vertical hot and cold tank pair. In addition to providing these two tanks, it is considered essential to provide a third salt storage tank which will serve three purposes:

1) To hold the salt inventory in heat exchangers, lines, receiver and other equipment in the event of plant shutdown.

2) To hold salt which is returned to storage at a temperature other than 288°C (550°F) or 566°C (1,050°F).

3) To serve as a spare storage tank in event either one of the other tanks requires maintenance.

Without provision of a third tank for this service, the event of a leak in either the hot or cold tanks could be economically unacceptable. The plant downtime and possible salt loss could easily outweigh the additional costs involved in providing a drain tank that is sized as a spare hot tank.

The hot and cold salt tanks are sized based on the required storage capacity of 380 MWh_t, the working temperature difference of 278°C (500°F), salt density at respective temperatures, heat capacity of 1,578 J/Kg °C (377 Btu/lb °F) and allowable soil bearing load of 220 kPa (4500 lb/ft^2) max. This last constraint together with most economical fabrication requirements entails the height of both tanks being 11 m (36 ft.). Each tank is designed to contain 3.27 x 10^6/Kg (7.21 x 10^6 lb) of molten salt which assumes a 5% heel in each. A 5% excess capacity is also provided as an overfilling precaution. Using this criteria and allowing 250 CM (10") of internal insulation, the hot salt tank diameter is 16.0 m (52.3 ft) whereas the cold salt tank diameter is 14.6 m (47.9 ft). The salt drain tank design duplicates the hot salt tank.

In this design, tank shells are designed for 320°C (600°F) and provided with a special floor-to-wall knuckle joint to accommodate thermal stresses and differential expansion between tank floor and walls. Carbon steel retains most of its strength characteristics at 320°C (600°F) and is also resistant to corrosion from molten salt at this temperature. The cold tank is constructed of carbon steel and is provided with external insulation to minimize heat losses.

The hot salt tank is constructed of carbon steel which is protected from the hot salt by an internal refractory brick lining. Since most refractories are susceptible to attack from molten salt at this temperature, a special expandable 304 stainless steel liner is used between the salt and the refractory surface. This liner is designed in a waffled membrane configuration similar to linings used in L.N.G. storage tanks. 304 stainless steel has proven resistant to corrosion from molten salt at 566°C (1,050°F) and the waffled configuration with an underlying refractory felt buffer accommodates the variable stresses during filling and emptying operations. The membrane protects the refractory from attack while the refractory maintains the carbon steel shell at a reasonable temperature. The shell of the hot salt tank is provided with external insulation and both internal and external insulation are designed to maintain this temperature at 320°C (600°F). The salt drain tank and both salt sumps are designed to the same criteria as the hot salt tank.

These tanks are supported on cooled foundations to avoid overheating the substructure. Little is known about the behavior of soil and rock at high tempera-

tures, therefore, a foundation design which takes into account heat flux from the tank bottom and the variation in substrate strength with temperature, requires considerable research. For the purposes of conceptual design, it has been assumed that a cooled foundation is required and the type proposed is considered inexpensive yet safe (see Figure 5.6-3). It consists of two layers of concrete supported on sand backfill which is contained in a concrete ring-type wall. The tank itself sits on the upper concrete layer consisting of vermiculite refractory. This affords thermal protection to the lower layer of ordinary concrete in which are embedded carbon steel cooling coils. This design will result in only small heat losses from the tank bottom. This heat is prevented from overheating the substructure by intermittent use of cooling water circulation through the coils.

For personnel and equipment safety and to prevent loss of salt, each salt storage tank is surrounded by a 1.2 m (3.9 ft) high dike. The volume within each dike sufficient to contain the entire contents of each tank. The salt drain tank dike is sized for hot salt conditions. Both the hot salt and salt drain sumps are included within the storage tank dikes. This concept of design could involve additional costs, however, these are considered a relatively insignificant in comparison to the potential disaster which could occur if the sumps were located outside the dikes and the level control valves on the storage tank discharge lines failed in the open position.

The vents on all three salt tanks are joined in a common line with one common vent. This will minimize the interchange between the ullage gas within the tanks and atmosphere. Consequently, the potentially deleterious effects of atmospheric water and carbon dioxide on the molten salt composition are minimized.

Although they resemble API tanks, none of these tanks fall under either the API or the ASME Pressure Vessel Code. Quality standards from either of these codes may be adopted for convenience, but because of the unusual density and temperature of contained material, the special design described is required.

Salt Pumps

The aggressive characteristics of molten salt on moving surfaces precludes the use of most standard pump seals. Molten salt pumps have typically been specified as vertical pumps. Because of the rapid attack of molten salt on bearing surfaces these pumps have been specified as cantilever shaft design. The mechanical limitations imposed by this configuration limit the maximum head that can be developed to the region of 76 m (250 ft). Consequently, this type of pump has been specified for the hot salt pumps PP-202, salt drain pump PP-203, and effluent separator pump PP-204, all of which have head requirements less than 76 m.

The head requirements for the cold salt pump is 360 m (1,180 ft) which precludes a vertical type pump. Four possible alternatives were considered for this service:

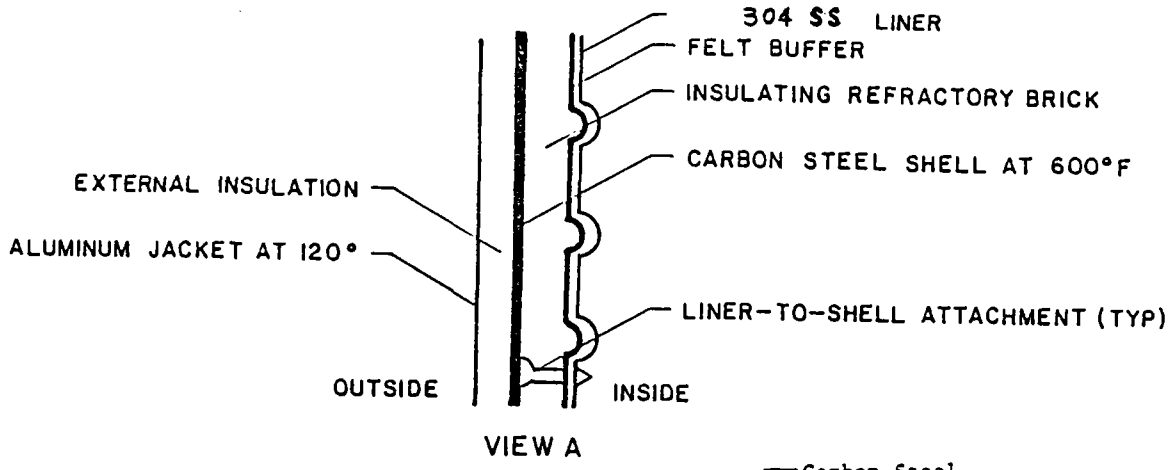

VIEW A

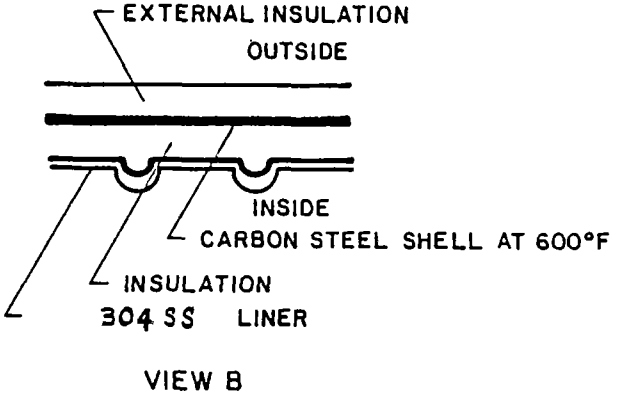

VIEW B

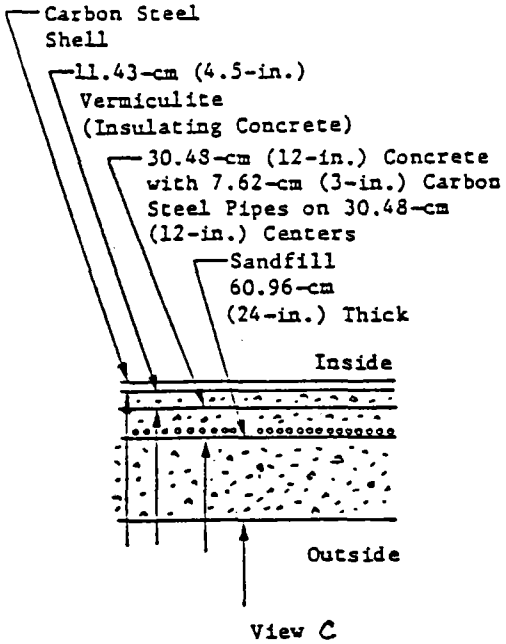

View C

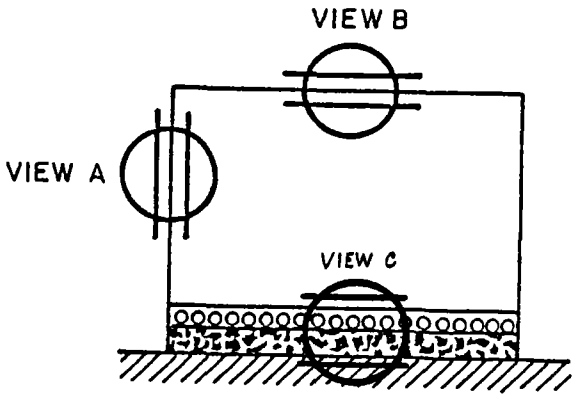

HOT TANK FOR THERMAL ENERGY STORAGE SYSTEM
Figure 5.6-3

1. A staged pumping system using vertical cantilever pumps. This alternative was discounted in view of expense and undersirable mechanical and operational problems.

2. Vertical cantilever pumps could be arranged in series in a single sump. This alternative was discounted because of undesirable operational and control problems.

3. A vertical pump with submerged bearings could be used. This alternative was considered least favorable because of the very high downtime expected due to bearing failure.

4. A horizontal pump with an effective seal could be used. A seal has been developed which the manufacturer believes will work in this service. Consequently this type of pump has been specified for the cold salt pumps pending testing of the seal in molten salt service.

Salt Melter

The salt melter is provided to melt solid salt, provide molten salt inventory makeup, and to provide auxilliary source of heat during long-term shutdowns to maintain the salt in the molten state. The melter is commercially available as a package unit which includes its own storage, combustion and pumping equipment. Heavy crude oil has been specified as the melter fuel source in order to minimize capital investment. The fuel oil storage and pumping facilities to be provided for the boilers will also be utilized for the salt melter.

Effluent Relief Separator

In the event of tube failure in any of the molten salt heat exchangers, the shell side pressure must be relieved. This relief protection is provided by bursting discs which will vent the salt/steam mixture to the relief effluent separator. This vessel is designed to separate the salt from the steam, thereby permitting recovery of the salt and venting of the steam to a safe location. The separated salt flows by gravity to the vessel sump from which it is pumped to storage by an insitu separator sump pump. The vessel is designed to contain the salt inventory of the turbine steam heat exchangers, the major subsystem salt inventory.

Salt Piping

The salt distribution piping has been designed to minimize capital investment while providing maximum energy efficiency and safety. 304 stainless steel has been selected as piping material in hot salt service since the most recent corrosion test data indicates satisfactory results. A-106 GrB carbon steel was chosen for the cold salt piping service and a corrosion allowance of 1.5 mm specified. Expansion loops will be provided in long piping runs wherever detailed stress analysis indicates their necessity.

All piping will be be fully welded and insulated to minimize cost, leakage and thermal losses. This will maximize the energy efficiency of the subsystem during operation, and permit short term shutdowns of the salt circulation without risk of salt freezing. All salt piping is provided with special high temperature electric heat tracers to preheat the lines prior to the introduction of molten salt. The tracers will achieve a pipe temperature of 300°C (570°F) to ensure no risk of salt solidification.

5.6.3 Operating Modes

The operating modes of this subsystem are dictated by the operating modes of its interfacing subsystems. The normal charge and discharge rates of the energy storage system depend entirely upon the capabilities of the receiver and steam subsystems respectively. The maximum charge rate is the maximum thermal rating of the receiver, 122 MW_t (35.5 MBtu/hr); the maximum discharge rate is the rate at which salt is pumped and cooled through the molten salt/turbine steam and molten salt/process steam exchangers when both these subsystems are operating, 67 MW_t (19.6 MBtu/hr).

The energy storage capacity selected (380 MWh_t) requires in excess of 3 million Kg of salt as the storage medium. Consequently, the initial start-up of this facility deserves special consideration.

5.6.3.1 Initial Start-Up

The initial start-up of this system has been envisaged as using temporary equipment for this once-only situation. It is anticipated that an outside contractor will supply all the ancilliary equipment necessary to obtain the molten salt inventory in the storage tanks. In order to prevent solidification of the molten salt on first entering these tanks, it is necessary to preheat this equipment. The procedure proposed for this is described below.

Hot water from the temporary melter will be pumped into the hot and cold salt and salt drain tanks MF-201/2/3 to establish a heel of liquid in each. Once the level in each tank is sufficient to provide suction to the pumps, a water circulation loop from the melter to and from each tank will be established. Solid salt will then be added to the melter and the firing rate increased. While salt is being added to the melter, water will be evaporated increasing the salt concentration and temperature of the circulating fluid. The temperatures of the storage tanks themselves will increase thereby achieving the desired preheat. Once all the water has been evaporated, the firing of the melter will be adjusted to maintain a molten salt temperature of 288°C (550°F).

The circulation around the hot salt tank and salt drain tank will then be stopped. The heel of molten salt in these tanks will be maintained at temperature by the permanent salt melter and transfer system G-201. The molten salt working inventory will then be established in cold salt tank MF-201. This

initial charging exercise is anticipated to last 30 days after which the normal cold start-up procedure will continue. The main requirement of this procedure is to ensure that all salt piping and equipment is preheated to at least 300°C (570°F) by means of the high temperature electrical heat tracing. After this temperature is achieved, salt flow may commence to the interfacing subsystems.

5.6.3.2 Hot Shutdown/Start-Up

In this operating mode, salt flows cease around the system, and the salt is left in the piping ready for an imminent restart. The design of insulation and tracing provided on the salt piping maintains the salt in a molten state during these short-term situations.

In view of the nightly shutdown of the receiver and turbine steam subsystems this type of shutdown/start-up will be the one most frequently encountered. Salt temperatures around the subsystem loop will continue to be monitored during these periods. If salt temperatures notably decrease at any point, a low salt flow can be established as required. In normal restart, salt flows are established as required by the interfacing subsystems.

5.6.3.3 Cold Shutdown

This operational mode differs from others in that all salt must be removed from the subsystem. The subsystem operation is dependent on the interfacing subsystems, so it is essential to coordinate requirements. The salt drain tank MF-203 is provided for holding salt drained from piping and equipment. Preferably, this would only be used for salt streams of temperatures other than 288°C (550°F) or 566°C (1,050°F) in order to minimize the quantity of rework salt. Thus, the receiver tower supply piping and the salt return header from the molten salt steam generation subsystems would be drained to the cold salt tank MF-201. That which cannot gravity flow to the tank would be drained to the salt drain sump for storage in the salt drain tank MF-203. Similarly, salt at a temperature of 566°C (1,050°F) would be drained to the hot salt tank MF-202. All other salt from the receiver and molten salt heat exchangers would be stored in the salt drain tank MF-203 for subsequent rework.

If is essential that all salt be removed from the system before temperatures reduce to 300°C (570°F). Consequently electric tracing should remain on until total salt drainage has occured. Depending on the duration of the shutdown, it may be necessary to add heat to the salt storage system by use of the salt melter G-201.

5.6.4 Energy Storage Subsystem Cost Estimate

The estimated direct cost for the energy storage subsystem (Account 5700) is $11.0 million.

5.7 ELECTRIC POWER GENERATING SUBSYSTEM (EPGS)

The EPGS converts thermal energy in the form of high pressure, superheated steam into electric power suitable for distribution to a utility grid. The major components are a turbine generator with accessories, heat rejection equipment, condenser, feedwater heaters and pumps, utility interface equipment, and a backup diesel generator. The majority of the equipment is located in or adjacent to the EPGS building at the tower base, close to the thermal storage and heat exchanger equipment. Table 5.7-1 summarizes the EPGS characteristics.

The turbine generator is required to produce electricity from the steam in a safe and efficient manner while supplying extraction steam at six pressures for feedwater heating and process preheating. A schematic of the turbine and feedwater heaters is shown in Figure 5.7-1. The turbine is a single reheat, multiple extraction, condensing type. Steam enters the high pressure (HP) turbine at 538°C and 8.27 MPa (1,000°F and 1,200 psia) and is exhausted at 2.76 MPa (400 psia). There is one feedwater heater extraction from the HP turbine and some of the exhaust goes to another feedwater heater. The balance of the exhaust is reheated in a molten salt heat exchanger and returned to the low pressure (LP) turbine at 538°C and 2.62 MPa (1,000°F and 380 psia). There are four extractions from the LP turbine, one of which provides the deaerator and the process preheater with 290 kPa (44 psia) steam. The LP turbine exhausts to the condenser at 6.75 kPa (2 in Hg).

The turbine generator always operates at the design conditions but over a variable number of hours each day. On days of maximum energy collection, it operates up to the full 14 hour peak period. On some days there is not enough thermal energy collected to operate the turbine at all. The turbine is provided with blanketing and seal steam when it is not producing power. This allows quick start-up and reduces thermal cycling of the unit. During the low insolation months of December and January, the turbine is shutdown completely. Scheduled maintenance of the turbine, heat exchangers and accessory equipment can be performed at this time.

The synchronous generator is direct driven by the turbine at 3,600 RPM and produces 20.4 MW_e of electric power at 12 kV. Considering the total heat input of 56.05 MW_t, the unit has a gross heat rate of 2.75 KW_t/KW_e (9,380 Btu/KWh). If the 4.87 MW_t process preheat extraction energy is credited against the boiler heat input, and the 0.8 MW_e direct EPGS parasistic electric load is subtracted from the generator output, the heat rate is 2.61 KW_t/KW_e (8,910 Btu/KWh) which is equivalent to a Rankine cycle efficiency of 38.3%.

The heat rejection equipment condenses the turbine exhaust steam and transfers the heat to the environment. The wet cooling tower is required to maintain a turbine exhaust pressure of 6.75 kPa (2 in Hg). Since wet cooling towers rely on the latent heat of vaporization to remove heat, large quantities of water are vaporized and carried away from the tower. This water is available from the existing agricultural activity that will be displaced by the installation of the heliostat field. In addition to evaporation losses, a small amount of the circulating water cascading over the fill becomes airborne in the form of drift

TABLE 5.7-1 EPGS Characteristics

Turbine Type	-	Single reheat, multiple extraction, condensing
Inlet Temperature	-	538°C (1,000°F)
Inlet Pressure	-	8.27 MPa (1,200 psia)
Steam Flow Rate	-	75,170 Kg/hr (165,760 lb/hr)
Reheat Temperature	-	538°C (1,000°F)
Reheat Pressure	-	2.62 MPa (380 psia)
Total Heat Input	-	56.05 MW_t (191.3 MBtu/hr)
Exhaust Temperature	-	38°C (101°F)
Exhaust Pressure	-	6.75 kPa (2 in Hg)
Condenser Heat Rejection	-	30.2 MW_t (103 MBtu/hr)

Extractions:

	Pressure kPa (psia)	Temperature °C (°F)	Mass Flow Rate Kg/hr (lb/hr)
1	4,540 (659)	463 (865)	4,415 (9,734)
2	2,760 (400)	399 (750)	4,625 (10,198)
3	1,590 (231)	475 (887)	3,532 (7,788)
4	750 (109)	373 (705)	3,400 (7,498)
5	303 (44)	285 (545)	11,292 (24,899)
6	60 (9.5)	146 (295)	2,419 (5,333)

Life	-	26 years
Speed	-	3,600 RPM
Generator Type	-	Revolving field, synchronous, 60 H_z
Coupling	-	Direct Drive
Generator Output	-	20.4 MW_e, 12 kV
Gross Heat Rate	-	2.75 KW_t/KW_e (9,380 Btu/kW-hr)

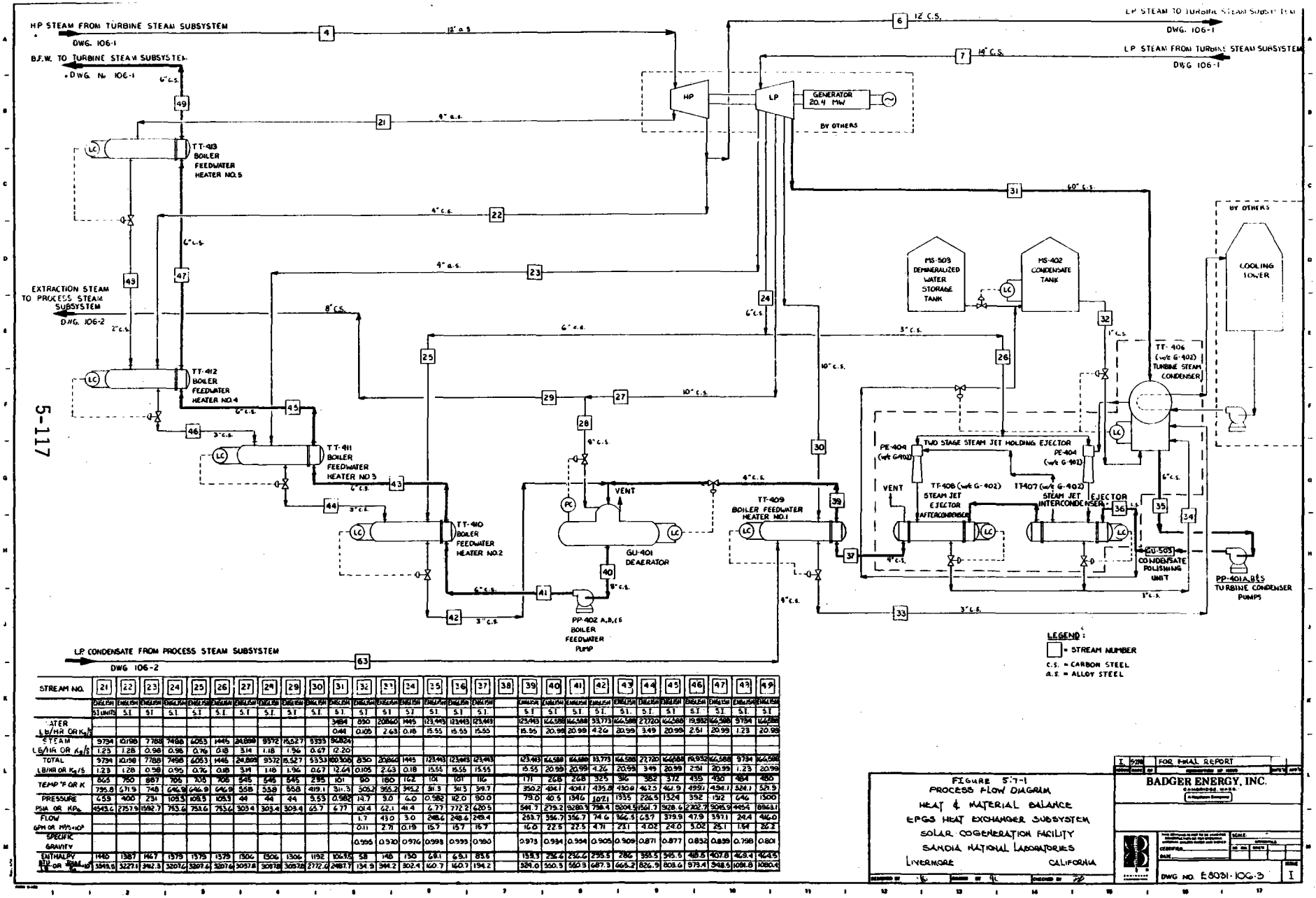

STREAM NO.	21	22	23	24	25	26	27	28	29	30	31	32	33	34	35	36	37	38	39	40	41	42	43	44	45	46	47	48	49
	ENGLISH	ENGLISH	ENGLISH	ENGLISH	ENGLISH	ENGLISH	ENGLISH	ENGLISH	ENGLISH	ENGLISH	ENGLISH	ENGLISH	ENGLISH	ENGLISH	ENGLISH	ENGLISH	ENGLISH		ENGLISH	ENGLISH	ENGLISH	ENGLISH	ENGLISH	ENGLISH	ENGLISH	ENGLISH	ENGLISH	ENGLISH	ENGLISH
	S.I. UNITS	S.I.	S.I.	S.I.	S.I.	S.I.	S.I.	S.I.	S.I.	S.I.	S.I.	S.I.	S.I.	S.I.	S.I.	S.I.	S.I.		S.I.	S.I.	S.I.	S.I.	S.I.	S.I.	S.I.	S.I.	S.I.	S.I.	S.I.
WATER LB/HR OR Kg/h											3484	850	20840	1445	123,445	123,445	123,445		123,445	164,588	164,588	53,773	164,588	27,720	164,588	19,932	164,588	9784	164,588
											0.44	0.105	2.63	0.18	15.55	15.55	15.55		15.55	20.99	20.99	4.26	20.99	3.49	20.99	2.51	20.99	1.23	20.99
STEAM LB/HR OR Kg/S	9734	10198	7788	7468	6053	1445	24,809	9572	15,627	8335	90,304																		
	1.23	1.28	0.98	0.95	0.76	0.18	3.14	1.18	1.96	0.67	12.20																		
TOTAL LB/HR OR Kg/S	9734	10198	7788	7468	6053	1445	24,809	9572	15,627	8335	90,308	850	20842	1445	123,445	123,445	123,445		123,445	164,588	164,588	53,773	164,588	27,720	164,588	19,932	164,588	9784	164,588
	1.23	1.28	0.98	0.95	0.76	0.18	3.14	1.18	1.96	0.67	12.64	0.105	2.63	0.18	15.55	15.55	15.55		15.55	20.99	20.99	4.26	20.99	3.49	20.99	2.51	20.99	1.23	20.99
TEMP °F OR K	865	760	887	705	705	705	545	545	545	295	101	90	180	162	101	101	101		116	226	228	325	314	382	372	456	460	464	460
	735.8	671.9	748	650.9	650.9	650.9	558	558	558	419.1	311.3	305.2	355.2	345.2	311.3	311.3	311.3		319.7	380.2	384.1	408.1	435.8	430.9	467.5	491.9	509.1	494.1	524.1
PRESSURE PSIA OR KPa	655	400	251	109.5	108.5	105.5	44	44	44	5.55	0.982	14.7	30	6.0	0.982	12.0	9.0.0		79.0	40.5	1346	1071	1335	226.5	1324	352	192	646	1300
	4543.6	2757.9	1592.7	755.6	753.6	753.6	303.4	303.4	303.4	65.7	6.77	101.4	62.1	41.4	6.77	772.2	620.5		546.7	279.2	9280.9	738.4	9204.5	1561.7	9128.6	2302.7	9052.9	4454	8863.1
FLOW GPM OR M³/HOP												1.7	49.0	3.0	248.6	248.6	248.4		253.7	356.7	356.7	74.6	366.5	65.7	379.9	47.9	387.1	24.4	446.0
												0.11	2.71	0.19	15.7	15.7	15.7		16.0	22.5	22.5	4.71	23.1	4.02	24.0	3.02	25.1	1.54	28.2
SPECIFIC GRAVITY											0.955	0.930	0.976	0.998	0.993	0.993	0.980		0.973	0.934	0.934	0.905	0.909	0.871	0.877	0.852	0.839	0.798	0.801
ENTHALPY BTU/LB OR KJ/KG	1440	1387	1467	1379	1379	1379	1304	1306	1306	1192	1016.8	58	148	130	68.1	68.1	85.6		158.1	256.4	252.6	295.5	286	388.5	345.5	488.8	407.8	468.4	464.6
	3345.6	3227.1	3412.3	3207.6	3207.6	3207.6	3057.8	3057.8	3057.8	2772.0	2487.7	134.9	344.2	302.4	160.7	160.7	194.2		384.0	560.5	560.5	687.3	665.2	826.9	803.6	979.4	948.6	1091.8	1080.4

FIGURE 5-7-1
PROCESS FLOW DIAGRAM
HEAT & MATERIAL BALANCE
EPGS HEAT EXCHANGER SUBSYSTEM
SOLAR COGENERATION FACILITY
SANDIA NATIONAL LABORATORIES
LIVERMORE CALIFORNIA

I	SUN	FOR FINAL REPORT

BADGER ENERGY, INC.
CAMBRIDGE, MASS.

DWG NO. E-8031-106-3 I

droplets. Approximately 50 percent of the drift fallout occurs within 150 m (500 ft) of the cooling tower. Since these droplets contain the concentrated dissolved solids of the circulating water, they could foul the heliostat mirror surfaces. To minimize the impact of drift fallout on the collector field, the cooling tower is specified with drift reduction baffling; the tower has been sited so the prevailing south-easterly winds blow the drift away from the field; and the tower is located 150 m (500 ft) from the field.

Boiler feedwater for turbine steam generation is produced in a conventional closed loop turbine condensate feedheater system with final exhaust steam condensed against cooling water in a surface condenser. The heaters, pumps and condenser are located below the turbine. The feedwater heaters are required to produce a final feedwater temperature of 250°C (480°F) to prevent possible freezing of the molten salt in the turbine steam heat exchangers. To prevent any contamination of the high purity turbine steam, the condensate is pumped through a polishing unit prior to the first feedwater heater. Makeup water is treated in a demineralizer and added in the deaerator. The feedwater is pumped to 9.3 MPa (1,350 psia) and then preheated to the required temperature in the next four feedwater heaters before passing to the turbine steam subsystem.

The utility interface equipment allows the power generated by the EPGS to be transferred onto the PG&E grid. PG&E, for the protection of life and property, requires that cogenerators meet mininum requirements for facility interface design and facility operation. Figure 5.7-2 is a schematic representation of the interface requirements for the Solar Cogeneration Facility.

Metering is required to measure instantaneous power output in MW, integrated power output in kW-hrs, and reactive power output in MVAR. PG&E requires that this metered output information be telemetered to its Energy Control Center in San Francisco.

The main transformer bank steps up the generator terminal voltage to PG&E's 70 kV transmission voltage. Main and generator circuit breakers, activated by various protective devices, are required to protect the PG&E system from faults occurring at the Solar Cogeneration Facility, and to protect the Solar Cogeneration Facility from faults occurring in the PG&E system. Specific PG&E minimum operating and protection requirements for the Solar Cogeneration Facility are described in Appendix C.

Preliminary transmission studies indicate power from the facility should be transmitted at 70 kV into the PG&E grid by building a 1/2 mile, 70 kV line from the turbine-generator site to connect to the existing 70 kV line supplying Lightner 70/12 kV Substation.

Lightner Substation was built in 1947 primarily to serve local aggricultural loads. The winter peak loads supplied by the substation are 1-2 MW_e. The summer peak loads supplied are 5-6 MW_e. The power from the Solar Cogeneration Facility in excess of the Lightner Substation load would be used to supply other loads served by the PG&E grid. On the 70 kV transmission system there is presently about 30 MW_e of summer peak load within 10 miles of the facility.

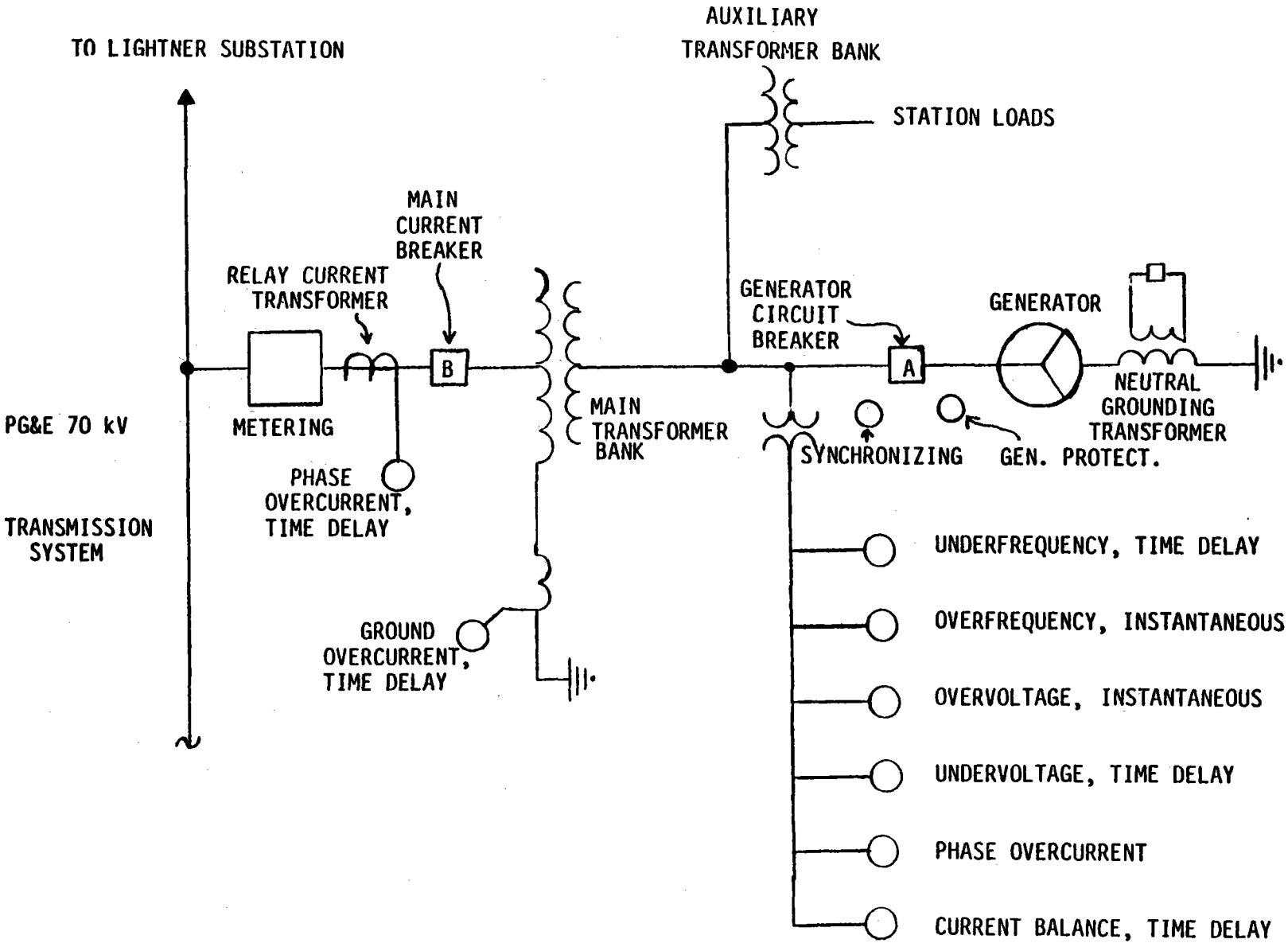

FIGURE 5.7-2 SINGLE LINE ELECTRICAL SCHEMATIC FOR UTILITY INTERFACE

The other transmission alternative proposes 115 kV transmission outlets for the Solar Cogeneration Facility. This alternative would require about 3 miles of 115 kV transmission to PG&E's nearest 115 kV line and would be more costly.

PG&E will review its transmission studies about 3 years prior to the operating date of the Solar Cogeneration Facility to determine if changes in system conditions indicate the 115 kV alternative is more favorable. Presently, no such changes are foreseen.

A 600 KW_e, quick start, diesel generator is included in the EPGS to provide emergency power. This backup power is required to stow the heliostat field and bring the plant to a safe shutdown condition in the event of a storm and loss of primary power.

The estimated direct cost of the electric power generation subsystem (Account 5800) is $9.0 million.

5.8 PROCESS STEAM SUBSYSTEM

The generation of 80% quality steam from the process steam subsystem is intended to supply about half the normal steam required for EOR purposes. Consequently, the steam conditions are compatible with those of the fossil fired steamers which supply the balance of total requirements. The equipment consists of conventional shell and tube heat exchangers with molten salt providing the major heat input requirements. The water for steam generation, from on-site wells is softened in separate water treatment facilities prior to use.

5.8.1 Functional Requirements

The primary requirement of this subsystem is to continuously generate 5.56 kg/s (44,000 lb/hr) of 80% quality steam at 293°C (560°F). It uses thermal energy in molten salt from the energy storage subsystem as the primary heat source for steam generation, and treated water from on-site wells as feed. To maximize the efficiency of the overall system it uses 290 kPa (42 psia) turbine extraction steam as a heat medium and provides preheat of feedwater for the steamers by use of this extraction steam. Since the turbine is not continuously operational the design provides the normal solar steam generation requirements during all turbine shutdown periods. The softened water for process steam requirements will be supplied from the water treatment equipment.

The equipment for this subsystem is to be contained in an individual area for which the structural environmental design requirements are:

Wind Velocity:	40 m/s (90 mph)
Seismic UBC:	Zone 4
Snow Load:	3.81 Kg/M^2 (0.78 lb ft^2)
Max Foundation Loading:	220 kPa (4,500 lb/ft^2)

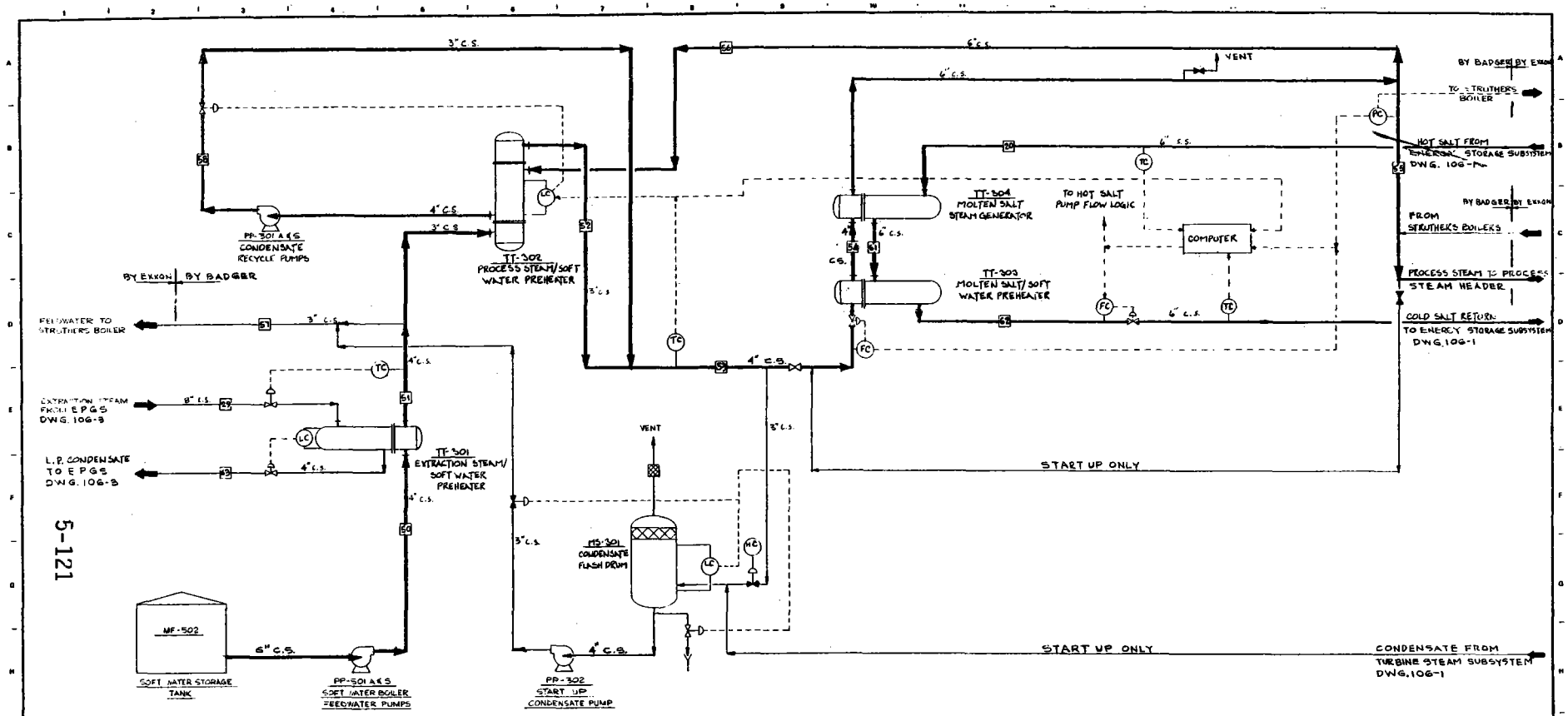

NOTE: MOLTEN SALT ENTHALPY IS TAKEN AS 0850°F (560.8K)

LEGEND

□ = STREAM NUMBER
C.S. = CARBON STEEL
S.S. = STAINLESS STEEL

STREAM NO	50		51		52		53		54		55		56		57		58		59		60		61		62		63	
	ENG. UNITS	S.I. UNITS	ENG. UNITS	S.I. UNITS	ENGLISH	S.I. UNITS	ENGLISH	S.I. UNITS	ENGLISH	S.I. UNITS	ENGLISH	S.I. UNITS	ENGLISH	S.I. UNITS	ENGLISH	S.I. UNITS	ENGLISH	S.I. UNITS					ENGLISH	S.I. UNITS	ENGLISH	S.I. UNITS	ENGLISH	S.I. UNITS
MOLTEN SALT LB/HR OR KG/S																							196793	24.85	196793	24.85		
STEAM LB/HR OR KG/S											35200	4.44	14208	1.79														
WATER LB/HR OR KG/S	92350	11.66	92350	11.66	44000	556	61760	7.80	61760	7.80	8800	1.12	3552	0.45	48350	6.10	17760	2.24									85521	1.96
TOTAL LB/HR OR KG/S	92350	11.66	92350	11.66	44000	556	61760	7.80	61760	7.80	44000	5.56	17760	2.24	48350	6.10	17760	2.24					196793	24.85	196793	24.85	85521	1.96
TEMP. °F OR °K	70	294.1	250	394.1	441	500.2	477	520.1	550	560.8	560	566.3	560	566.3	250	394.1	559	565.8					621.3	600.4	550	560.8	964	401.9
PRESS. PSIA OR KPA	122.4	8439.4	121.7	8391.1	1192	8218.8	1190	8205.0	1183	8156.7	1133	7812.0	1133	7812.0	1216	8384.3	1218	8398.1					96	661.9	94	648.1	41.85	288.5
FLOW LBM/HR OR KG/S	185.1	11.63	196.1	12.32	105.8	6.65	152.7	9.59	170.1	10.69					102.65	6.45	46.6	2.93					211.6	13.3	208.3	13.09	33.9	2.09
SPECIFIC GRAVITY	0.998	0.998	0.942	0.942	0.832	0.832	0.809	0.809	0.726	0.726					0.942	0.942	0.762	0.762					1.86	1.86	1.89	1.89	0.936	0.936
ENTHALPY BTU/LB OR KJ/KG	38.05	88.5	218.6	508.5	420.1	977.3	461.1	1072.7	548.5	1276.1	1062.6	2471.9	1062.6	2471.9	218.6	508.5	561.1	1305.3					28.2	65.6	0	0	233.6	542.0

DESIGNED BY	PP
DRAWN BY	LL
CHECKED BY	

FIGURE 5.8-1
PROCESS FLOW DIAGRAM
HEAT AND MATERIAL BALANCE
SALT/PROCESS STEAM SUBSYSTEM
SOLAR COGENERATION FACILITY
SANDIA NATIONAL LABORATORIES
LIVERMORE CA

FOR FINAL REPORT

BADGER ENERGY, INC.
CAMBRIDGE, MASS.
A Foster Wheeler Company

SCALE	
CERTIFIED	
DATE	

DWG NO E8031-106-2
ISSUE 1

The process steam subsystem includes all equipment, instrumentation, controls, piping, foundations, civil and any other work necessary to meet these requirements. It will be designed to meet all statuatory regulations and codes currently in force. The layout will provide reasonable access for proper operation, inspection, maintenance and repairs of the equipment, lines and instrumentation.

5.8.2 Design Description

The process steam subsystem consists of a heat exchange train of four shell and tube units which generate 5.56 kg/s (44,000 lb/hr) 80% quality steam at 7.81 MPa (1,133 psia). One of the exchangers also serves to preheat feedwater for the steamers in addition to feedwater for the molten salt steam generator. This exchanger uses turbine extraction steam as the heat source which is only available when the turbine is operating. Consequently the design provides for normal steam generating capacity without the heat input of the extraction steam. The design includes its own equipment for preheating prior to introduction of molten salt.

5.8.2.1 Flow Description

The schematic flow diagram for this subsystem is shown in Figure 5.8-1. Water from wells located near the site is softened in the water treatment equipment and pumped by soft water boiler feedwater pump PP-501 A/B thru the heat exchangers in series. Initial preheat is gained in the extraction steam/soft water preheater TT-301 which is a conventional turbine steam boiler feedwater heater. The water temperature is raised from 21°C (70°F) to 121°C (250°F) by heat exchange with 290 kPa (42 psia) turbine extraction steam. The extraction steam condensing in the shell of the exchanger is discharged under its own pressure to the EPGS feedwater subsystem. The preheat temperature of 121°C (250°F) is the maximum boiler feedwater preheat acceptable at the steamers.

To prevent solidification of the salt, the feedwater stream at 121°C (250°F) must then achieve further preheat before entering the molten salt exchangers. This preheat is obtained in the process steam/soft water preheater TT-302 which uses process steam recycled from the outlet of the steam generator to heat the feedwater to 227°C (441°F). The feedwater temperature is increased to 247°C by addition of process steam condensing in the exchanger shell using the condensate recycle pump PP-301. The feedwater flows to the molten salt/soft water preheater TT-303 where its temperature is increased to near saturation before passing to the molten salt steam generator TT-304 where 80% quality steam is generated at a pressure of 7.81 MPa (1,133 psia). In both TT-303 and TT-304 the heat exchange is with molten salt which flows in series first through molten salt steam generator entering at 566°C (1,050°F) and then through the molten salt/soft water preheater leaving at 288°C (550°F). The salt flow is controlled by the pressure of the process steam as monitored at the header. A portion of the steam generated is recycled to the process steam/soft water preheater TT-302 leaving a net production of 5.56 Kg/s (44,000 lb./hr.) at 7.81 MPa (1,133 psia).

5.8.3 Control Description

The instrumentation and controls for this subsystem are shown in Figure 5.8-1 and Figure 5.8-2. The controlling functions for this subsystem are: feedwater flow, feedwater temperature for both the molten salt and fossil fired steam systems, molten salt flow and associated process steam capacity.

5.8.3.1 Steam Pressure

Steam pressure at the process steam header is monitored and used at the master controller for both water and salt flows. The output signal from this controller is used as set point for the feedwater flow controller at the inlet to boiler feedwater preheater TT-303. The transmitter output signal from this controller and the feedwater temperature controller are fed into a minicomputer to determine the overall heat content of the feedwater.

The temperature of the molten salt entering the steam generator TT-304 and leaving the preheater TT-303 are also inputs to the minicomputer. This is programmed to perfom a heat balance around the system and varys the salt flow to generate the desired steam pressure. A signal from this salt flow controller is fed back to the hot salt pump control logic for summation with the turbine steam salt flow to ensure sufficient pumping capacity.

5.8.3.2 Boiler Feedwater Temperature

The water temperature at the inlet of the fossil steamers must not exceed 121°C (250°F). This is controlled by varying the flow of extraction steam entering the shell side of TT-301.

Water temperature to the molten salt water preheater TT-303 must be maintained above 247°C (477°F). This is controlled by monitoring the temperature at this point to reset the level controller on the shell side of TT-302. This varies the heat exchange area and consequently, the flow of condensate injected by condensate recycle pump PP-301.

5.8.4 Design Features

The four units in this heat exchanger train are all shell and tube type. All welded connections are specified for reasons of economy and to minimize joint leakage. The exchangers are specified to be shop fabricated, tested,and shipped assembled. They will be located on site in an individual area defined on the facility plot plan. This is adjacent to the hot salt pumps and soft water treating facilities minimizing installation and operation costs. A maintenance area is adjacent facilitating tube bundle removal.

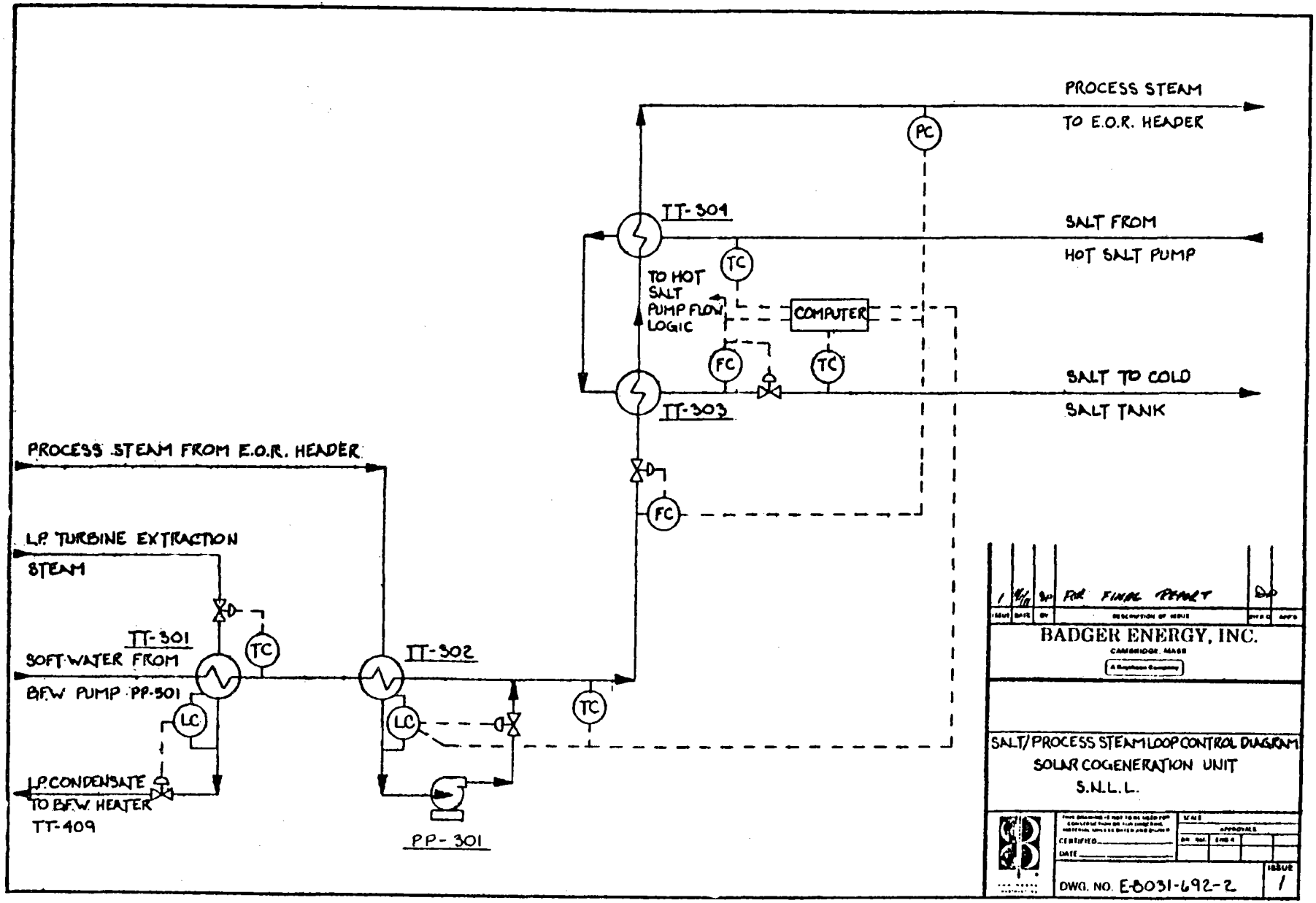
PROCESS STEAM
TO E.O.R. HEADER
PC
IT-304
SALT FROM
HOT SALT PUMP
TC
TO HOT SALT PUMP FLOW LOGIC
COMPUTER
FC
TC
SALT TO COLD
SALT TANK
IT-303
PROCESS STEAM FROM E.O.R. HEADER
FC
L.P. TURBINE EXTRACTION STEAM
IT-301
SOFT WATER FROM B.F.W. PUMP PP-501
TC
IT-302
TC
LC
LC
L.P. CONDENSATE TO B.F.W. HEATER TT-409
PP-301
1 4/18 DP FOR FINAL REPORT DP
BADGER ENERGY, INC.
CAMBRIDGE, MASS.
SALT/PROCESS STEAM LOOP CONTROL DIAGRAM
SOLAR COGENERATION UNIT
S.N.L.L.
CERTIFIED
DATE
DWG. NO. E-8031-692-2
ISSUE 1

Figure 5.8-2

Since this system must be capable of stand-alone operation, individual start-up facilities are provided. Due to the high melting point of the salt, it is impossible to cold start this system using molten salt. The startup sequence (See Operational Modes) must raise the entire system including all contained water to at least 242°C (467°F) before any molten salt flow . All salt piping and equipment is electrically traced to exceed this temperature. The startup heating duty for the feedwater will be provided by steam from the fossil steamers. A condensate flash drum MS-301 and startup condensate pump PP-302 are provided to utilize this steam during the startup mode.

The design features of each individual exchanger in this system are described below:

5.8.4.1 Extraction Steam/Soft Water Preheater - TT-301

This heat exchanger is designed for initial preheat of the softened well water for the molten salt and the fossil fired steamers. The heating medium is 290 MPa (42 psia) extraction steam from the turbine with condensate return to the EPGS boiler feedwater (BFW) system. The decision to use this heat medium was based on availability of this steam and the desire to minimize the amount of fossil fuel consumed by the steamers.

The exchanger is a standard BFW preheater/turbine steam condenser U-tube type. Contruction is all carbon steel with expanded tube/tubesheet joints and welded-end nozzles.

5.8.4.2 Process Steam/Soft Water Preheater - TT-302

This exchanger heats the feedwater for the molten salt steam generator above the solidificaftion temperature of the molten salt. The water inlet temperature to the first molten salt preheater was selected as 247°C (477°F) in order to give a safe operating margin above the salt solidification temperature.

Since this process steam system must operate independently of the turbine steam system, the only continuously available heating medium to preheat this soft water stream is 7.8 MPa (1133 psia) process steam recycled from the process steam header. The condensate produced in the exchanger is reinjected into the soft water stream at the exit of the exchanger using the condensate recycle pump PP-301.

The mixed soft water/condensate stream is maintained at the required temperature of 247°C (477°F) by controlling the amount of process steam recycled. The condensate is injected downstram rather than upstream of the exchanger in order to maximize the heat transfer and minimize the water flow rate through the exchanger.

The design duty of the exchanger is set by the need to preheat the soft water when no turbine extraction steam is available. In this case, feedwater enters the exchanger at 21°C (70°F) rather than 121°C (250°F) requiring increased process steam/condensate throughputs. The condensate injection configuration chosen eliminates the problem of mixing recycled steam condensate and soft water at 21°C (70°F).

The exchanger is a vertical, single pass design which minimizes the problem of controlling the exit water temperature by flooding the tube bundle with condensate. All carbon steel construction is used with expanded tube/tubesheet joints and welded end nozzles.

5.8.4.3 Molten Salt/Soft Water Preheater and Steam Generator - TT-303/304

These exchangers heat soft water from 247°C (477°F) and generate 80% quality steam at 7.8 MPa (1133 psia). A net steam production of 5.56 kg/s (44,000 lb/hr) is required from the system but because of the process steam preheat requirements when the turbine extraction steam is not available, the required gross duty becomes 9.45 kg/s (74,978 lb/hr).

The separation of preheat and boiler duties was dictated by considerations of process control and heat exchanger design. In order to minimize installation space, and equipment construction and maintenance costs, the two units have been specified as duplicate exchangers stacked upon each other. In the preheater, the soft water is preheated to 287°C (550°F) with further preheat and generation of 80% quality steam occurring in the steam generator.

All 304 stainless steel material is specified in order to eliminate problems of dissimilar materials for this high temperature, high pressure service. Strength welded tube/tubesheet joints are specified to minimize leakage. In event of tube rupture, each exchanger shell is equipped with a rupture disc to relieve shell side pressure. Each rupture disc and associated nozzles will be electrically traced to prevent salt solidifying at these points. The disc outlet nozzles will be piped via a manifolded system to the relief effluent separator MS-206 located in the exchanger area. In the event of tube failure, the salt will be separated from the steam in this vessel and will gravity flow to the separator sump. Steam will be vented from the separator to a safe location and the salt pumped to salt drain tank MF-203 by the effluent separator pump PP-204. To prevent any risk of salt solidification, the exchanger shells can be drained back to the effluent separator.

5.8.5 Operating Modes

In normal operation of this system, the EPGS subsystem is operational and provides 290 kPa (42 psia) extraction steam. When operating under these conditions, salt flow through the subsystem will be 25 Kg/s (196,800 lb/hr) with a working temperature difference of 278°C (500°F). Variations in insolation do not affect this operation since the molten salt storage capacity decouples this system from the receiver subsystem. The other principal operating modes are long term (cold) and short term (hot) start-up and shutdown conditions.

5.8.5.1 Cold Start-Up

This start-up procedure assumes the system to have been drained and the molten salt steam exchangers to be empty. Depending on whether or not the EPGS system is operating, feedwater will be available at 21°C (70°F) or 121°C (250°F). In either case, the procedure uses the following sequence of events.

The tubeside of the molten salt exchangers is isolated from the steam exchangers to prevent any risk of salt solidification.

Process steam is introduced from the steam header to the process steam/soft water preheater TT-302 to warm up the shellside of the unit. The steam condensate mixture from this exchanger will bypass the condensate recycle pumps and flow to condensate flash drum MS-301.

Next, a low feedwater flow to the tubeside of TT-302 is initiated with flow returning to the condensate flash drum. Increase pressure in the system using the control valve at the inlet flash down inlet line and start-up condensate pump PP-302 and pump hot water accummulating in flash drum to fossil steamers.

Gradually increase steam flow to TT-302 to increase exit water temperature.

Start flow of process steam from the header through the tubesides of molten salt exchangers TT-303/4 to vent.

Commission all electric tracing on salt lines and equipment and warm up both sides of molten salt exchangers to 260°C (500°F).

Introduce a low flow of molten salt through the exchangers with salt returning to cold salt tank or salt drain tank depending on temperature and status of other subsystems. Once the temperatures of the mixed water/condensate stream from TT-302 is at normal conditions of 247°C (477°F) open the isolation valve upstream of TT-303 to establish normal water flow path.

Increase molten salt flow through the exchangers while reducing water return to flash drum. Build up steam pressure in system to normal conditions while venting to atmosphere. Once normal operating conditions are established, open up steam to header and shutdown the start-up condensate pump PP-302.

5.8.5.2 Hot Shut-Down

In view of the continuous steam generation requirement from the unit, a hot shutdown will be of infrequent occurence. Under these conditions, the salt flow through the exchangers is stopped but the shutdown duration is not consi-

dered sufficient to cause any solidification problems. Salt temperature around the loop will be monitored during the shutdown and a low flow through the exchanger may occasionally be established as required. The water/steam system will be held at normal pressure by maintaining a small process steam flow to the process steam/soft water preheater. The tubeside of the molten salt exchangers will be kept hot by recycling a small steam flow from the process steam header venting to atmosphere.

5.8.5.3 Hot Start-Up

Start-up from the conditions described above will be a relatively simple operation. Steam flow from the header passing through the molten salt exchanger to the atmosphere is increased to enable salt flow to be established through the exchanger shells. Steam flow through the process steam/soft water preheater is increased and water flow established. While increasing feedwater temperatures to normal conditions, flow is passed to the flash drum, then to the fossil steamers.

Once the temperature of the water is satisfactory as feed to TT-303, flow is established and the procedure continues as described for cold start-up.

5.8.5.4 Cold Shutdown

This operational mode differs from the others since it is necessary to remove all salt from the system. In view of the independence of this subsystem, the main salt supply and return headers may remain in operation. Consequently, in this case it would be impossible to drain the subsystem to the salt drain tank MF-203. This subsystem salt piping and equipment is designed to be drained to the relief effluent separator MS-206. Salt accummulating in this vessel is transferred to storage by the effluent separation pump PP-206. All salt must be drained from the system prior to any temperatures appraoching 247°C (447°F) and the electric tracers will remain in operation until total salt drainage is ensured. The water system may be partially drained back to the condensate flash drum and/or soft water storage tank MF-502.

5.9 TURBINE STEAM SUBSYSTEM

The production of superheated steam from this subsystem is designed for use as motive fluid for a 20.4 MW_e turbine generator. The superheated steam is produced by heat exchange with molten salt which provides the total heat requirements for the subsystem. The subsystem interfaces with the energy storage and the electric power generation subsystems and together with these interfacing subsystems is capable of independent operation. The feedwater is supplied from the EPGS at a temperature of 250°C (480°F) at 9.03 MPa (1,310 psia).

5.9.1 Functional Requirements

The turbine steam subsystem is required to generate 20.9 Kg/s (165,800 lb/hr) of superheated steam at 538°C (1,000°F) and 8.27 MPa (1,200 psia). The steam must be of suitable quality for use as motive fluid for a 20.4 MW_e turbine generator. The subsystem is required to reheat 18.4 Kg/s (145,800 lb/hr) of steam from 400°C (750°F) to 538°C (1,000°F) at a pressure of 2.62 MPa (380 psia) for use in the second stage of the turbine. It uses the thermal energy contained in molten draw salt as the heat source for this steam generation and uses feedwater at 250°C (480°F) supplied from the EPGS. The molten salt is supplied from the energy storage subsystem at a temperature of 566°C (1,050°F) can be returned at 288°C (550°F). The energy storage capacity of the molten salt is designed to provide only a few hours of electricity generation, consequently the subsystem must start-up and shutdown on a daily basis.

The equipment for this subsystem is to be located in an individual area for which the structural environmental design requirements are:

Wind Velocity:	40 m/s (90 mph)
Seismic:	UBC Zone 4
Snow Load:	3.81 Kg/m^2 (0.78 lb/ft)
Max Foundation Loading:	216 kPa (4,500 lb/ft^2)

The turbine steam subsystem includes all piping equipment, instrumentation controls, foundations, civil and any other work necessary to meet these requirements. It will be designed to meet all statuatory regulations and codes currently in force. The layout will provide reasonable access for proper operation, inspection and maintenance of the equivalent piping and instrumentation.

5.9.2 Design Description

The turbine steam subsystem equipment consists of four shell and tube heat exchangers and one steam drum. Molten salt is the heating medium. Two exchangers serve to preheat boiler feedwater (BFW) from 250°C (480°F) and generate saturated steam at 8.54 MPa. The remaining two exchangers act as a steam superheater and steam reheater increasing steam temperatures to 538°C (1,000°F), in both cases. The subsystem is capable of operating independently of the process steam subsystem although process steam is used as the heat medium in equipment provided for cold start-up of this unit.

5.9.2.1 Flow Description

The schematic flow diagram for this subsystem is shown in Figure 5.6-1. Boiler feedwater at 9.03 MPa flows through the boiler feedwater preheater TT-401 for preheat against molten salt. This stream is raised from a temperature of 250°C (480°F) to near saturation temperature of 288°C (550°F) before flowing into the

steam drum MS-401. Water in the steam drum circulates naturally through the tubeside of steam generator TT-402. Steam is mechanically separated from entrained water in the top of the steam drum. A slip stream of boiler water from the steam drum may also be injected into the feedwater steam upstream of the boiler feedwater preheater TT-401 by means of start-up circulation pump PP-403. This keeps the water temperature at a safe margin above the molten salt solidification temperature.

Steam leaving the steam drum flows through the tubeside of steam superheater TT-403. The steam temperature is raised to 538°C (1,000°F) before delivery to the turbine at 8.27 MPa. The steam quality required at the turbine may be adjusted within the desired limits by varying the solids removal rate from the steam drum in the blowdown stream.

After use in the HP turbine, the majority of the steam is returned for reheating before use in the LP turbine. This steam stream flows through the tubeside of the steam reheater TT-404 for heat exchange against molten salt. The steam temperaure is raised to 538°C (1,000°F) before delivery to the turbine at 2.62 MPa (380 psia).

Molten salt enters this subsystem at a temperature of 566°C (1,050°F). The salt flows in parallel through the shell sides of the steam superheater and reheater before recombining to flow through the steam generator TT-402. Salt flows in series through the shell sides of the steam generator and BFW preheater leaving the subsystem at 288°C (550°F). The total salt flow through the system is controlled at the exit of the BFW preheater. This flow controller is reset by monitoring superheated steam pressure as supplied to the turbine.

5.9.2.2 Control Description

The instrumentation and controls for this subsystem are shown in Figure 5.6-1 and 5.9-1. Controlling functions for this subsystem are: steam temperature as delivered to the HP and LP turbine casings, feedwater flow and temperature, steam raising capacity and salt flow.

Steam Temperature

Steam temperature to the HP turbine is controlled by varying the flow of hot salt bypassing the steam superheater TT-403. Steam temperature to the LP turbine is controlled by varying the salt flow through the shell side of steam reheater TT-404.

Steam Flow

Steam flow leaving the steam drum MS-401 is monitored and the transmitter signal is combined in a conventional 3-element regulator system monitoring steam flow, feedwater flow and drum level. This is the method of controlling feedwater flow to maintain constant drum level at varying steam flows.

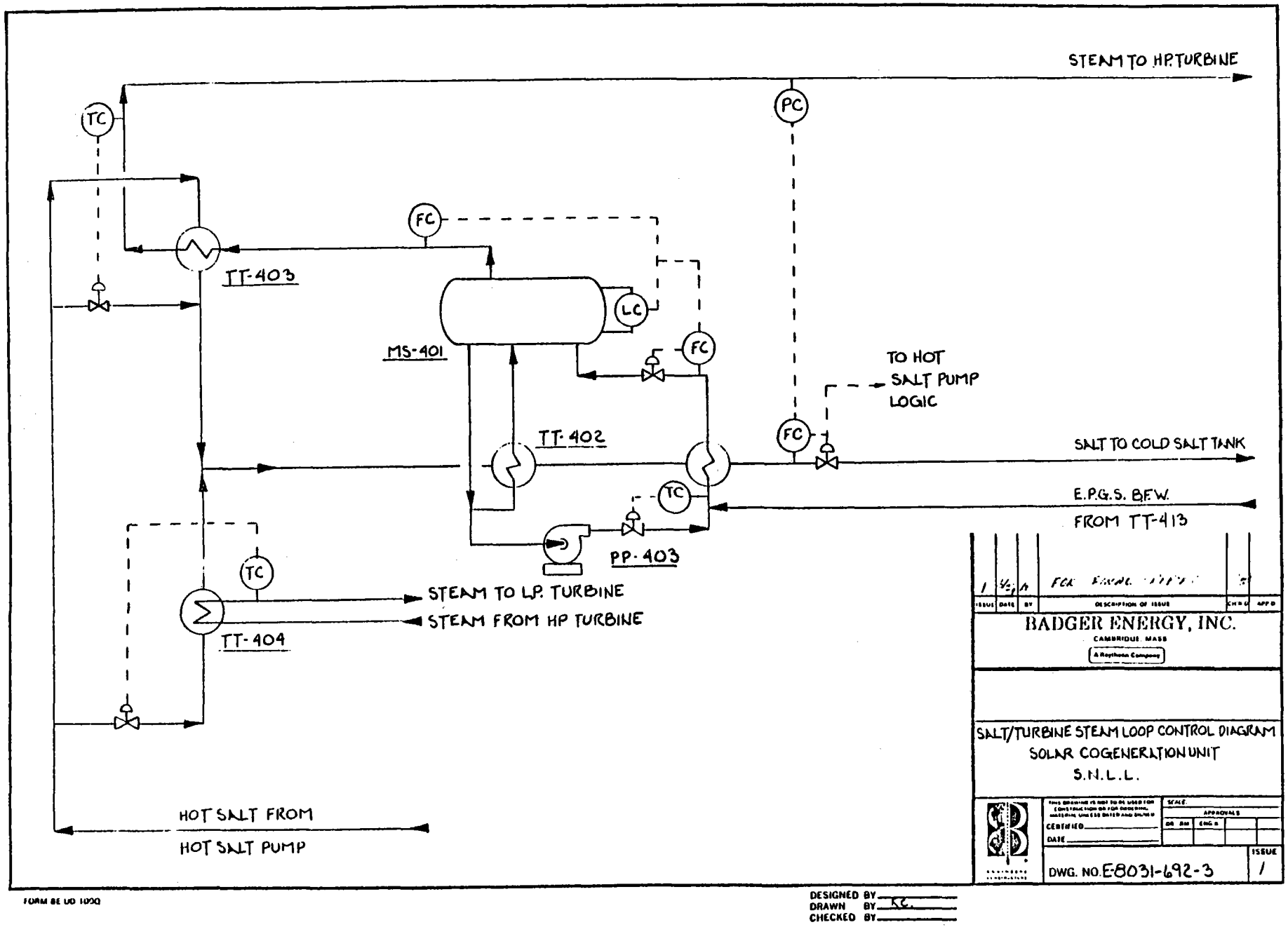
STEAM TO HP TURBINE
TC
PC
FC
TT-403
LC
MS-401
FC
TO HOT
SALT PUMP
LOGIC
TT-402
FC
SALT TO COLD SALT TANK
TC
E.P.G.S. B.F.W.
FROM TT-413
PP-403
TC
STEAM TO LP. TURBINE
STEAM FROM HP TURBINE
TT-404
HOT SALT FROM
HOT SALT PUMP
BADGER ENERGY, INC.
CAMBRIDGE MASS
A Raytheon Company
SALT/TURBINE STEAM LOOP CONTROL DIAGRAM
SOLAR COGENERATION UNIT
S.N.L.L.
DWG. NO. E-8031-692-3
ISSUE 1
DESIGNED BY
DRAWN BY
CHECKED BY

Figure 9-1

Salt Flow

The signal from the controller monitoring steam pressure to the HP turbine is used as set point to the salt flow controller at the exit of the boiler feedwater preheater TT-401. This varies salt flow through the steam and water exchanger in accordance with the HP turbine steam demand. A signal from the salt flow controller is transmitted to the hot salt pump control for summation with the process steam salt flow signal to maintain desired hot salt pumping capacity.

Feedwater Temperature

The feedwater temperature entering the subsystem is controlled to maintain a safe operating margin between the water and molten salt temperatures. If the water temperature starts to approach the salt solidification temperature, the controller will inject water from the Steam Drum.

5.9.3 Design Features

The four molten salt heat exchangers are of shell and tube design. The salt, on the shell side of each unit flows counter to the water/steam. Construction is all 304 stainless steel to eliminate thermal stresses inherent with dissimilar materials in high temperature designs. All welded connections are specified to minimize joint leakage and materials costs. Strength welded tube/tubesheet joints are specified to minimize leakage. In event of tube rupture, each exchanger is fitted with a rupture disc to relieve shell side pressure. These rupture discs and associated nozzles will be electrically traced to prevent salt solidifying at these points. The disc outlet nozzles will be piped to the relief effluent separator MS-206 to permit recovery of the salt. This separator is located in the exchanger area. The steam will be vented from the vessel while the salt will gravity flow to the separator sump. The effluent separator pump PP-204 will be used to return the salt to the salt drain tank MF-203. The exchanger shells may also be drained to the relief effluent separator.

The parallel salt flow configuration for the superheater and reheater was dictated by turbine steam inlet temperatures. A vertical thermosystem steam generator was selected because it allows simpler piping and control systems. Any variation in salt operating conditions will be accommodated with the design circulation ratio of approximately 10:1. The boiler feedwater preheater design was dictated by process and economic factors. The water outlet temperature of 288°C (550°F) was selected in order to retain a single shell unit.

The exchangers are located on site in an individual area defined on plot plan (Figure 5.1-1). This location is adjacent to the hot salt pumps and process steam system exchangers to minimize installation and operational costs. A maintenance area is adjacent for tube bundle removal.

In view of the frequent start-up and shutdown of this subsystem and the requirement for operation independent of the process steam subsystem, separate start-up facilities are provided; a pump and heat exchanger to heat-up the boiler feedwater. In view of the melting point of the salt, is impossible to execute a cold start-up of this system using molten salt. The start-up sequence (see Operational Modes) must raise the entire system to at least 242°C (467°F) before any molten salt flow. All salt piping and is electrically traced with special high temperature elements in order to exceed this temperature. However, for a cold start-up, the feedwater entering the subsystem would be at ambient temperature. Consequently, a start-up heater TT-405 is provided with a separate start-up circulation pump PP-403. The exchanger uses process steam. The start-up circulation pump is used during normal operation if the temperature of feedwater entering the subsystem falls below normal.

5.9.4 Operating Modes

The turbine generator system is intended for operation only at its rated capacity. When operating under these conditions, salt flow through the subsystem will be 128 kg/s (1,016,000 lb/hr) with a working temperature difference of 278°C (500°F). Total heat duty will be 56.1 MW (191.5 x 10^6 Btu/hr) which will generate 20.9 kg/s (165,800 lb/h.) steam at 538°C (1,000°F) and 8.27 MPa (1,200 psia). It will also reheat 18.4 kg/s (145,800 lb/hr) steam from 400°C (750°F) to 538°C (1,000°F) at 2.62 MPa (380 psia).

Variations in insolation do not affect operation of this unit since the molten salt storage capacity decouples this subsystem from the receiver subsystem. Consequently, the only other principal operating modes are long term (or cold) and short term (hot) start-up and shutdown.

5.9.4.1 Cold Start-Up

Start-up under cold conditions assumes the system to have been entirely drained. Cold boiler water (appropriately treated) may have been left in the steam drum/generation equipment. In either case, the start-up procedure would be similar involving the following sequence of events: Establish a working level in steam drum. Set up water circulation around the BFW heater/steam generation system using start-up circulation pump PP-403.

Commence heat-up of circulating water by heat exchange with process steam in start-up heater TT-405.

Utilize condensate produced from TT-405 by injection into process steam boiler feedwater stream using start-up condensate pump-PP302. Commission electric tracers on salt piping and equipment.

Increase steam pressure in the system until water temperatures achieve 243°C (470°F), then start a flow of steam through the superheater to vent.

With the whole system (except reheater TT-404) above 243°C (470°F) introduce molten salt through the steam generator and BFW preheater with main flow bypassing the superheater. Increase steam pressures, temperatures and vent flow while starting to establish normal conditions. Once steam flow and temperature is satisfactory, commission flow to the turbine and once the extraction steam is at a satisfactory temperature, start flow through the reheater.

As the turbine is brought on line, the temperature of the feedwater entering the subsystem will increase enabling the start-up heater to be taken off line and normal operating conditions to be established.

5.9.4.2 Hot Shutdown

Since part daily operation of the turbine generator is intended, hot shutdown will occur on a daily basis. The salt flow through the unit is stopped and salt left in the piping and equipment. The salt piping and equipment tracing and insulation is designed to prevent any salt solidification. Salt temperatures around the subsystem loop will continue to be monitored during this normal ten hour nightly shutdown. A low salt flow can be established through the system as required. This heat input together with heat input from the start-up heater will enable steam pressure to be maintained and conditions ready for immediate start-up.

5.9.4.3 Hot Start-Up

Start-up from the conditions described above will normally occur on a daily basis. A steam flow through the superheater is established using the start-up heater to provide generating requirements. A Salt flow may then be established through the system and the start-up then proceeds accurding to the cold start-up proceedure of paragraph 5.9.4.1.

5.9.4.4 Cold Shutdown

This operational mode differs from others in that all salt must be removed from the subsystem. Since the subsystem operation is independent of the process steam system, the main salt supply and return headers may remain in operation. This subsystem salt piping and equipment is designed to be drained to the relief effluent separator pump PP-204. All salt must be removed from the system prior to any temperature approaching 247°C (477°F) and the electric tracing will remain on until total salt drainage is ensured. Depending on the duration of the shutdown, the boiler water system may be drained or may be treated and left full of water.

5.9.5 Process and Turbine Steam Subsystems Cost Estimate

The estimated direct cost for the process and turbine steam subsystems combined (Account 5600) is $5.0 million.

5.10 SPECIALIZED EQUIPMENT

5.10.1 Water Treatment Subsystem

The water treatment subsystem consists of two independent units to purify the local well-water to be suitable for the process steam and turbine steam generation subsystems. The water treatment system for the process steam will purify the water required for both molten salt and fossil fired steam generators. The water treatment system for the turbine steam subsystem provides water to make up the boiler blowdown and turbine seal losses. Storage and pumping facilities for both product water streams are provided.

5.10.1.1 Functional Requirements

The water treatment subsystem has two primary requirements:

1) To provide 11.6 x 10^{-3} m^3/s (185 gpm) feedwater suitable for 80% quality steam generation at 7.8 MPa (1,133 psia) for EOR purposes.

2) To provide boiler feedwater make up for the turbine steam and EPGS subsystems. This water is to be of suitable quality for generation of superheated steam at 538°C (1,000°F) and 8.27 MPa (1,200 psia) for use as turbine motive fluid.

The water treatment subsystem includes sufficient surge capacity to accommodate start-up and other high make up demand modes.

5.10.1.2 Design Descriptions

The subsystem equipment consists of storage tanks, pumps and the water softening and demineralizing systems which are specified as skid mounted packaged units.

The water source is drawn from 300 m (1,000 ft) wells located on the site. This well water is stored in a 1,200 m^3 (32,000 gal) tank which provides storage capacity in case of loss of well-water supply. The well-water is pumped through parallel granular media filters for removal of suspended solids. A poly electrolyte flocculating agent will be added to the water upstream of the filters in order to increase the removal efficiency of the filtration. Each filter will be capable of treating normal water flow to allow for filter backwashing. After filtration, the water receives further treatment depending on its use. Water for process steam generation is softened by passing through parallel trains of cation exchange beds. This softener is sized to treat the total water requirements for both the fossil steamers and the process steam generation subsystem. Water required for makeup purposes for the turbine is fully demineralized by passing through parallel trains of cation and anion resin vessels before final polishing in parallel mixed resin beds. Storage tanks with capacities for 24 hours normal operation are provided for both product water streams.

6.0 ECONOMIC ANALYSIS

Two important objectives of the economic assessment of the Solar Cogeneration Facility are to determine the near-term economic viability of the project and to examine the impact of variations in major economic parameters such as capital and operating and maintenance costs on economic viability. Two measures of economic viability used in this analysis are levelized energy cost ($\overline{LEC}$) and net present value (NPV).

The economic analysis shows that for the base case capital costs and realistic economic assumptions, the $\overline{LEC}$ of the Solar Cogeneration Facility is somewhat higher than the conventional oil fired boiler $\overline{LEC}$. However, the analysis also shows the high degree of sensitivity of the Solar Cogeneration Facility economic viability to capital costs, tax credits and depreciation.

6.1 METHODOLOGY

The economic methodology used to assess the Solar Cogeneration Facility is based on a consideration of all costs and revenues which would be incurred by Exxon as an industrial user. Two common economic measures are used in this analysis: levelized energy cost and net present value. The levelized energy cost is calculated from

$$\overline{LEC} = [(\overline{FCR} \times CI_{PV}) + (1 - t)(CRF)\ (OM_{PV} + Elect_{PV} + Fuel_{PV})]/\text{Annual Energy Output}$$

where $\overline{FCR}$ is the levelized fixed charge rate, CRF the capital recovery factor, and t the applicable corporate tax rate. CI_{PV} accounts for all capital expenditures prior to commercial operation; OM_{PV}, $Elect_{PV}$ and $Fuel_{PV}$ are the present values of all recurring costs incurred during operation over the system life, namely operations and maintenance (OM), electricity purchases (Elect) and any fuel burned (Fuel). For the solar facility cases, no fuel is consumed ($Fuel_{PV} = 0$) and the net revenues from the sale of electricity to PG&E results in $Elect_{PV} < 0$. The levelized fixed charge rate ($\overline{FCR}$) is a value that, when applied to the capital investment over the life of the plant, expresses the constant fixed charges required to recover the investment, allowing for depreciation and investment tax credit effects. For this project, the $\overline{FCR}$ is calculated by

$$\overline{FCR} = [1 - t(DPF) - a]\ CRF + (1 - t)\ (B_1 + B_2)$$

where DPF is the depreciation factor for the applicable depreciation method and period, a is the investment tax rate percentage, and $B_1 + B_2$ is the combined insurance and property tax rate.

The net present value is calculated from

$$NPV = -\frac{\overline{FCR}}{CRF} \times CI_{PV} + (1 - t)\ [-OM_{PV} - Elect_{PV} - Fuel_{PV}]$$

For the solar facility cases $Electpv < 0$ and $Fuelpv < 0$, since both are revenue streams. NPV is, then, the difference between revenues and expenses over the lifetime of the project.

The economic analysis allows a direct comparison between the proposed solar cogeneration facility and conventional oil fired steamers. For the anticipated steam drive operation at Edison, it was determined that the energy output of four 7.33 MW_t (25 MBtu/h) steamers would be required. Since two of the four steamers are already in use at Edison, the economic comparisons considered two new energy facility cases: a solar cogeneration facility and a coventional oil fired facilty, each producing approximately the same amount of steam which equals the annual output of two fossil fired steamers.

6.2 ASSUMPTIONS AND RATIONALE

The economic assumptions which enter into the base case calculations of $\overline{LEC}$ and NPV are shown in Table 6.2-1.

Table 6.2-1 Economic and Fuel Cost Assumptions

System Life	26 years
Initial Year of System Operation	1986
Discount Rate	15%
Depreciation Lives	11 years (Federal), 3 years (State)
Depreciation Methods	Asset Depreciation Range with first year averaging (Federal), Sum of years digits on 75% of Book Value (State)
Investment Tax Credit	10%
Solar Tax Credits	15% (Federal) + 13.5% (State), (net of US income tax)
Tax Rates	46% (Federal), 9% (State), 50.86% (Combined)
Property Tax and Insurance	2.25% (Levelized)
General, Capital and O&M Escalation	8%
Fuel Cost	$4.00/MBTU (1980)
Fuel Escalation Rate	12% (including general escalation) (not an Exxon forecast or an Exxon endorsed forecast)
Electricity Escalation	Per PG&E Private Proprietary Forecast
Fixed Charge Rate (after tax)	.0624 (Existing taxes, depreciation methods)

These assumptions are a realistic set which account for existing income tax rates and solar tax credits for both federal and California state governments.

The federal depreciation method, asset depreciation range (ADR), is a composite accelerated depreciation calculation where the double-declining method is used for the first two calendar years, sum-of-the years digits are used for the next nine calendar years, with the residual (if startup occurs midyear) taken in the last year of operation. The federal depreciation factor (DPF) used in the FCR equation is equal to 0.5825. The composite tax rate of 50.86% accounts for the deduction of the state tax during calculation of the federal tax.

The solar investment tax credit of 38.5% is made up of several state and federal tax credits including 10% federal investment tax credit, 15% federal solar tax credit and an effective state solar tax credit of 13.5%.

Fuel costs of \$13.7/MWh_t (\$4.00/MBtu) are assumed, based on economic parameters supplied by Sandia Labs for the cogeneration program. This assumption is realistic for 1980 costs at the Edison field. It should be noted that the net effect of the various taxes and royalties on oil sold from the Edison field is to lower the price of oil which is produced and used onsite for fuel for the steamers. Higher taxes result in higher costs to Exxon for oil purchased at market prices and consumed at Edison and thus there is a greater economic incentive to consume a portion of the oil produced at Edison which is not subject to taxes. Higher oil prices impose a lower LEC target for solar in this application than would be encountered for solar in a non-oil producing application.

Escalation rates for general, capital and O&M are assumed to be 8% which is a Sandia supplied assumption. Fuel escalation rate of 12% (4% above inflation) is also based on Sandia supplied information.

Finally, the price schedules for electricity which is generated at the Edison field and sold to Pacific Gas and Electric Company are based on the rates and capacity payment described in Section 2 of this report and escalated according to a PG&E proprietary forecast.

6.3 PLANT AND SYSTEM SIMULATION MODELS

The performance of the Solar Cogeneration Facility was determined by a detailed computer simulation of the solar subsystem coupled with calculations of system losses, energy storage status, EPGS performance and facility operating schedules to yield daily, monthly and annual system performance. Solar subsystem performance was determined from three computer models - MIRVAL, TRASYS and STEAC. MIRVAL and TRASYS model the performance of the collector field and receiver and provide inputs to the solar subsystem performance model STEAC. Insolation and weather data from the Fresno Solmet TMY data tape was also input to STEAC.

Overall system performance was calculated on a daily basis by modifying the solar subsystem energy output to account for balance of plant thermal losses, turbine performance, electrical energy consumption and facility operating schedules. System performance is summarized in Section 4 of this report.

Economic calculations are based on the equations presented in Section 6.1 for levelized energy cost and net present value.

6.4 RESULTS AND CONCLUSIONS

The levelized cost of energy was determined for both the Solar Cogeneration Facility and a conventional oil fired facility as explained in Section 6.1. The total capital and first year operating and maintenance costs for both facilities and the annual performance of both facilities are summarized in Table 6.4-1. Details on capital costs for the Solar Cogeneration Facility are given in Appendix A and Section 4 of this report. Results of the base case calculations for conventional and solar facilities are shown in Table 6.4-2.

Table 6.4-1 Cost and Performance Summary $1980

	Conventional Oil-Fired Steamers (2)	Solar Cogeneration Facility
Capital Cost (Total)	$1.33 x 10^6	120 x 10^6
Operation Maintenance (First Year)	$ .68 x 10^6	2.4 x 10^6
Fossis Fuel Cost (Annual)	$3.34 x 10^6	- 0 -
Net Thermal Output to Process (Annual)	110,000 MWh_t (375,000 MBtu)	105,600 MWh_t (360,300 MBtu)
Fuel Consumed (Annual)	140,000 MWh_t (478,300 MBtu) 80,700 BBL)	- 0 -

Table 6.4-2 Levelized Cost of Energy, Baseline Economics, $1980

Conventional Oil Fired Steam Facility	Solar Cogeneration Facility
$35/$MWh_t$ ($10/MBtu)	$51/$MWh_t$ ($15/MBtu)

The baseline economic results show the Solar Cogeneration Facility to have a higher $\overline{LEC}$ than the conventional oil fired steamer facility by a factor of 1.44. The results of NPV for the baseline solar case is a negative NPV of $13.8 million when discounted at 15%.

However, the solar economic results are very sensitive to a number of key assumptions which can result in substantially higher and lower $\overline{LEC}$ and NPV. These sensitivities are presented in the following section.

6.4.1 Sensitivity Analysis

6.4.1.1 Operations and Maintenance Expense

Two sensitivities around the base case first year O&M expense of 2% of initial capital costs were examined. These cases are 1% and 3% of the initial capital cost and the results are displayed in Figure 6.4-1. O&M expense has a significant impact on both $\overline{LEC}$ and NPV as Figure 6.4-1 indicates. A halving of the first year O&M from the base value of 2% results in a 20% reduction in $\overline{LEC}$, from about $50 to $40/MWh$_t$.

The NPV, however, remains negative for all O&M sensitivities using base case assumptions. The base case of 2% was arrived at by a separate "bottoms up" calculation for the Solar Cogeneration Facility (also see Section 4.8) which approximated the 2% of capital cost number. Until solar facility O&M costs are determined from the Barstow 10 MW$_e$ Pilot Plant, the Almeria IEA Central Receiver System, and other central receiver solar facilities, there will remain some uncertainty which should be bounded by the sensitivity analysis.

6.4.1.2 Capital Costs

The economic attractiveness of the Solar Cogeneration Facility is strongly affected by the facility capital costs. Two sensitivities around the base case of $120 million were examined. The low capital cost case of $75 million was taken from the baseline estimate modified by the assumption of no-charge for heliostats (this case was requested by Sandia Labs). This "free heliostat" case includes $20/m^2 of direct heliostat costs. The high capital cost case of $135 million resulted from modifying the base case with the assumption of direct heliostat costs of $260/m^2 installed ($370/m^2 including all indirects and contingency) which has been the Sandia supplied assumption for the preliminary economic calculations for this program.

Results are shown in Figure 6.4-2 for the range of assumed capital costs. The $75 million capital solar cost assumption results in an $\overline{LEC}$ of $16/MWh$_t$ which is considerably less than the $35/MWh$_t$ $\overline{LEC}$ of the conventional fossil system. It is also highly improbable for a system of this size and complexity. The higher capital cost assumption of $135 million realizes an $\overline{LEC}$ of $62/MWh$_t$

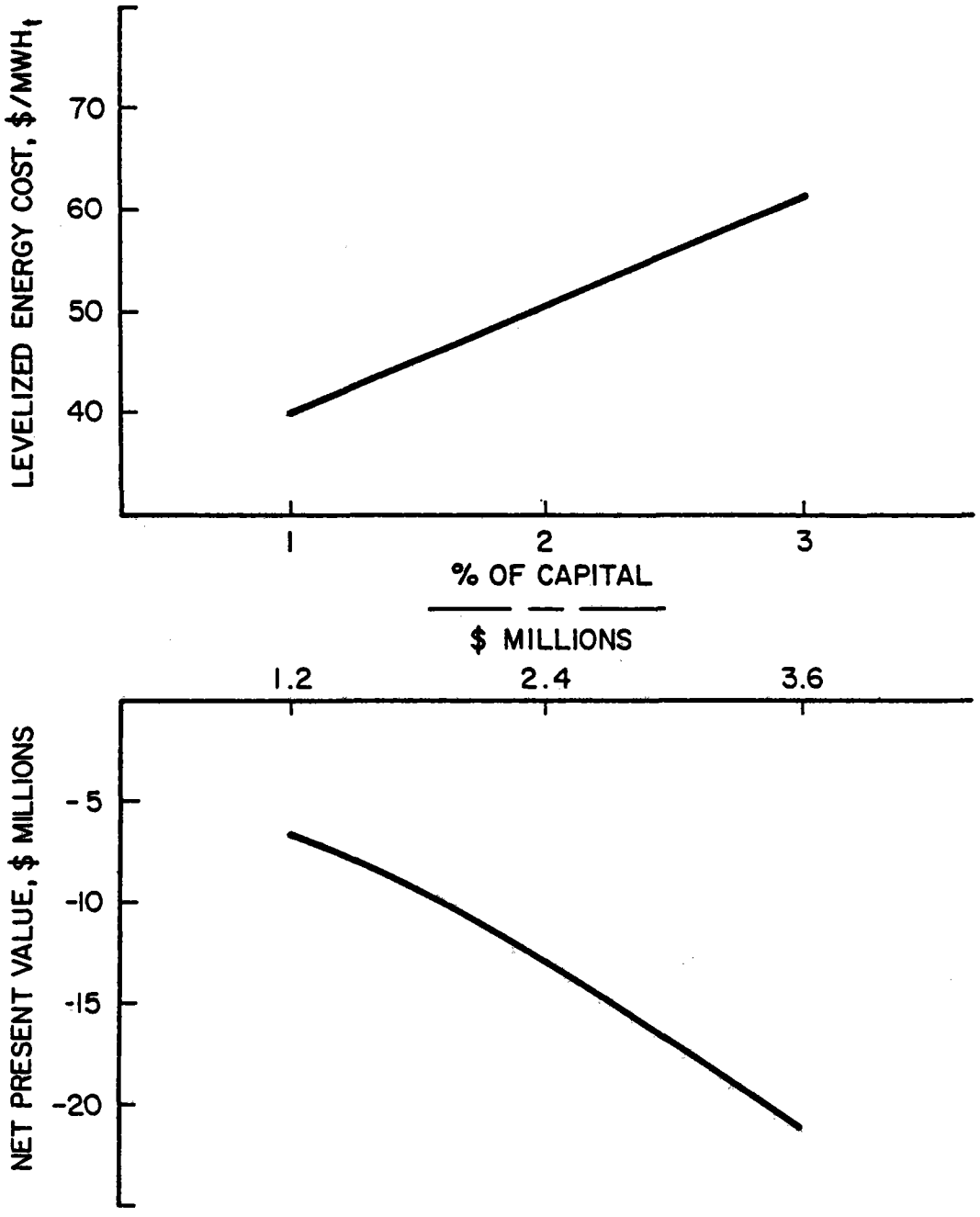

Figure 6.4-1
Solar O and M Sensitivity

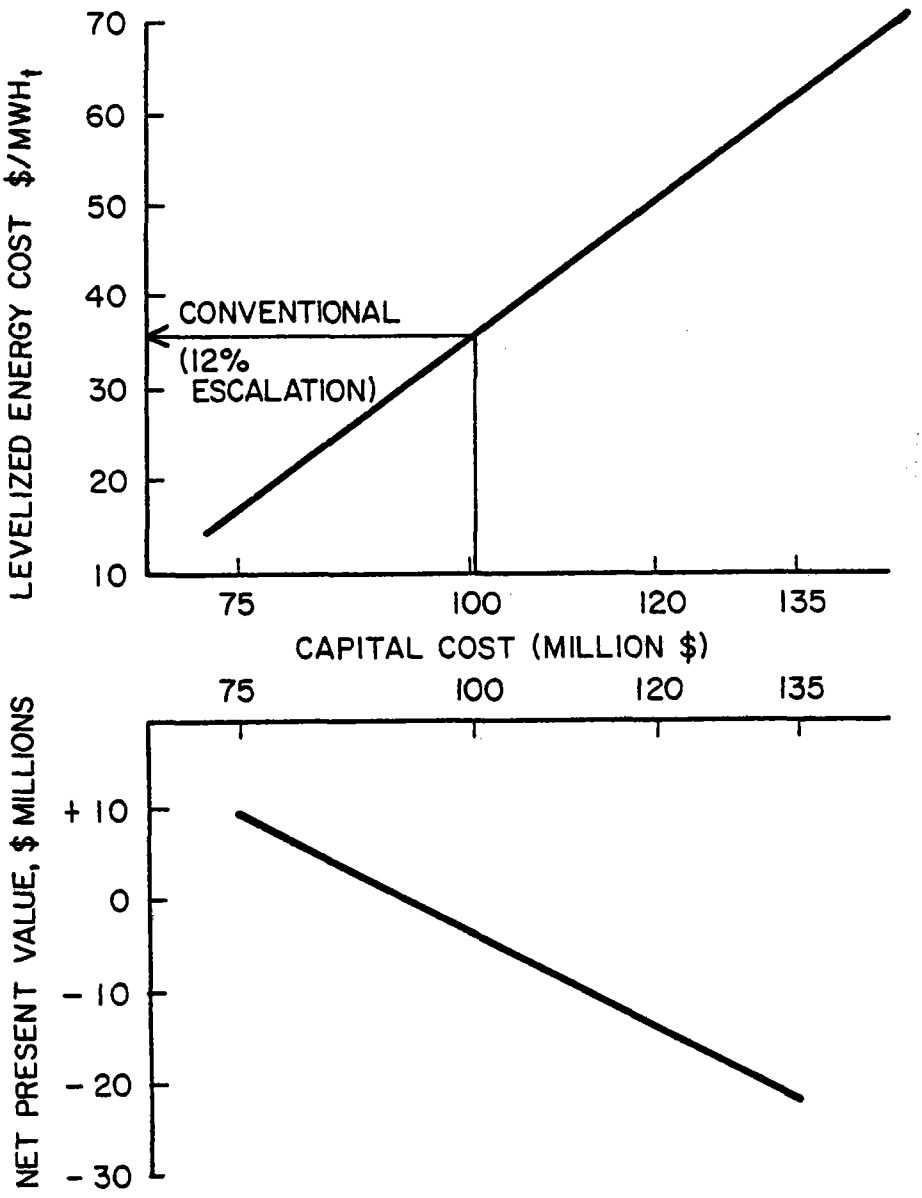

Figure 6.4-2
Solar Capital Cost Sensitivity

and has an NPV of -$22 million. The interesting point on this curve is the crossover with the conventional system which occurs at a capital cost of $100 million. This represents a reduction of 20% from the baseline capital estimate and would require a reduction in direct capital cost of about $12 million, which results in a $20 million change in capital cost after the indirect costs are added. The important message Figure 6.4-2 conveys is that small changes in the Solar Cogeneration Facility capital cost can effect large swings in $\overline{LEC}$.

6.4.1.3 Fixed Charge Rate

The impact of three alternative fixed charge rates on the Solar Cogeneration Facility economics was determined. These fixed charge rates represent varying scenarios of solar tax credits and depreciation allowances and are summarized in Table 6.4-3. Case 2 is the base case and represents no change in existing depreciation laws and a continuation of the federal and state solar tax credits which are due to expire in 1983 (state) and 1985 (federal). Case 1 assumes enactment of the proposed "10-5-3" depreciation rules by both federal and state governments and continuation of all solar tax credits. This is the most favorable scenario for the solar case.

Table 6.4-3 Fixed Charge Rates

Case	$\overline{FCR}$ after tax	Basis
1	0.0494 (1)	38.5% Solar Credits and 5 year SOYD (Federal and State)
2 Base	0.0624	38.5% Solar Credits, 11 year ADR (Federal), 3 year SOYD (State)
3	0.0923 (1,2)	No Solar Credits & 5 year SOYD
4	0.1067 (2)	No Solar Credits, 11 year ADR (Federal and State)

Notes: (1) Assumes new "10-5-3" depreciation rules enacted by US and copied by California. This would allow a 10 year depreciation on structures, 5 years on equipment and 3 years on vehicles.

(2) Solar Credits expire by 1985 (Federal) and by 1983 (State). California depreciation also expires in 1983 per AB 2036.

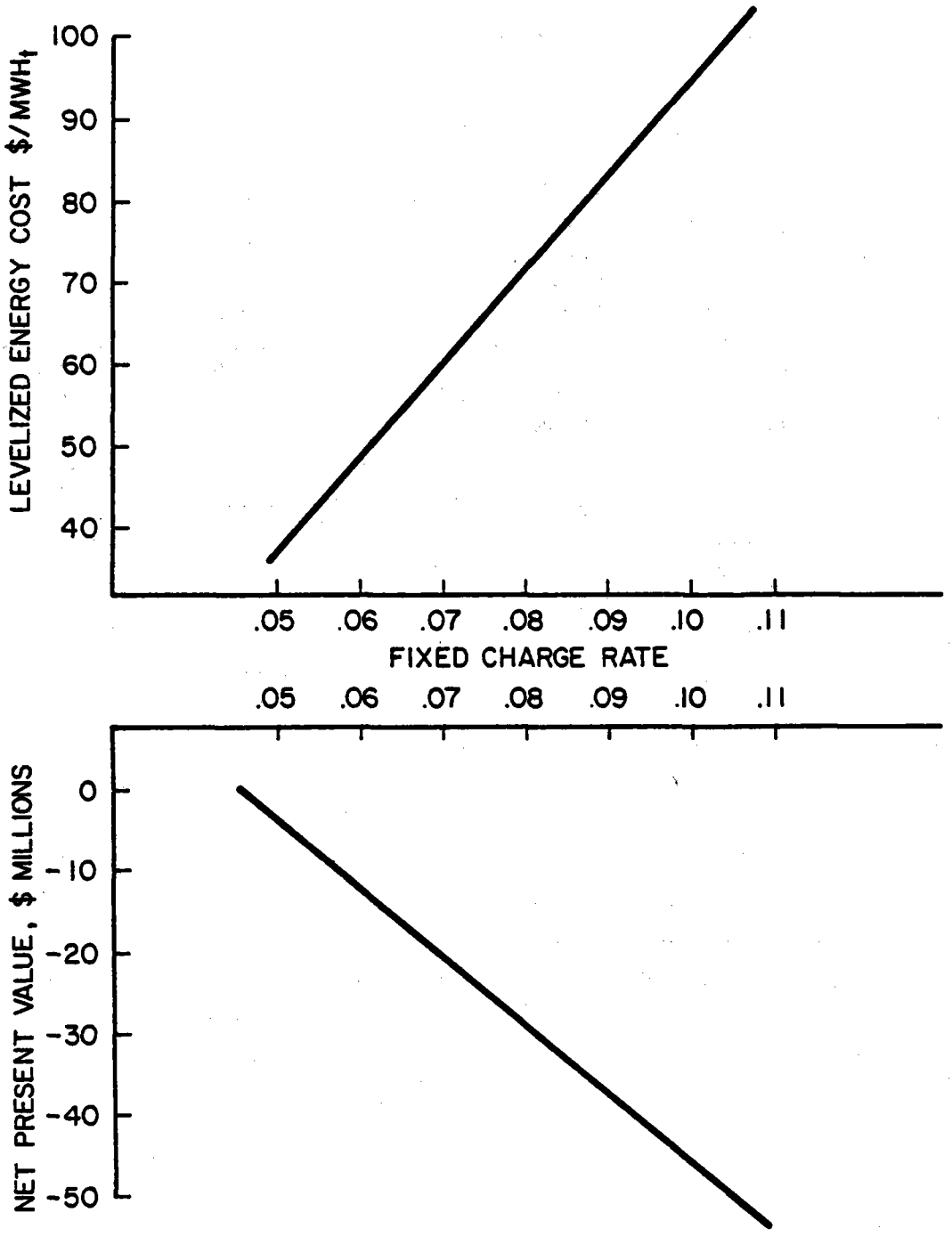

Figure 6.4-3
Solar $\overline{FCR}$ Sensitivity

Two cases which are least favorable toward solar are Cases 3 and 4 which assume that all solar tax credits expire and 10-5-3 depreciation rules are enacted (Case 3) or current depreciation laws stand (Case 4).

Results are shown in Figure 6.4-3. Once again the $\overline{LEC}$ is shown to be very sensitive to a key economic parameter, in this case the fixed charge rate. The change in $\overline{LEC}$ over the range of $\overline{FCR}$'s is from \$36/MWh$_t$ to \$101/MWh$_t$. This is an important economic uncertainty which has a major impact on the attractiveness of the Solar Cogeneration Facility.

6.4.1.4 Fuel Escalation Rates

Changes in the escalation rates of fuel for the conventional oil fired facility case were examined, ranging from 8% (0% real growth) to 16% (8% real). The base case assumption is 12% (4% real) which was supplied by Sandia Labs. Results are depicted in Figure 6.4-4 which shows a range of $\overline{LEC}$ for the conventional oil fired facility case of from \$63/MWh$_t$ at 16% escalation to a low of \$22/MWh$_t$ for the 8% escalation case. Fuel escalation, like capital, O&M, and $\overline{FCR}$, can have a significant influence on the relative merits of a conventional steaming facility versus the Solar Cogeneration Facility.

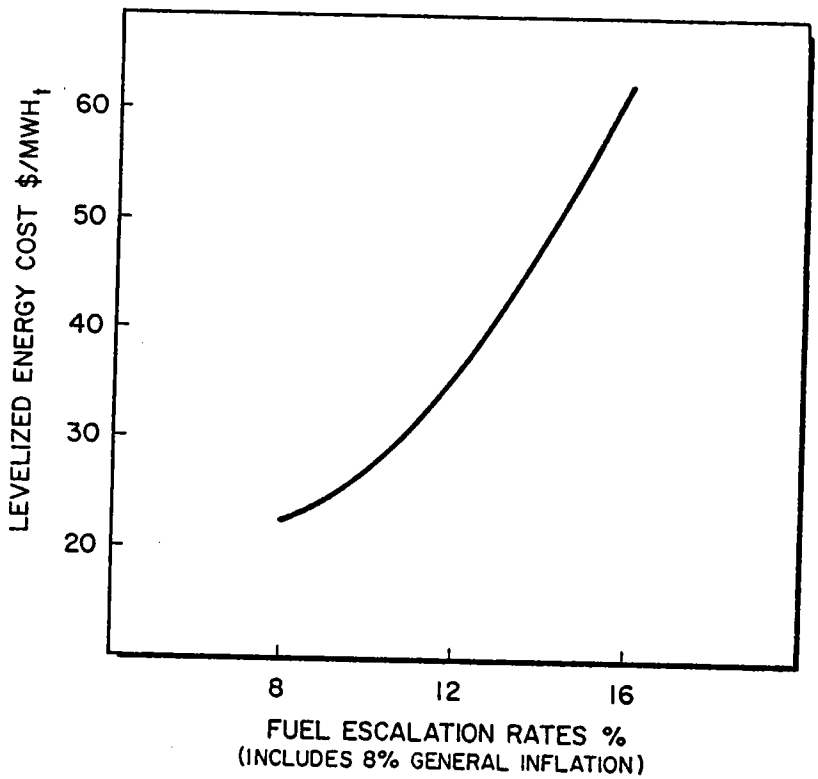

Figure 6.4-4
Conventional Fuel Escalation

6.4.1.5 Combined Sensitivities

Two additional cases were examined for the solar facility, i.e., the combinations of O&M, and $\overline{FCR}$ which would yield the most favorable and least favorable comparisons of the solar facility to the oil fired case. Table 6.4-4 displays the results, which show the most favorable combination for solar to be the 1% O&M plus lowest $\overline{FCR}$ case plus 16% fuel escalation (fuel escalation affects only the NPV and not the solar $\overline{LEC}$). This case results in $\overline{LEC}$ and NPV of \$26/MWh_t and +\$22 million, respectively. The least favorable solar sensitivity combination results in $\overline{LEC}$ of \$112/MWh_t and NPV of -\$65 million. It is clear that changes in several individual key economic parameters and combinations of changes in these parameters have significant impact on the solar vs. conventional economic comparisons.

Table 6.4-4 Combined Sensitivities, Solar Cogeneration Facility

Capital \$ Million	O&M (% of Capital)	$\overline{FCR}$	Fuel Escalation (%)	$\overline{LEC}$ \$/MWh_t	NPV \$ Million
120	1	.0494	16	\$ 26	+22
120	3	.1067	8	\$112	-65

6.4.2 Summary

The base case economic set for the Solar Cogeneration Facility compared to the base case oil fired steamer facility economic assumptions shows the solar case to be at an economic disadvantage. A number of economic scenarios were examined which result in the solar case being equal to or less than the conventional case, considering levelized energy costs. Likewise, a number of economic scenarios resulted in the solar case having higher $\overline{LEC}$ than conventional.

From an Exxon project viewpoint, the uncertainties surrounding the solar facility case are much larger than the uncertainty of the conventional case which is simply fuel cost escalation. Therefore, it would be very risky to attempt to make a project decision in 1981 when the economic climate in 1986 may be considerably different and make the solar project even less economically attractive than it appears in 1981.

7.0 DEVELOPMENT PLAN

The following development plan is a requirement of the subject DOE contract and should not imply any Exxon plans to pursue this project at this time. This development plan describes the detailed design, startup and operation of a solar cogeneration facility at the Edison field. It is consistent with the completion of the conceptual design study in mid-1981 and the startup of the cogeneration facility in 1986.

7.1 DESIGN PHASE

The design phase commences after completion of the conceptual design and includes the development testing, detailed design and engineering of the facility and the securing of all required legal permits.

Two important development tests have been identified as necessary before detailed design of the facility can be completed. The first of these is a steam drive pilot at the Edison field which will determine the suitability of the field to respond to the steam drive mode of enhanced recovery. This pilot is already underway at Edison and is scheduled for completion by the end of 1982. The second development test would be an accelerated life test of the cold salt pump. This pump is required to move the salt from the cold storage tank up the tower to the solar receiver and has not been tested under the specific pressure conditions required by the cogeneration design.

This test is designed to complement other development tests of salt related equipment and heliostats which DOE has completed or is planning, including molten salt solar receivers, internally lined salt storage tanks and second generation heliostats. The two cogeneration development tests can be run in parallel.

The detailed design and engineering work will incorporate results from these development tests as well as design and operating data from other solar central receiver pilot plants including the Barstow 10 MW_e Pilot Plant, and pilot plants in Spain and Italy, all of which will be fully operational in early 1982.

The detailed engineering design will cover all major subsystems including solar, energy storage and transfer, electric power generation and process steam, site preparation and site development. Startup procedures and tests will also be defined in the detailed design phase, and all information required for legal permits including construction and tower will be generated in the detailed design phase. At the completion of the detailed design phase, all required permit applications will be filed.

7.2 CONSTRUCTION PHASE

The construction phase begins when all permits have been issued. Initial construction activities include site preparation and procurement of long lead items including heliostats, receiver, salt storage tanks, turbine generator and master controller. The fabrication and installation of the major components is the next major construction activity followed by piping, site buildings, final system interconnections and charging the system with molten salt.

7.3 FACILITY CHECKOUT & STARTUP PHASE

Following the construction phase, tests will be run on each major subsystem to check all normal and emergency operating modes. These include heliostats, solar receiver, salt storage and transfer, electric power generation, process steam and master controller.

Facility startup will follow the checkout phase and will include careful monitoring of key parameters such as temperature, pressures and flow rates to insure that all design conditions are being achieved.

7.4 SCHEDULE AND MILESTONES

The cogeneration project schedule and milestones are shown in Figure 7.4-1. Phase II could begin in April 1982 with detailed engineering and permits complete by February 1984. Construction would commence and continue until October 1986 with normal facility operation projected for December 1986.

The schedule is consistent with the DOE conceptual design milestones which call for completion of conceptual design in mid-1981 and startup of the facility in late 1986.

*U.S. GOVERNMENT PRINTING OFFICE: 1981-740-145/2571

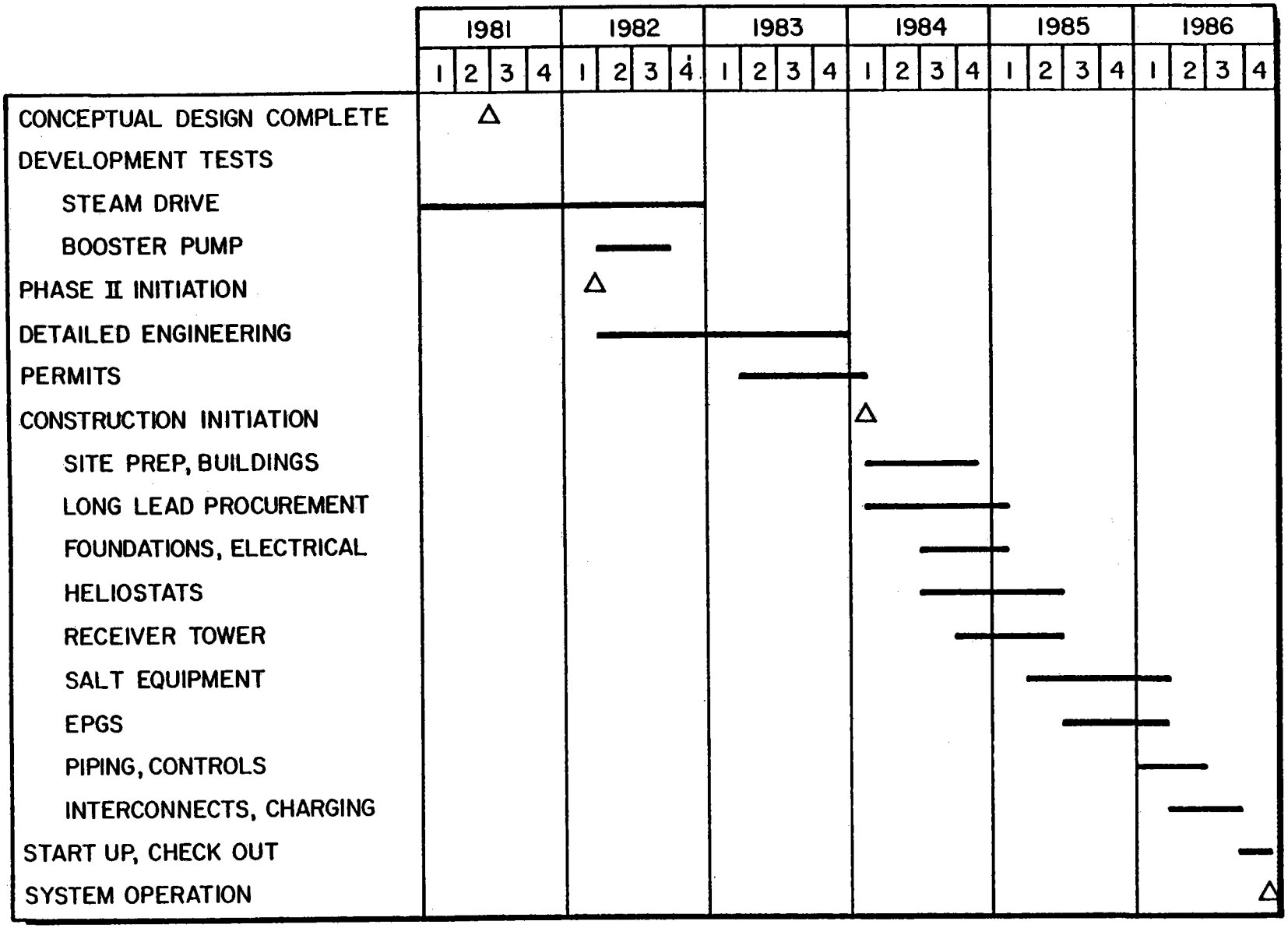

Figure 7.4-1 Cogeneration Project Schedule